PERFORMANCE STUDY OF A NOVEL SOLAR COLLECTOR USING PHASE CHANGE MATERIAL IN RISER TUBE

BUNDARITH NHEL

MASTER OF ENGINEERING IN RENEWABLE ENERGY ENGINEERING

MAEJO UNIVERSITY

2020

PERFORMANCE STUDY OF A NOVEL SOLAR COLLECTOR USING

PHASE CHANGE MATERIAL IN RISER TUBE

BUNDARITH NHEL

A THESIS SUBMITTED IN PARTIAL FULFILLMENT

OF THE REQUIREMENTS FOR THE DEGREE OF MASTER OF ENGINEERING

IN RENEWABLE ENERGY ENGINEERING

ACADEMIC ADMINISTRATION AND DEVELOPMENT MAEJO UNIVERSITY

2020

PERFORMANCE STUDY OF A NOVEL SOLAR COLLECTOR USING
PHASE CHANGE MATERIAL IN RISER TUBE

BUNDARITH NHEL

THIS THESIS HAS BEEN APPROVED IN PARTIAL FULFLLMENT

OF THE REQUIREMENTS FOR THE DEGREE OF MASTER OF ENGINEERING

IN RENEWABLE ENERGY ENGINEERING

APPROVED BY   Advisory Committee

Chair ....

(Assistant Professor Dr. Sarawut Polvongsri)

………………./………………/ ……………

Committee ....

(Associate Professor Dr. Akarin Intaniwet)

………………./………………/ ……………

Committee ....

(Assistant Professor Dr. Attakorn Asanakham)

………………./………………/ ……………

Program Chair, Master of Engineering ....

in Renewable Energy Engineering (Assistant Professor Dr. Tanate Chaichana)

………………./………………/ ……………

CERTIFIED BY ACADEMIC   ....

ADMINISTRATION AND DEVELOPMENT

(Associate Professor Dr. Yanin Opatpatanakit)

Acting Vice President for the Acting President of

Maejo University

………………./………………/ ……………

ชื่อเรื่อง	การศึกษาสมรรถนะของตัวเก็บรังสีอาทิตย์แบบใหม่ที่ใช้วัสดุเปลี่ยนเฟสใน ท่อไรเซอร์
ชื่อผู้เขียน	Mr.Bundarith Nhel
ชื่อปริญญา	วิศวกรรมศาสตรมหาบัณฑิต สาขาวิชาวิศวกรรมพลังงานทดแทน
อาจารย์ที่ปรึกษาหลัก	ผู้ช่วยศาสตราจารย์ ดร.สราวุธ พลวงษ์ศรี

บทคัดย่อ

งานวิจัยนี้มีวัตถุประสงค์เพื่อศึกษาสมรรถนะของตัวเก็บรังสีอาทิตย์แบบแผ่นเรียบที่ไม่มี
วัสดุเปลี่ยนเฟส (PCM) และใช้วัสดุเปลี่ยนเฟสชนิด RT42 มีจุดหลอมเหลว 38-40 °C เติมลงในท่อไร
เซอร์ที่มีเส้นผ่านศูนย์กลางขนาด 10 mm และ 16 mm ที่ติดตั้งภายในท่อดูดกลืนความร้อนมีเส้น
ผ่านศูนย์กลางขนาด 28 mm ตัวเก็บรังสีอาทิตย์ที่ทำการทดสอบมีขนาดกว้าง 220 mm ยาว 1,000
mm สูง 100 mm ติดตั้งหันหน้าไปทางทิศใต้ทำมุม 18° กับพื้นโลก ณ วิทยาลัยพลังงานทดแทน
มหาวิทยาลัยแม่โจ้ จังหวัดเชียงใหม่ ประเทศไทย ใช้ปั๊มน้ำในการหมุนเวียนน้ำผ่านตัวเก็บรังสีอาทิตย์
และวัดอัตราการไหลน้ำด้วยเครื่องวัดอัตราการไหล ในถังเก็บน้ำร้อนมีการติดตั้งขดลวดความร้อนเพื่อ
ควบคุมอุณหภูมิน้ำ ทำการทดสอบตามมาตรฐาน ASHRAE Standard 93-2003 โดยมีค่ารังสีอาทิตย์
ตั้งแต่ 790 W/m² ความเร็วลม 2.2-4.5 m/s อุณหภูมิแวดล้อมไม่เกิน 30 °C และทำการเพิ่มอุณหภูมิ
น้ำขาเข้าตั้งแต่ 35°C - 65 °C โดยเพิ่มขึ้นทีละ 5 °C แล้วทำศึกษาโดยปรับอัตราการไหลของน้ำ 3 ค่า
(0.01 0.02 และ 0.03 kg/s·m²) จากนั้นนำข้อมูลไปวิเคราะห์การถ่ายเทความร้อนของตัวเก็บรังสี
อาทิตย์และสมรรถนะทางความร้อนของระบบตามลำดับ

จากการทดสอบพบว่า อุณหภูมิน้ำขาเข้าและอัตราการไหลของน้ำมีผลต่อสมรรถนะทาง
ความร้อนของตัวเก็บรังสีอาทิตย์ โดยเมื่ออุณหภูมิน้ำขาเข้าตัวเก็บรังสีอาทิตย์สูงขึ้นความร้อนที่ตัวเก็บ
รังสีอาทิตย์ได้รับและสมรรถนะของตัวเก็บรังสีอาทิตย์จะมีค่าลดลงเนื่องจากมีการสูญเสียความร้อน
ไปสู่สิ่งแวดล้อมมากขึ้น เช่นเดียวกันเมื่อให้อัตราการไหลน้ำเพิ่มขึ้น โดยสมรรถนะทางความร้อนของ
ตัวเก็บรังสีอาทิตย์ที่ใช้วัสดุเปลี่ยนเฟสขนาดเส้นผ่านศูนย์กลางท่อไรเซอร์ 16 mm ที่อัตราการไหล
0.03 kg/s·m² มีสมรรถนะทางความร้อนสูงสุด ซึ่งมีค่า เท่ากับ 0.835 และค่า เท่ากับ 9.68 W/m²·K
รองลงมาเป็นตัวเก็บรังสีอาทิตย์ที่ใช้วัสดุเปลี่ยนเฟสขนาดท่อไรเซอร์ 10 mm และตัวเก็บรังสีอาทิตย์
แบบทั่วไปที่การทดสอบอัตราการไหล 0.02 kg/s·m² โดยมีค่า เท่ากับ 0.828, 0.713 และ เท่ากับ
11.304 W/m²·K 10.642 W/m²·K ตามลำดับ

ในส่วนคุณลักษณะการถ่ายเทความร้อนของของตัวเก็บรังสีอาทิตย์ พบว่า อัตราการไหล
ของน้ำที่ใช้ในการทดสอบอยู่ในช่วงการไหลแบบราบเรียบ เมื่ออัตราการไหลและขนาดของท่อไรเซอร์
เพิ่มขึ้นค่าสัมประสิทธิ์การพาความร้อนจะมีค่าเพิ่มขึ้นเช่นเดียวกับค่าตัวเลขพรันด์เทิล จากการ
ทดสอบสามารถสร้างสมการความสัมพันธ์ของค่าตัวเลขนัสเสลท์ (Nu) ที่มีความสัมพันธ์ต่อ ค่าตัวเลข
เรย์โนลด์ (Re) และค่าตัวเลขพรันด์เทิล (Pr) ในการไหลแบบราบเรียบได้ดังสมการ

$$Nu=0.143\ Re^{0.193}\ Pr^{1.821}\ \text{เมื่อ } 2 < Pr < 5$$

คำสำคัญ : สมรรถนะ, ตัวเก็บรังสีอาทิตย์, ลักษณะการถ่ายเทความร้อน, วัสดุเปลี่ยนสถานะ

Title	PERFORMANCE STUDY OF A NOVEL SOLAR COLLECTOR USING PHASE CHANGE MATERIAL IN RISER TUBE
Author	Mr. Bundarith Nhel
Degree	Master of Engineering in Renewable Energy Engineering
Advisory Committee Chairperson	Assistant Professor Dr. Sarawut Polvongsri

ABSTRACT

This research aims to study the performance of flat-plate solar collector without phase change material (PCM) and with RT42 PCM type with a melting point at 38-40 $^{\circ}$C filled in the riser tube with a diameter of 10 mm and 16 mm that inserted into the absorber tube of 28 mm outside diameter. The experiment flat-plate solar collector has 220 mm of width, 1,000 mm of length, and 100 mm of height facing to the south at 18° of tilt angle at School of Renewable Energy, Maejo University, Chiang Mai, Thailand. The electrical pump is used to circulate water through the collector and measured the mass flow rate by flow rate meter. In the hot water storage tank the electric heater is installed the water temperature regulation. The test method is carried out following the ASHRAE standard 93-2003 in a condition of the solar radiation is equal or more than 790 W/m^2, the wind speed is between 2.2-4.5 m/s, the ambient temperature is not more than 30 °C, the inlet water temperature of solar collector is varied from 35°C - 65 °C and has adjusted increment of 5 °C. The three conditions of mass flow rate 0.01 0.02 and 0.03 kg/s•m^2 are adjusted. The obtained data would be analyzed the heat transfer and thermal performance of solar collector, respectively.

From the experiment showed that the inlet water temperature and mass flow rate effected on the thermal performance of solar collector. When the inlet water temperature increased, the heat gain from solar collector and the thermal performance would be decreased because of the heat gain loss to the surrounding as same as in the case study of mass flow rate increasing. The thermal performance of

solar collector integrated with PCM riser of 16 mm diameter at the mass flow rate of 0.03 kg/s·m^2 was given the highest thermal performance presented of the and were 0.835 and 9.68 W/m^2·K. The next was the solar collector integrated with PCM riser of 10 mm diameter and the last was the conventional solar collector at the mass flow rate of 0.02 kg/s·m^2 which showed the are 0.828, 0.713 and were 11.304 W/m^2·K, 10.642 W/m^2·K, respectively.

For the heat transfer characteristic of solar collector discussion. It was found that the observation of water mass flow rate was a laminar flow. When the mass flow rate and the riser tube increased, the convection heat transfer coefficient would be increased as same as the Prandtl Number. From the study could obtain the relation of Nusselt number (Nu) that relates to the Reynold number (Re) and Prandtl number (Pr) as following equation

$$Nu = 0.143 \, Re^{0.193} \, Pr^{1.821} \quad \text{which } 2 < Pr < 5.$$

Keywords :   Performance, Solar collector, Heat transfer characteristic, Phase Change material

ACKNOWLEDGEMENTS

Bundarith Nhel

TABLE OF CONTENTS

Page

List of Tables

List of Figures

List of Abbreviations

PCM	Phase Change Material
CO2	Carbon dioxide
IEA	International Energy Agency
UN	United Nation
AEDP	Alternative Energy Development Plan
SWH	Solar water heater

List of Symbols

Symbol	Description	Unit
I_T	Total solar radiation on tile surface	W / m^2
$(\tau\alpha)_e$	Transmittance-Absorptance product	-
F_R	Collector heat removal factor	-
F'	The collector flow efficiency factor	-
U_L	Collector overall heat loss coefficient	$W / m^2 \cdot K$
h_{p-c}	The heat transfer from the absorber plate to the cover	$W / m^2 \cdot K$
$h_{r,p-c}$	The radiation heat transfer from the absorber plate to the cover	$W / m^2 \cdot K$
$h_{r,c-s}$	The heat transfer from the cover to the sky	$W / m^2 \cdot K$
h_w	Wind heat transfer coefficient	$W / m^2 \cdot K$
T_p	The absorber plate temperature	K
T_c	The cover glazed temperature	K
T_a	The ambient temperature	K
T_f	Fluid temperature	K
T_i	Inlet water temperature	K
$T_{s,m}$	The PCM solid melting temperature	K
$T_{m,l}$	The PCM melting to liquid state temperature	K
T_{ref}	The temperature reference	K
T_m	The melting temperature	K
ΔT	The mean temperature difference of collector and water	K
$\dot{m}$	Mass flow rate circulating in the collector system	kg / s
C_p	Specific heat of the water	$kJ / kg \cdot K$
ρ	Water density	kg / m^3
μ	Dynamic viscosity	$N \cdot s / m^2$
η_{coll}	The thermal performance of solar collector	-
A_c	The collector area of solar collector	m^2
A_p	The Aperture are of solar collector	m^2
D_i	The inside diameter of the tube	m
D_o	The outside diameter of the tube	m

C_b	The bond conductance	-
h_i	The heat transfer between fluid and absorber plate	$W / \mathrm{m}^2 \cdot K$
h	The enthalpy of the Phase Change Material	$kJ / kg \cdot K$
C_{ps}	The specific heat of PCM in solid state	$kJ / kg \cdot K$
C_{pl}	The specific heat of PCM in liquid state	$kJ / kg \cdot K$
l	The heat fusion of the PCM	kJ
f	The factor of PCM	-
ε_p	The emittance of plate	-

Chapter 1

Introduction

This chapter offers a general global issue relate to energy production by fossil fuel source and the factor impacts to environment. The global energy demand has been increasing slightly and will be double by 2050, for security of energy around glob, IEA has been proposing the renewable energy. In ASEAN region, the committee of each partners make own plan for future energy security around region by giving existence on renewable energy for the target reduce fossil fuel demand. Thailand government has own goal to achieve 30% of energy from renewable energy by 2030 within wind power generator, biomass and solar photovoltage are the first production and solar thermal energy presents low-temperature for heater or pre-heat system. In Literature review is offered to the new technologies have been using and present themes.

1.1. Statement of purpose

Every year, the world population has been increasing continuously the United Nation reports that population of 7.6 billion in 2017 is expected to reach 8.6 billion, 9.8 billion in 2050 and 11.2 billion in 2100 (UN, 16 Oct 2018). The modern industrial revolution is a period of unprecedented economic and social development changes energy is a fundamental input to economic activity. The global energy consumption grows significantly to driving habitants and industrials demand that is forced to expand the amount energy resource as fossil fuel. However, the energy products from fossil fuel also have important impacts which releases carbon dioxide (CO_2) and other greenhouse gases the fundamental driver of global climate change and environment pollution. The International Energy Agency (IEA) is guided by four main areas of focus: Energy security, Economic development, Environmental awareness and engagement worldwide has been wily proposing the renewable energy technologies (IEA, 2019). In the ten countries of the Association of Southeast Asia Nations (ASEAN), the total population is nearly 640 million and the number is signal for higher energy consumption around the region and an estimate of at least $2.7 trillion of energy investment is needed by 2040 to achieve ASEAN energy targets alone. With greater

energy demand, it is inevitable that rising consumption of all fuel will be witnessed in the near future.
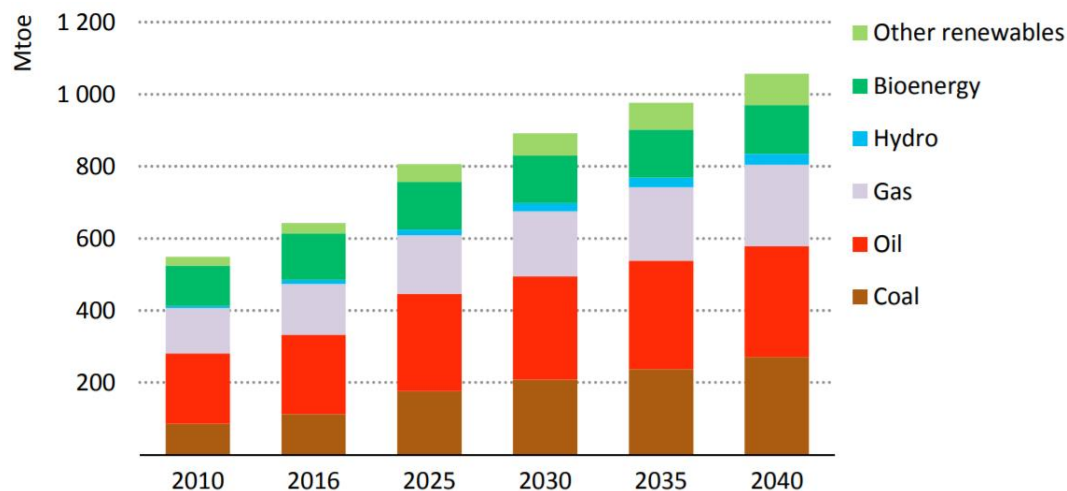
Figure 1 Primary energy demand in Southeast Asia (EnergyOutlook2017, 16 Oct 2018).

Coal alone accounts for almost 40% of the growth, and overtakes gas in the coal fire to generate electricity mix. The demand of crude oil expands from 4.7 million barrels per day (mb/d) to around 6.6 mb/d in 2040. This is due to the expansion in transportation vehicles increase by two-thirds to around 62 million. The demand for natural gas also grows strongly, around 60% by 2040, due to higher consumption in power generation and industrial section (EnergyOutlook2017, 16 Oct 2018). At the same time, energy-related air pollution issue, both indoor and outdoor, also presents a major risk to public health. Rising CO_2 emission is contrary to the objectives of the Paris Climate Change Agreement. It's a challenging for the ASEAN nation committee achieves the target of reducing the fossil fuel energy by ordering around the region to use the new source of energy which is clean and is abundant on the earth. Alternative energy consists of the energy from hydro, geothermal, wind, solar, biomass and wave energies as the solution to the existing energy problem. In Thailand, the government has set a new renewable energy target of 30% of final energy consumption by 2036 in its Alternative Energy Development Plan (AEDP) 2015. there is a large amount of hydropower generating capacity, including 1,000 MW of pumped storage, in all scenarios. This can be used as regulating power when needed, especially in the

scenario that the share of variable energy sources, such as solar photovoltaic (PV) and onshore wind power, in the power system increase substantially. the industrial facilities that can potentially use biomass for process heat are large-scale, centralized plants operating at economies of scale, which would require large energy flows to be brought from within and across national borders. Renewable thermal energy utilization accounts for nearly two-thirds of the total increment of renewables in final energy in the same year 2036, if the AEDP 2015 target is met as projected in the plan. The majority of this is expected to come from biomass according to the plan. Solar thermal represents "low-hanging fruit" in the end-use sectors, and can be scaled up significantly in buildings for water heating and in industry for low-temperature heating and pre-heating (Ministry of Energy, 2019).

Solar energy is one energy that provide light and radiation heat to every living things on earth, also one of the most promising energy resources that has been using every day and one of other alternatives energy has been wily using for product both heat and electric in the same time. Solar cells rely on the interaction between light that hits the electron hole-pair on the semi-conductor and making potential difference in circuit then it took electron cross circuit which generating electricity while the solar collectors use to attach to the radiation directly absorb heat to produce thermal energy. Both systems have been under development with techniques while the solar hot water system has been attracted by scientist to search the way to improve abilities collect, store thermal energy and its performance. Solar flat plate collector is not yet quire development by many researchers. The recent techniques were published as such as Nano fluid which increase heat absorption capacity from the collector plate surface (Syam Sundar et al., 2018) (Sarawut and Kiatsiriroat, 2014) (Liu et al., 2013). Otherwise, the solar hot water system with Nano-fluid offers high thermal efficiency but it gives disadvantages during and offer operation. Other scientists have studied about thermosiphon solar collector by using twisted tapes inside and have found that the system gives sloop flow and high heat transfer (Jaisankar et al., 2009) (Wongcharee and Eiamsa-ard, 2011) (Murugan et al., 2019). This technique is increased face side affected and turbulent flow inside the absorber tube plate where working fluid was collected thermal energy during operate than simple solar collector. Furthermore, the

conventional solar collector system operates upon various solar radiation intensity and suffers from the sporadic nature solar energy across a given time interval in daylight. Adding thermal energy storage device into solar hot water system is an alternative to solve the issue (Cabeza et al., 2011; Gond et al., 2012; Khalifa et al., 2013; Naghavi et al., 2015; Reddy, 2007; Wu et al., 2018). The phase change material (PCM) which its chemical composites that are systematized according to the energy procedure store: sensible heat, latent heat and chemical reaction (heat fusion) of thermal energy storage. Latent heat of PCM can store a large amount of heat fusion when it's melting. The energy store of PCM is changed by the chemical components that are given the different form of the melting process such as isothermal and non-isothermal process. Solar collector integrated with the latent heat of PCM to store the thermal energy when collecting heat from high radiation solar intensity and is released to the working fluid, its thermal store can keep exit water temperature stability than a conventional collector solar water heat collector.

1.2. Literature review

A traditional solar water heating system consists of collectors and a storage tank which is working fluid circulated by electric pump or gravity flow through. the solar hot water system converts solar energy into thermal energy than it transfers energy to working fluid from low to high temperature. water is stored in a well-insulated tank. it still gives interested by many researchers where were published relate to investigated the performance of system. Improving tech can continuously produce or keep hot working fluid when absent incident solar radiation by using the heat thermal energy storage device. This paper will present the solar collector which solar collected integrated with PCM inside collector which were improving the thermal performance enhance from collected surface to the working fluid and discharge heat from the phase change material (PCM) which is latent heat energy storage can store a large amount of heat to working fluid when solar radiation intensity drops.

1.2.1. Phase change materials (PCM)

Non-Isothermal process and Isothermal Process of PCM
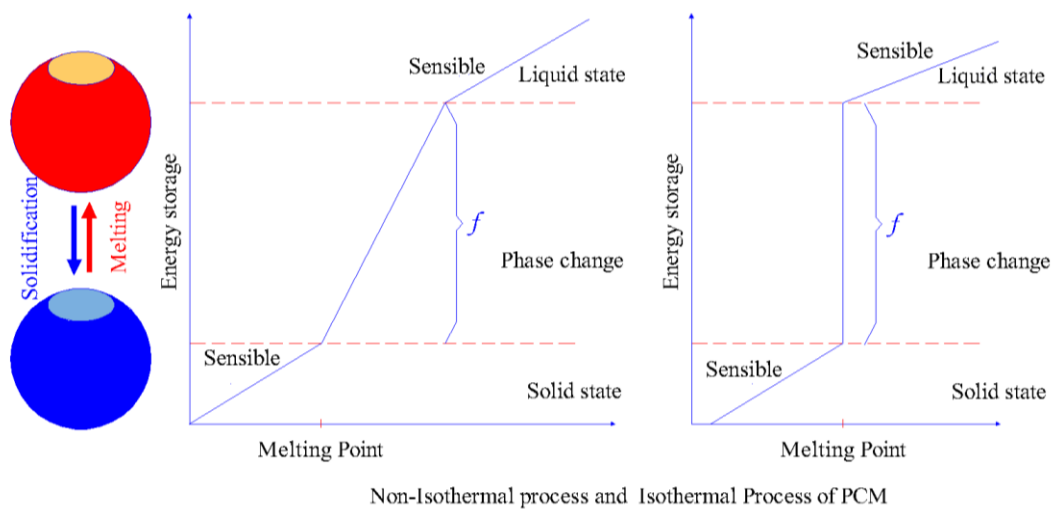
Figure 2 Energy storage of Phase Change Material (ICNQT, 2018).

It is deal because the latent heat associated with melting and freezing is capable of storing much more heat than sensible thermal storage alone. Once the heat generating component is shut-off the PCM will begin to solidify by releasing the stored energy. The most common applications that benefit from PCM include those with known duty cycles. It has a high heat of fusion per unit weight and volume, have a relatively high thermal conductivity for non-metals, and show small volume changes between solid and liquid phases. These are not commonly used for electronics heat sinks, since they are corrosive and long-term reliability (thousands of cycles) is uncertain. The most common application is for very large thermal storage applications. where much lower cost is very attractive. The phase change material is stored thermal energy when the period of solar radiation and release heat to the water when the temperature of water low then temperature of PCM. Paraffin PCM's also have a low thermal conductivity, so designing sufficient conduction paths is another key design consideration. Solar collector integrated with paraffin wax PCM which is melting point between 38 °C to 42 °C showed **Table 1**.

Table 1 Properties of the PCM (Bellan et al., 2015; Loem et al; RUBITHERM, 2018).

Properties	Value
Melting temperature	38-43 $^\circ$C
Specific heat in liquid state	2 (KJ/kg·K)
Specific heat in solid state	2 (kJ/kg·K)
Thermal conductivity in liquid state	0.2 (W/m·K)
Thermal conductivity in solid state	0.2 (W/m·K)
Density in liquid state	0.76 (kg/l)
Density in solid state	0.88 (kg/l)
Volume expansion	12.5 (%)
Latent heat of fusion	170 (kJ/kg)
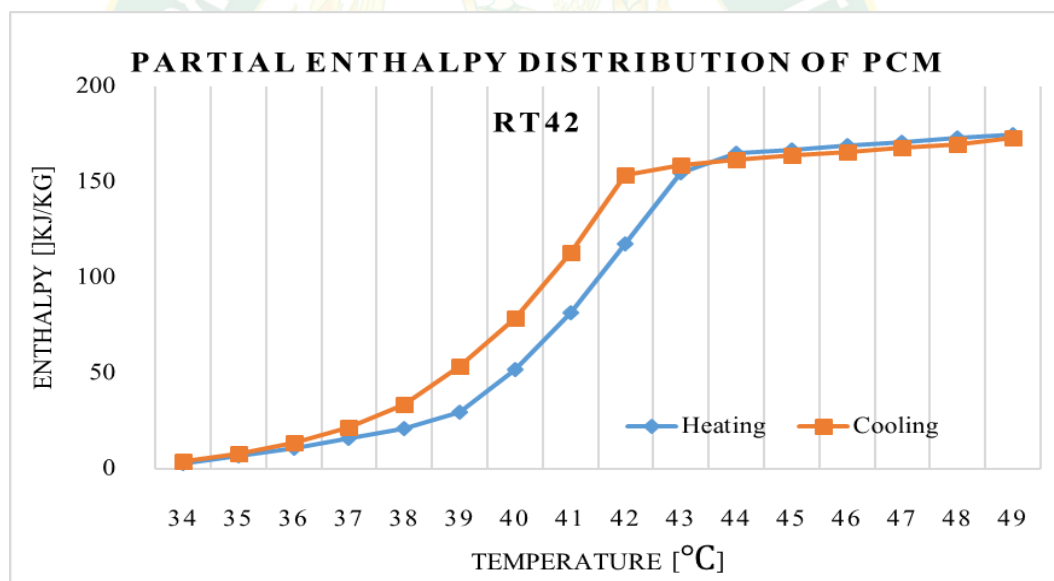
Figure 3 The partial enthalpy distribution of PCM RT42 (RUBITHERM, 2018).

Papadimitratos et al (Papadimitratos et al., 2016) studied the performance of a solar water heater with evacuated tubes integrated with phase change materials. The results show that phase change material integrated inside the inner tubes of evacuated tube solar collectors can effectively store energy (form of latent heat) next to the heat pipes and enable a delayed cooling after sunset or late evening. The proposed solar collector utilizes two distinct phase change material (dual-PCM), Tritriacontane and Erythritol with melting temperature 72°C and 118°C. The operation of solar water

heater with the proposed solar collector is investigated during both normal and on demand operation. The feasibility of this technology is tested via large scale commercial solar water heaters. This study shows a significant efficiency improvement of 26% for the normal operation and 66% for the stagnation mode of dual-PCM solar water heaters for both normal and stagnation operation, compared with standard solar water heaters that lack PCM.
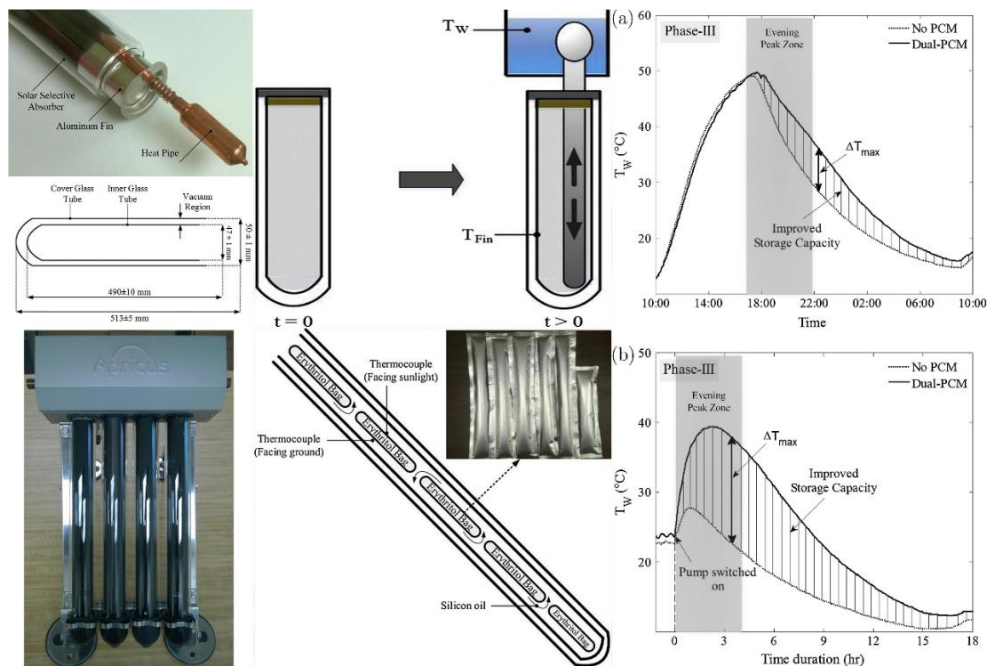
Figure 4 Schematic of evacuated solar collector filled with PCM and experimental apparatus (Papadimitratos et al., 2016).

Koca, Ahmet et al (Koca et al., 2008) studied the energy and exergy analysis of a latent heat storage of PCM into solar collector which copper pipe was used as heat exchanger with 10 mm outer diameter and 1 mm thickness into the tank PCM. The heat transfer fluid as allowed to flow inside the serpentine pipe to discharge the heat by the phase change materials. The variations of radiation become almost constant during morning and it increases until noon. The bell-shaped variations were obtained for stored energy during all day. It was observed that the net energy efficiency 45% but the area of collector surface is smaller than that of PCM surface area. As result of this, low outlet temperature was obtained but it increased the cost of the latent heat storage system.
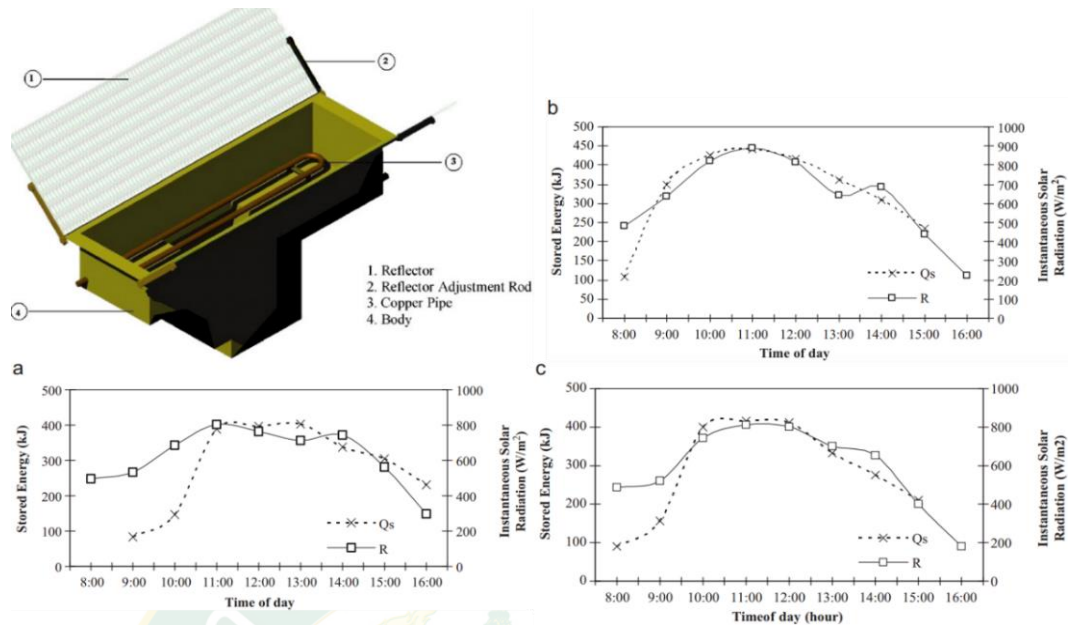
Figure 5 Variations of storage heat with radiation (Koca et al., 2008).

Taheri et al (Taheri et al., 2013) studied the water heater potential to enhance heat transfer by dining the black colored sands immersed into the water storage tank established the main portion of the collector absorber section. Water storage tank was construction from galvanized sheet of 0.0015m in thickness and the volume of 1.45 x 0.56 x 0.17 m^3 with the collected surface absorb 0.67 m^2.
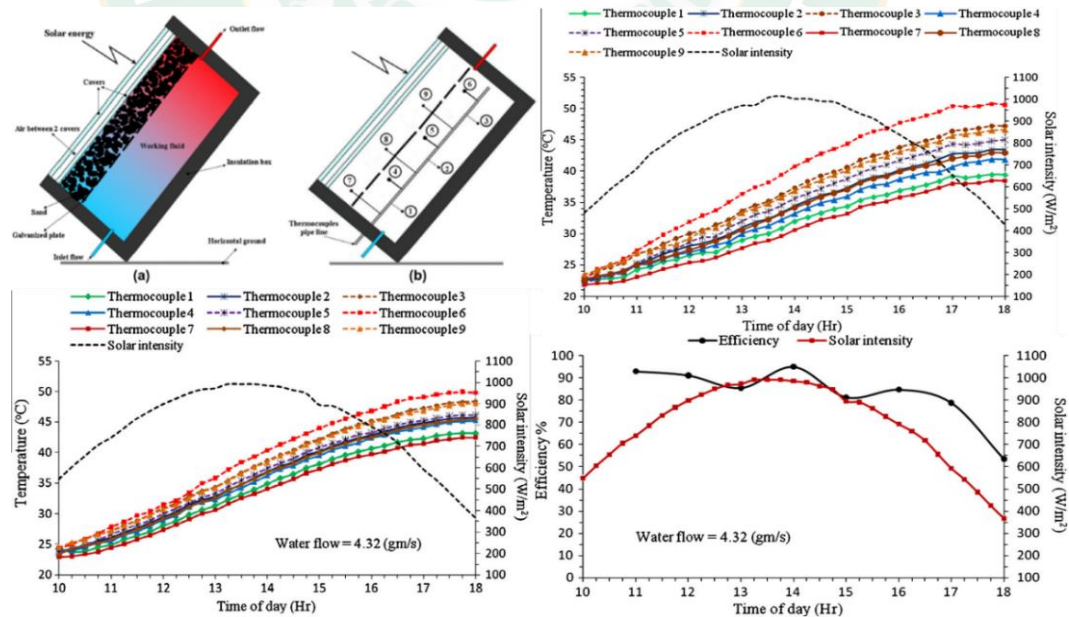
Figure 6 The curves of hourly solar radiation, thermocouple temperatures in natural convection and force convection and collector efficiency (Taheri et al., 2013).

According to figure below, the both hourly Nusselt number and hourly heat transfer coefficient grew continuously, which is forced convection condition showed that the daily average efficiency was obtained about 82.88%, mass flow rate was 4.32 gm/s. it is seen that efficiency of the CSWH system has been increased due to the forced flow operation of the CSWH system. Hussain (Al-Madani, 2006) constructed a cylindrical solar water heater consists of a cylindrical tube glass having a length of 0.8 m and 0.14 m outer diameter with thickness of 6 mm. The copper coil tube in shape of spiral rings within 2 mm and 3.175 mm inner and outer diameter tube and painted black were installed inside glass. The result is showed that the maximum temperature difference of 27.8 °C between inlet and outlet of the mass flow rate 9 kg/h. During the experiemntal perioud was found the maximum efficiency of cylindrical water heater 41.8%.
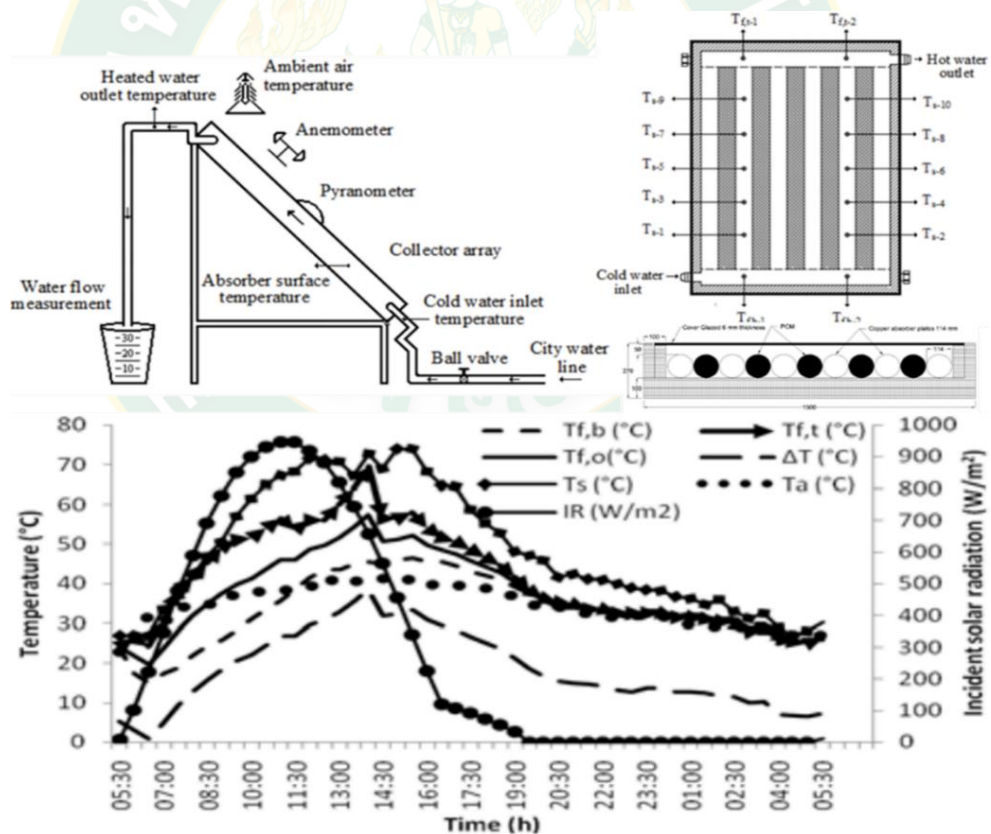
Figure 7 Domestic chromium solar collector with PCM and data experiment stored inside (Koyuncu and Lüle, 2015).

Koyuncu and Lüle (Koyuncu and Lüle, 2015) studied Thermal performance of a domestic chromium solar water collector with phase change material. It constructed

and tested for the thermal efficiency according to EN (European Union Norms) 12975-2. Thermal energy was stored for short term period (from day to night) using paraffin (melting temperature point: 55 °C, melting latent heat: 50 kcal/kg and density: 900 kg/m3) as a phase change material (PCM). Each test was replicated two times. As a result, the thermal efficiency of the collector was obtained as 65% and 59% for first and second test period respectively, while fluid flows as 0.02 kg/s·m^2.

Abdul Jabbar et al (Khalifa et al., 2013) integrated a storage solar collector water heater by using paraffin wax (PCM) as back layer, test and conducted during clear and semi-cloudy in January, February and March the intensity solar radiation 6.22, 6.39 and 6.23 W/m^2, the plate temperature is found to increase up to a distant of 2.5m form water inlet. At hour 14:00 pm, the steady temperature was 50 °C in January, 60 °C in February and 46 °C in March. The efficiency useful energy gains of the system divided by the total solar radiation incident on collector plane, which range 45% - 54%. Consequently, the water continues to receive heat after sunset as the PCM acts as a heat source, the wax PCM temperature was found to greater than the absorber temperature signifying the storage capacity of the PCM.
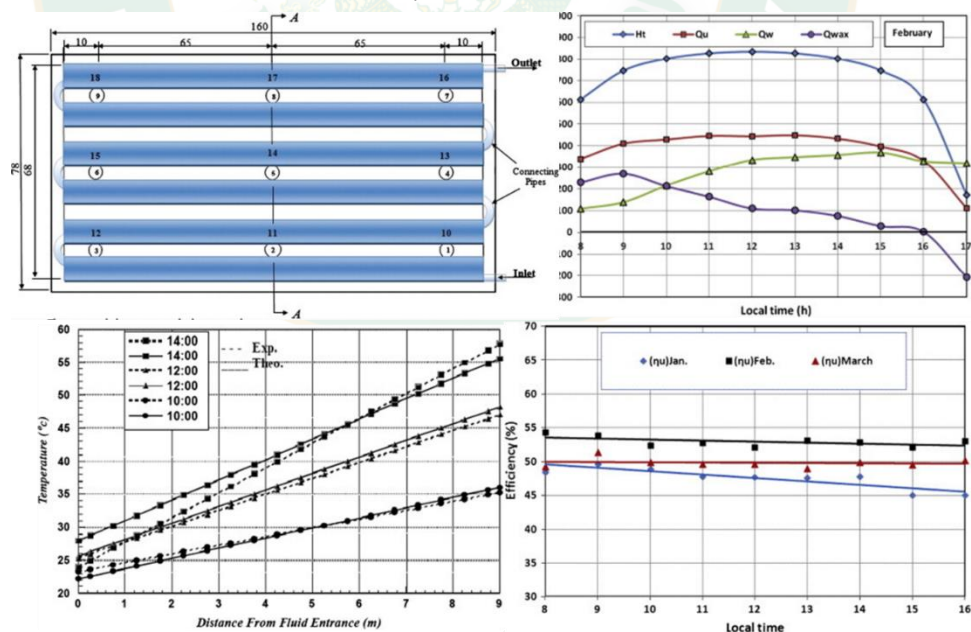
Figure 8 Schematic of solar water heater storage system, variation of solar radiation insolation, Useful energy gain, heat gain of water, heat gain of PCM, Pipe surface temperature and instantaneous efficiency (Khalifa et al., 2013).

The PCM melts and the heat is stored in the melted PCM as a sensible heat. During low and off-sunshine hours, the system cools down and the liquid PCM transfers heat to the circulating water as a useful heat until the PCM solidifies. Consequently, the water continues to get heated after sunset as the PCM acts as heat source. Malvi and Gupta et al (Gupta et al., 2017) experimental investigated of heat removal factor and report the performance of solar collector for various flow configurations and compare evaluation. A sheet and tube type collector where the tube is bonded to the absorber plate by a suitable adhesive, as the result indicated that when the mass flow rate of water is 1, the parallel wall to wall flow is 0.88, respectively. It was also observed that for the case of PCM, F_R is a quantity and its value ranges flow and is proportional to the melting temperature of PCM, but it was observed that in a conventional water heater with parallel wall to wall flow the factor does not increase significantly beyond a mass flow rate of 4 kg/h.
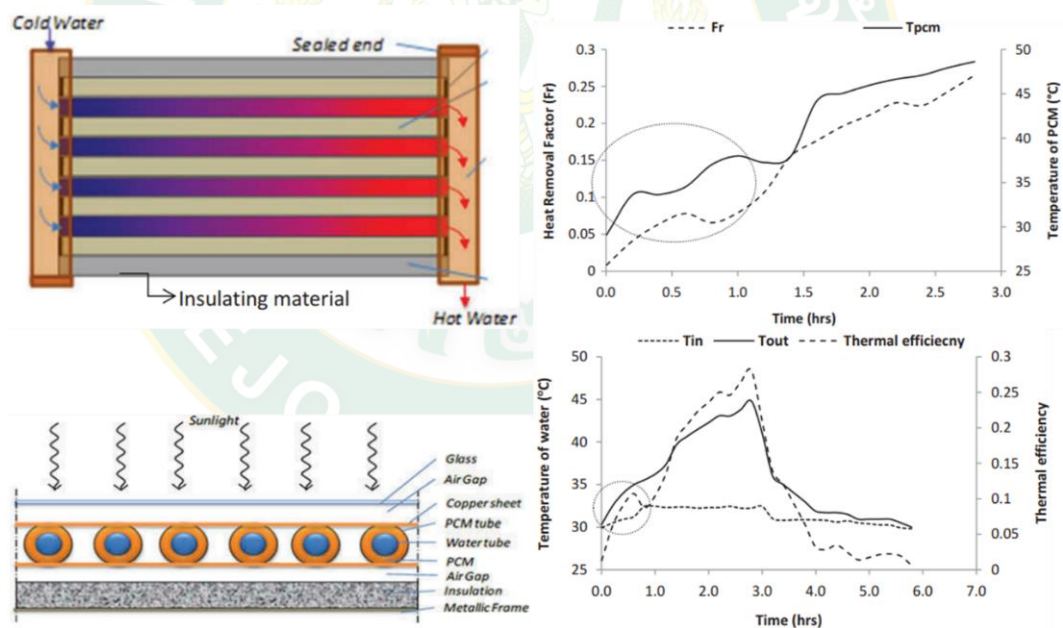
Figure 9 Water flow parallel Channels-schematic plan view, Heat removal factor and temperature profile of water (Gupta et al., 2017).

The heat removal factor F_R function to PCM melting phases rather than mass flow rate. The factor decreases during phase change because in the charging stage the PCM itself absorbs heat. The factor increases during the sensible heat stage of the PCM. Variable values of F_R from 0 to 0.28 are obtained. The effect of the PCM's heat of

fusion is observed in the first hours of charging, which is encircled. Lin, Saw Chun et all (Lin et al., 2012) studied the flat-plate solar collector integrated with phase change materials below the absorber plate as thermal energy storage. The absorber plat was modified by installing extended surfaces into the PCM reservoir to increase the heat transfer area. Their showed that the comparison of flat plate solar collector in different inclination angles 10 to 20° with and without phase change materials can provide promising 38 °C hot water temperature for day time demand with 52 % efficiency.
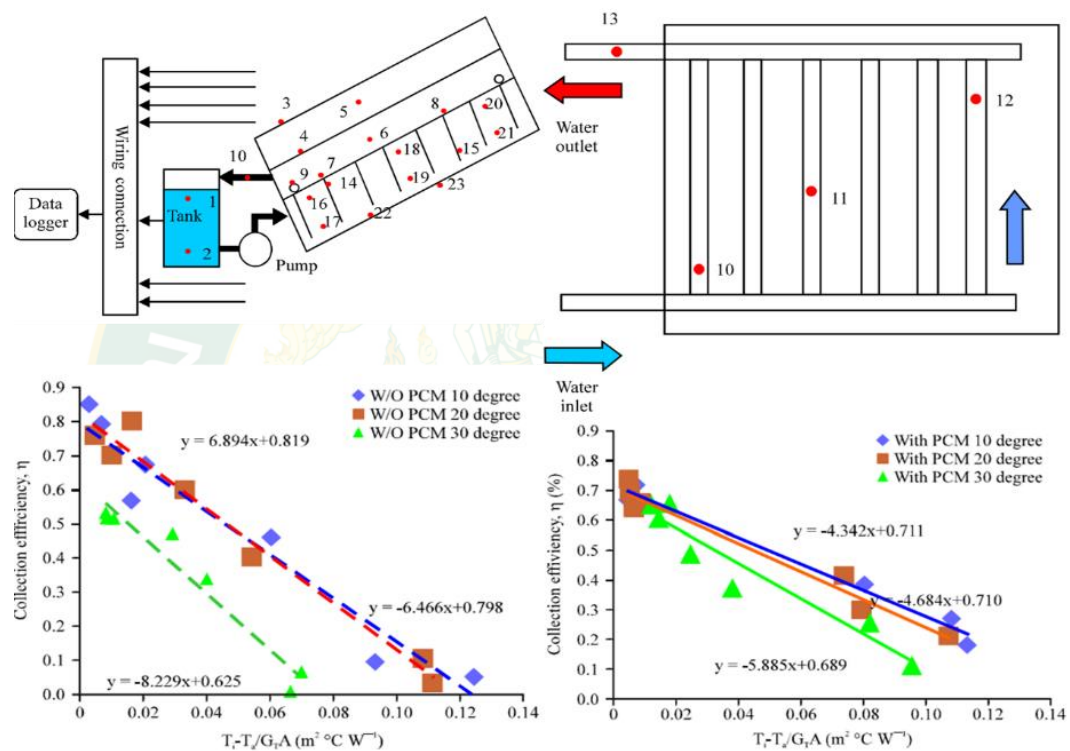
Figure 10 Flat-plate solar collector integrated with PCM and the collection efficient different degree with and without PCM (Lin et al., 2012).

1.2.2. Performance enhancement flat plate solar collector

Generally, the flat-plate solar collector has collected efficiency approximately 40 to 70% while the standard of water mass flow rate is around 1,200 cm^3/m^2.min (Bhowmik and Amin, 2017; Duffie and Beckman, 2013; Gary, 2006; Hollands, 1965; Jafarkazemi and Ahmadifard, 2013; Struckmann, 2008; Zambolin and Del Col, 2010). Many flat-plate typically of solar collector is used in the temperature range not over 60 °C since high temperature will be given high heat loss during operating. Jafarkazemi

et al (Jafarkazemi and Ahmadifard, 2013) studied energetic and energetic evacuation of flat-plate solar collectors. The verification and confirmation of the model based on the experimental data, effect of parameters such as fluid flow rate and temperature, type of working fluid and thickness of the back insulation on the energy and exergy efficiency of the collector has been examined and based on the analysis and comparison. The results showed that energy and exergy efficiencies have conflicting behaviors in many cases. While an increase in fluid inlet temperature leads to a decrease in energy efficiency of collector, it leads to an overall increase in exergy efficiency even to its maximum. While an increase in mass flow rate 0.03, 0.04 and 0.05 kg/s leads to an increase in energy efficiency of the collector. Increasing inlet water temperature and decreasing water mass flow rate can be effective on decreasing these destructions. designing the system with inlet water temperature approximately 40° more than the ambient temperature as well as a lower flow rate may enhance the overall performance.
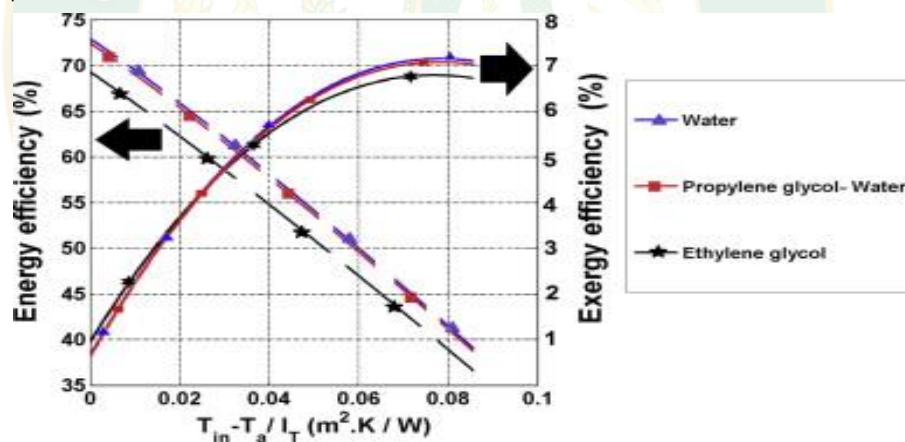
Figure 11 The comparison between the energy and exergy efficiencies of flat plate collector in terms of $(T_i-T_a)/I_T$ (Jafarkazemi and Ahmadifard, 2013).

The flow rate for three different working fluids including water, ethylene glycol, and a mixture of water and propylene glycol with the concentration of 15.6%. As it can be seen, water is the best working fluid. Bhowmik et al (Bhowmik and Amin, 2017) studied the solar reflector used here with the solar collector to increase the reflectivity of the collector. The radiation emitted by the absorber plate of the collector cannot escape through the glass, and the reflector on the other hand used to concentrate the solar heat on the collector surface, thus maximize the collector efficiency. The

collector efficiency is obtained here, without reflector as 51%, and with reflector as 61%. Thus, the overall efficiency of the flat plate solar collector is increased approximately 10% by using the reflector with the collector.
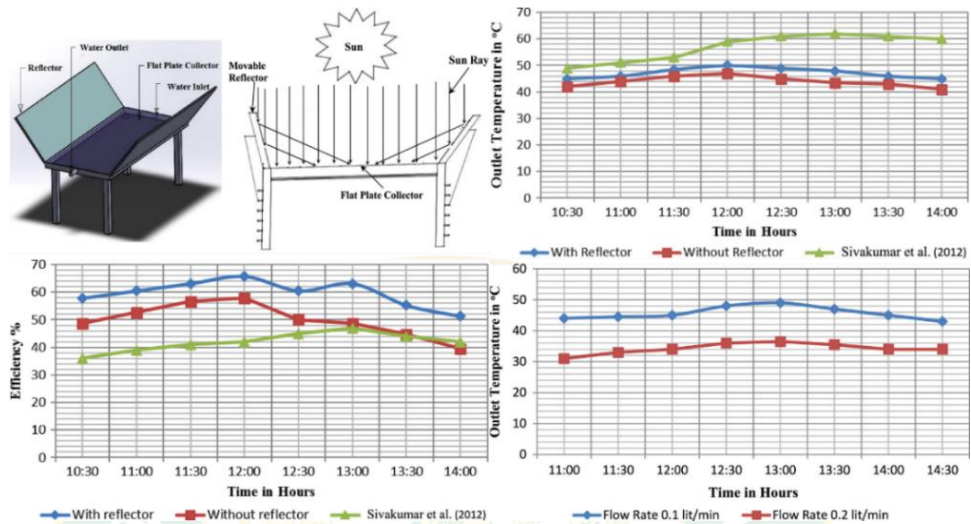
Figure 12 Prototype reflective solar collector, and thermal efficiency with time

(Bhowmik and Amin, 2017).

Balaji et al (Balaji et al., 2017) studied the convective heat transfer by reducing the cross sectional area between the absorbing fluid and inner wall of the tube. The heat transfer enhancers are frictionally engaged with the inner side of the tube wall, and it is kept in the axial flow direction of the fluid flow path. Designing of Eight heat transfer enhancers were arranged parallel to the fluid flow at an angle of 45° to each other from the center of the tube.
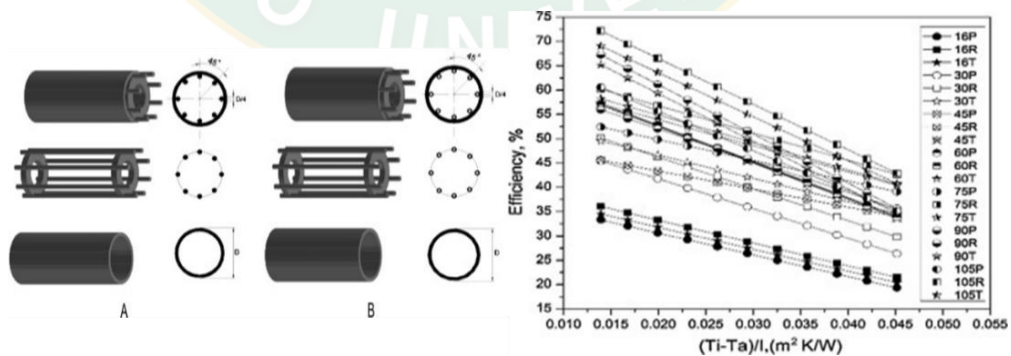
Figure 13 Heat transfer enhancer absorber tube (A) rod heat transfer enhancer, (B) tube heat transfer enhancer and variation of independent parameter with efficiency

(Balaji et al., 2017).

The effect of reduced temperature on the collector instantaneous efficiency for various mass flow rates eat loss from the collector is high when the slope of the efficiency curve is high, and it reduces the convective heat transfer. The higher heat transfer coefficient due to increase in Reynolds number overshadows the efficiency enhancement due to heat transfer enhancer. The rod heat transfer enhancer increases the efficiency by 14% at 0.0125 reduced temperature compared with a plain tube. At the same time, tube heat transfer enhancer achieves about 11%.

From the literature reviews, the conventional solar flat-plate collector was given the average thermal efficiency up to 70% with wildly research such techniques twist-plate and wire-coil with difference ratios inserted into absorber plate of collector, while the phase change material can be stored the thermal energy during its phase change. Using the energy stores of PCM filled in the riser which welded with baffle plate inserted into absorber plate of Flat-Plate solar collector could be effected on thermal performance and convective heat transfer of the novel flat-plate solar collector integrated, providing the suitable outlet temperature and its integrated with phase change material (PCM) inside riser tube to improve thermal performance of the solar collector. The system will be tested in a real environment with various flow rates and following to the ASHRAE Standard, the thermal performance of the novel solar collector compares to the normal collector. the temperature of riser tube, plate surface and others parameters are collected and carried out.

Objective

1. To study the phenomena of different riser tube Phase Change Material inserts novel solar water heater collector integrated.
2. To study the performance of the solar collector system for the whole year.

Benefits

1. Phase change material stores large amount of its latent heat when changing phase from solid to liquid or liquid to solid.
2. Suitable mass flow rate gives high performance of novel solar hot water system.
3. Predict the thermal performance of the solar hot water collector with PCM.

Scopes

1. The absorber plate copper tube of the novel solar hot water is about 28 mm for outside diameter and the thickness of 1.25 mm.
2. The Phase Change Material has a melting point between 38 $^\circ$C to 43 $^\circ$C and is inserted into the absorber tube plate of the solar hot water collector.
3. Comparison experiments of the conventional solar collector and the one integrated with phase change material.
4. The flow rate is varied between 0.01 kg/s·m^2, 0.02 kg/s·m^2 and 0.03 kg/s·m^2 to obtain the optimal performance of the solar water heating system as following as ASHRAE Standard Test.
5.   The tilt angle of the novel solar water heater is the latitude of Chaing Mai province (18°) and the collector is faced to the south.

Chapter 2

Theories

2.1. Solar collector analysis

The thermal analysis of the solar collecting system is very complicated; therefore, some assumptions need to be made in order to simplify the analysis. The theory of first law thermodynamics, law of conservation of energy principle, states that the net change (increase or decrease) in the total energy of the system during a process is equal to the difference between the total energy entering and leaving the system during that process for an open system of control volume is used to predict the thermal performance of a solar collector.

$$\begin{pmatrix} \text{Energy balance at} \\ \text{the solar collector} \\ \text{rate energy in} \end{pmatrix} = \begin{pmatrix} \text{Rate of energy} \\ \text{Out} \end{pmatrix} + \begin{pmatrix} \text{Rate of energy} \\ \text{Accumleted} \end{pmatrix} \qquad \text{Eq. 1}$$

converted to heat energy which results in higher temperature of a working fluid and attributes to heat loss at the back of the collector.
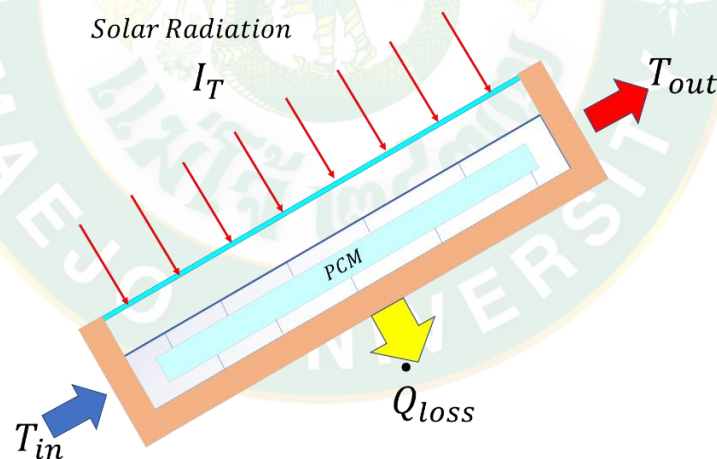
Figure 14 Energy balance of solar in storage.

2.1.1. The overall heat loss coefficient of solar water heater

The overall loss coefficient of the solar collector in the mathematic analysis was considered the thermal network for a single glass cover of the system in **Figure 15**. At some typical location on the absorber plate. The absorbed energy is distributed to thermal losses through the top, the bottom and the useful energy gain.
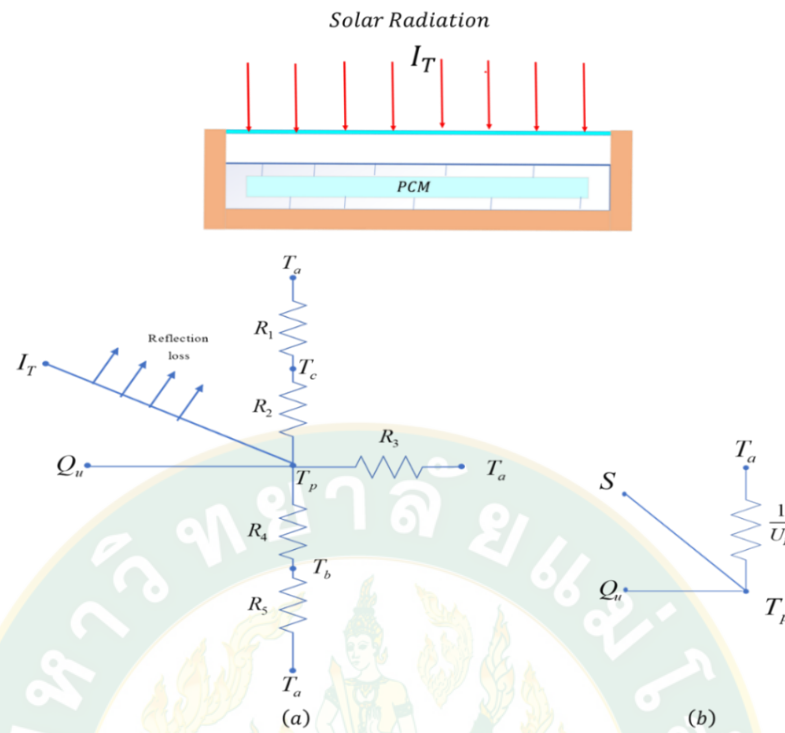
Figure 15 (a) Thermal network of solar storage collector, (b). Equivalent network.

The thermal energy loss through the top is the result of convention and radiation between plates. In the steady-state energy transfer between the plate and the cover glazed equal to the energy lost the surrounding from the top cover. The loss through the top per unite area in then equal to the heat transfer from the absorber plate to the glass cover is given as (Duffie and Beckman, 2013). The design or modelling purposes these energy exchanges are usually described in terms of a top surface heat loss coefficient U_t, which combines both the radiative and convective heat transfer processes. A more empirically based technique to estimate U_t was first proposed by Hottel and Woertz (1942) (Duffie and Beckman, 2013), who produced a semi-empirical equation for U_t. The top lost cam be calculated by:

$$U_t = \left(\frac{n}{\frac{C}{T_{pm}}\left[\frac{(T_{pm}-T_a)}{(n+f)}\right]^e} + \frac{1}{h_w} \right)^{-1} + \frac{\sigma(T_{pm}+T_a)(T_{pm}^2+T_a^2)}{\frac{1}{\varepsilon_p + 0.00591 n h_w} + \frac{2n+f-1+0.133\varepsilon_p}{\varepsilon_g} - n}$$

Eq. 2

Where

$$f = (1+0.089h_w - 0.1166h_w\varepsilon_p)(1+0.07866n)$$

Eq. 3

Factor in Eq. 2.

$$C = 520\left(1 - 0.000051\beta^2\right) \tag{Eq. 4}$$

The emissive power, base of natural logarithm

$$e = 0.430\left(1 - \frac{100}{T_{pm}}\right) \tag{Eq. 5}$$

The efficiency collecting factor (F') of the solar collector can be given as:

$$F' = \frac{U_L^{-1}}{w\left[\dfrac{1}{U_L(D + w_d F)} + \dfrac{1}{C_b} + \dfrac{1}{\pi D_i h_i}\right]} \tag{Eq. 6}$$

The efficiency collecting factor to the standard fin efficiency was calculated as:

$$F = \frac{Tanh\left[m(w-D)/2\right]}{m(w-D)/2} \tag{Eq. 7}$$

$$m = \sqrt{\frac{U_L}{\delta k}} \tag{Eq. 8}$$

The heat removal factor of the solar collector could be calculated as:

$$F_R = \frac{\dot{m}c_p}{A_c U_L}\left[1 - \exp\left(\frac{A_c U_L F'}{\dot{m}c_p}\right)\right] \tag{Eq. 9}$$

2.1.2. Solar collector analysis of the thermal performance

The solar water heater collector without phase change material will be given the characteristics of the collector.
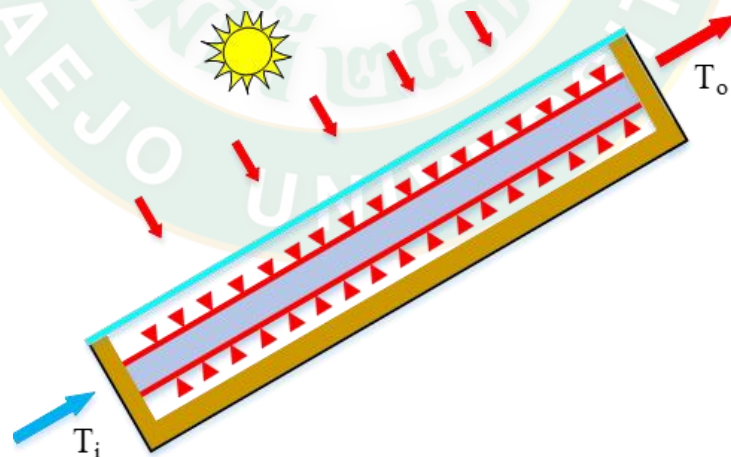
Figure 16 Solar collector generated thermal energy from solar radiation.

The thermal efficient of collector is (Bliss, 1959; Duffie and Beckman, 2013; Polvongsri, 2013). The general of the energy collected by solar collector relates to the mass flow rate $\dot{m}$ through to the collector, the water temperature different between inlet and outlet (T_o-T_i) and the specific heat of water C_p was given as Eq. 13:

$$\dot{Q} = \dot{m}C_p\left(T_o - T_i\right) \qquad\qquad \text{Eq. 10}$$

The thermal efficiency of solar collector is defined as the ratio between the heat gain from working fluid and the total incident solar radiation on the absorber plate area of solar collector were given as Eq. 11 and Eq. 12:

$$\eta = \frac{\dot{m}c_p\left(T_o - T_i\right)}{I_T A_C} \qquad\qquad \text{Eq. 11}$$

$$\eta = F_R\left(\tau\alpha\right)_e - F_R U_L \frac{\left(T_i - T_a\right)}{I_T} \qquad\qquad \text{Eq. 12}$$

The thermal efficiency test is presented at near normal incidence conditions therefore, that F_R is constant of maximum efficient, F_R and U_L are constant within the range of temperature. The linear will result when the efficiency is obtained from averaged data plated against $(T_a\text{-}T_i)/I_T$ according to Eq. 12. The intersection of the vertical line of efficiency axis is equal to $F_R(\tau\alpha)_e$ at this axis the temperature of working fluid that entered the collector near ambient temperature means that the collector efficient is nearly maximum. So, the slope of the linear line is equal to $F_R U_L$ shows that the way energy has lost from the solar collector. At the intersection of the line with the horizontal axis collector efficiency is zero and this point normally calls the stagnation, usually occurs when no fluid flows in the collector.
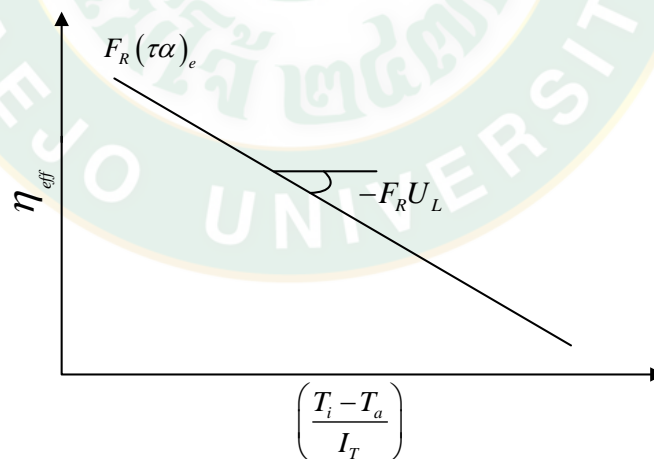
Figure 17 The thermal efficiency curve.

The temperature of PCM varied to the phase change by the relation of enthalpy as shown in of the enthalpy method change with temperature, which have three states can be calculated enthalpy as following (Khalifa and Abdul Jabbar, 2010; Khalifa et al., 2013; Koyuncu and Lüle, 2015; Taheri et al., 2013):
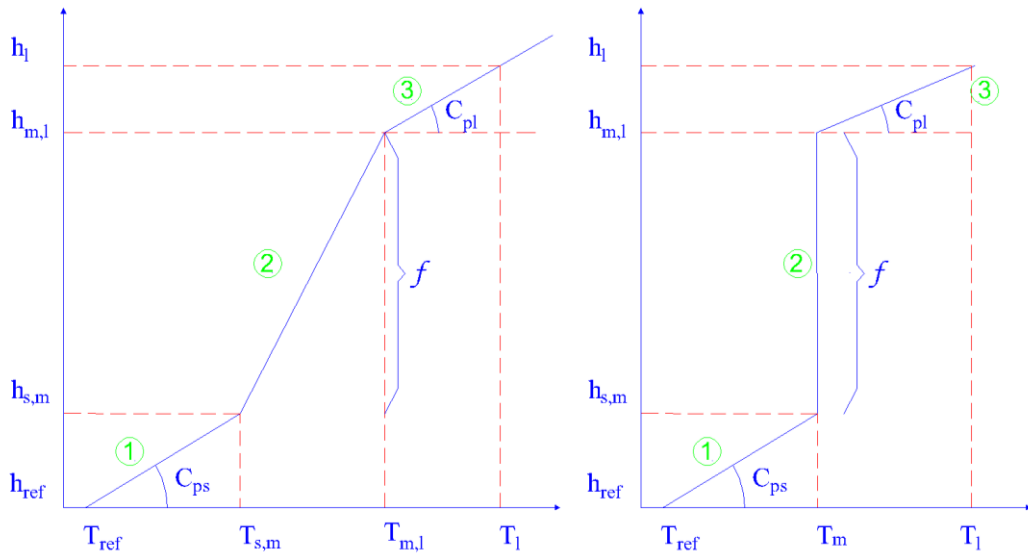
Figure 18 Isothermal and non-isothermal of phase change material.

State 1 as: In the solid phase of PCM which enthalpy varies temperature between T_{ref} and $T_{s,m}$

State 2 as: In melting period of PCM which enthalpy varies temperature between $T_{s,m}$ and $T_{m,l}$

Stage 3 as: In liquid phase of PCM which enthalpy varies temperature between T_l and $T_{m,l}$

$$\begin{cases} h = c_{ps}\left(T - T_{ref}\right) \\ h = c_{ps}\left(T_{s,m} - T_{ref}\right) + \dfrac{T - T_{s,m}}{T_{m,l} - T_{s,m}} \times f \quad where, \begin{bmatrix} T < T_m \\ T_{s,m} < T < T_{l,m} \\ T > T_m \end{bmatrix} \\ h = c_{ps}\left(T_{s,m} - T_{ref}\right) + f + c_{pl}\left(T - T_{m,l}\right) \end{cases} \qquad \text{Eq. 13}$$

The heat transfer coefficient of fluid to the surface outside the cylindrical capsule was evaluated from the following empirical correlation. The correlation was developed for forced convection of fluid flowing across bundles of tubes:

$$Nu = 0.8\,\mathrm{Re}^{0.4}\,\mathrm{Pr}^{0.36} \qquad \text{Eq. 14}$$

The Reynolds number, Re for the water was based on the capsule diameter.

From Eq. 1, Eq. 10, Eq. 11, Eq. 12 and Eq. 13 the thermal efficiency of the novel solar collector with the thermal energy stores of the phase change material could be calculated as:

$$\eta_{coll+PCM} = \frac{\dot{m}C_{P,water}\left(T_o - T_i\right) + M_{PCM}C_{p,PCM}\left(\dfrac{dT}{dt}\right)}{I_T A_C}$$ Eq. 15

2.1.3. Heat transfer analysis of the solar collector

The solar collector was collected and absorbed the solar radiation intensity of the sun which its converts into thermal energy, while the flowing fluid inside the system was collected those heat during operation. The energy collected (Q_{coll}) of the circulating fluid inner the absorber tube from the inner surface of absorber plate (A_i) which gave the actual heat flux (q''), its was given as :

$$q'' = \frac{Q_{coll}}{A_i}$$ Eq. 16

Where the collected energy was calculated following to the Eq. 10, the mean temperature of the flowing fluid (T_w) and the absorber temperature (T_T) which gave the convection heat transfer coefficient of the solar collector calculated as:

$$h_i = \frac{q''}{T_T - T_w}$$ Eq. 17

The convection heat transfer coefficient of water flowing in the solar water heater collector tube (h_i) will be calculated by:

$$h_i = \frac{N_u k}{L}$$ Eq. 18

Where the k is thermal conductivity of the copper tube, L is the thickness of the copper tube.

The Reynolds number is dimensionless quantity of the flow regime depends mainly on the ratio of inertial forces to viscous forces in the fluid. It is expressed for internal flow of circular pipe as:

$$\text{Re} = \frac{4\dot{m}}{\mu \pi D}$$ Eq. 19

The Prandtl number is dimensionless quality

$$\text{Pr} = \frac{C_p \mu}{k}$$ Eq. 20

It turns out that the transition from laminar to turbulent flow also depends on the degree of disturbance of the flow. Under most practical conditions, the flow in a circular pipe is laminar and transitional.

Table 2 Practical conditions of the Reynold number (Cengel and Cimbala, 2013).

$Re \leq 2300$	Laminar flow
$Re \geq 2300$	Turbulent flow

The novel solar collector integrated with phase change material was studied and found the thermal collected of the convective heat transfer coefficient which could give the correlation of convective heat transfer as the Nusselt Number form as following Eq. 21:

$$Nu = a\,\mathrm{Re}^b\,\mathrm{Pr}^c \qquad \text{Eq. 21}$$
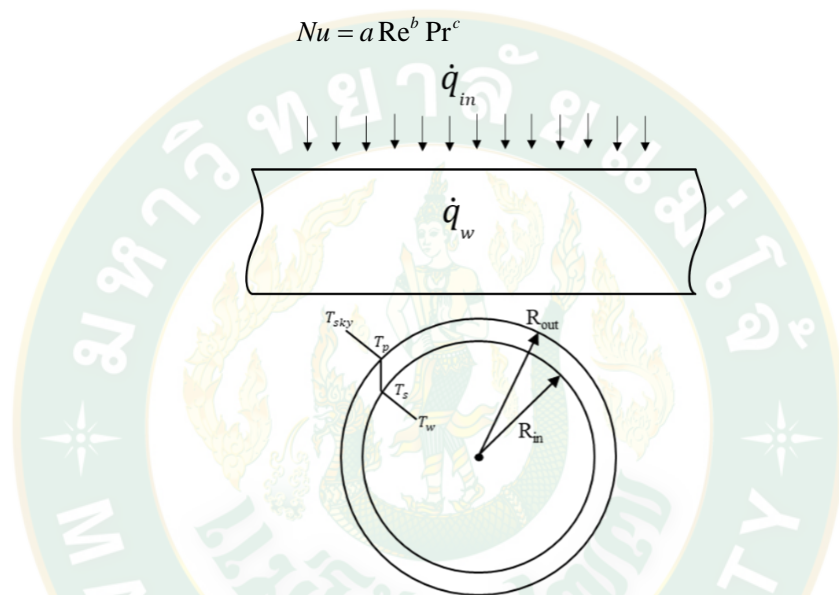
Figure 19 The heat generates from outside to inside with constant heat flux.

2.1.4. The prediction of the solar radiation intensity

The solar energy is an abundant and a reliable renewable resource that is sustainable and can be used for centuries to heat water and continues to be an option for heating and producing electric today. Almost all of the Earth's energy input comes from the sun which is generally considered to produce a constant amount of power with a surface intensity of 6.33×10^7 W/m^2. Not all of the solar energy that reaches the Earth's atmosphere by Earth which is due to the Earth's energy budget. This budget accounts for the fact some of the energy incident on the outer atmosphere of the planet is immediately reflected back inti space. The reflection by the atmosphere, clouds, and Earth's surface. In Thailand, the maximum solar radiation level during April-May of which the value is in a range of 20-24 MJ/m^2. The maximum radiation in the

northern region and some part in the central zone about 19-20 MJ/m^2 with the average daily radiation is around 18.2 MJ/m^2 (Ministry of Energy, 2019). The solar radiation is depending declination angle between the sun angular position with respect to the equator plane could be given as (Duffie and Beckman, 2013):

$$\delta = 23.45\sin\left[360\left(\frac{284+n}{365}\right)\right] \qquad \text{Eq. 22}$$

The total daily solar radiation

$$H_o = 24\frac{3600}{\pi}I_{sc}\left[1+0.033\cos\left(\frac{360n}{365}\right)\right]\left[\begin{array}{c}\cos(\phi)\cos(\delta)\sin(\omega_s)\\+\frac{2\pi\omega_s}{360}\sin(\phi)\sin(\delta)\end{array}\right] \qquad \text{Eq. 23}$$

For Thailand, daily diffuse radiation (H_d) could estimate from the global solar radiation (H) as:

$$\frac{H_d}{H} = -4.6408+26.5495\left(\frac{H}{H_o}\right)-28.3422\left(\frac{H}{H_o}\right)^2-31.4546\left(\frac{H}{H_o}\right)^3+46.4421\left(\frac{H}{H_o}\right)^4 \qquad \text{Eq. 24}$$

Where the H is daily global solar radiation on horizontal plane is given in **Table 3**:

The hourly diffuse radiation (I_d) could be calculated from:

$$I_d = H_d\frac{\pi}{24}\left[\frac{\cos(\omega)-\cos(\omega_s)}{\sin(\omega_s)-\left(\frac{2\pi\omega_s}{360}\right)\cos(\omega_s)}\right] \qquad \text{Eq. 25}$$

The solar radiation on the horizontal plane, (I_b)

$$\frac{I}{H} = \frac{\pi}{24}\left(a+b\cos(\omega)\right)\left[\frac{\cos(\omega)-\cos(\omega_s)}{\sin(\omega_s)-\left(\frac{2\pi\omega_s}{360}\right)\cos(\omega_s)}\right] \qquad \text{Eq. 26}$$

Where a_1, a_1, b_1 and b_2 are constants are given for Chaing Mai province, Thailand: 0.514, 0.228, 0.512 and 0.514:

$$\begin{aligned}a &= a_1+a_2\sin(\omega_s-60)\\b &= b_1+b_2\sin(\omega_s-60)\end{aligned} \qquad \text{Eq. 27}$$

The total solar radiation on the tilt surface can be calculated as:

$$I_T = I_b.R_b+I_d\frac{1+\cos(\beta)}{2}+I.\rho_g\frac{1-\cos(\beta)}{2} \qquad \text{Eq. 28}$$

Table 3 Average of the month and daily solar radiation (Weather, 2019).

Average day of the month	

Month	Date	Date of the year	Daily solar radiation, H (MJ/m^2 day)
January	17	17	17.25
February	16	47	19.28
March	16	75	21.04
April	15	105	20.62
May	15	135	19.08
June	11	162	16.35
July	17	198	15.79
August	16	228	17.73
September	15	256	17.78
October	15	288	16.14
November	14	318	15.71
December	10	344	18.02

The daily efficiency of Active solar water heater which system had pump to drive water through the collector, in the collector was converted solar energy into thermal exchange to working fluid inside then go to the storage tank while the daily efficient of the system could be calculated as:

$$\eta_{daily} = \sum \frac{Q_S}{I_T A_C \Delta t}$$ Eq. 29

Chapter 3

Experiment set-up

The novel solar collector is built in a single copper tube as absorber plate tube 28.7 mm, 1 mm thickness and 1,000 mm long inserted with riser copper. On the copper tube is welded with copper plate for increasing aperture surface absorber of collector with Ordinary black colored was painted to absorb maximum heat from solar radiation while its working. In the riser tube was filled with RT42 Phase Change Material (PCM) by its melting is contented of latent heat energy stores and semi-circle of copper to increase the heat transfer of working fluid and PCM in daytime operation as showed in **Figure 20**.

Figure 20 The novel and conventional solar collector (PCM1,PCM2 and without PCM) installed.

The length of PCM riser is equal to the absorber copper tube which is different riser PCM diameter of the novel solar collector is tested in the same condition to find out the thermal performance of each systems. The properties of PCM were showed in **Table 1** with the volume expansion 12.5% which was filled in the riser tube in each side of diameters. The specific of riser PCM is showed in **Figure 21**.
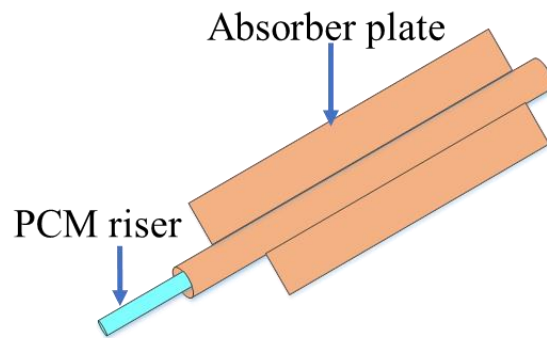
Figure 21 The novel solar collector frame, copper plate and riser PCM.

Table 4 The characteristic of solar collector integrated with PCM 1, PCM 2 and without PCM.

Category	Diameter	Unit	Inside
PCM 1	Ø 16	mm	RT 42
PCM 2	Ø 10	mm	RT 42
Without PCM	-	-	-

On the back and side of the solar collector were used aroflex foam rubber insulation thickness 25 mm to maximize heat retention. On top of the solar collector is a single glazed has 3 mm thickness and frame of the collector is made of aluminum.
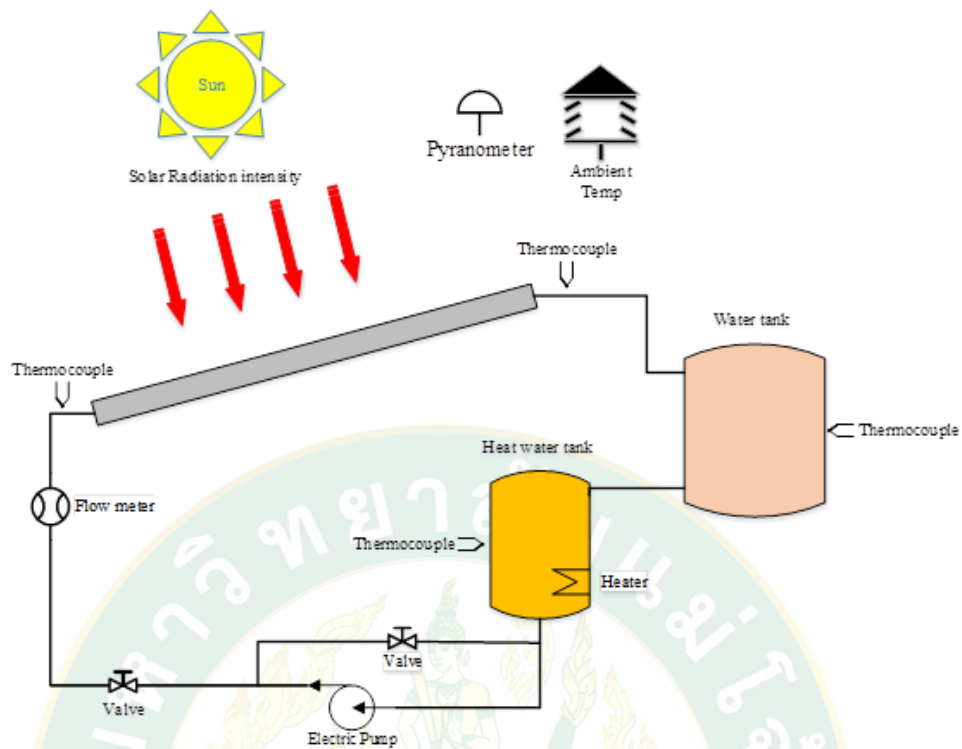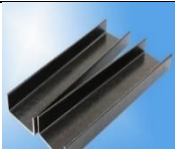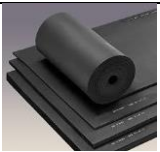
Figure 22 The experimental set-up of the novel solar water heater system.

On the cover glass was put a pyranometer is radiometer used to measure the global total solar radiation incident upon a surface per unite time per unite area which is pyranometer type apogee to record the beam radiation from the sun. The electric pumping is driving force the water flow inside the system while mass flow rate crosses in the system is regulated by the gauge valve and reading by flow meter and Bypass system was also installed to protect the pump from overload by over pressure. The complete se-up can be demonstrated in **Figure 22**.

Table 5 Equipment with its specification for installing and testing.

N°	Equipment	Photos	Specifications
1	Glazed cover		Thickness 3 mm Glass Emittance
2	Copper plate and tube		The copper plate to extend aperture area. The copper tube 28 mm and Riser PCM 16 and 10 mm k=thermal conductivity 385 W/m·°C

N°	Equipment	Photos	Specifications
3	Aluminum frame		-
4	Insulation aroflex		Aroflex insulation density 40 t0 70 kg/m^3 installed in edge and back of collector. Thickness 25 mm to minimize heat loss thermal conductivity
5	Flow control valve Green pipe PPR		Glove valve used to regulate flow circulated in the system and bypass when it's over pressure. The diameter 20 mm of green pipe connected in system.
6	Water flow meter		The flow meter measures flow rate from 4.5 to 15 L/h with accuracy ±2 %.
7	Driving water pump		Used to driving fluid circulated in the solar collector system with maximum flow rate 800 L/h.
8	Thermocouple wire type K		Measuring range from -200 °C to 1350 °C with accuracy ±0.5 °C.
9	Data logger 4 channels TM-1947SD		Used to record data experiment with accuracy ±0.4 %. + 1 °C with thermocouple type K

N°	Equipment	Photos	Specifications
10	Pyranometer Apogee (USA)		Measures global horizontal or plan of array irradiation range 0-350 mV. Accuracy ±5 %.
11	Data logger Adam 5000 TCP		The data logger Adam has accuracy ±5 % and operating temperature 10 – 70 °C.
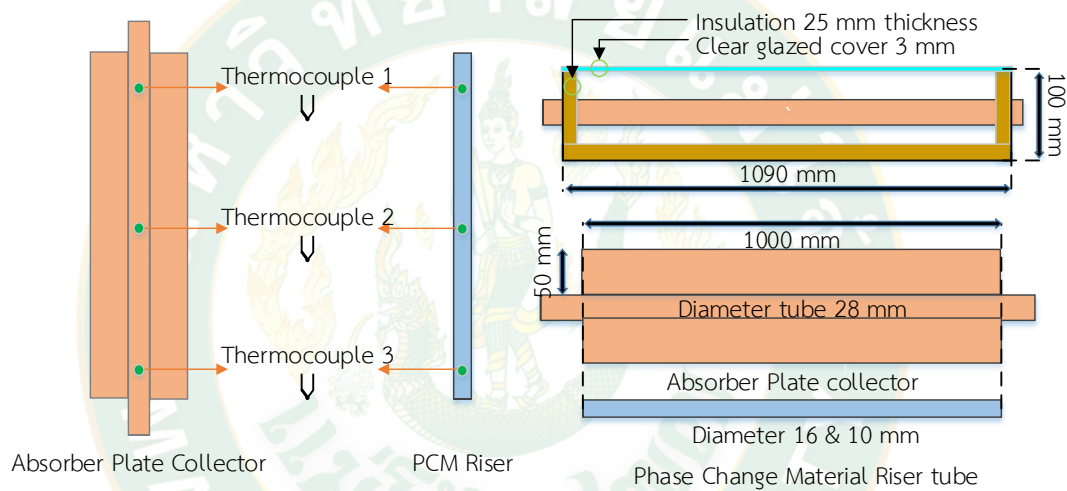
Figure 23 The dimension of the novel solar collector.

In piping system has control temperature of the inlet water temperature and outlet water temperature of the system and then all data was recorded in the same time. Water temperature in the system is measured by thermocouples type K record temperature data logger TM-1947SD and Ex 9018. The storage tank obtains the water for circulating in the system test. It is constructed as a metal material and cover by the insulation. The insulation was installed to minimize the heat loss as convective and conductive heat to the environment. The electric heater was used to regulate the water for experimental testing and the water temperature in the tank, there are three points of measuring in the tank. top, middle, and bottom by the thermocouple type K are installed to measure for analyzing the performance. The temperature data of the tank is given the amount of hot water will provide to the stationary.
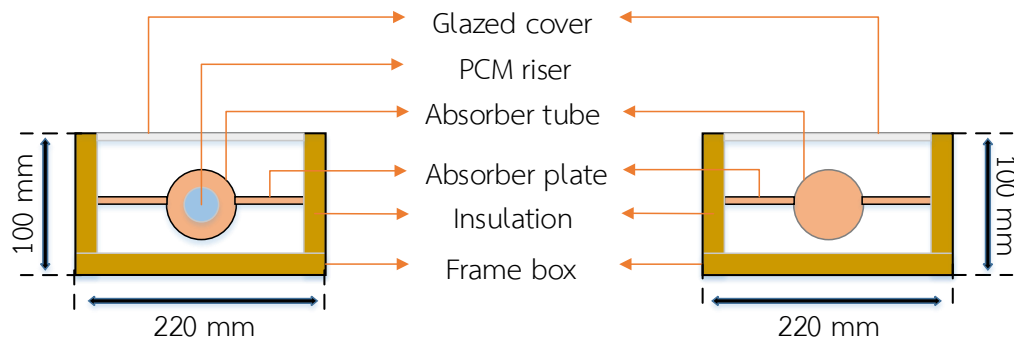
Figure 24 Section view of the novel solar hot water system.

3.1.   Experiment procedure

The solar collector system is constructed to do the experimental test which conducting with a single tube to find out the primary parameter to analytical with the mathematic for the big system that distributes and follows to the ASHRAE standard test (Polvongsri, 2013). Many standard tests were used to predict and analysis on the solar water heating collector performance as like as ASHRAE Standard, European. Even though, those standards are similarities ways, giving the specifics condition for testing as such as wind velocity, solar radiation intensity, mass flow rate, accuracy of equipment, ambient temperature, inlet and outlet temperature. The different between those standard are the mathematical analysis on the solar collector test with graphic cure. Moreover, the standard tests are giving the efficiencies of each test were collected the temperature, flow rate test, radiation.

In this novel solar water heating collector is following to the ASHRAE Standard test that is provides as followed below:

- The Ashrae standard was given the average flow rate 0.02 kg/s·m^2 that given the maximum heat collected form the radiation of the daytime,
- The experiment condition test when the clear sky following to the ambient collected data test.
- In this standard test is given the maintain steady-state or quasi-steady-state conditions with an incident solar flux of greater than 790 W/m^2 while the solar collector tile angle is faced to the south in 18° latitude of Chaing Mai, Thailand.

The collector is used pump to driving force the water inside system flowing with measuring the water temperature inlet and outlet. In this study is going to test in different water temperatures started from lowest in 35 °C to 65 °C the highest and detail in **Table 6** and **Table 7**.

Table 6 The novel collector tests temperature radiation (Polvongsri, 2013).

Temperature Test	35	40	45	50	55	60	65
Time	The data collected in each interval time in 5 minutes						
Radiation	Started when radiation higher than 790 W/m^2						

Table 7 Steady condition of the ASHRAE 93-2003 outdoor test (Polvongsri, 2013).

Variable	Maximum variation		Lower limit	Upper limit	
	In between data periods	Within data periods			
Total irradiation normal to sun	-	±32 W/m^2 (± 10 Btu/ft^2.h)	790 W/m^2	-	-
Fraction of diffuse radiation	-	-	-	20%	-
Incident angle modifier	-	±2%	-	-	-
Ambient Temperature	Range < 30 °C	± 1.5 °C	-	-	-
Wind	-	-	2.2 m/s	4.5 m/s	-
Flow rate	0.02 kg/s.m^2	± 0.005 gpm	-	-	-
Inlet Temperature	-	± Max of (0.1 °C, 2%)	-	-	-
Incident angle	-	± 2.5 °	-	-	-
Symmetry to solar noon	-	-	-	-	-

The steady state conditions of the ASHRAE Standard 93-2003 describes test methods for steady-state or quasi-steady-state thermal performance with time response and angular tests. The purpose of performing the tests under steady state conditions is to avoid transient influences during the test that could inflate the "measured" performance of a collector. Several of the variable have extremely tight tolerances on variability. It makes the test in both difficult and time consuming.

The test period is defined as the time over which steady state condition are maintained for a single measured efficiency point. The test period as defined in the standard consists of the pre-data period and the data period defined as below **Figure 25**:

Test period		
In general:	Pre-data period	Pre-data period
Outdoor test:	15 min	Max (5 min, τ)
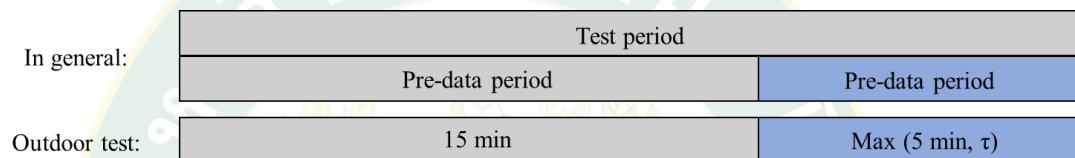
Figure 25 Test and pre-data periods for thermal efficiency of solar collector

(τ =constant time) (Polvongsri, 2013).

The novel and conventional solar collector were tested as following to the ASHRAE standard 93-2003 was showed the process below **Figure 26** of the solar collected parameter data related:
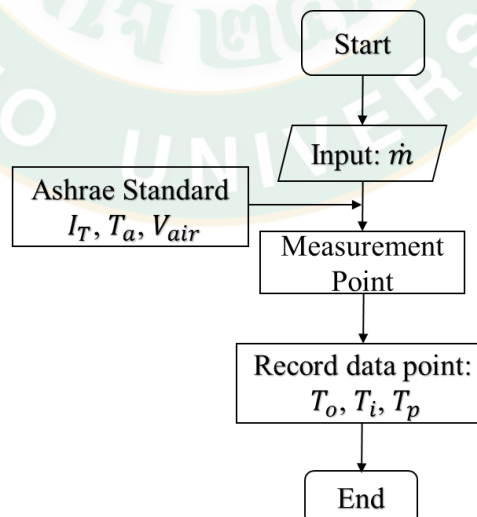
Figure 26 The solar collector tests process.

Start

Input:
$\dot{m}, C_p, T_o, T_i, T_a, A_c, I_T$

Calculate : $Q_{coll}, \eta_{coll}, (T_o - T_i), \frac{(T_i - T_a)}{I_T}$

Following Equation:

$$Q_{coll+PCM} = \dot{m}C_p(T_o - T_i) + (MC_P)_{PCM}\left(\frac{dT}{dt}\right)$$

$$Q_{coll+PCM} = A_c[F_R(\tau\alpha)_e I_T - F_R U_L(T_i - T_a)]$$

$$\eta_{coll} = \frac{Q_{coll+PCM}}{I_T A_c}$$

$$\eta_{coll} = F_R(\tau\alpha)_e - F_R U_L\left(\frac{T_i - T_a}{I_T}\right)$$

Plot :
Q_{coll} with T_i
$(T_o - T_i)$ with T_i
Linear regression :
η_{coll} with $\frac{(T_i - T_a)}{I_T}$

Output:
$F_R(\tau\alpha)_e, F_R U_L$

End
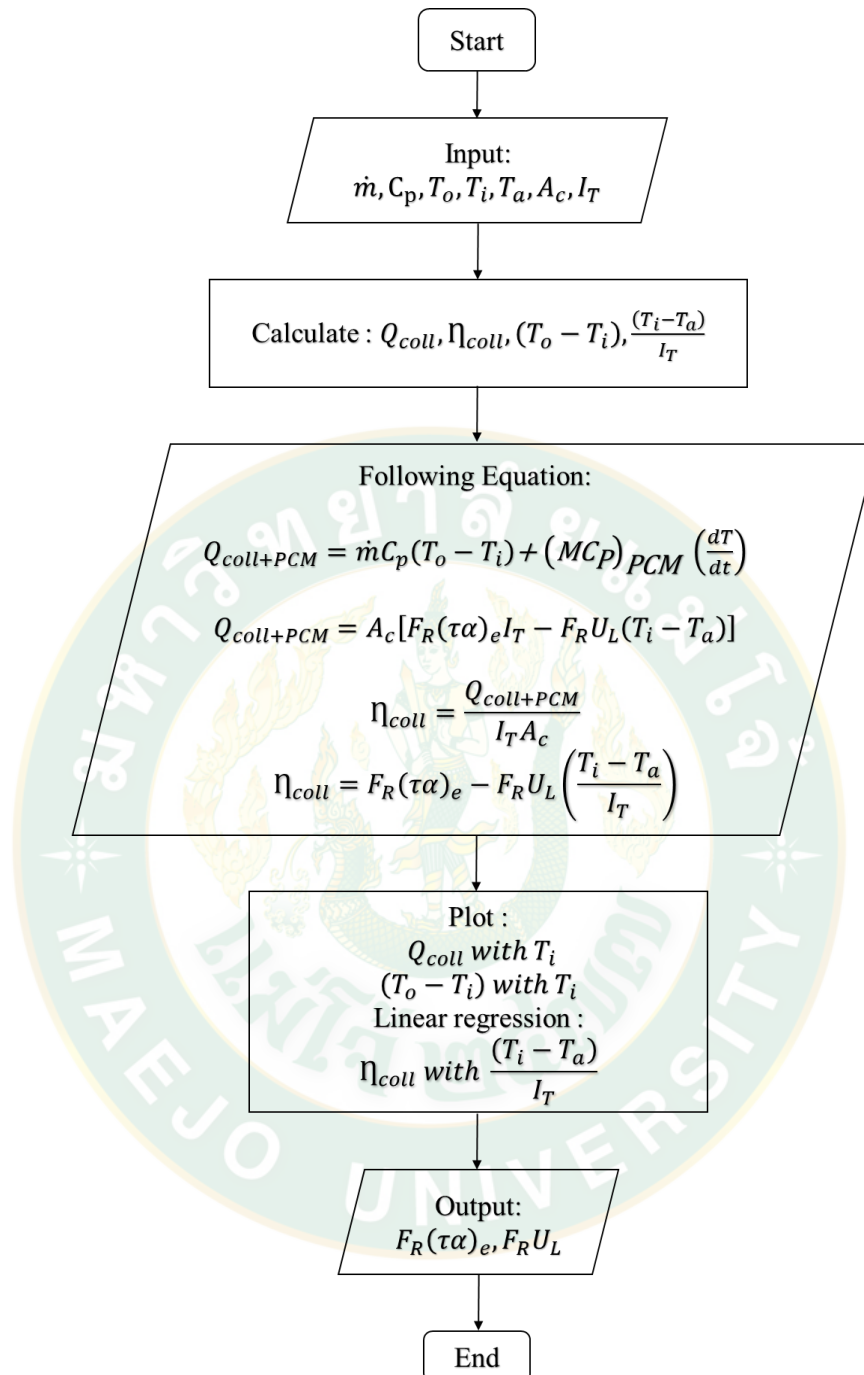
Figure 27 The analysis process of the solar collector.
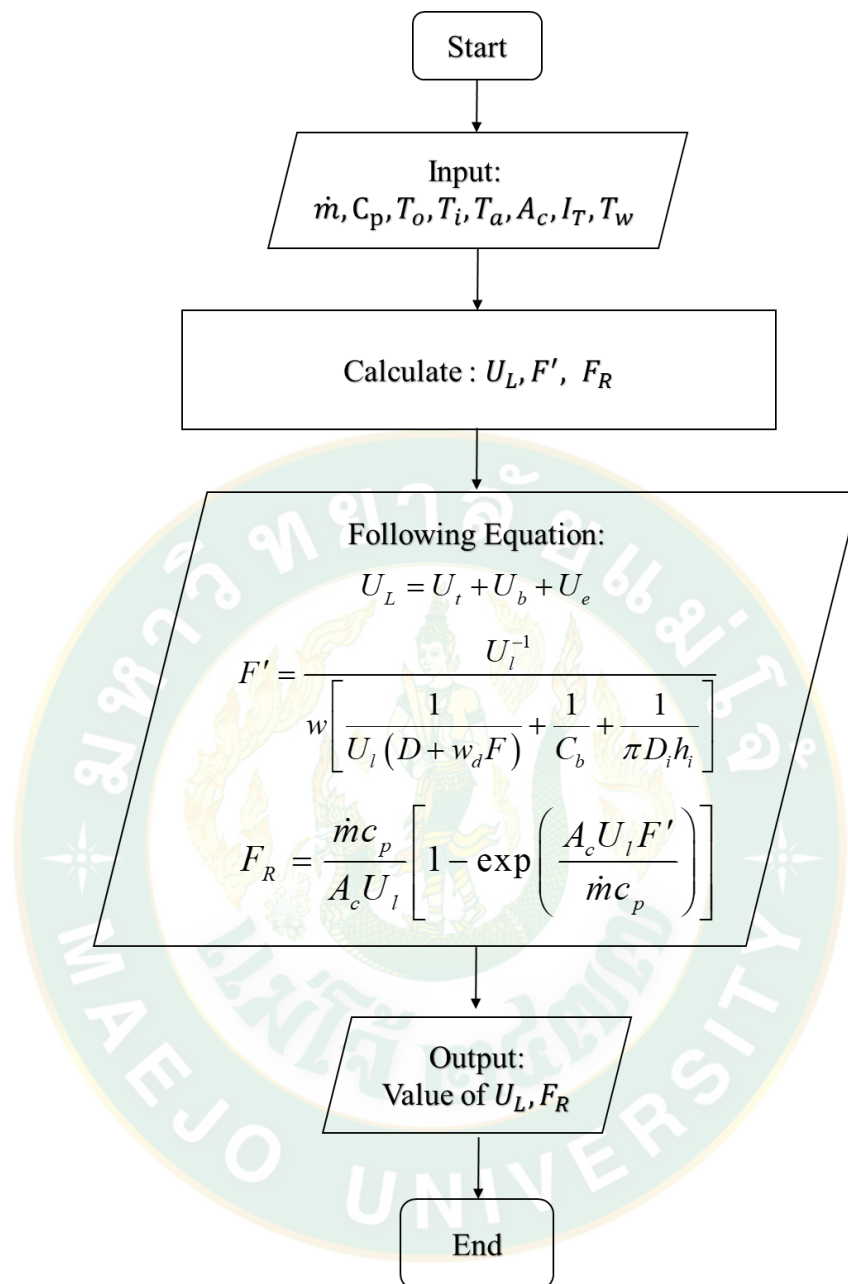
Figure 28 The calculation process of overall heat loss (U_L),

collected efficiency of fin (F') and heat removal factor (F_R).

```
          ┌─────────┐
          │  Start  │
          └─────────┘
               │
               ▼
    ╱─────────────────────────────────────╲
   ╱              Input:                    ╲
  ╱  ṁ, Cₚ, Tₒ, Tᵢ, Tₐ, A_c, A_in, I_T, T_w, T_av ╲
 ╱─────────────────────────────────────────╲
               │
               ▼
  ┌─────────────────────────────────────┐
  │     Calculate : Q_coll, q", hᵢ       │
  └─────────────────────────────────────┘
               │
               ▼
 ╱───────────────────────────────────────────╲
╱          Following Equation:                 ╲
│                                              │
│       Q_coll = ṁCₚ(Tₒ − Tᵢ)                  │
│                                              │
│              q" = Q_coll/A_in                │
│                                              │
│          hᵢ = q"/(T_w − T_av)                │
╲──────────────────────────────────────────────╱
               │
               ▼
       ╱─────────────────╲
      ╱     Output:       ╲
     ╱     Value of        ╲
    ╱    Q_coll, q", hᵢ     ╲
   ╱─────────────────────────╲
               │
               ▼
          ┌─────────┐
          │   End   │
          └─────────┘
```

$$Q_{coll} = \dot{m}C_p(T_o - T_i)$$
$$q'' = \frac{Q_{coll}}{A_{in}}$$
$$h_i = \frac{q''}{(T_w - T_{av})}$$
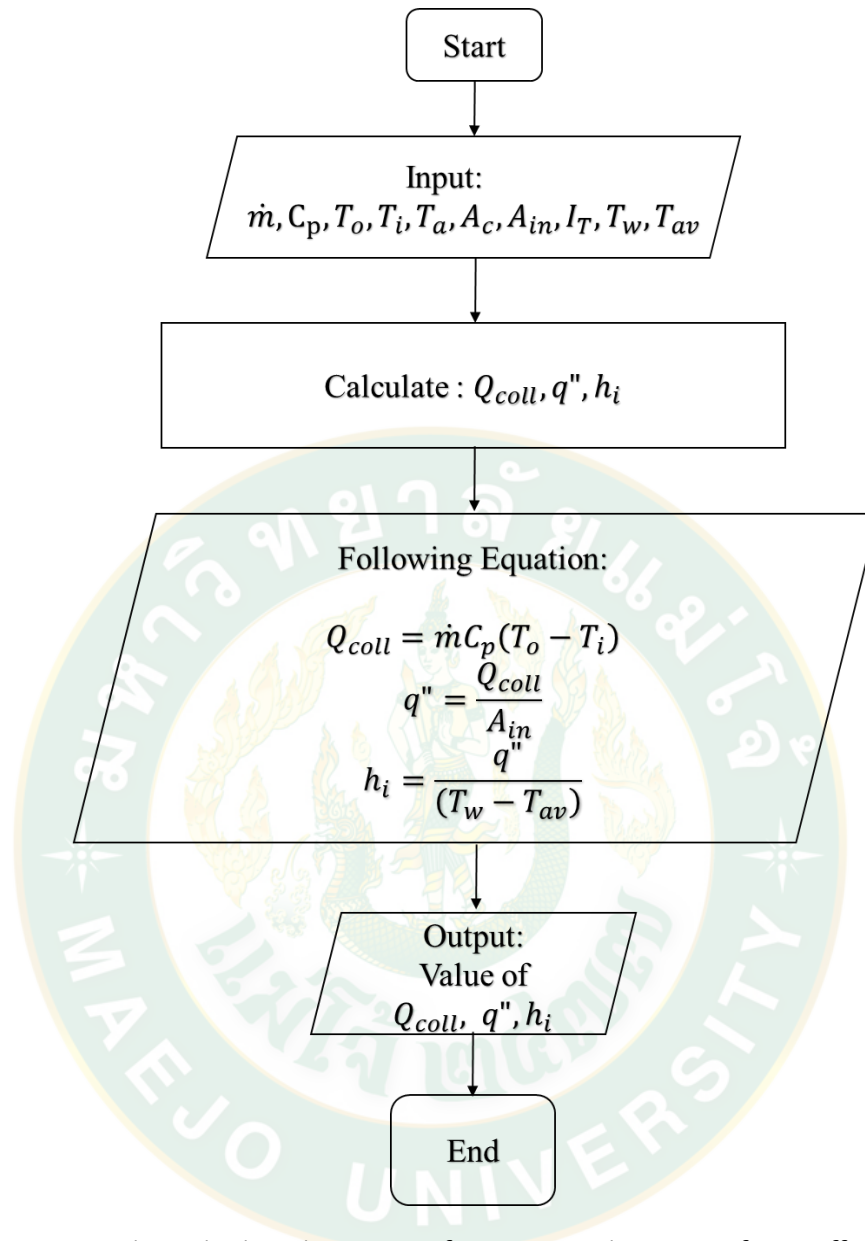
Figure 29 The calculated process of convective heat transfer coefficient (hi).

The heat removal factor was calculated following to the **Figure 28** and the heat transfer coefficient of each solar collector was calculated following to the **Figure 29**.

3.1.1. The various diameters of riser tube Phase Change Material inserts in collector with thermocouple points and predicted over the year

The experimental test in different diameter of riser the copper tube inserts in copper absorber tube of the solar water heater collector for experimental test. The

riser PCM is picked in three points to measure the temperature which is to study about the phenomena of the PCM when collector operating. The various diameters are d_1 and d_2 with 9 and 16 mm and thickness 1 mm.
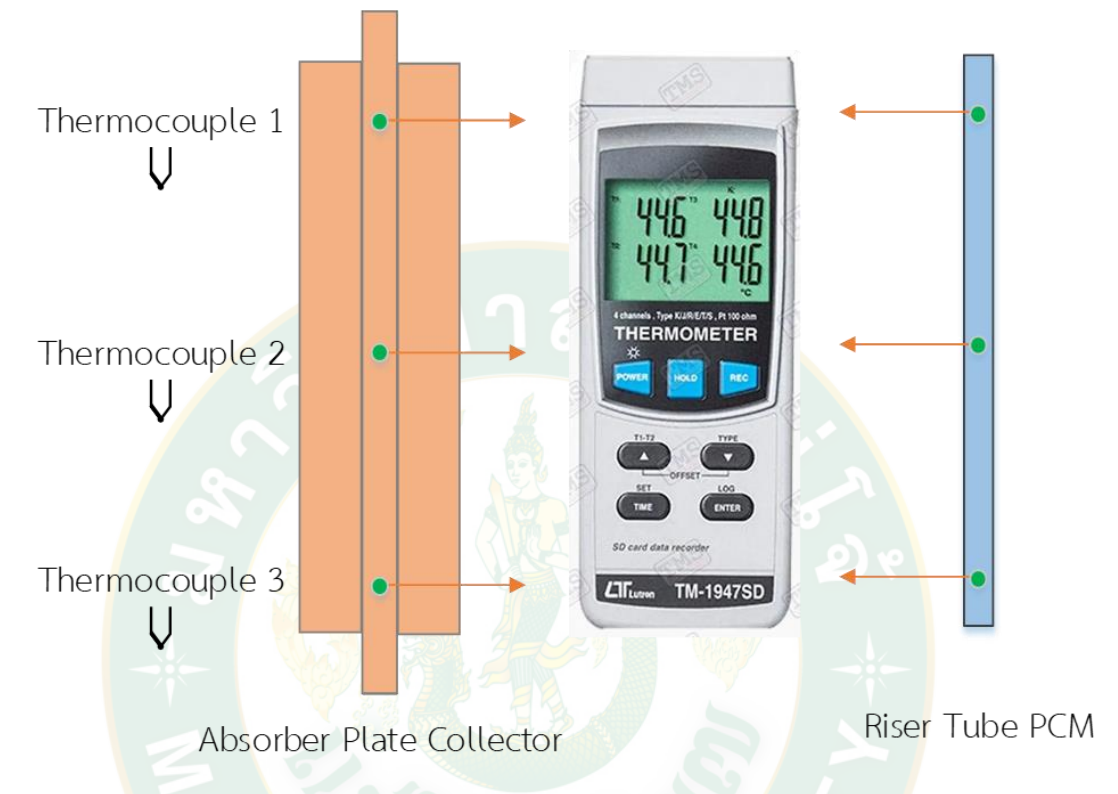
Figure 30 The riser tube phase change material with thermocouple.

The novel solar collectors were predicted the energy storage (Q_s) and daily efficiency (η_s) in a whole year which using the predicted equation of solar intensity and ambient temperature of Chiang Mai, Thailand and following to processing calculation showed in **Figure 31**.
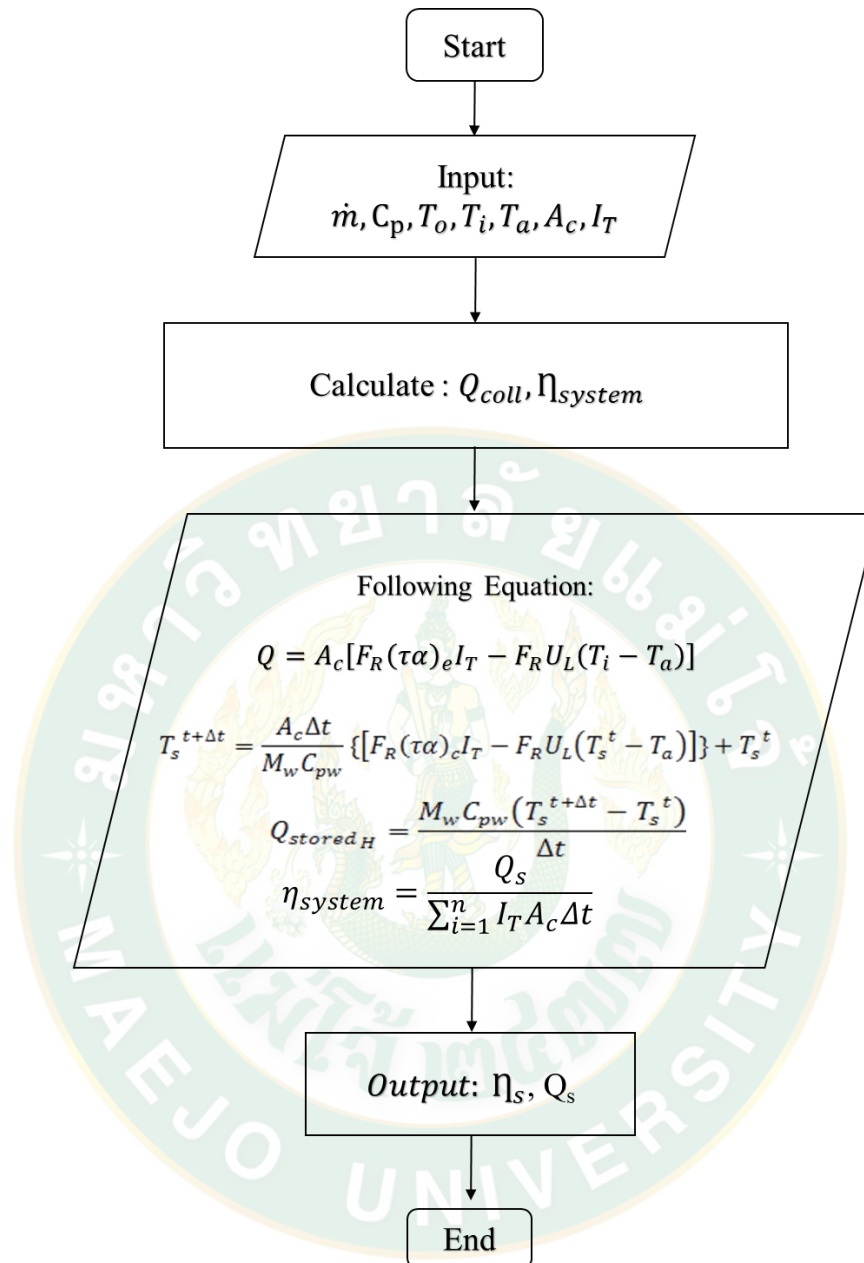
Figure 31 The prediction of energy stores in water tank (Q_s) and daily efficiency (η_s).

Chapter 4
Result and discussion

The novel solar collector integrated with phase change material riser was tested to determine the thermal performance following to ASHRAE STANDARD 93-2003. According to the test condition as ruling when testing, the novel solar collector was divided into two collectors which inserted different phase change materials riser diameter as 10 mm and 16 mm filled with RT42 PCM (a melting point 38-42 $^{\circ}$C). Even though, the ASHRAE Standard mass flow rate 0.02 kg/s·m^2 was used on experiment of thermal efficiency and full day experiment was tested to qualify the thermal efficiency, while, the various mass flow rate 0.01, 0.02 and 0.03 kg/s·m^2 were tested as following the similar condition test which were showed the performance of different mass flow rate, indeed, was found the best water flow rate with daily experiment also tested. The convection heat transfers coefficient (hi) of the novel solar collector integrated was calculated as following to the Nusselt number correlation (Nu).

4.1. The thermal performance of novel solar water heater integrated using ASHRAE standard 93-2003 condition and mass flow rate 0.02 kg/s·m^2

The experiment was conducted in outdoor experiment following ASHRAE standard 93-2003 where the water mass flow rate each collector is equal to 0.02 kg/s·m^2 and the inlet water temperature is controlled by the electric heater at 35 $^{\circ}$C, 40 $^{\circ}$C, 45 $^{\circ}$C, 50 $^{\circ}$C, 55 $^{\circ}$C, 60 $^{\circ}$C, and 65 $^{\circ}$C, respectively. The solar radiation, ambient temperature, inlet water temperature, outlet water temperature, and hot water temperature in a storage tank were collected during the day at School of Renewable Energy, Chiangmai, Thailand. From the experiment, it was showed that the inlet water temperature increases, with the increasing of heat loss from the collector. The thermal performance of the novel solar collector with PCM riser provided higher values than the conventional flat plate solar collector. The novel solar collector with PCM in 10 mm diameter riser (PCM2) gave the highest $F_R(\tau\alpha)_e$ and F_RU_L of 0.828 and 11.30 W/m^2·K following by 16 mm diameter riser (PCM1), the $F_R(\tau\alpha)_e$ and F_RU_L of 0.808 and 10.93

$W/m^2 \cdot K$ and the conventional solar collector gave the $F_R(\tau\alpha)_e$ and $F_R U_L$ of 0.713 and 10.642 $W/m^2 \cdot K$.

For solar collector performance analysis of the presenting the useful heat gains due to the inlet water temperature variation. Both of heat gains from the novel solar collectors integrated with PCM (PCM 1and PCM 2) showed that were higher than the collector without PCM at the mass flow rate of 0.02 $kg/s \cdot m^2$. The PCM 2 with riser of 10 mm diameter was given higher heat gain than the PCM 1 with riser of 16 mm diameters which effecting on the energy stored in the phase change material that filled in the riser. Due to the useful heat gains of collector was influence with the temperature, therefore, the heat gains at the low inlet water temperature had less overall heat loss into environment while the high inlet temperature would give a slightly increase amount losing thermal energy. In the **Figure 33** shows the thermal efficiency of the novel and conventional solar collectors were analyzed following the ASHRAE standard 93-2003. The linear equations of both collectors PCM2 and PCM1 could identify of the better system performance than the conventional solar collector without PCM. The range of inlet temperature, ambient temperature and solar radiation were given the relation of $(T_i-T_a)/I_T$ at X-axis, its value changed cause of the variation of inlet temperature during testing with steady state condition while the intersection on Y-axis presented the thermal efficiency $F_R(\tau\alpha)_e$. According to Eq. 12, if the relation $(T_i-T_a)/I_T$ was slightly different, the collected thermal energy was closely to the maximum energy input as solar radiation. On the opposite, when the relation of $(T_i-T_a)/I_T$ had grown up, the energy loss would increase cause of the ambient temperature variation that showed as the slope of the linear equation or $F_R U_L$. The results showed that $(T_i-T_a)/I_T$ was varied from 0.01-0.05 $°C \cdot m^2/W$. Both the novel solar collectors integrated with PCM were performed that PCM 1 and PCM 2 provided the $F_R(\tau\alpha)_e$ of 0.808, 0.828 and $F_R U_L$ was 10.93, 11.34 $W/m^{2 \cdot °}C$, respectively while the solar collector without PCM got 0.713, and 10.64 $W/m^{2 \cdot °}C$ as shown as in **Table 8** with all case studies had the correlation on coefficient over than 0.98.
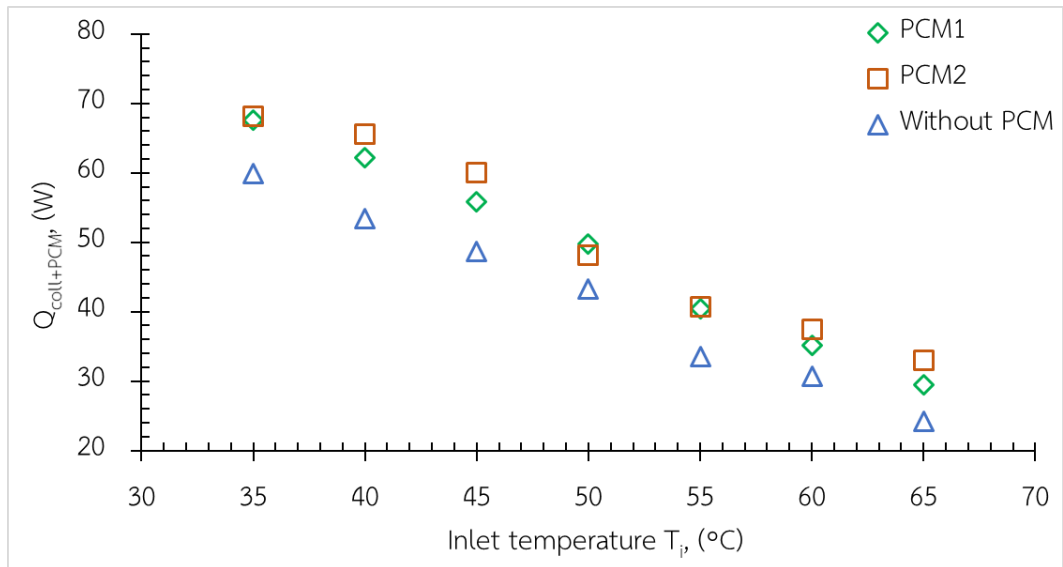
Figure 32 The heat gains of novel and conventional solar collector.
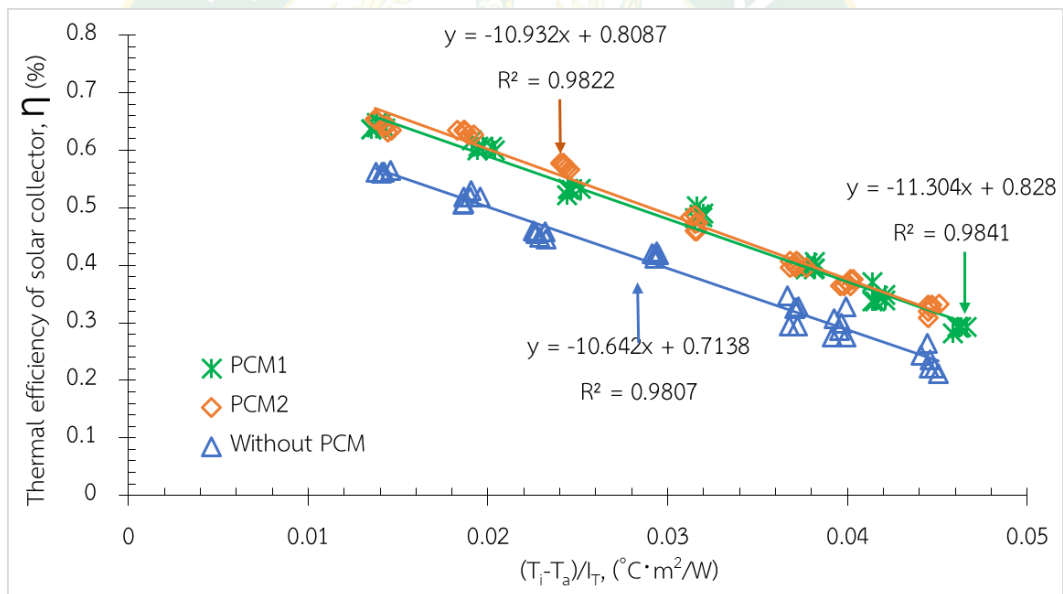
Figure 33 The thermal efficiency of novel and conventional solar collector with Ashrae standard 93-2003 mass flow rate 0.02 kg/s·m^2 with term of PCM energy store.

Table 8 The values of $F_R(\tau\alpha)_e$ and F_RU_L for the novel solar collectors (PCM1 and PCM2) comparing to the conventional solar collector (Without PCM).

The standard test mass flow rate 0.02 kg/s.m^2			
Category	$F_R(\tau\alpha)_e$	F_RU_L	R^2
PCM 1	0.808	10.932	0.982
PCM 2	0.828	11.304	0.984
Without PCM	0.713	10.642	0.981

In the **Figure 34** was showed the heat removal factor of the novel and conventional solar collector (F_R). The changing of the inlet temperature was effected to the collected energy could presents as removal factor characteristic while the inlet temperature from 35 to the 65 $^{\circ}$C were tested on novel collector (PCM1, PCM2) and conventional. Using the data thermal analysis of the thermal performance in **Table 8**, its each factors were showed that the novel solar collector PCM1 was given high value which is 0.86 to 0.78 following to the set inlet temperature, the novel collector PCM is 0.83 to 0.67 while the conventional solar collector was given 0.82 to 0.58.
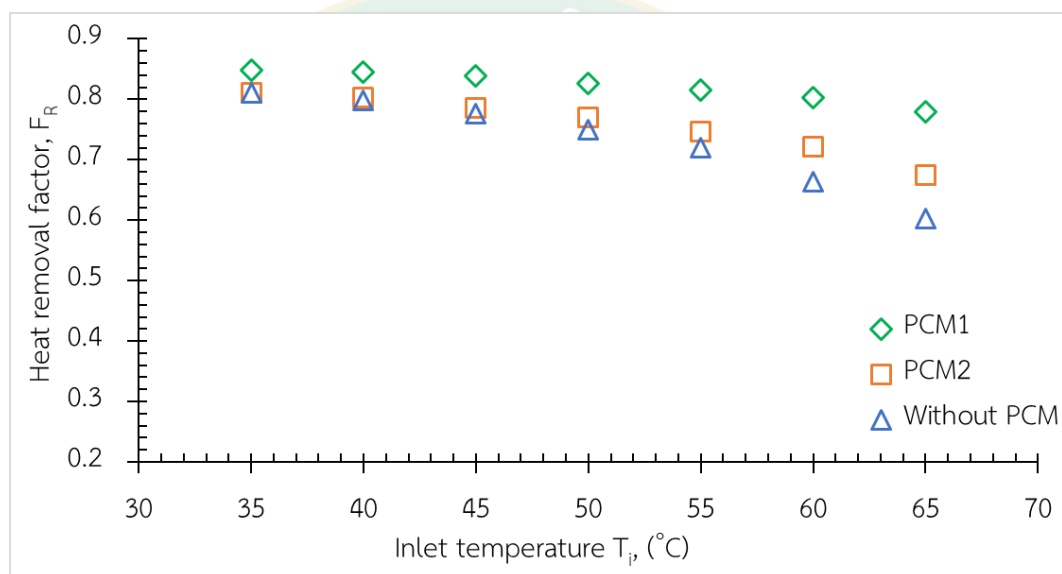
Figure 34 The heat removal factor of the novel and conventional solar collector.

4.2. The effect of mass flow rate to the thermal efficiency of the novel solar collector integrated with phase change material and conventional

The solar energy is clean, environmentally renewable energy and can be used in both electricity and heat functional. In part of heat production, commonly used a solar collector that can integrate with many techniques are offered the highest thermal performance which one method is to use the phase change material (PCM). The goal of this research is to study the thermal performance of solar collector with and without phase change material (PCM) riser. The various water mass flow rates per collector area were observed at 0.01, 0.02 and 0.03 kg/s·m^2, respectively. The novel solar collectors were installed for thermal performance testing following ASHRAE standard 93-2003 comparing with the solar collector without PCM riser. The experiment results show

that both of the novel solar collectors were given the thermal performance greater than the solar collector without PCM riser. The novel solar collector that integrates with phase change material riser of 16 mm diameter (PCM1) at 0.03 kg/s·m^2 demonstrated the best of $F_R(\tau\alpha)_e$ and F_RU_L of 0.835 and 9.681 (W/m^2·K) following by the mass flow rate of 0.02 kg/s·m^2 and 0.01 kg/s·m^2, respectively. For the novel solar collector integrated with phase change materials riser of 10 mm diameter (PCM2) gave the $F_R(\tau\alpha)_e$ and F_RU_L of 0.828 and 11.304 (W/m^2·K) at 0.02 kg/s·m^2 following by the results of mass flow rate 0.03 kg/s·m^2 and 0.01 kg/s·m^2, respectively.

4.2.1. Thermal performance of novel solar collector integrated with phase change material riser 16 mm outside diameter (PCM1)

The novel solar collector integrated with RT42 (melting point 38 to 43 $^\circ$C) phase change material riser 16 mm outside diameter (PCM1) was studied effected mass flow rate from 0.01 to 0.03 kg/s·m^2. on thermal performance. The experimental tested following to Ashrae standard 93-2003 (Polvongsri, 2013) and inlet temperature various from 35, 40, 45, 50, 55, 60, 65 $^\circ$C, respectively. In the **Figure 35**, **Figure 36** and **Figure 37** was showed the temperature different (T_o-T_i) was changed to the mass flow rate, while the low mass flow rate was given the low (T_o-T_i) and energy gains $Q_{coll+PCM}$ opposite to high mass flow rate. However, the inlet temperature is also effected to the temperature different and thermal energy gains while operating, when testing with low inlet temperature (T_i), the solar collector was collected a lot more of heat gains $Q_{coll+PCM}$ and high temperature different (T_o-T_i), neither, the high inlet temperature (T_i) was collected low heat gains $Q_{coll+PCM}$ and low temperature different (T_o-T_i). The flow rate 0.03 kg/s·m^2 was showed the temperature different (T_o-T_i) from 4.9 to 2.6 $^\circ$C while the heat gains from solar radiation $Q_{coll+PCM}$ was 78.9 to 44.84 W, the flow rate 0.02 kg/s·m^2 gives heat gains Q_{coll} was 67.60 to 29.5 W and (T_o-T_i) was 6.1 to 2.4 $^\circ$C while the flow rate 0.01 kg/s·m^2 gives heat gains $Q_{coll+PCM}$ was 71.8 to 31.23 W and (T_o-T_i) was 10.1 to 4.2 $^\circ$C, respectively.
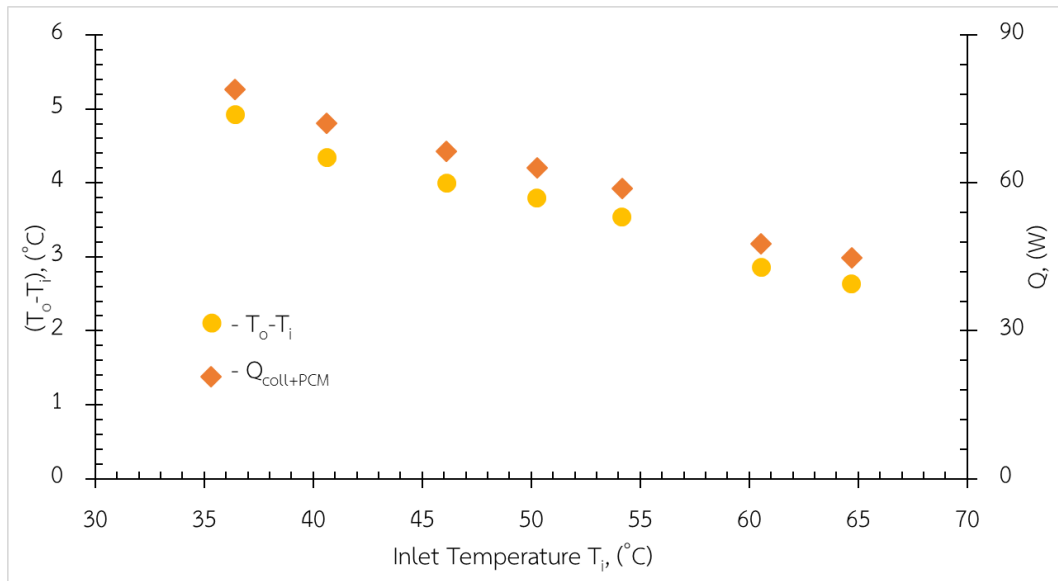
Figure 35 Temperature difference (T_o-T_i) and heat gains ($Q_{coll+PCM}$) of PCM1 integrated solar collector with mass flow rate 0.03 kg/s·m^2.
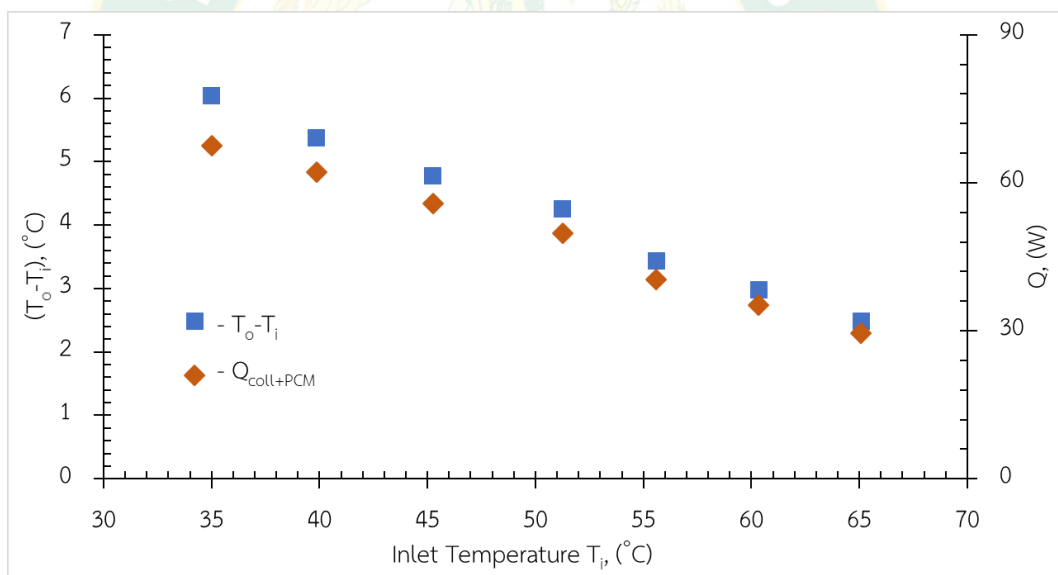
Figure 36 Temperature difference (T_o-T_i) and heat gains ($Q_{coll+PCM}$) of PCM1 integrated solar collector with mass flow rate 0.02 kg/s·m^2.

The effected various mass flow rates on thermal efficiency on novel solar collector integrated with phase change material (PCM1) The results represented by the linear regression function between (T_i-T_a)/I_T and thermal efficiency (η). The $F_R(\tau\alpha)_e$ in each case mass flow rate were performed on the intersection of Y-axis represented the maximum efficiency and the slope of the equation as the heat loss to environment by following the Eq. 11 and Eq. 12. The novel solar collector integrated with PCM of

riser tube 16 mm outside diameter was given the value $F_R(\tau\alpha)_e$ of 0.766, 0.808 and 0.835 and heat loss $F_R U_L$ of 10.506, 10.932 and 9.68 $W/m^2 \cdot K$ by testing various flow rates was showed in **Table 9** and **Figure 38** of (PCM1). The novel collector PCM1 tested with mass flow rate at 0.03 $kg/s \cdot m^2$ is given a highest thermal performance with $F_R(\tau\alpha)_e$ of 0.835 and $F_R U_L$ of 9.68 $W/m^2 \cdot K$ with term of the phase change material energy stores.
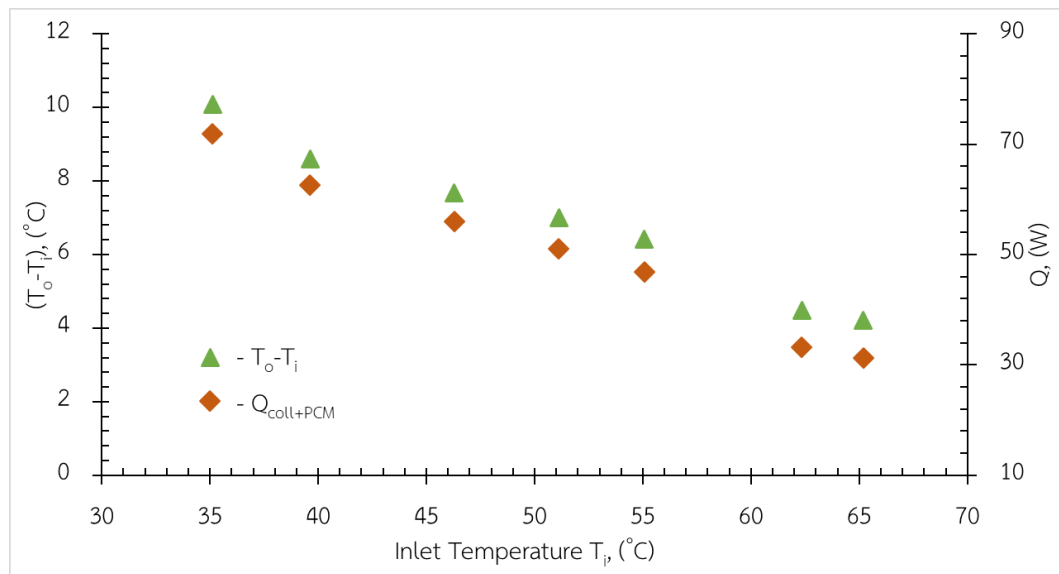
Figure 37 Temperature difference $(T_o - T_i)$ and heat gains $(Q_{coll+PCM})$ of PCM1 integrated solar collector with mass flow rate 0.01 $kg/s \cdot m^2$.

Table 9 The thermal efficiency analysis data.

PCM 1 (The novel solar collector integrated with riser PCM 16 mm of diameter)			
Flow rate (kg/s·m²)	$F_R(\tau\alpha)_e$	$F_R U_L$	R^2
0.01	0.766	10.506	0.98
0.02	0.808	10.932	0.98
0.03	0.835	9.680	0.98
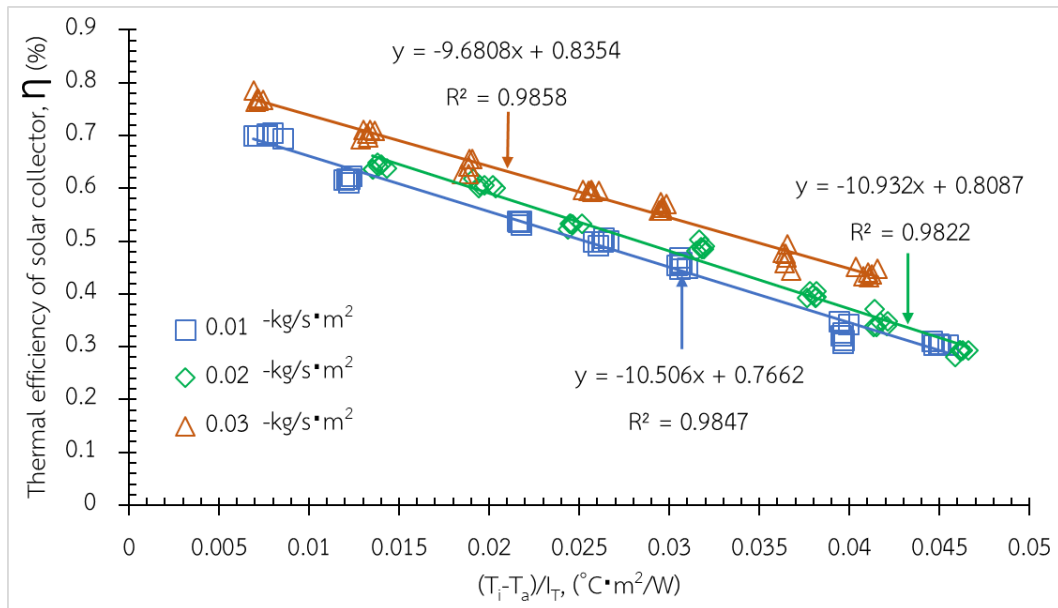
Figure 38 Thermal efficiency of novel solar collector integrated with PCM1 tested with various mass flow rate from 0.01 to 0.03 kg/s·m^2.

4.2.2. Thermal performance of novel solar collector integrated with Phase change material riser 10 mm outside diameter (PCM2)
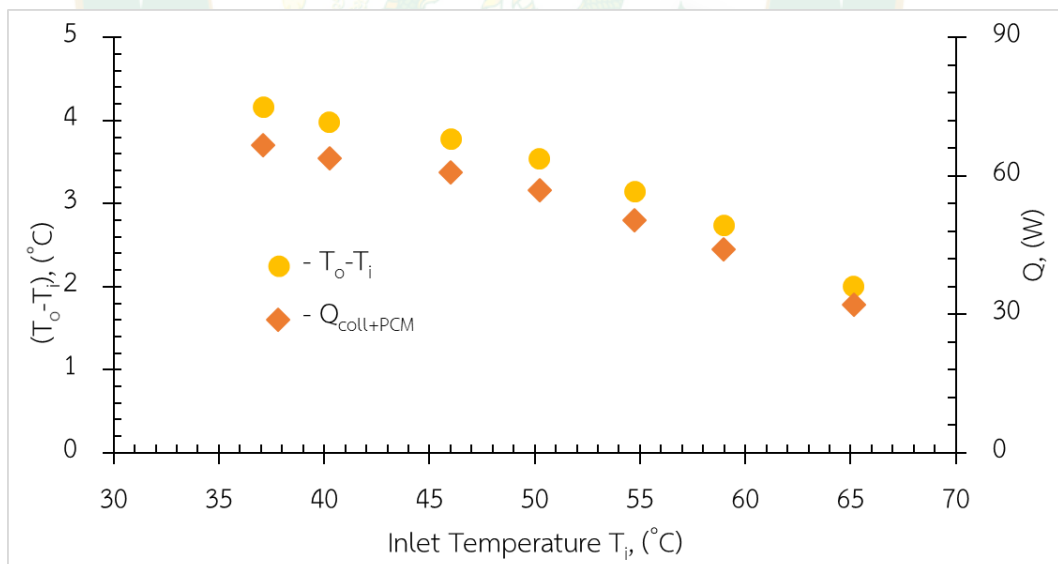
Figure 39 Temperature difference (T_o-T_i) and heat gains ($Q_{coll+PCM}$) of PCM2 integrated solar collector with mass flow rate from 0.03 kg/s·m^2.

The novel solar collector integrated with RT42 (melting point 38 to 43 °C) phase change material riser 10 mm outside diameter (PCM2) was studied of thermal performance effect by mass flow rate from 0.01 to 0.03 kg/s·m^2.
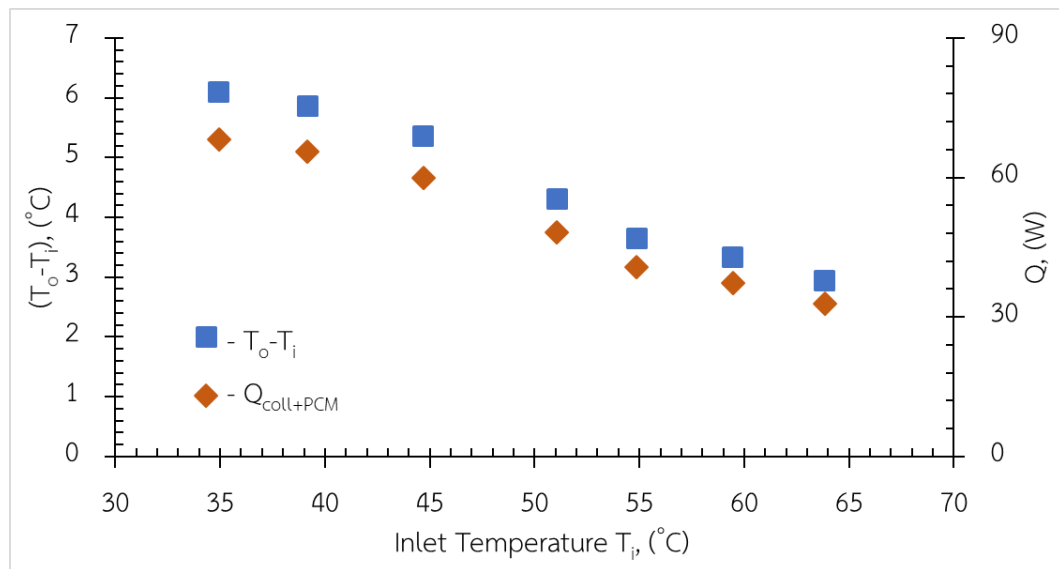
Figure 40 Temperature difference (T_o-T_i) and heat gains $(Q_{coll+PCM})$ of PCM2 integrated solar collector with mass flow rate from 0.02 kg/s·m².
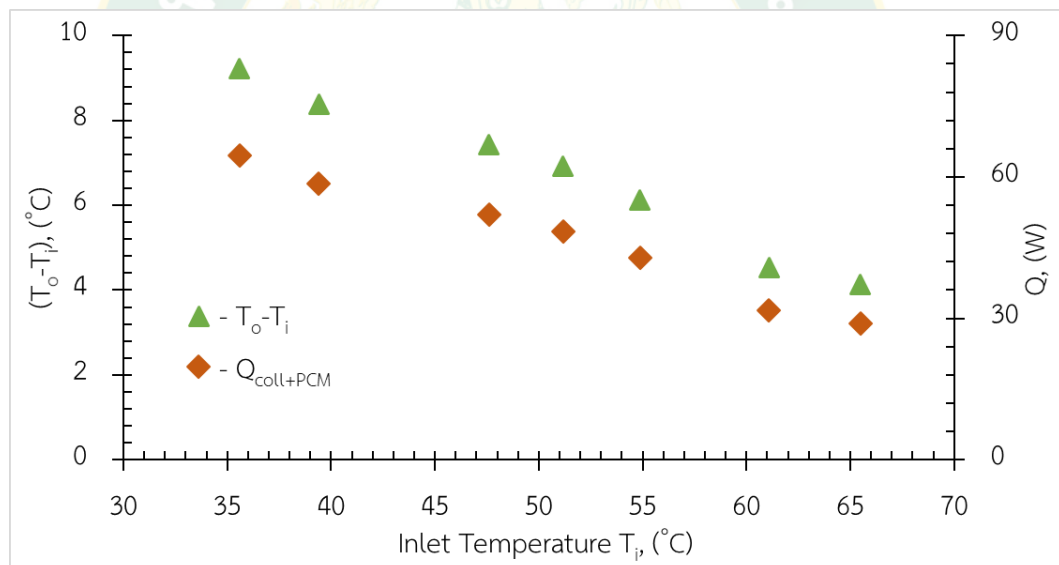
Figure 41 Temperature difference (T_o-T_i) and heat gains $(Q_{coll+PCM})$ of PCM2 integrated solar collector with mass flow rate from 0.01 kg/s·m².

The experimental tested following to Ashrae standard 93-2003 (Polvongsri, 2013) such specific condition as: the solar radiation intensity higher than 970 W/m², air velocity from 2.2 to 4.4 m/s and inlet temperature various from 35, 40, 45, 50, 55, 60, 65 °C, respectively. In the **Figure 39**, **Figure 40** and **Figure 41** was showed the temperature different (T_o-T_i) was changed to the mass flow rate, while the low mass

flow rate was given the low (T_o-T_i) and heat gains $Q_{coll+PCM}$ opposite to high mass flow rate.

However, the inlet temperature is also effected to the temperature different and energy gains while operating, when testing with low inlet temperature (T_i), the solar collector was collected a lot more of heat gains ($Q_{coll+PCM}$) and high temperature different (T_o-T_i), neither, the high inlet temperature (T_i) was collected low heat gains ($Q_{coll+PCM}$) and low temperature different (T_o-T_i). The flow rate 0.03 kg/s·m^2 was showed the temperature different (T_o-T_i) from 4.1 to 2.0 °C while the collected thermal energy from solar radiation which heat gains were ($Q_{coll+PCM}$) was 66.7 to 32.1 W, the flow rate 0.02 kg/s·m^2 gives heat gains $Q_{coll+PCM}$ was 68.3 to 32.9 W and (T_o-T_i) was 6.2 to 2.9 °C while the flow rate 0.01 kg/s·m^2 gives energy gains $Q_{coll+PCM}$ was 64.5 to 29.0 W and (T_o-T_i) was 9.2 to 4.1 °C following to inlet temperature (T_i), respectively.

In the **Table 10** and **Figure 42** were represented the effected various mass flow rates on thermal efficiency on novel solar collector integrated with phase change material (PCM1) The results represented by the linear regression function between (T_i-T_a)/I_T and thermal efficiency (**η**). The $F_R(\tau\alpha)_e$ in each case mass flow rate were performed on the intersection of Y-axis represented the maximum efficiency and the slope of the equation as the heat loss to environment by following the Eq. 11 and Eq. 12. The novel solar collector integrated with PCM of riser tube 16 mm outside diameter was given the value $F_R(\tau\alpha)_e$ of 0.711, 0.828 and 0.743 and heat loss F_RU_L of 11.304 , 8.764 and 9.625 W/m^2·K by testing various flow rates was showed in **Table 10** and **Figure 42** of (PCM2). The novel collector PCM1 tested with mass flow rate at 0.02 kg/s·m^2 is given a highest thermal performance with $F_R(\tau\alpha)_e$ of 0.828 and F_RU_L of 11.304 W/m^2·K with term of Phase Change Material energy stores.

Table 10 The thermal efficiency analysis data from tested of PCM energy stores.

PCM 2 (The novel solar collector integrated with riser PCM 10 mm of diameter)			
Flow rate (kg/s·m^2)	$F_R(\tau\alpha)_e$	F_RU_L	R^2
0.01	0.711	9.625	0.95
0.02	0.828	11.304	0.98
0.03	0.743	8.764	0.97
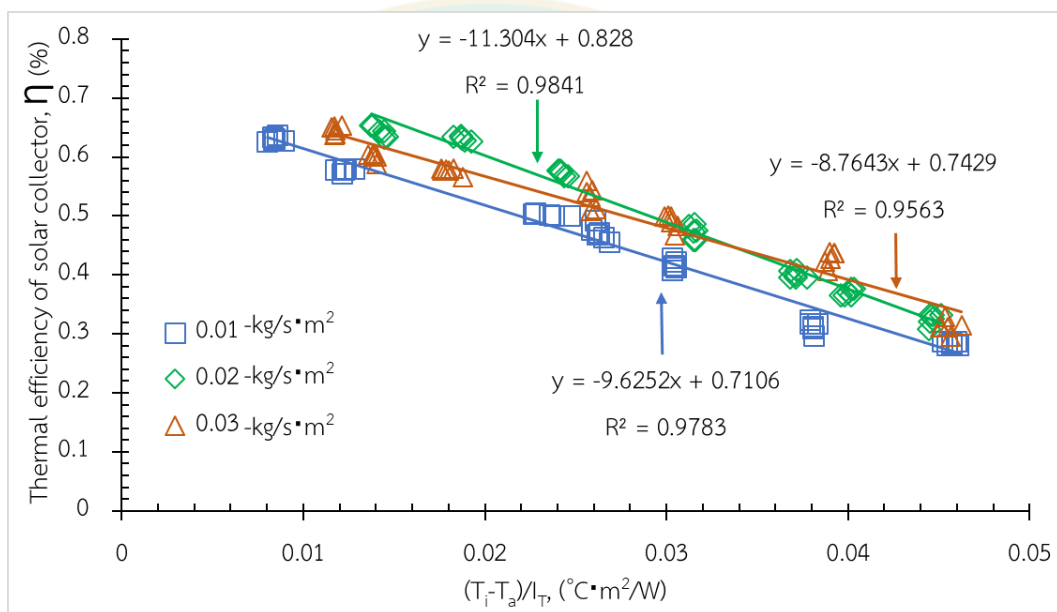
Figure 42 Thermal efficiency of novel solar collector integrated with PCM2 tested with mass flow rate 0.01 to 0.03 kg/s·m^2.

4.2.3. Thermal efficiency of conventional solar collector

The conventional solar collector (without PCM) was studied of thermal performance effect by mass flow rate from 0.01 to 0.003 kg/s·m^2. The experimental tested following to Ashrae standard 93-2003 (Polvongsri, 2013) such specific condition as: the solar radiation intensity higher than 970 W/m^2, air velocity from 2.2 to 4.4 m/s and inlet temperature various from 35, 40, 45, 50, 55, 60, 65 $^\circ$C, respectively. In the **Figure 43**, **Figure 44** and **Figure 45** was showed the temperature different (T$_o$-T$_i$) was changed to the mass flow rate, while the low mass flow rate was given the low (T$_o$-T$_i$) and energy gains Q$_{coll}$ opposite to high mass flow rate. However, the inlet temperature

is also effected to the temperature different and collected energy while operating, when testing with low inlet temperature (T_i), the solar collector was collected a lot more of heat gains (Q_{coll}) and high temperature different (T_o-T_i), neither, the high inlet temperature (T_i) was collected low thermal energy (Q_{coll}) and low temperature different (T_o-T_i).
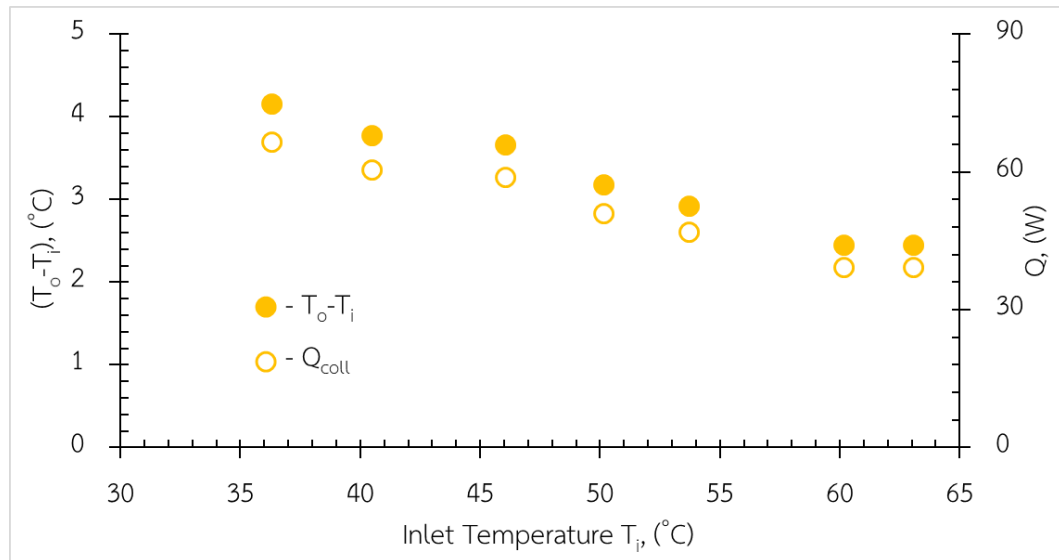
Figure 43 Temperature difference (T_o-T_i) and heat gains (Q_{coll}) of conventional solar collector with mass flow rate 0.03 kg/s·m^2.
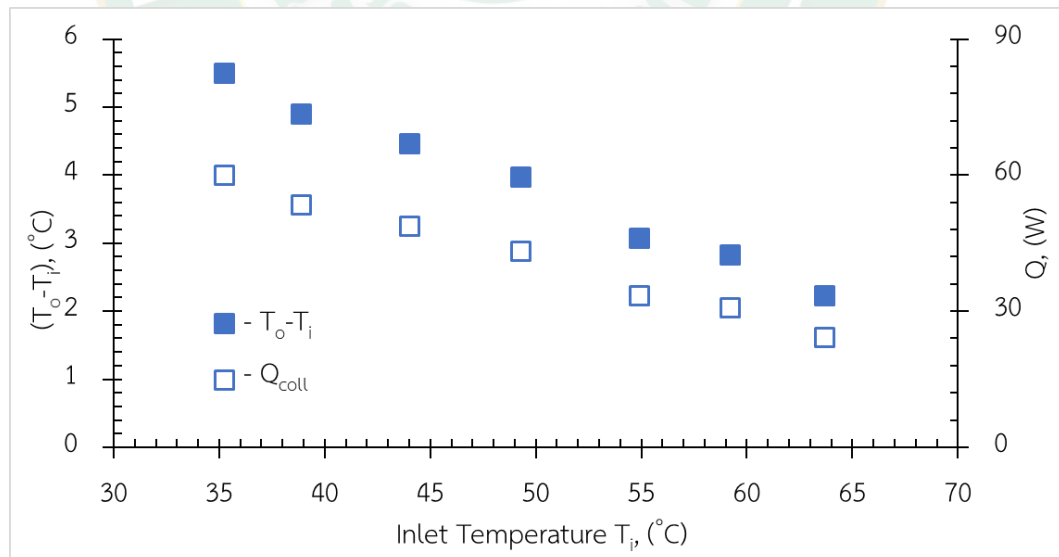
Figure 44 Temperature difference (T_o-T_i) and heat gains (Q_{coll}) of conventional solar collector with mass flow rate 0.02 kg/s·m^2.

In the **Figure 45** with flow rate 0.03 kg/s·m^2 was showed the temperature different (T_o-T_i) from 4.1 to 2.4 $^\circ$C while the collected thermal energy from solar radiation of heat gains (Q_{coll}) was 67.3 to 39.3 W, the flow rate 0.02 kg/s·m^2 gives heat gains Q_{coll} was 59.8 to 24.2 W and (T_o-T_i) was 5.5 to 2.2 ℃ while the flow rate 0.01 kg/s·m^2 gives heat gains Q_{coll} was 58.7 to 28.6 W and (T_o-T_i) was 8.4 to 4.1 ℃ following to inlet temperature (T_i), respectively.
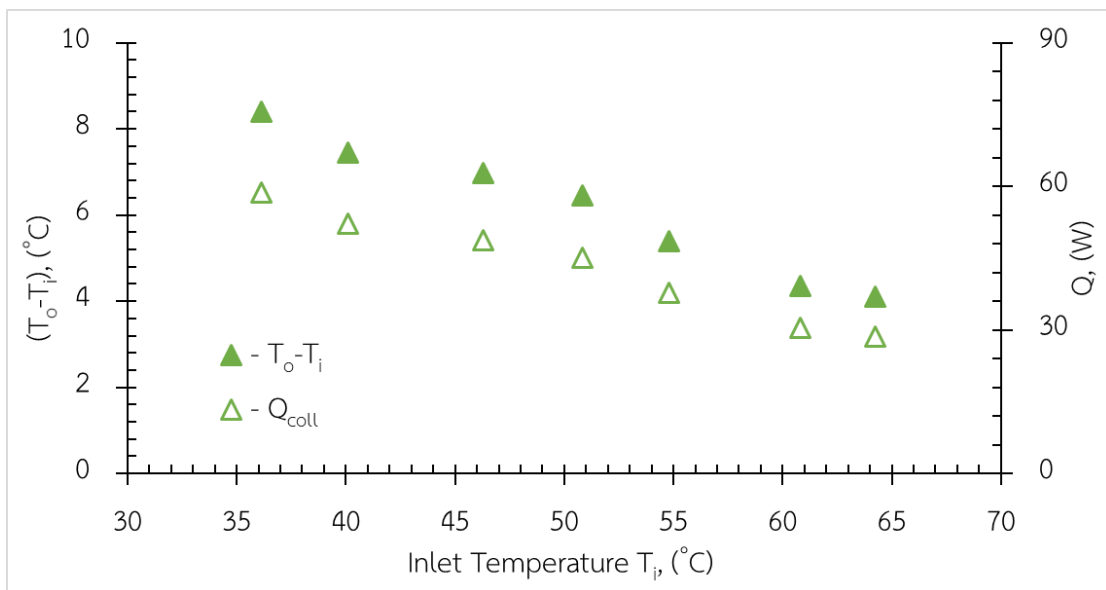
Figure 45 Temperature difference (T_o-T_i) and heat gains (Q_{coll}) of conventional solar collector with mass flow rate 0.01 kg/s·m^2.

In the **Figure 46** was represented the effected various mass flow rates on thermal efficiency on conventional solar collector (without PCM) The results represented by the linear regression function between (T_i-T_a)/I_T and thermal efficiency (η). The $F_R(\tau\alpha)_e$ in each case mass flow rate were performed on the intersection of Y-axis represented the maximum efficiency and the slope of the equation as the heat loss to environment by following the Eq. 11 and Eq. 12. The conventional solar collector was given the value $F_R(\tau\alpha)_e$ of 0.637, 0.714 and 0.702 and heat loss F_RU_L of 8.77, 10.64 and 8.69 W/m^2·K by testing various flow rates was showed in **Table 11** (without PCM). The novel collector PCM1 tested with mass flow rate at 0.02 kg/s·m^2 is given a highest thermal performance with $F_R(\tau\alpha)_e$ of 0.714 and F_RU_L of 10.642 W/m^2·K.

Table 11 The thermal efficiency analysis data from tested.

PCM 1 (The novel solar collector integrated with riser PCM 16 mm of diameter)			
Flow rate (kg/s·m^2)	$F_R(\tau\alpha)_e$	F_RU_L	R^2
0.01	0.637	8.774	0.971
0.02	0.714	10.642	0.981
0.03	0.702	8.695	0.975
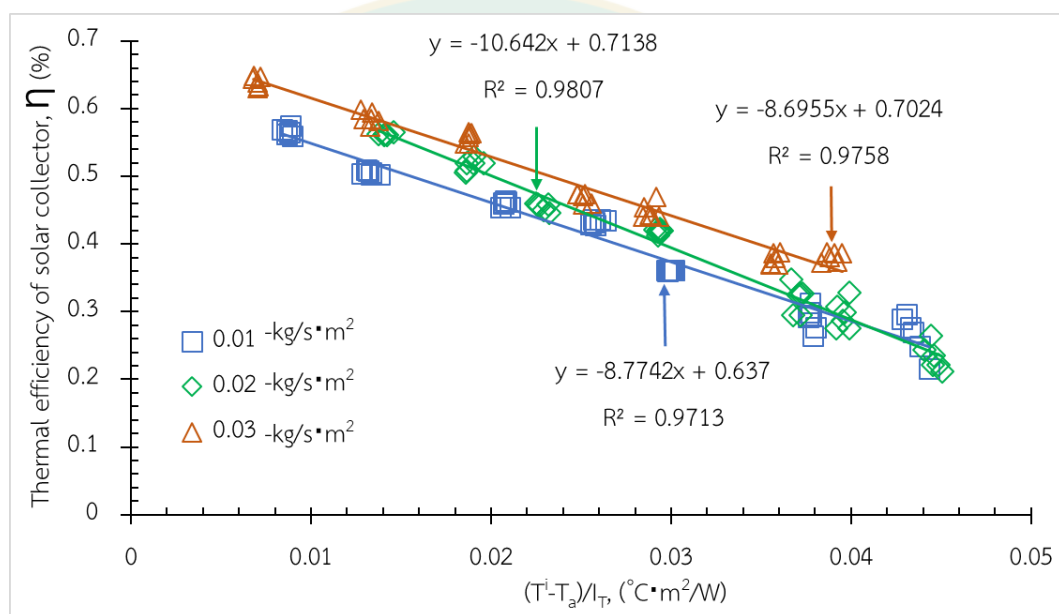
Figure 46 Thermal efficiency of conventional solar collector.

4.2.4. Thermal efficiency of the novel and conventional solar collector

The novel solar collector integrated with phase change material (RT42 melting point 38-43 °C) with difference riser diameters as 16 and 10 mm of outside diameter and convention were experimented following to the ASHRAE Standard 93-2003 condition such as Ambient temperature (T_i), Air velocity (V_{air}), Solar radiation intensity (I_T), various flow rates 0.01 to 0.03 kg/s·m^2, Inlet temperature 35, 40, 45, 50, 55, 60 and 65 °C of each solar collector.
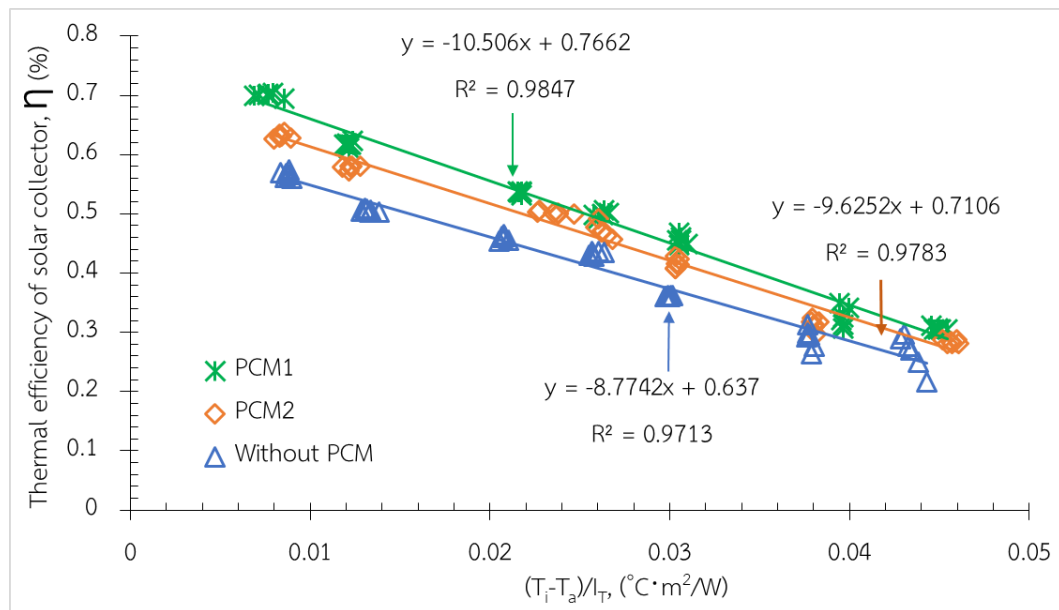
Figure 47 The thermal efficiency of solar collector with mass flow rate 0.01 kg/s·m^2.
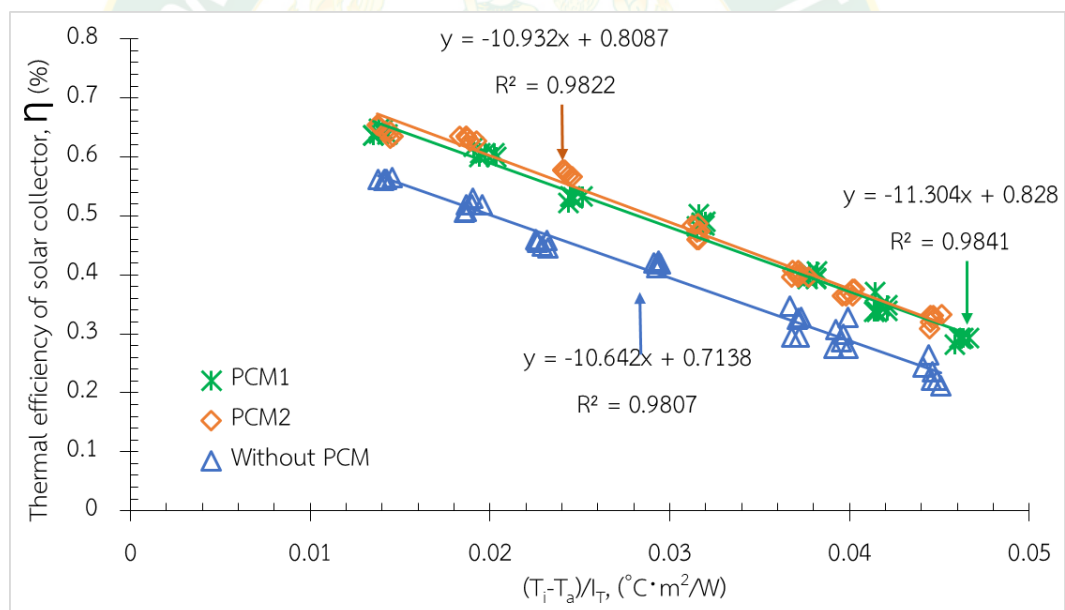
Figure 48 The thermal efficiency of solar collector with mass flow rate 0.02 kg/s·m^2.

The various mass flow rates were tested in each novel solar collector and conventional collector as seen in **Figure 47**, **Figure 48** and **Figure 49**. In the thermal solar collector performance tested with mass flow rate 0.01 kg/s·m^2 seen that the novel solar collector integrated with phase change material riser 16 mm outside diameter (PCM1) was gave highest thermal performance than others collector seen as in the **Table 12** which represented of the thermal performance data $F_R(\tau\alpha)_e$ and F_RU_L were 0.766 and 10.506 W/m^2·K. The thermal efficiency of solar collector tested with

mass flow rate 0.02 kg/s·m^2 was found that the efficiency of novel solar collector integrated with phase change material riser 10 mm outside diameter (PCM2) is a highest thermal efficiency as seen in the **Table 12** which $F_R(\tau\alpha)_e$ and F_RU_L were 0.828 and 11.304 W/m^2·K, while the tested with mass flow rate 0.03 kg/s·m^2 the novel collector PCM1 also showed in the **Table 12**, the highest efficiency with $F_R(\tau\alpha)_e$ and F_RU_L were 0.835 and 9.680 W/m^2·K, respectively.
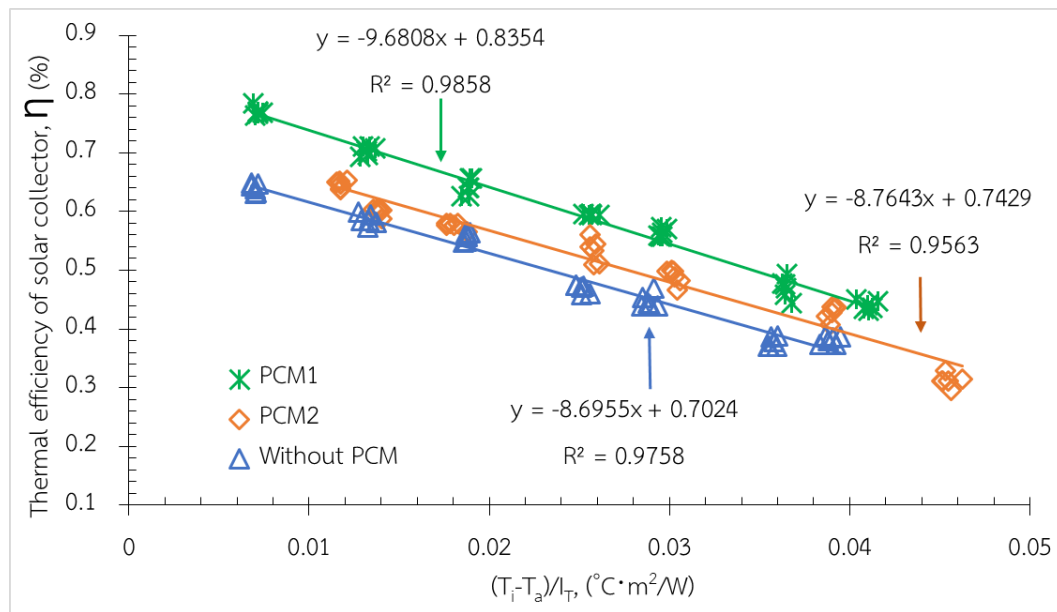
Figure 49 The thermal efficiency of solar collector with mass flow rate 0.03 kg/s·m^2.

The both novel solar collector and conventional collector had experimented following to the ASHRAE Standard test condition, in the same time, each solar collector also loss the thermal energy to the environmental round the collector which represented the heal loss (U_L) (Eq. 2) and the parameter (F_R) could showed the ability of solar collector call heat removal factor (F_R) (Eq. 9) where found out with various flow rate 0.01, 0.02 and 0.03 kg/s·m^2. The energy loss following to the temperature on the plate absorber and temperature inlet, while operating with low inlet temperature both heat loss and heat removal factor were given low heat loss and high energy collected, neither, increasing inlet temperature of the solar collector system made the collector loss maximum energy to the environment and small energy collector or small value of the heat removal factor.

Table 12 Thermal efficiency of the novel and conventional solar collector.

Thermal efficiency of solar collector with mass flow rate 0.01 kg/s·m^2			
Category	$F_R(\tau\alpha)_e$	$F_R U_L$	R^2
PCM1	0.766	10.506	0.98
PCM2	0.710	9.625	0.97
Without PCM	0.637	8.774	0.971
Thermal efficiency of solar collector with mass flow rate 0.02 kg/s·m^2			
Category	$F_R(\tau\alpha)_e$	$F_R U_L$	R^2
PCM1	0.808	10.932	0.98
PCM2	0.828	11.304	0.98
Without PCM	0.714	10.64	0.97
Thermal efficiency of solar collector with mass flow rate 0.03 kg/s·m^2			
Category	$F_R(\tau\alpha)_e$	$F_R U_L$	R^2
PCM1	0.835	9.680	0.98
PCM2	0.742	8.764	0.95
Without PCM	0.702	8.695	0.97
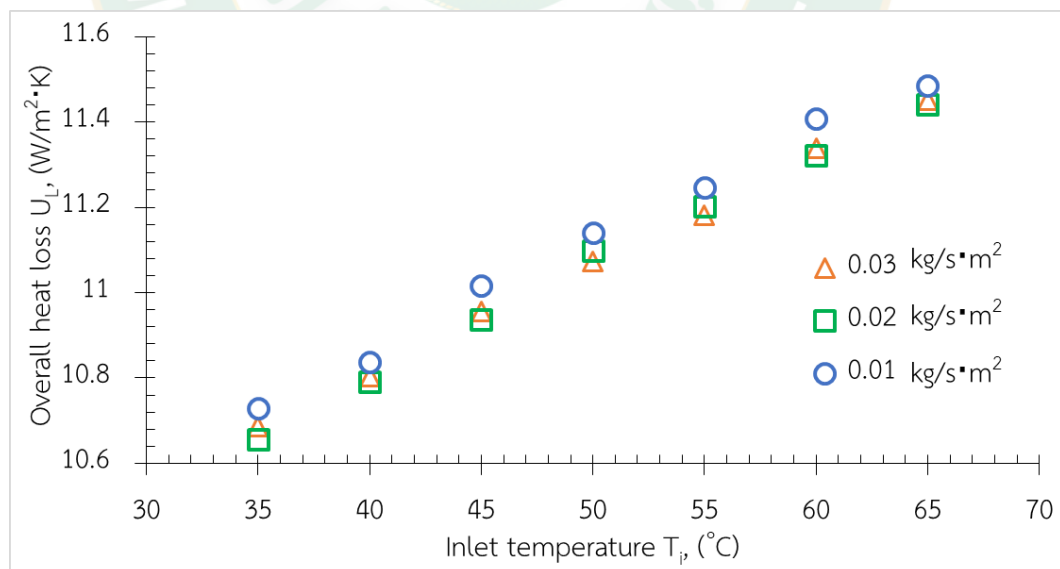
Figure 50 The overall heat loss (U_L) of PCM1 integrated solar collector.

In the **Figure 50**, **Figure 51 Figure 52**, **Figure 53**, **Figure 54** and **Figure 55**, the novel solar collector PCM1, PCM2 and conventional collector without PCM was seen that the heat loss various from 13.01 to 15.78 W/m^2·K, 12.1 to 15.68 W/m^2·K and 11.15 to 15.02 W/m^2·K of mass flow rate 0.01 kg/s·m^2 and the heat removal factor (F$_R$) was 0.78 to 0.65, 0.78 to 0.6 and 0.79 to 0.58, respectively.
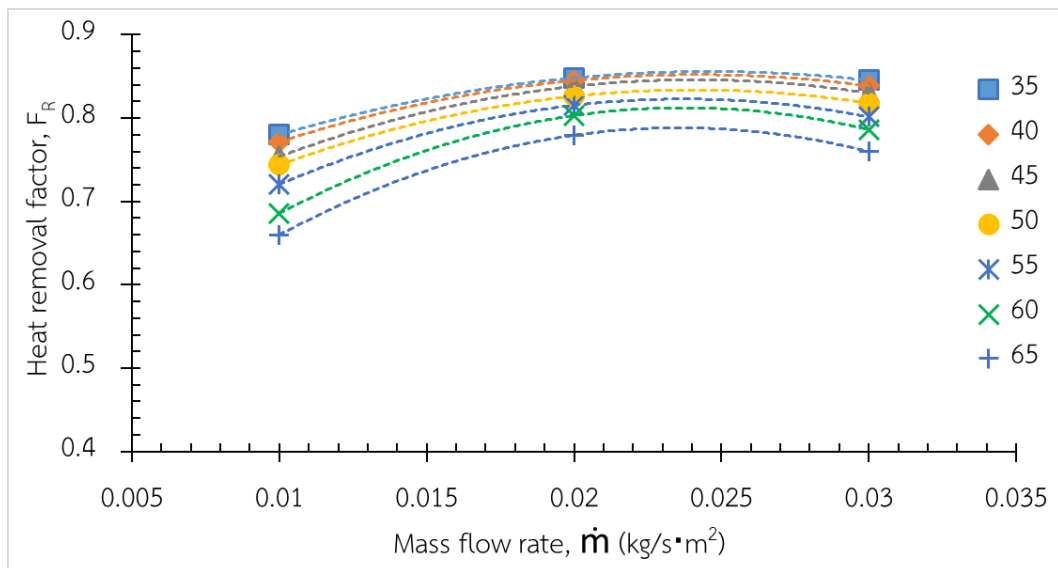
Figure 51 The heat removal factor (F$_R$) of with PCM1 integrated solar collector.
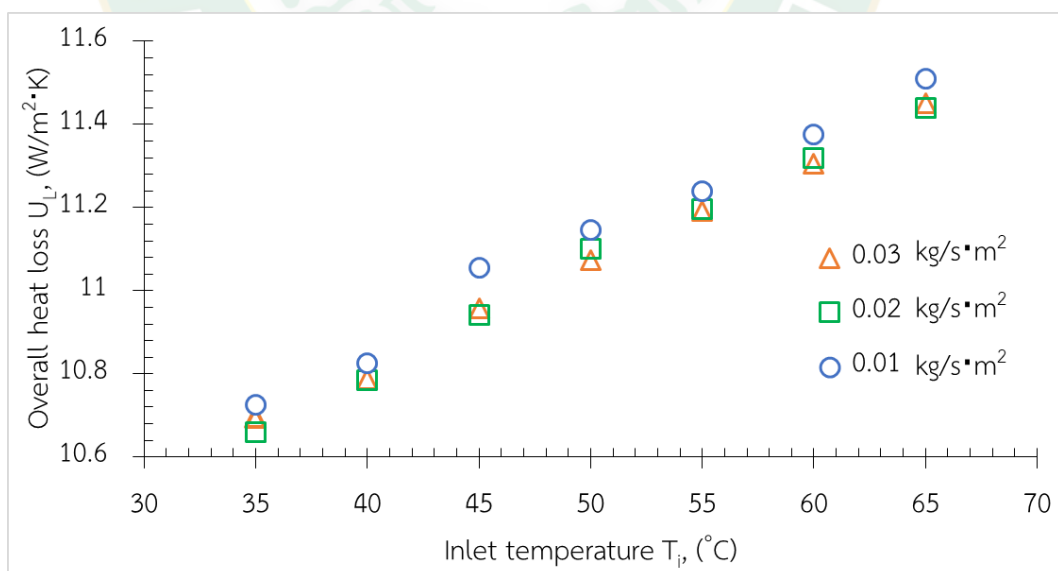
Figure 52 The overall heat loss (U$_L$) of PCM2 integrated solar collector.

Moreover, the solar collector tested with the mass flow rate 0.02 kg/s·m^2 was found that the heat loss (U$_L$) between 13.03 to 14.31 W/m^2·K, 13.64 to 16.5 W/m^2·K and 13.13 to 18.32 W/m^2·K and the heat removal factor (F$_R$) was 0.84 to 0.77, 081 to 0.67 and 0.81 to 0.58, respectively. The test with mass flow rate 0.03 W/s·m^2, the heat loss was 11.5 to 13.16 W/m^2·K, 10.3 to 11.9 W/m^2·K and 10.45 to 13.04 W/m^2·K, while the heat removal factor was 0.84 to 0.74, 0.83 to 0.71 and 0.83 to 0.67.
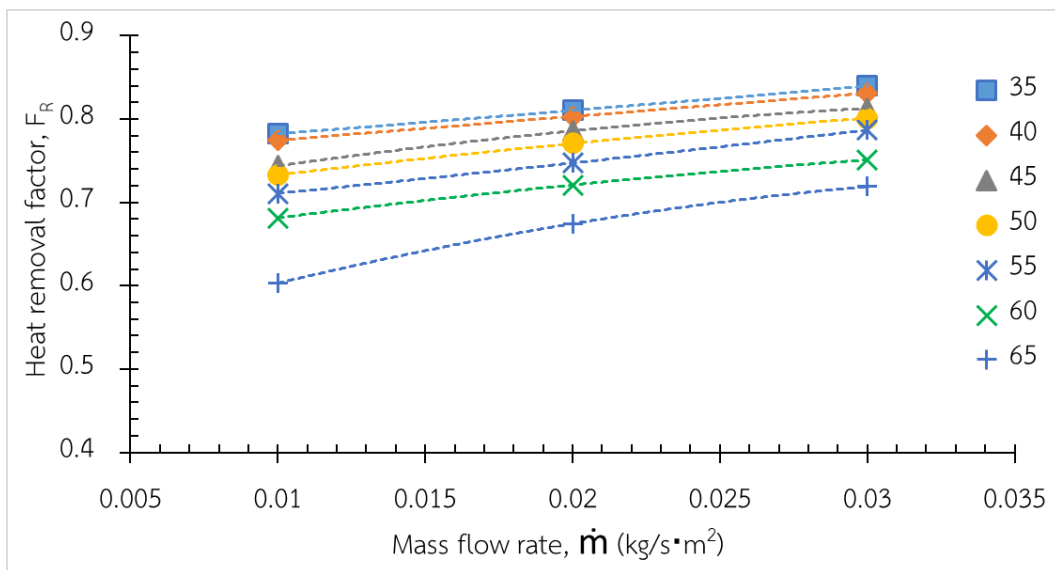
Figure 53 The heat removal factor (F$_R$) of with PCM2 integrated solar collector.
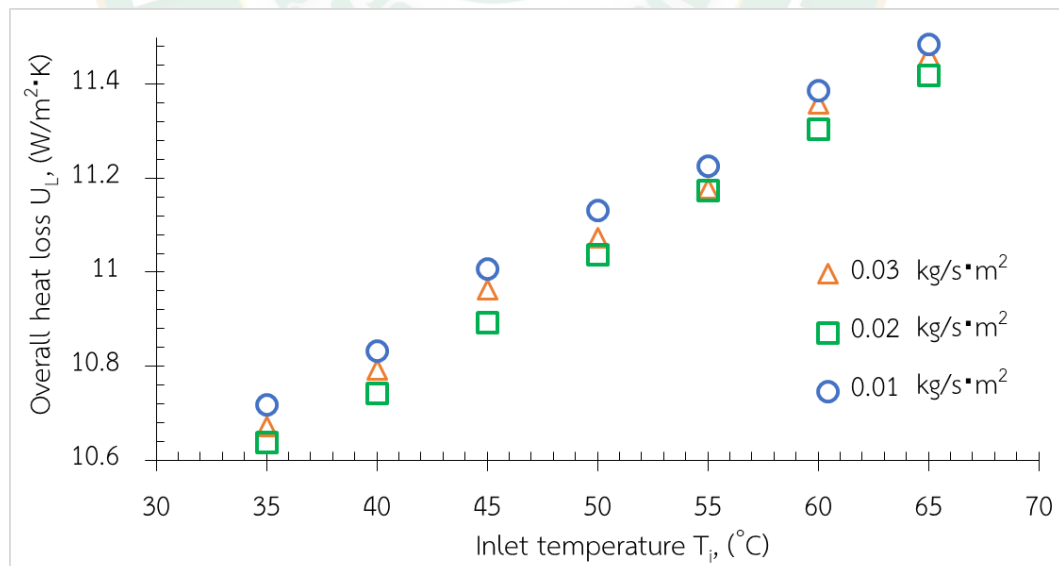
Figure 54 The overall heat loss (U$_L$) of conventional solar collector (without PCM).
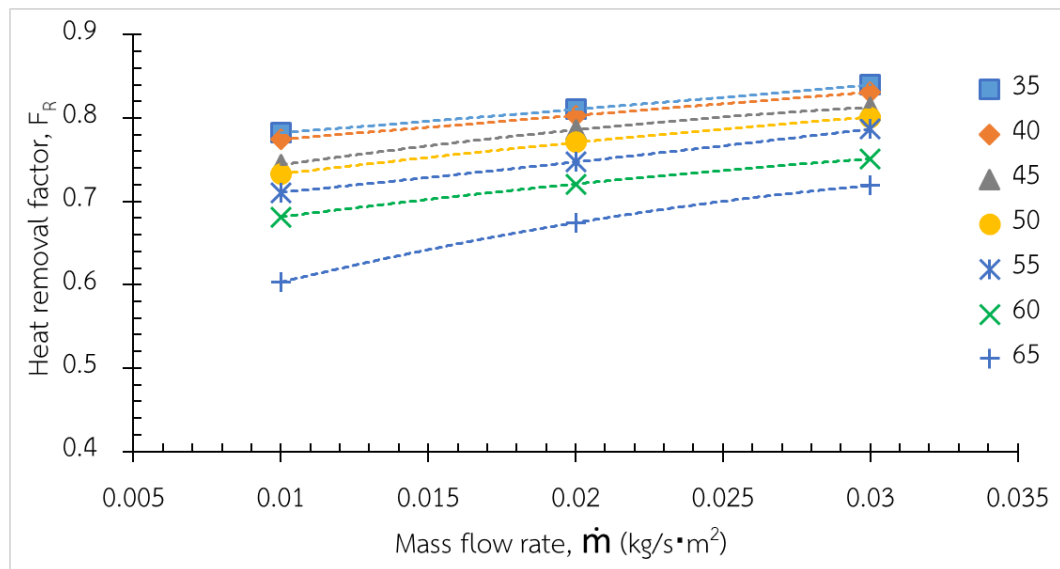
Figure 55 The heat removal factor (F_R) of without PCM conventional solar collector.

The novel solar collectors were given the high thermal performance which mean the value of other factors were also represented as the heat loss (U_L) and heat removal factor (F_R). experimental of the solar collector tested with the various inlet temperature also effected to these parameters as seen above which low heat loss and high heat removal factor at the small temperature inlet temperature, either than, high inlet temperature was found that high heat loss and low heat removal factor. Moreover, another factor could be effected to these parameters was the mass flow rate which the experimental tested with novel and conventional solar collector with 0.01, 0.02 and 0.03 kg/s·m^2 showed that the high thermal efficiency of mass flow rate was given high heat loss to environmental cause of the F_RU_L which represented the maximum heat loss of the solar collector performance.

4.3. **The heat transfer enhancement of novel solar collector integrated with phase change material**

The experimental of the novel and normal solar collector integrated with phase change material riser in difference of diameter and without integrated were tested following to the Ashrae standard 93-2003 various mass flow rates 0.01, 0.02 and 0.03 kg/s·m^2.
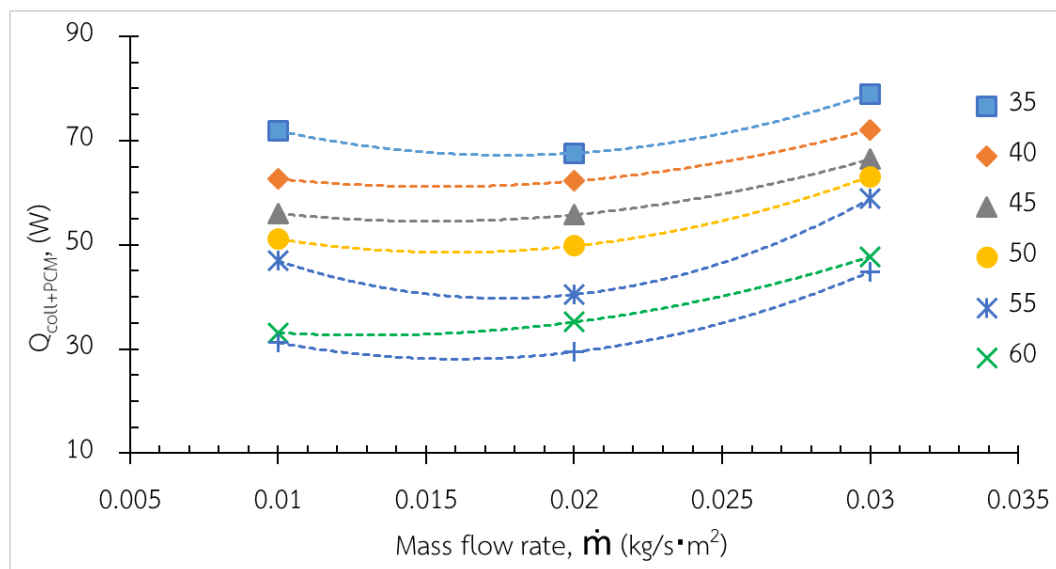
Figure 56 The heat gains of novel solar PCM1of riser 16 mm with various mass flow rates 0.01, 0.02 and 0.03 kg/s·m^2.

The heat gains ($Q_{coll+PCM}$) of the novel solar collector PCM1 and PCM2 were showed in the **Figure 56**, **Figure 57** and. **Figure 58** Both collectors were absorbed peak amount thermal energy when circulating water at low intel temperature, either, when water circulating in the system at high inlet temperature the novel collectors were collected the small amount of thermal energy during testing. Moreover, the mass flow rate was a factor effected to the heat gains ($Q_{coll+PCM}$) of solar collector, while the operating the big mass flow through to the collector which water could absorbed high thermal energy than low mass flow rate as seen the novel collector PCM1 of mass flow rate 0.03 kg/s·m^2 was 79.0 to 44.8 W following the inlet temperature 35 to 65 $^\circ$C, respectively. Other, the novel solar collector PCM2 and conventional solar collector are collected maximum energy while experimental tested with Ashrae standard mass

flow rate 0.02 kg/s·m² was 68.2 to 32.92 W following to inlet temperature 35 to 65 °C, respectively.
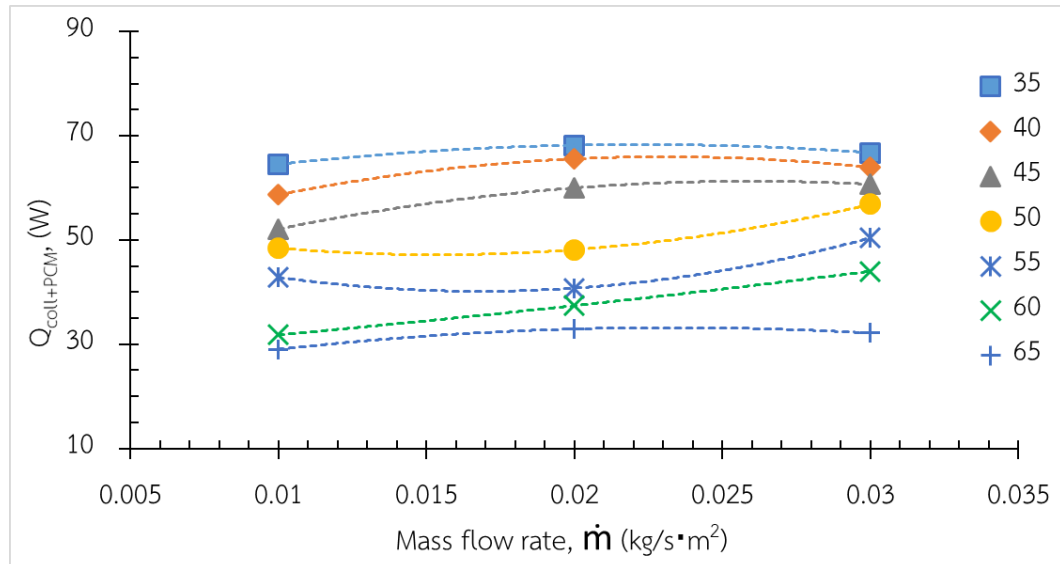
Figure 57 The heat gains of novel solar PCM2 riser 10 mm with various mass flow rates 0.01, 0.02 and 0.03 kg/s·m².
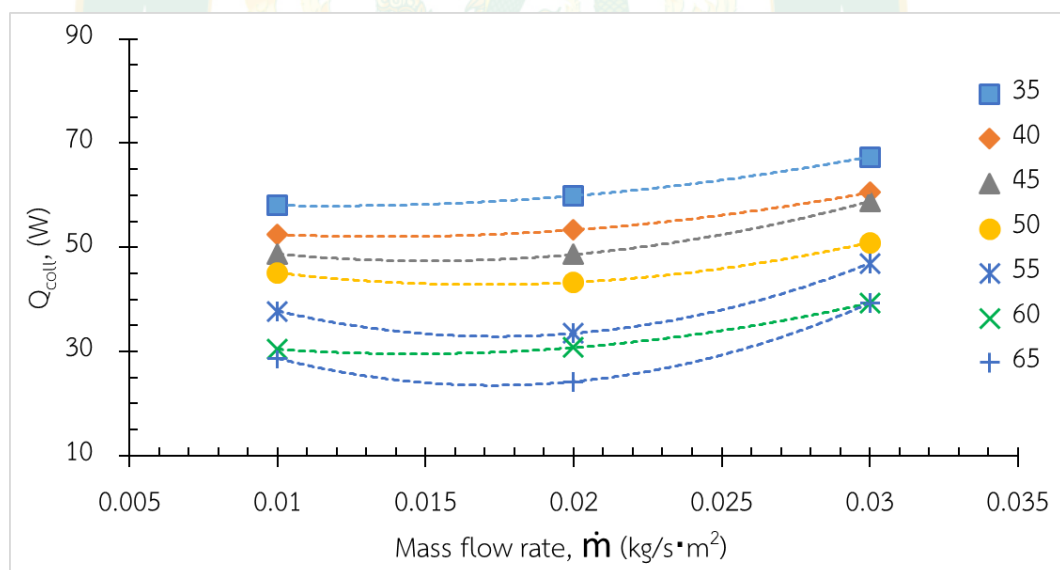
Figure 58 The heat gains of novel solar without PCM with various mass flow rates 0.01, 0.02 and 0.03 kg/s·m².

The conventional solar collector was seen that the thermal energy collected 66.5 to 39.3 W at mass flow rate 0.03 kg/s·m², 59.8 to 24.2 W at mass flow rate 0.02 kg/s·m² and at mass flow rate 0.01 kg/s·m² was 58.7 to 28.6 W.
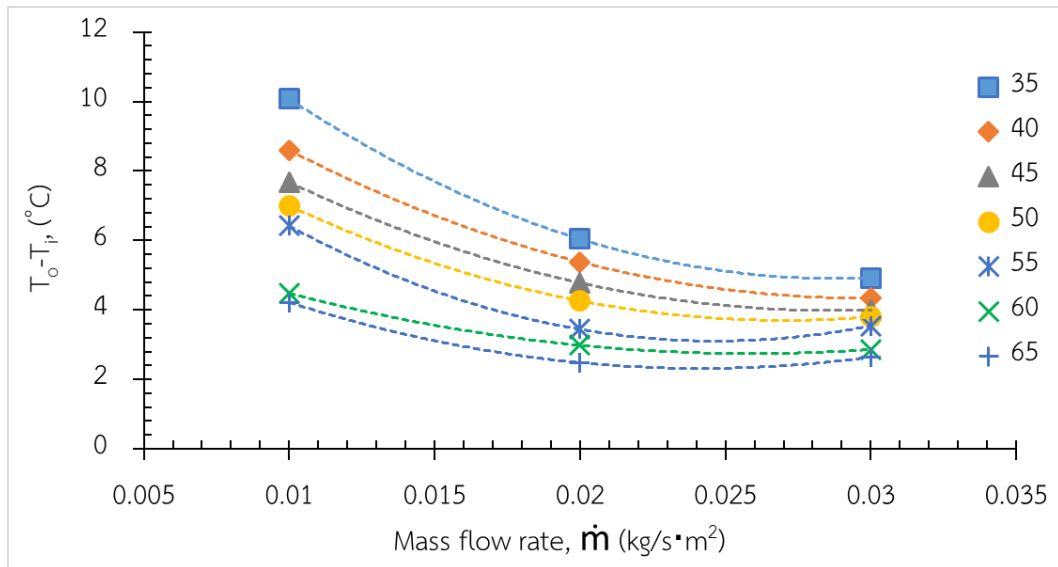
Figure 59 The temperature difference (T_o-T_i) of novel solar PCM1 with various mass flow rates 0.01, 0.02 and 0.03 kg/s·m².
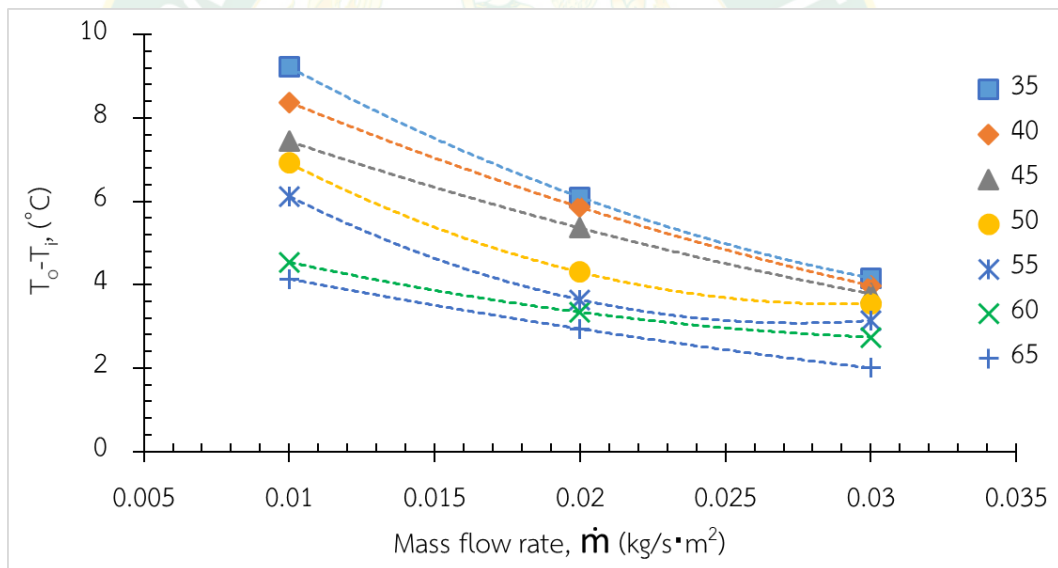
Figure 60 The temperature difference (T_o-T_i) of novel solar PCM2 with various mass flow rates 0.01, 0.02 and 0.03 kg/s·m².

In the **Figure 59**, **Figure 60** and **Figure 61** were showed that the different temperature (T_o-T_i) of novel solar collector PCM1 and PCM2 by various mass flow rates. The temperature difference (T_o-T_i) was various follow to the inlet temperature and various mass flow rates which the low mass flow rate was absorbed and transfer heat into circulating water with the small velocity flow rate, its made the water at high temperature, while high mass flow rate was absorbed and heat transfer of the collector

to the circulating water with high velocity flow rate on the inner tube which could made the inlet and outlet temperature going to smaller. The experimental tested with various inlet temperature also effected to the temperature (T_o-T_i) at low inlet temperature was high value than the high inlet temperature. The novel solar collector PCM1 and PCM2 were 10.1 to 4.22 $^\circ$C and 9.22 to 4.1 $^\circ$C at mass flow rate 0.01 kg/s·m^2, 6.1 to 2.9 $^\circ$C and 5.5 to 2.22 $^\circ$C at mass flow rate 0.02 kg/s·m^2 and at the mass flow rate 0.03 kg/s·m^2 the temperature (T_o-T_i) were 4.92 to 2.4 $^\circ$C and 4.1 to 2.0 $^\circ$C, while without PCM was 8.4 to 4.1°C, 5.5 to 2.2 $^\circ$C and 4.1 to 2.4 $^\circ$C as following to the various inlet temperature, respectively.
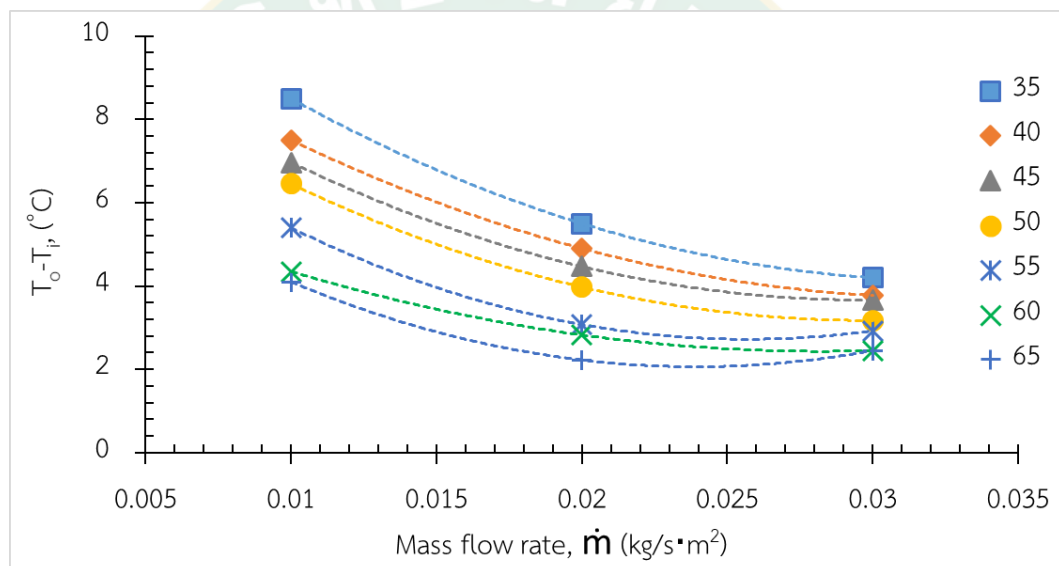
Figure 61 The temperature difference (T_o-T_i) of novel solar PCM1 with various mass flow rates 0.01, 0.02 and 0.03 kg/s·m^2.

In the **Figure 62** was showed the change of Prandtl number (Pr) following to the inlet temperature (T_i), the solar collector were tested with range of inlet temperature of the water which temperature was effected to the Prandtl number factor as changing from 4.51 to 2.7 following to temperature tests, respectively.
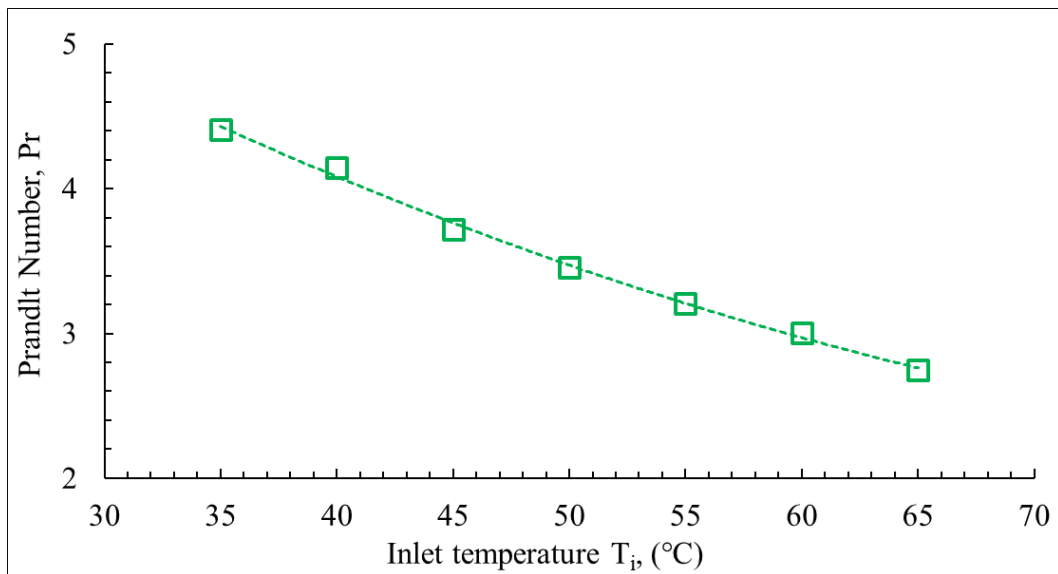
Figure 62 The Prandtl number (Pr) various with intel temperature (T$_i$).
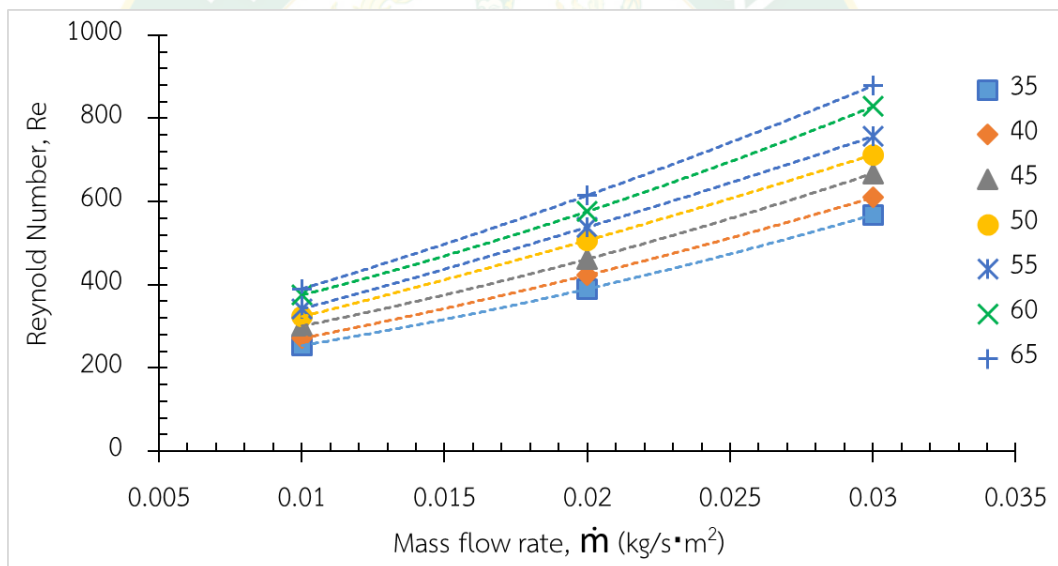
Figure 63 The Reynold Number (R$_e$) of novel solar collector (PCM1) of riser

16 mm with various mass flow rates 0.01, 0.02 and 0.03 kg/s·m^2.

In the **Figure 63**, **Figure 64** and **Figure 65** were showed the Reynold number of the novel solar collector PCM1 and PCM2 which its changed to the mass flow rate and temperature of the working fluid (water). The Reynold number could have indicated the resume of the flow rate inside the solar collector which the temperature of the water effected on its factor as the kinematic viscosity and density of the fluid. Moreover, the mass flow rate also one of main factor effected to the factor with diameter of the tube and velocity flow rate.
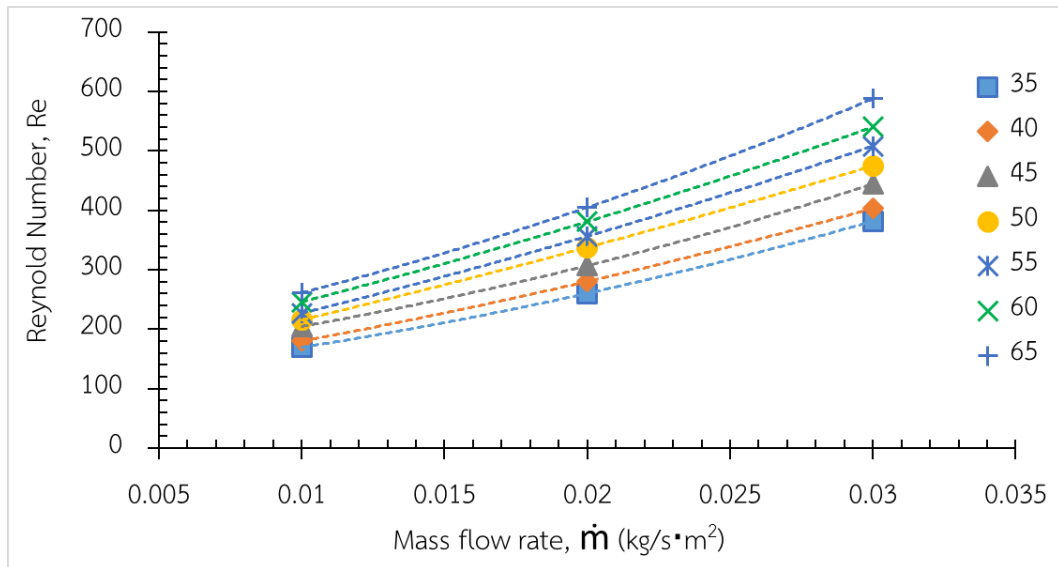
Figure 64 The Reynold number (R_e) of novel solar collector (PCM2) of riser 10 mm with various mass flow rates 0.01, 0.02 and 0.03 kg/s·m^2.
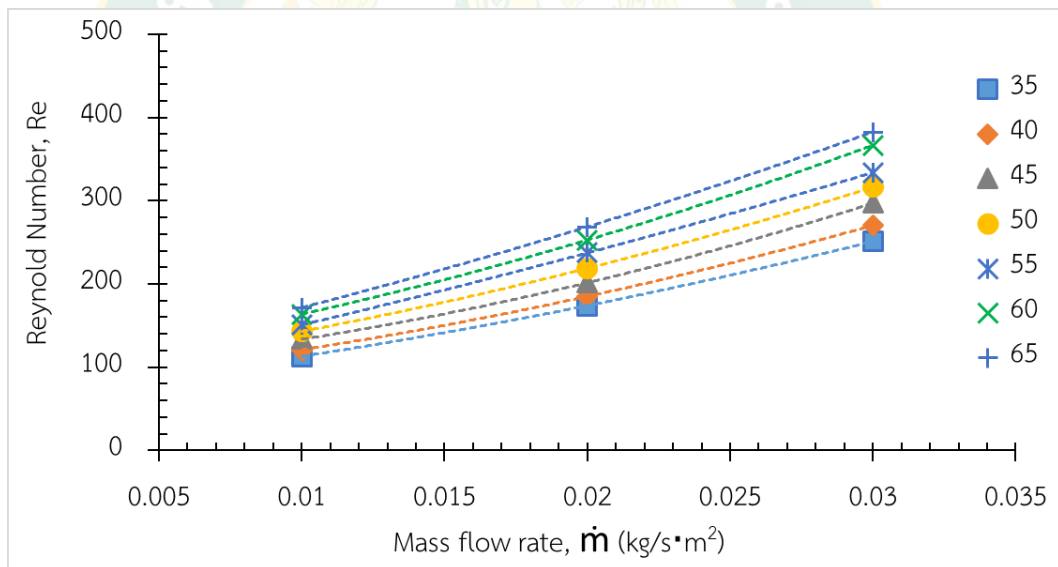
Figure 65 The Reynold number (R_e) of conventional solar collector with various mass flow rates 0.01, 0.02 and 0.03 kg/s·m^2.

The different riser s PCM risers were effected to factors which carried out the different of Reynold number of PCM1 and PCM2 as seen as the Reynold number 253.63 to 389.9 and 169.6 to 261.5 at mass flow rate 0.01 kg/s·m^2, 389.9 to 614.8 and 260.5 to 405.1 at mass flow rate 0.02 kg/s·m^2 while at mass flow rate 0.03 kg/s·m^2 the Reynold number was 568.3 to 878.2 and 381.0 to 587.9, while the collector without

PCM was 113.6 to 171.6, 174.04 to 268.7 and 251.6 to 382.7 following to the inlet temperature, respectively.

The solar collector was designed with the greenhouse effect which has black colored absorber plate converts radiation into thermal energy then the circulating fluid exchange heat inner absorber tube through to the storage tank. The critical integrated of novel solar collector with the riser phase change material inserted into the absorber tube was increasing the velocity flow rate inner of absorber plate which increased the thermal energy transfer into working fluid (water) by presenting the convective heat transfer coefficient (h_i). In the **Figure 66**, **Figure 67**and **Figure 68** were presented about the heat transfer (h_i) with various mass flow rate and inlet temperature of the novel solar collector PCM1 and PCM2. Both collectors were seen that the convective heat transfer coefficient (h_i) are increased by flow rate and decreased by high inlet temperature which were 132.2 to 49.34 W/m^2·K and 127.24 to 36.48 W/m^2·K within mass flow rate 0.01 kg/s·m^2, 142.72 to 67.86 W/m^2·K and 136.27 to 49.1 W/m^2·K of mass flow rate 0.02 kg/s·m^2 and at mass flow rate 0.03 kg/s·m^2 were 157.73 to 72.36 W/m^2·K and 139.76 to 56.1 W/m^2·K, while the collector without PCM was 119.6 to 32.06, 133.9 to 32.8 and 134.7 to 35.2 following inlet temperature, respectively.
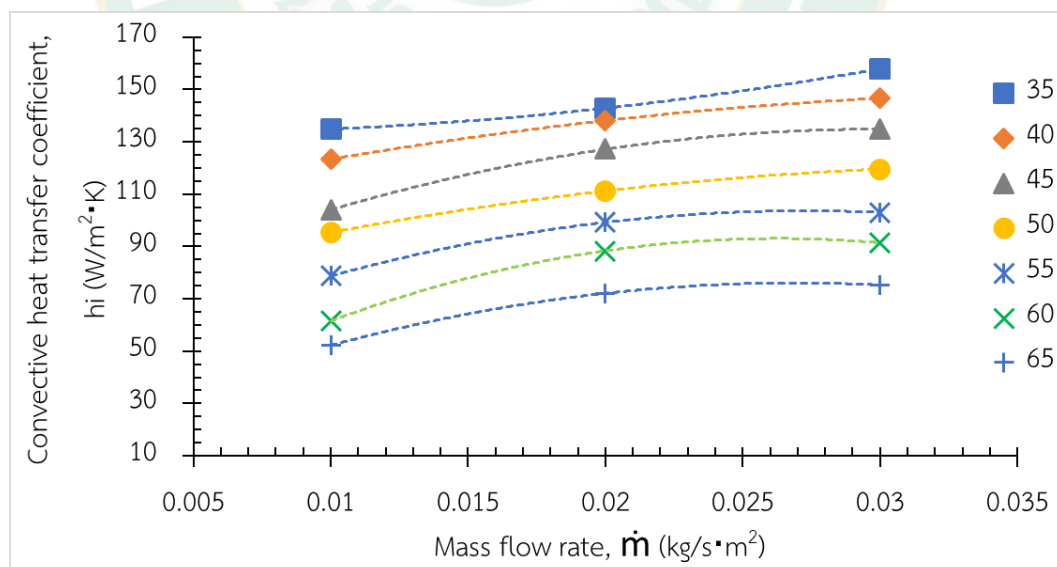
Figure 66 The convective heat transfer coefficient (h_i) of novel solar PCM1 of riser 16 mm with various mass flow rates 0.01, 0.02 and 0.03 kg/s·m^2.
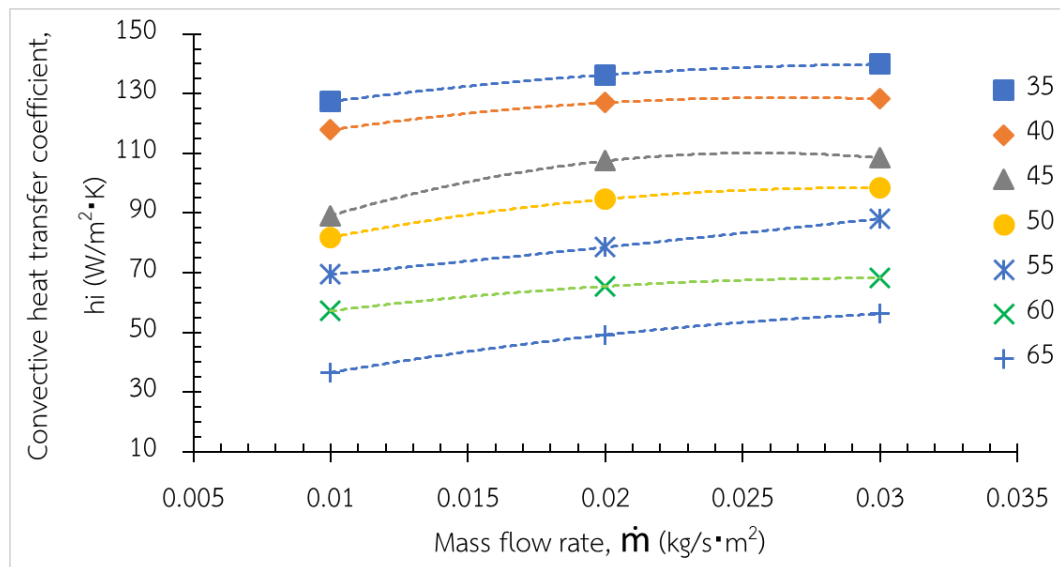
Figure 67 The convective heat transfer coefficient (h_i) of novel solar PCM2 of riser 10 mm with various mass flow rates 0.01, 0.02 and 0.03 kg/s·m^2.
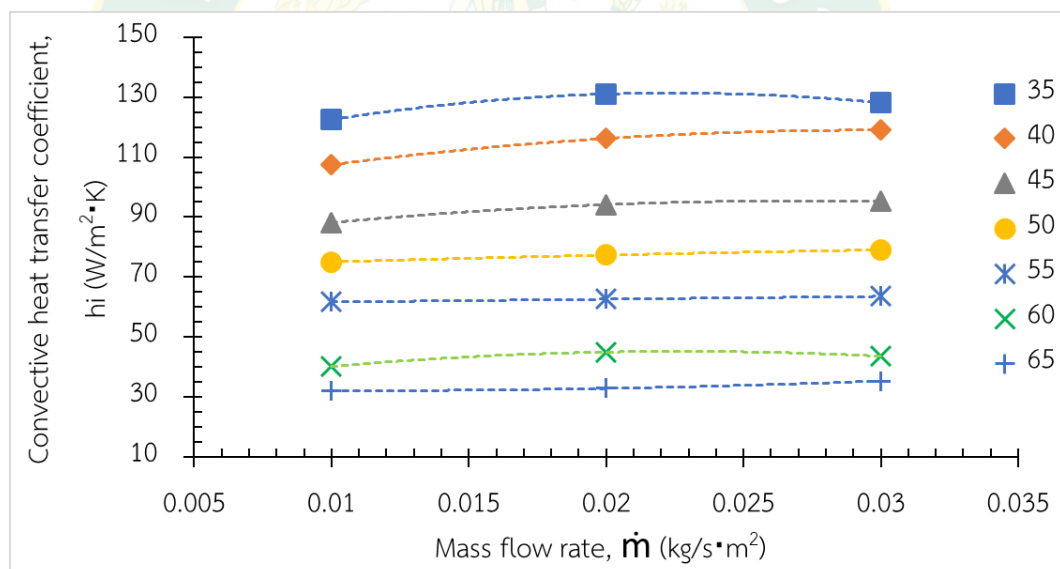
Figure 68 The convective heat transfer coefficient (h_i) of conventional solar collector with various mass flow rates 0.01, 0.02 and 0.03 kg/s·m^2.

In the **Figure 69 Figure 70**, and **Figure 71** showed about the Nusselt Number (Nu) of novel solar collector with various mass flow rates and inlet temperature. The heat transfer inner of the absorber plate to working fluid (water) was presented as the factor of Nusselt Number (Nu) factor of the PCM1 and PCM2 were 5.98 to 2.11 and 5.76 to 1.55 at mass flow rate 0.01 kg/s·m^2, 6.5 to 2.9 and 6.2 to 2.1 at mass flow rate 0.02 kg/s·m^2 while at mass flow rate 0.03 kg/s·m^2 the Nusselt number was 7.16 to 3.1

and 6.34 to 2.4, while the conational was 5.4 to 1.37, 6.1 to 1.41 and 6.13 to 1.5, following to the inlet temperature and Reynold Number, respectively.
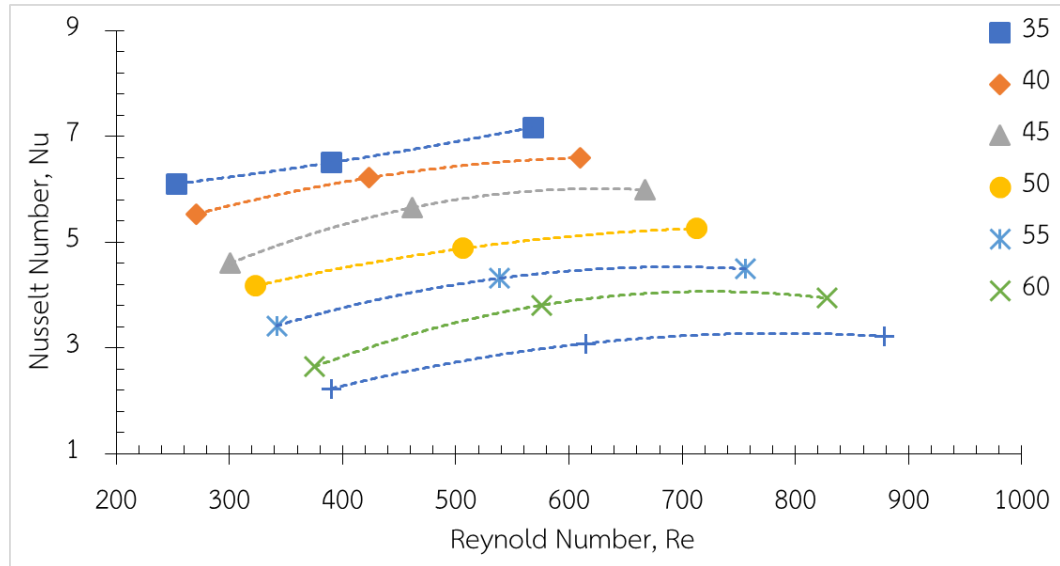
Figure 69 The Nusselt number (N_u) of novel solar collector (PCM1) of riser 16 mm.
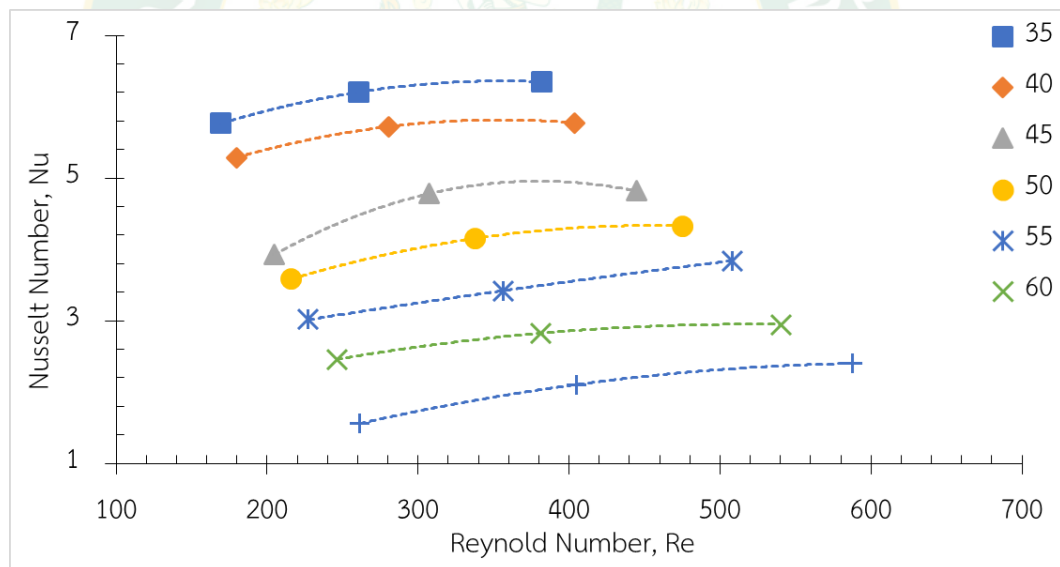
Figure 70 The Nusselt number (N_u) of novel solar collector (PCM2) of riser 10 mm.

From the experimental tested novel solar collector PCM1 and PCM2 were derived the correlation of the Nusselt number (Nu) relates to the Reynold number (Re) and Prandtl number (Pr) as: Correlation: $Nu = 0.143 \, \mathrm{Re}^{0.193} \, \mathrm{Pr}^{1.821}$

Which is 2 < Pr < 5, was showed the relationship of Nusselt number (Nu) between equation and experiment in **Figure 72**.
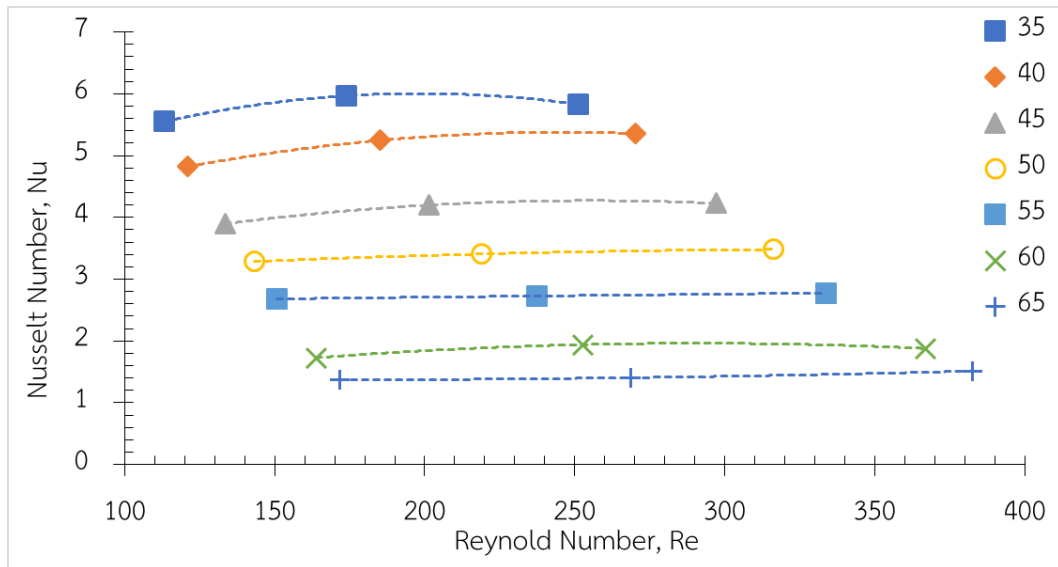
Figure 71 The Nusselt number (Nu) of conventional collector (without PCM).
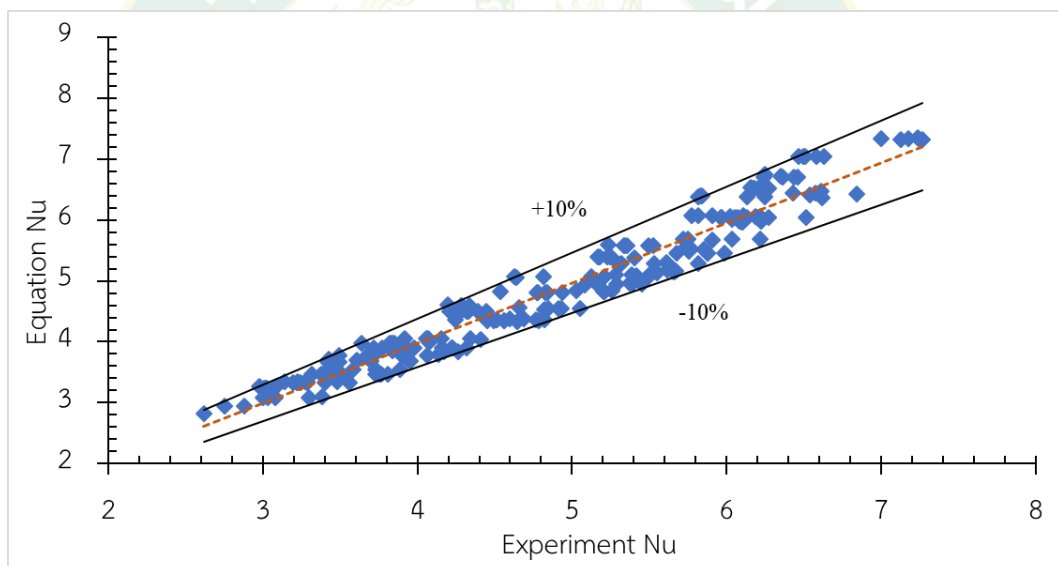
Figure 72 The relationship of Nusselt number (Nu) between equation and experiment.

4.4. The daily tested and the thermal energy predicted in a whole year.

In order to analyze the system analysis, the novel solar collectors and conventional collector were tested in daytime since 8:40 AM to 15:55 PM. The experimental results presented that described the collector performance and showed the several of inlet temperature, outlet temperature and the storage tank temperature. In the **Figure 73** shows the changing of the solar radiation intensity and ambient

temperature during daytime. The maximum solar radiation was around 800 W/m^2 and the ambient temperature was about 31 °C.
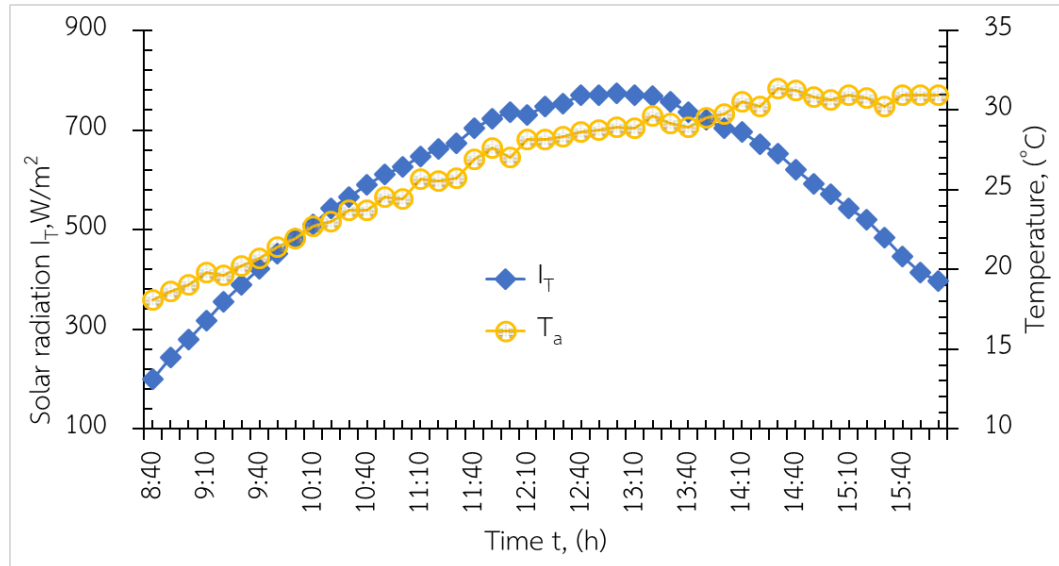
Figure 73 The daily experimental tested, Solar radiation and ambient temperature.
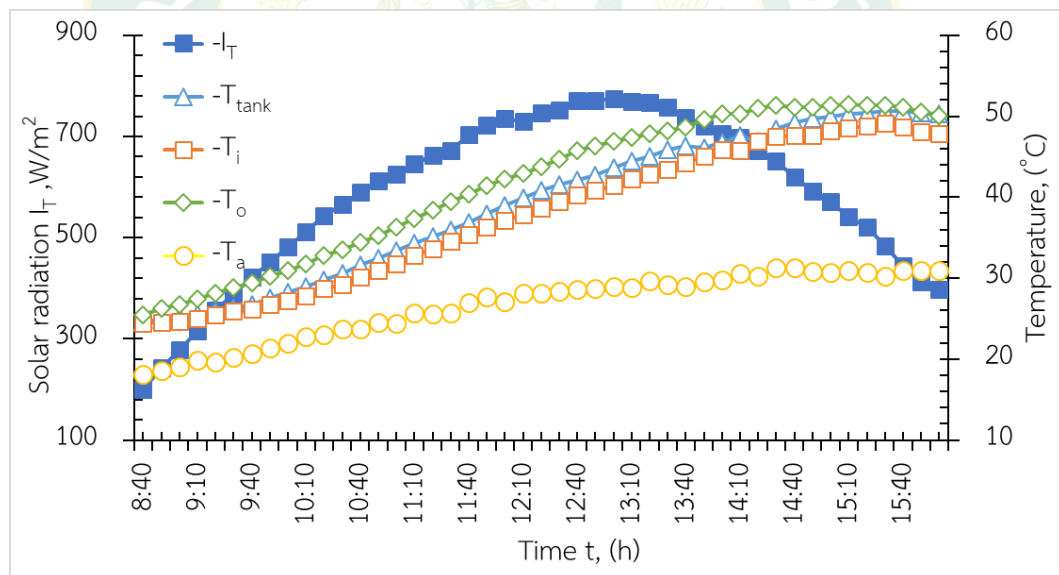
Figure 74 The novel solar collector (PCM1) of riser 16 mm teste.

The experiment was investigated at the initial temperature in 10-liter storage tank of 25 °C and set the water mass flow rate of 0.02 kg/s·m^2. In the **Figure 74** and **Figure 75** were presented the variation of temperature change of the novel solar collector (PCM 1 and PCM 2). The maximum temperature different between inlet and outlet temperature was around 5.1 and 5. 5 °C, respectively during peak solar radiation and the ambient temperature average of 27.2 °C. For the maximum temperature of

both water storage tanks were 50.2 and 51.5 $^{\circ}$C, respectively while the conventional solar collector in **Figure 76** shows the temperature different was around 4.8 $^{\circ}$C and temperature close to the 50 $^{\circ}$C.
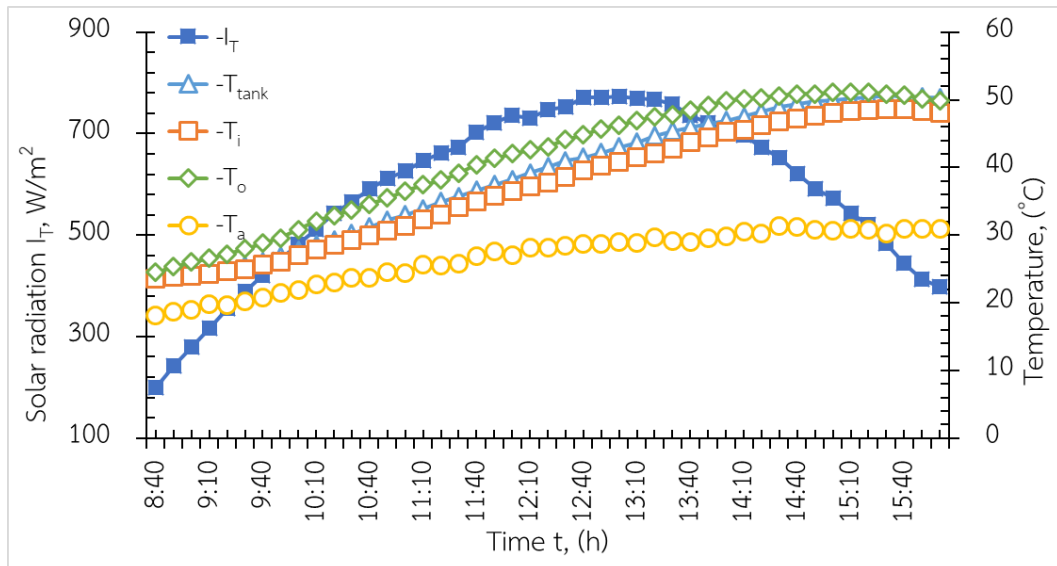
Figure 75 The novel solar collector (PCM2) of riser 10 mm tested.
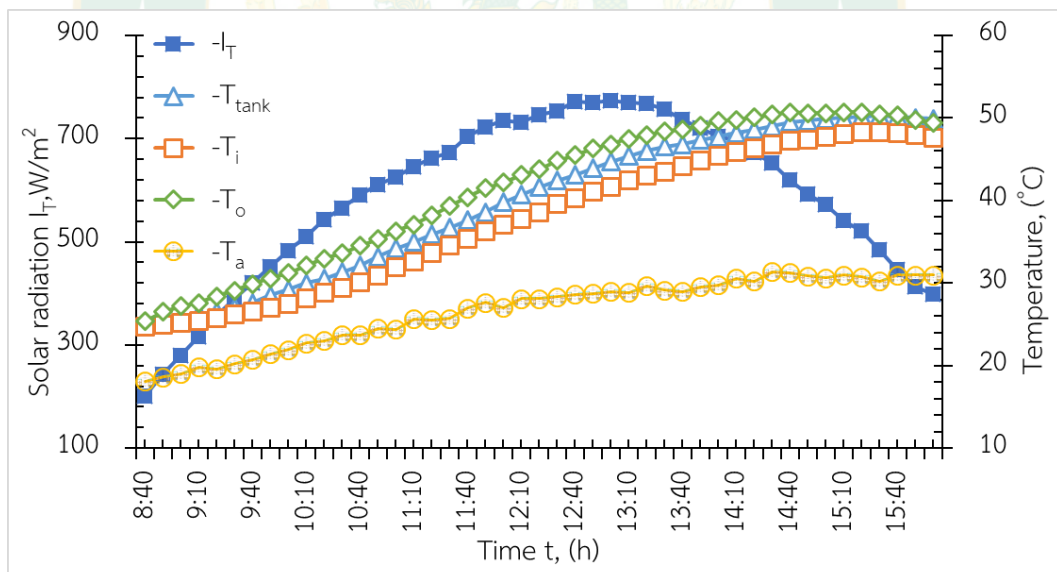
Figure 76 The conventional solar collector (Without PCM) tested.

In **Figure 77** shows the heat gain in the storage tank of each case studies. The heat gain (Q_s) would be varied by the solar radiation variation. At the solar radiation lower than 600 W/m^2, the heat gains both the novel collectors (PCM 1 and PCM 2) and conventional collector (without PCM) were similar. When the solar radiation more than 600 W/m^2, the heat gain of both novel collectors were higher than the conventional

solar collector. The calculated heat gains of using PCM 1, PCM 2 and without PCM were 1,126.3, 1,219.7 and 1,059.01 kJ, respectively. When considered in the term of thermal efficiency, both PCM collectors given the greater thermal efficiency about 8-10%. The novel solar collectors and the conventional collector were experimented for analysis system operation since 8:30 a.m. to 03:00 p.m. under clear sky day condition. The system was operated at the best mass flow rate of 0.03 kg/s·m^2 and circulated the water from the 10-liters storage tank to the collector.
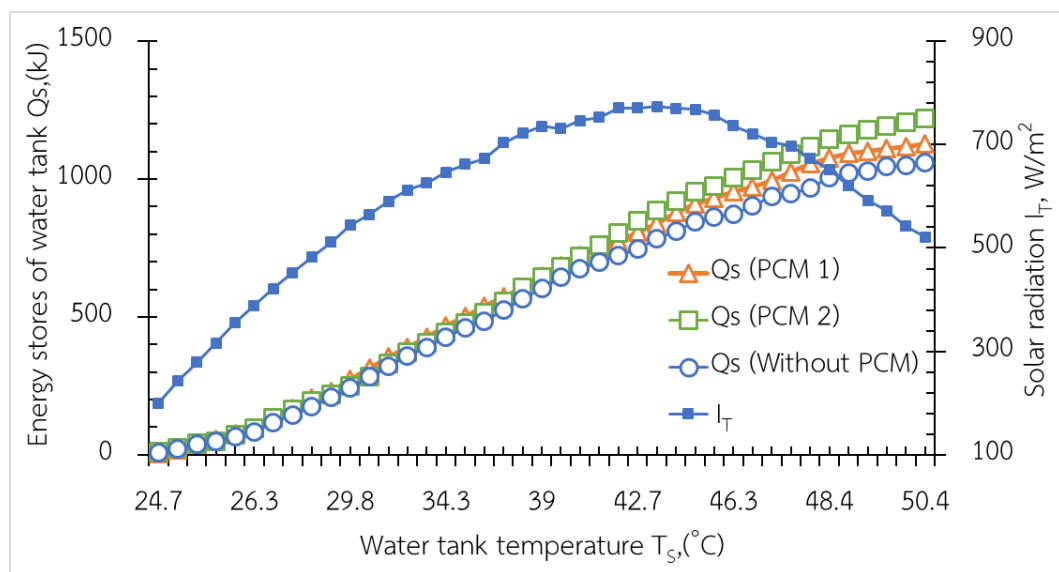
Figure 77 The energy stores of water tank of novel and conventional solar collector tested with the mass flow rate 0.02 kg/s·m^2.
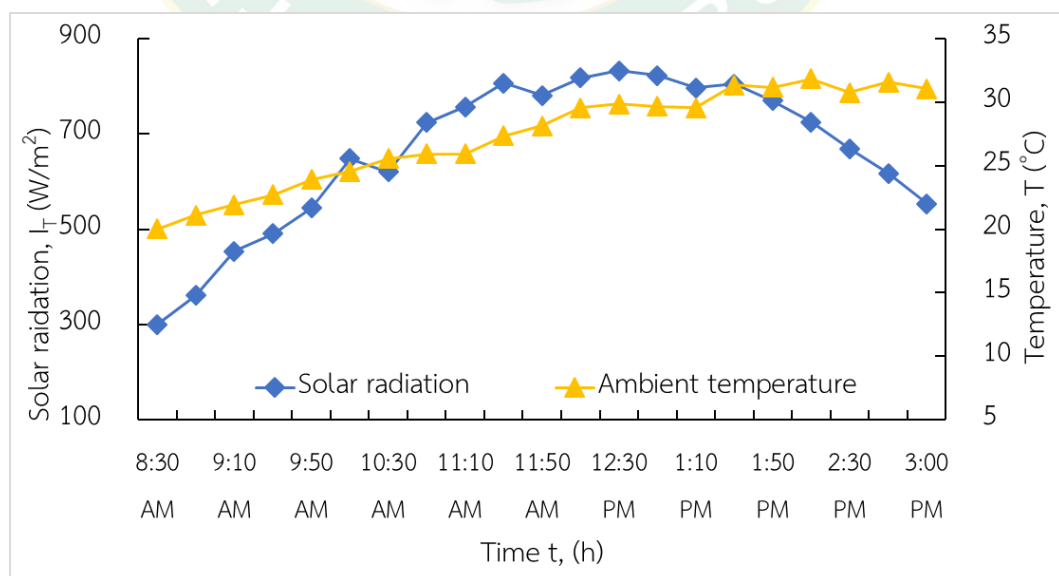
Figure 78 Solar radiation (I_T) and ambient temperature (T_a).
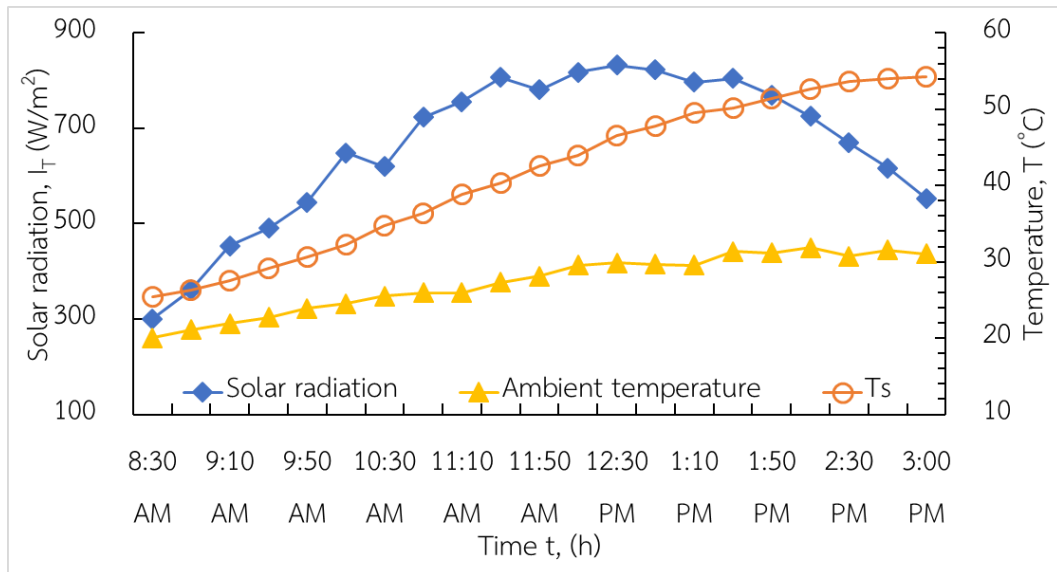
Figure 79 The result of daily system operation of novel solar collectors (PCM 1) tested with mass flow rate of 0.03 kg/s·m^2.
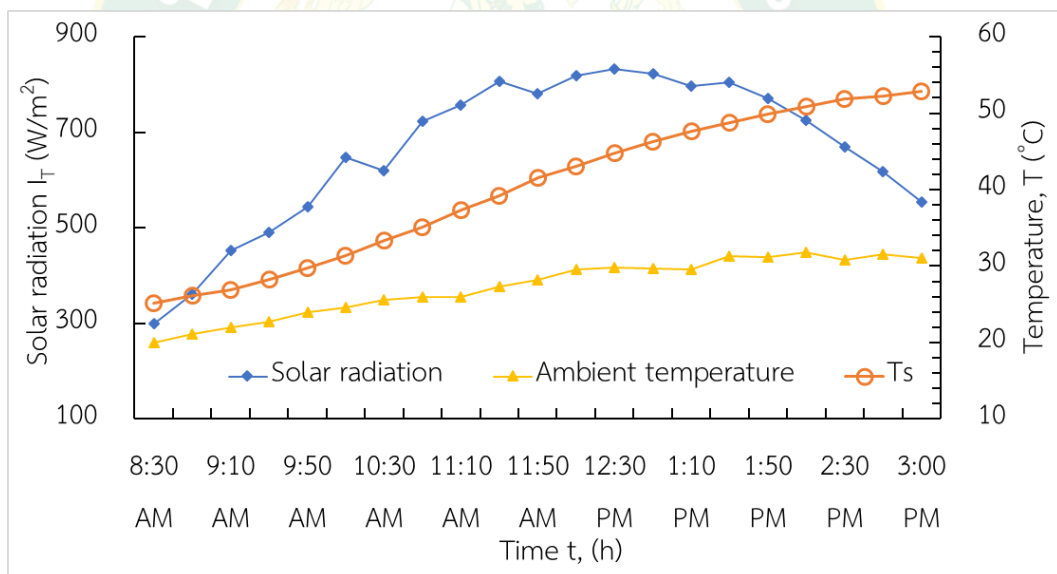
Figure 80 The result of daily system operation of novel solar collectors (PCM 2) tested with mass flow rate of 0.03 kg/s·m^2.

The results in **Figure 78**, **Figure 79**, **Figure 80** and **Figure 81** showed that the storage tank with initial temperature (T_s) was about 25 $^\circ$C and when the solar radiation (I_T) increased, the storage tank temperature was raised continuously following the variation of solar radiation. The maximum solar radiation was around 830 W/m^2 at 12:30 PM, the temperature T_s of storage tank were increased to 45, 46, and 44 $^\circ$C, respectively. The PCM 1 was collected more thermal energy than other collectors until

the end operating at 3:00 p.m. which the storage tank temperature was 55 °C while PCM 2 and without PCM was 53 ℃ and 51°C, respectively.
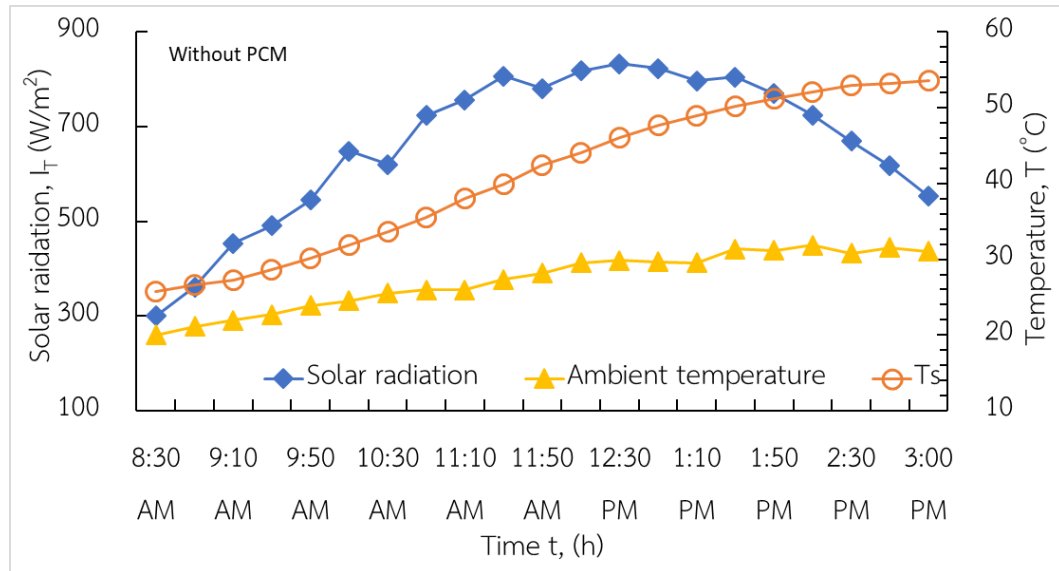
Figure 81 The result of daily system operation of conventional solar collectors (without PCM) tested with mass flow rate of 0.03 kg/s·m².

4.4.1. The thermal energy predicted in a whole year.

The amount of solar energy incident on earth each could be equivalent to 1.9 x 10^{14} tCOE while the globe consumes annual amount of energy at 9 x 10^9 which is 0.005 % of solar energy incidence cause of wind, rainfall, wave, biomass and so forth. In Thailand, the solar radiation map was developed by department of energy indicates that the maximum solar radiation level during April – May of the value is in a range of 20 – 24 MJ/m²-d. the area that has highest solar radiation level in the northeastern part which is around 19-20 MJ/m²-d.
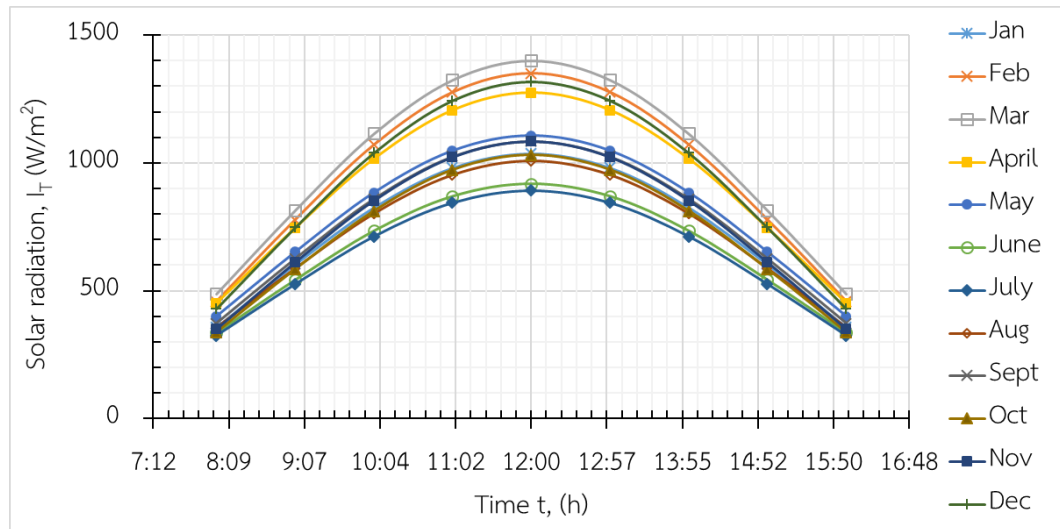
Figure 82 Prediction daily average solar radiation of monthly in Chiangmai, Thailand.
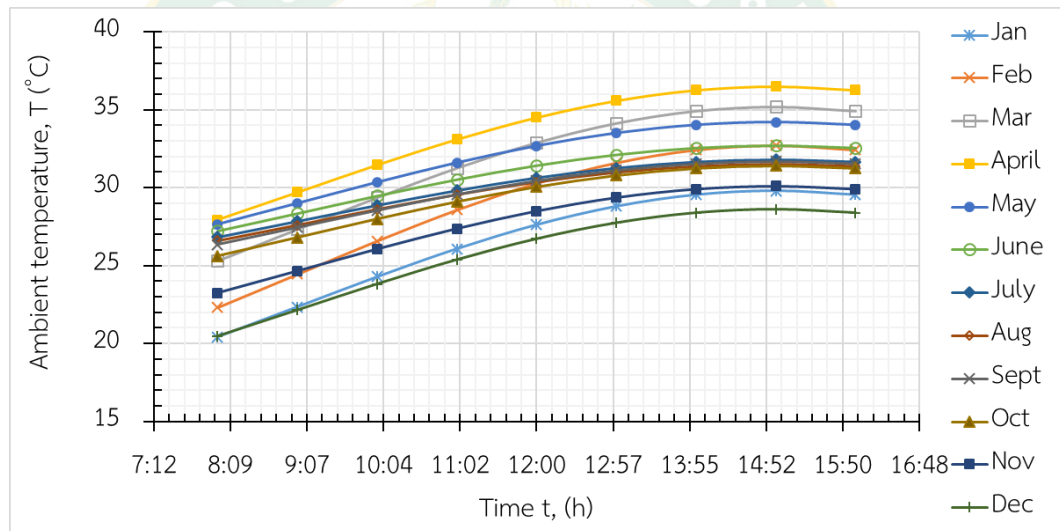
Figure 83 Prediction monthly ambient temperature of the year in Chiangmai, Thailand.

The average value for the whole country is 18.2 MJ/m^2-d. The developed of mathematic modeling of the solar radiation incidences on this area in the theory of the novel solar collector performance in the whole year was calculated to perceive the performance over the year as seen in the **Figure 82** of the solar radiation and **Figure 83** of the ambient temperature. The solar radiation and ambient temperature in the Chiangmai province, Thailand could be estimated using the equation and latitude of the location which could the data predicted to find out the thermal performance in the whole year of each solar collectors were installed with the storage

tank 11 kg of water. In the **Figure 82**, prediction daily average solar radian in average of the month. The data predicted from 8:00 to 16:00 each month while the solar radiation of the January radiation value was 357.3 to 1036.9 W/m^2 in average, February was 457.3 to 1350.2 W/m^2, March was 486.9 to 1401.1 W/m^2, April was 451.5 to 1274.2 W/m^2, on May was 400.3 to 1107.1 W/m^2, June was 324.06 to 892.17 W/m^2, August was 356.36 to 1007.58 W/m^2, September was 372.08 to 1085.31 W/m^2, October was 337.08 to 1031.31 W/m^2, November was 350.51 to 1084.64 W/m^2 and December was 429.8 to 1317.5 W/m^2 in average. The data predicted of ambient temperature in the **Figure 83** was 20.4 to 29.8 $^\circ$C in January, 22.3 to 32.7 $^\circ$C in February, 25.3 to 35.2 $^\circ$C in March, 27.9 to 36.5 $^\circ$C in April, 27.6 to 34.2 °C in May, 27.2 to 32.7 $^\circ$C in June, 26.8 to 31.8 $^\circ$C in July, 26.5 to 31.5 $^\circ$C in August, 26.3 to 31.7 $^\circ$C in September, 23.6 to 31.4 $^\circ$C in October and 23.3 to 30.1 $^\circ$C in December. Solar collector was simulated using the prediction equation of the solar radiation and ambient temperature where located in Chiang Mai province, Thailand. While, thermal efficiency of solar collector has been using into the whole year prediction of the thermal energy storage of each solar collector. In this, the storage tank was 21 kg and final predicted of tank temperature was 50 $^\circ$C of water was predicted in average of solar radiation and ambient temperature of each month of the year.

In the **Figure 84**, **Figure 85** and **Figure 86**, The novel solar collector integrated with phase change material riser 16 mm outside diameter (PCM1) was estimated with the mass flow rate 0.03 kg/s·m^2 which the storage tank temperature (T$_s$) were 25 $^\circ$C, 15 $^\circ$C, 10 $^\circ$C, 15 $^\circ$C, 20 $^\circ$C, 20 $^\circ$C, 30 $^\circ$C, 30 $^\circ$C, 25 $^\circ$C, 25 $^\circ$C, 25 $^\circ$C, 25 $^\circ$C, while the thermal storage of the system was 1992.55 kW, 2964.19 kW, 3317.65 kW, 2985.66 kW, 2468.42 kW, 1760.07 kW, 1685.62 kW, 2041.45 kW, 2174.82 kW, 2041.09 kW and 2615.2 kW in average following the daily efficiency and monthly, while the initial temperature was change following to the month predicted, respectively.
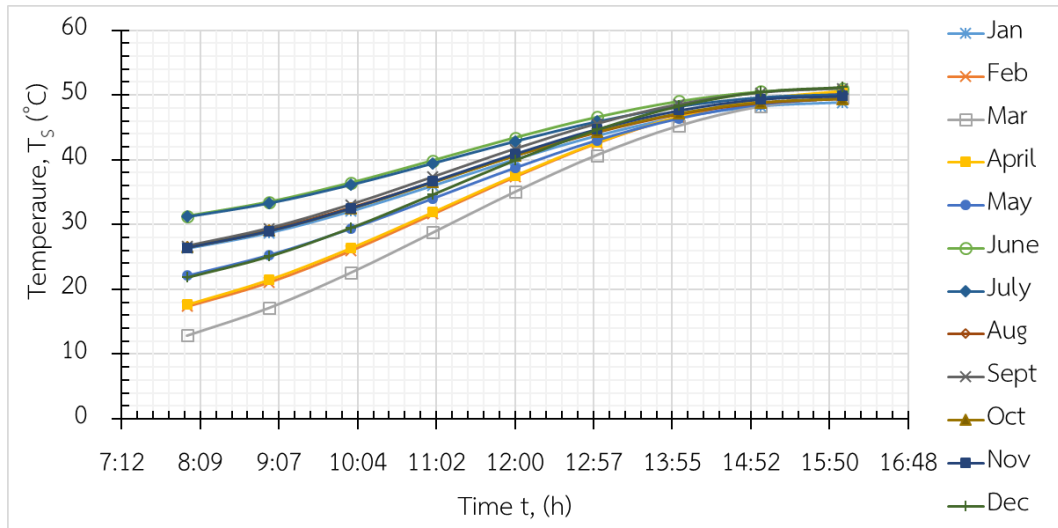
Figure 84 The prediction of water tank temperature of the novel solar collector
integrated with PCM riser 16 mm (PCM1).
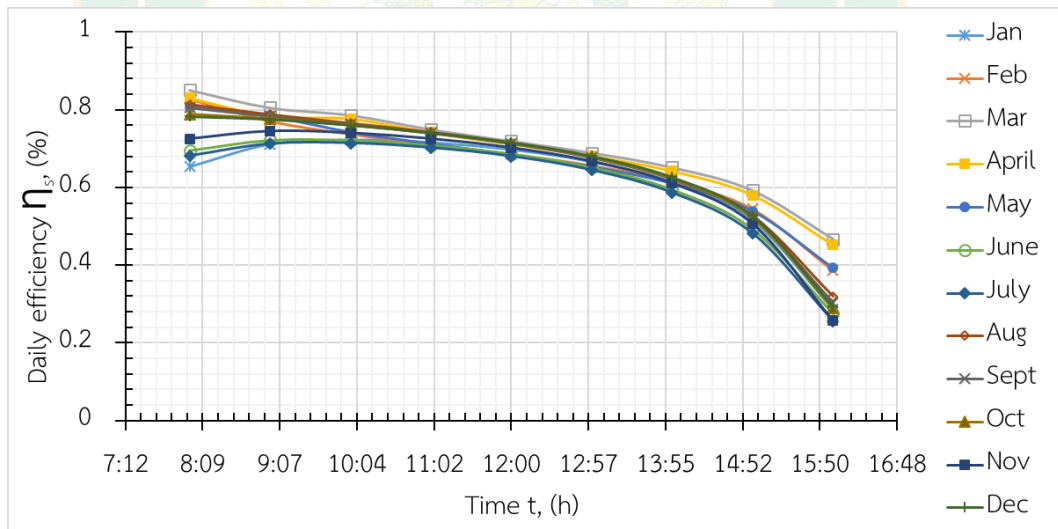
Figure 85 The daily efficiency of the novel solar collector (PCM1).
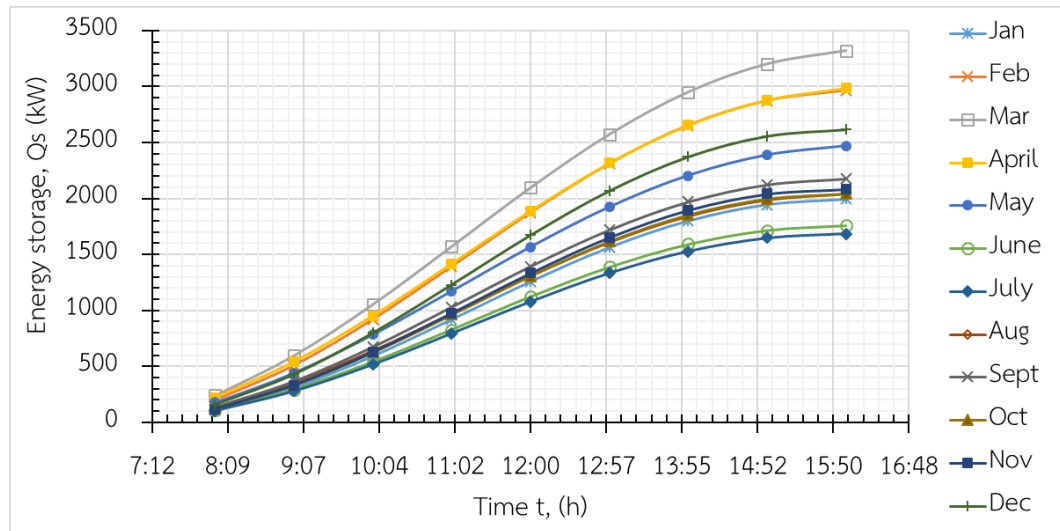
Figure 86 The energy storage of water tank by the novel solar collector (PCM1).

In the **Figure 87**, **Figure 88** and **Figure 89**, The novel solar collector integrated with phase change material riser 10 mm diameter (PCM2) which the storage tank temperature (T_s) was 30 °C, 20°C, 15 °C, 20 °C, 25 °C, 30 °C, 35 °C, 30 °C, 25 °C, 30 °C, 30 °C, 20 °C, while the thermal energy of the system was 1709.05 kW, 2603.49 kW, 2926.06 kW, 2619.81 kW, 2144.09 kW, 1638.37 kW, 1425.55 kW,1752.86 kW,1793.06 kW, 2430.38 kW in average following to the daily efficiency and monthly, while the initial temperature was change following to the month predicted, respectively.
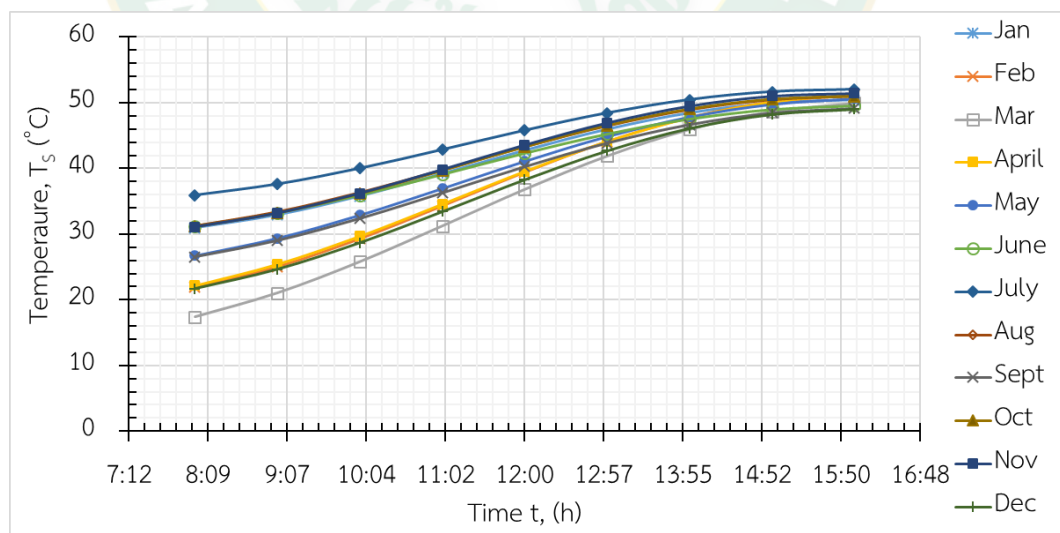
Figure 87 The tank temperature of the novel solar collector (PCM2).
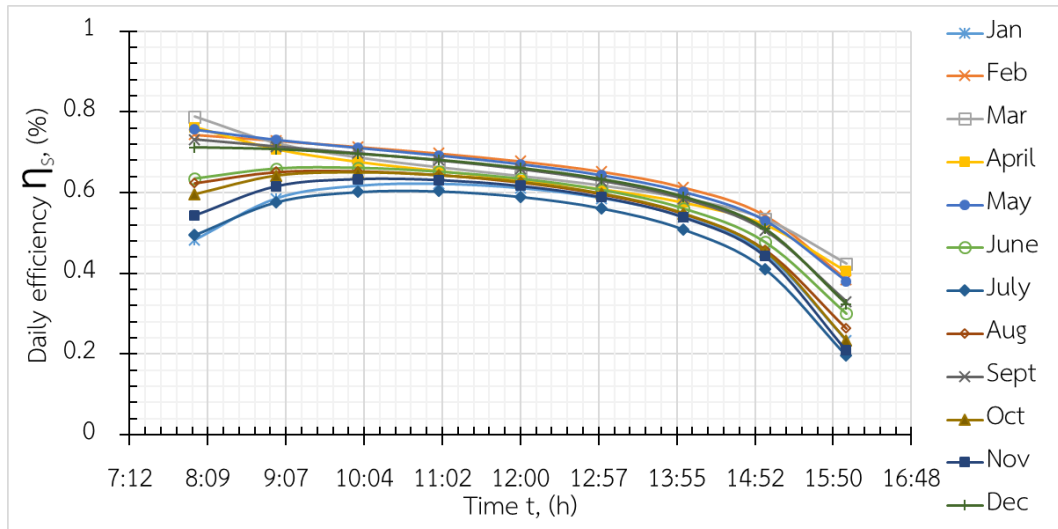
Figure 88 The daily efficiency of the novel solar collector (PCM2).
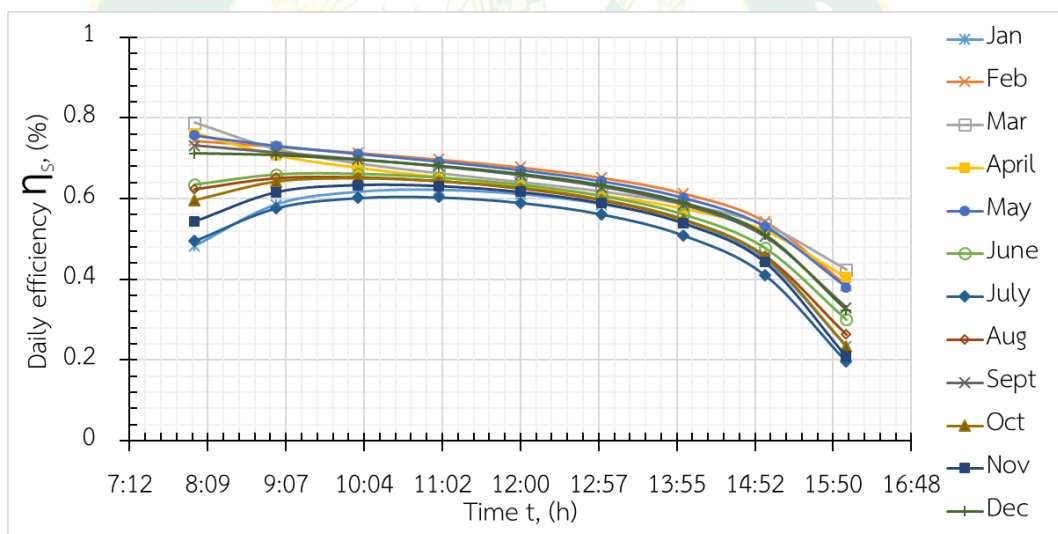
Figure 89 The energy stores of water tank by the novel solar collector (PCM2).
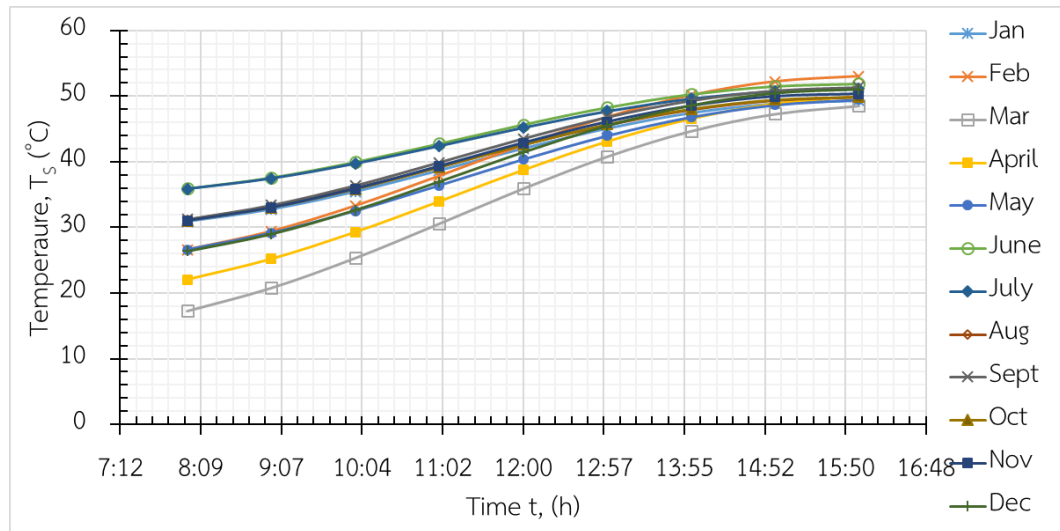
Figure 90 The temperature of water tank by the conventional solar collector (without PCM).

In the **Figure 90**, **Figure 91** and **Figure 92**, The conventional solar collector without phase change material integrated was estimated the storage tank temperature (T_s) was 30 °C, 25 °C, 15 °C, 20 °C, 25 °C, 35 °C, 35 °C, 30 °C, 30 °C, 30 °C, 25 °C while the thermal energy of the system was 1620.3 kW, 2345.81 kW, 2810.55 kW, 2513.92 kW, 2050.54 kW, 1414.11 kW, 1347.36 kW, 1666.71 kW, 1784.89 kW,1666.03 kW and 2175.58 kW, in average following to the daily efficiency and monthly while the initial temperature was change following to the month predicted, respectively.
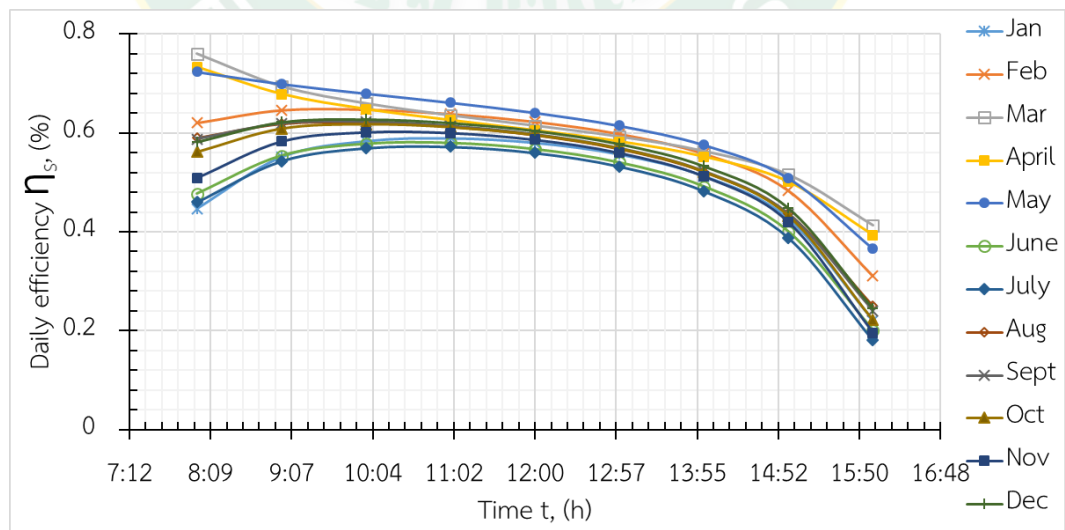
Figure 91 The daily efficiency of the conventional solar collector (without PCM).
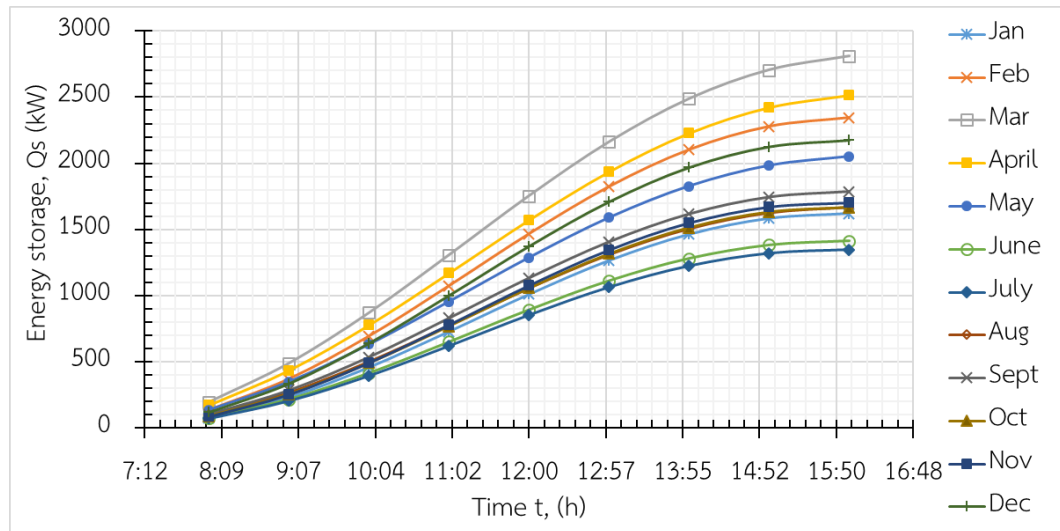
Figure 92 The energy stores of water tank by the conventional solar collector (without PCM).

The novel solar and conventional solar predicted in average value of monthly were showed in the **Figure 93**, the thermal energy of each solar collector was using the average data in a day and the day of the month which found the average of the monthly energy produced over a year.
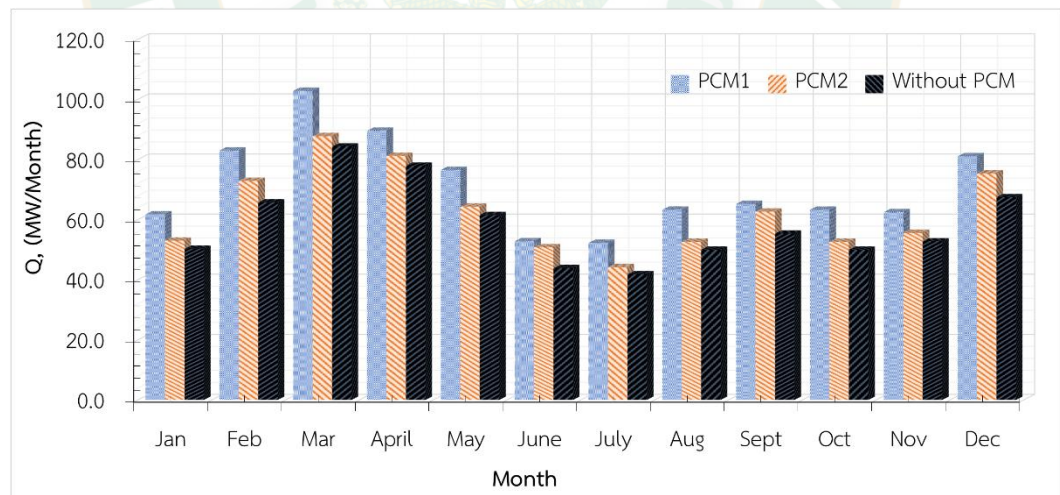
Figure 93 The energy consumption of the novel and conventional solar collector in the whole year.

Both the solar collector's thermal energy produced of PCM1, PCM2 and without PCM were 61.8 MW, 53.MW and 50.2 MW in January, 83.0 MW, 72.9 MW and in February, 102.8 MW, 87.8 MW and 84.8 MW in March, 89.6 MW, 81.2 MW and 77.9

MW in April, 76.5 MW, 64.3 MW and 61.5 MW in May, 52.8 MW,50.8 MW and 43.8 MW in June,52.3 MW, 44.2 MW and 41.8 MW in July, 63.3 MW, 52.6 MW and 50 MW in August, 65.2 MW, 62.7 MW and 55.3 MW in September, 63.3 MW, 52.6 MW and in October, 62.5kM, 55.6 MW and 52.7 MW in November and in December were 81.1 MW, 75.3 MW and 67.4 MW, respectively.

4.5. The phase change material in the riser tube

The novel solar collector integrated with phase change material (RT42) riser absorbed thermal energy during melting or freezing (a melting point is 38 to 43 °C) which could be stored a lot of amount of energy. The PCM riser 10 and 16 mm outside diameter inserted into the absorber plate and storage the energy during experimental which the pneumonia of the phase change material could be effected during the daily experimental in period of phase change and the melting temperature 38 to 43 °C with the heat storage capacity ± 165 kJ/kg which the properties, in the **Figure 94**:

- High thermal energy storage capacity

- Heat storage and release take place at relative constant temperatures

- No supercoiling effect, Chemically inert

- Long life product, with stable performance through the phase change cycles

- Melting temperature range between 38-42 °C available

- Price $ 14.76 per kilogram (Australia Dollar)
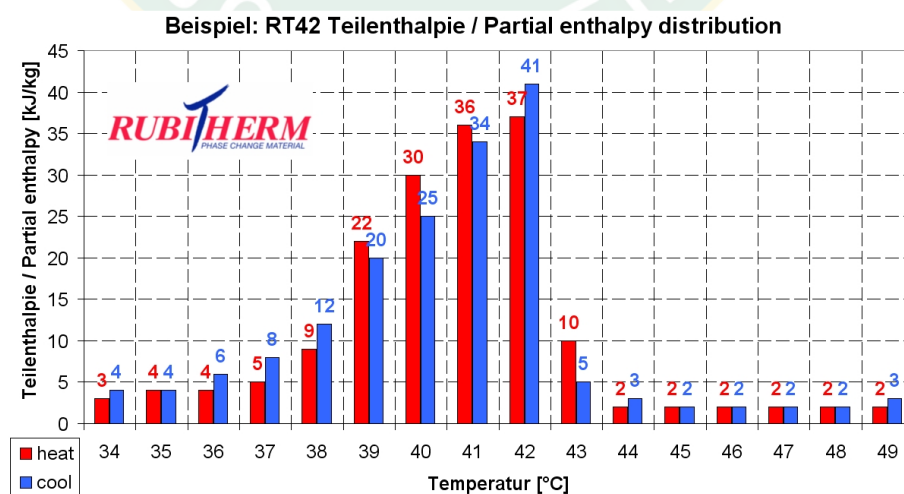
Figure 94 Measured with 3-layer calorimeter (RUBITHERM, 2018).

The novel solar collector integrated with phase change material filled in different riser diameter of 10 and 16 outside diameter with the volumetric of the riser were 5 x 10 $^{-2}$ and 1.6 x 10 $^{-1}$ liters which amount of the phase change material riser were 4.4 x 10^{-2} and 1.4 x 10^{-1} kg of (RT42).
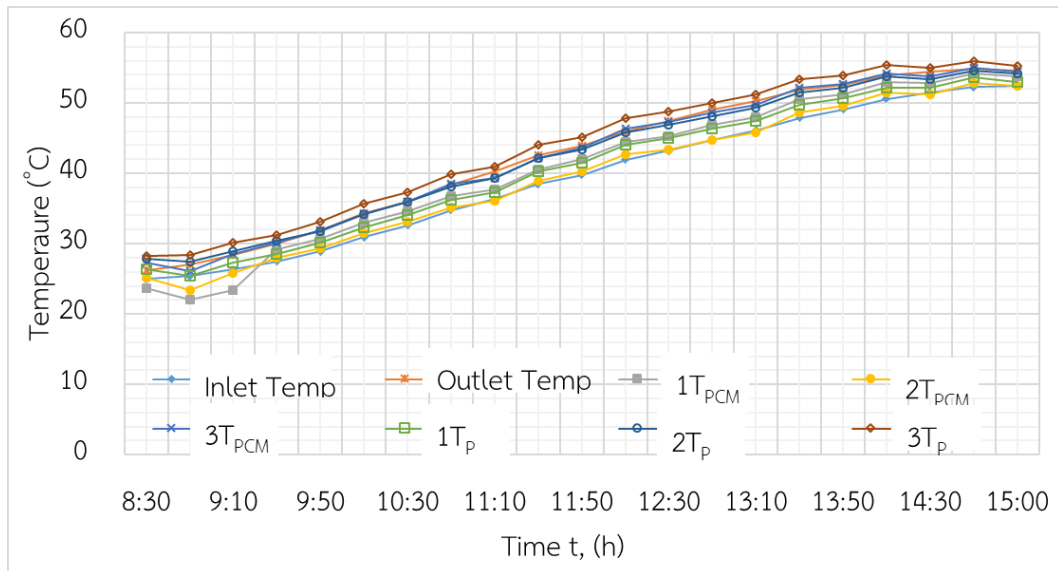
Figure 95 The absorber plate temperature and phase change material riser temperature of PCM1.
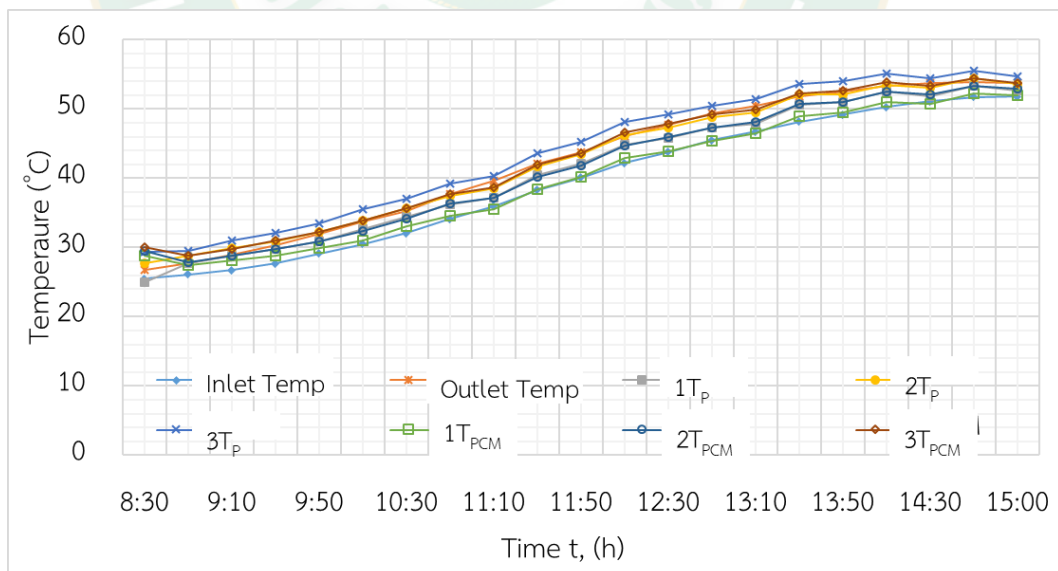
Figure 96 The absorber plate temperature and phase change material riser temperature of PCM2.
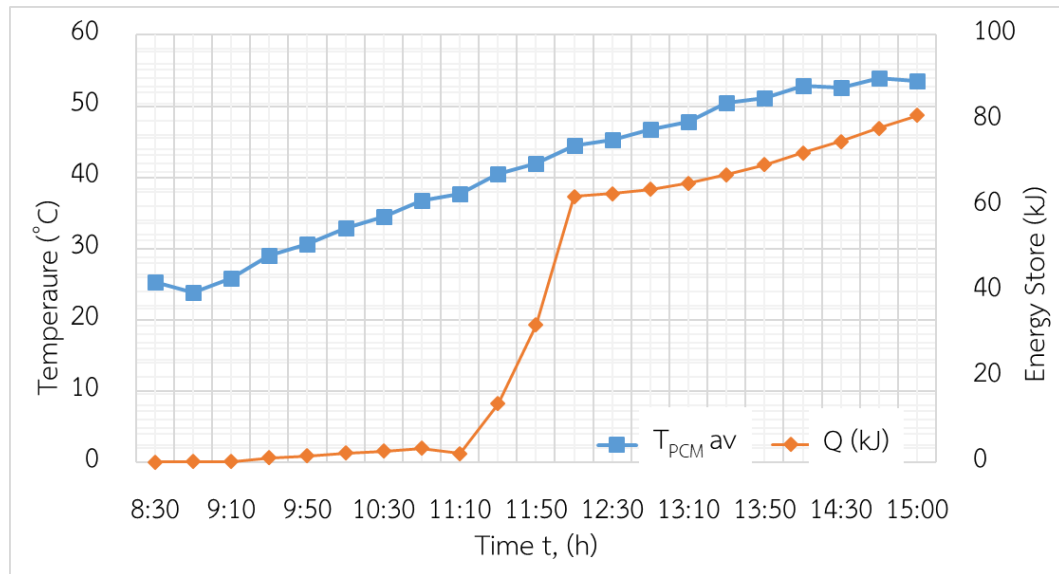
Figure 97 Average PCM temperature and Energy store of PCM1.
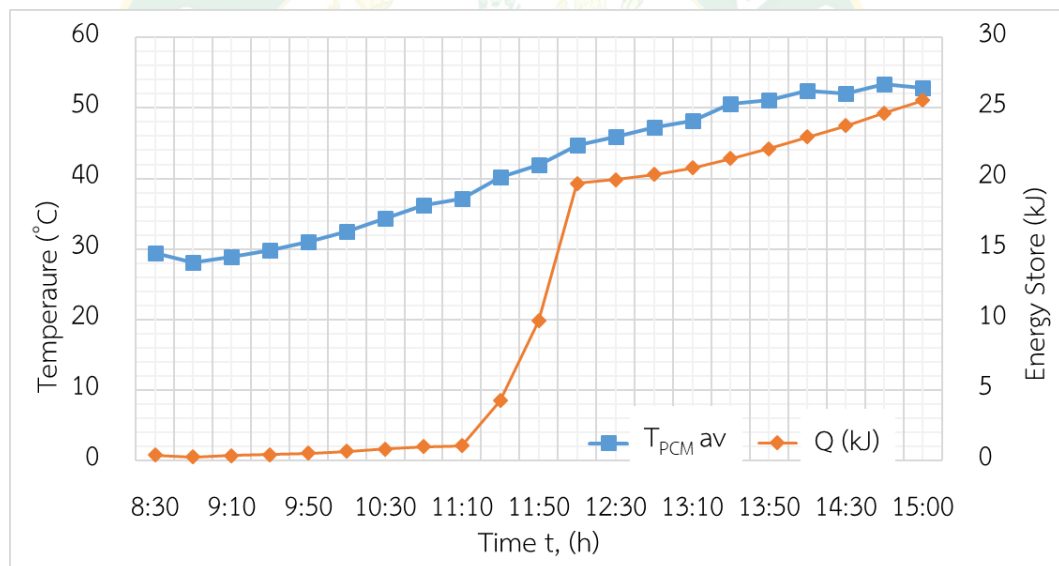
Figure 98 Average PCM temperature and Energy store of PCM2.

The daily experimental with the mass flow rate 0.03 kg/s·m^2 which the thermal energy store of the storage tank was showed in the **Figure 79** and **Figure 80** while the absorber plate temperature and the PCM riser temperature was various following to the dimension of the collector as the inlet water temperature point with the lowest then rising to the highest closed to the outlet temperature of the solar collector showed in **Figure 95** and **Figure 96**, while the energy store of the phase change material was showed in **Figure 97** and **Figure 98**.

Chapter 5

Conclusion and further work

In this research of the Flat-Plate solar collector integrated with the phase change material riser in different diameter were tested with the ASHRAE Standard 93-2003 of thermal efficiency effecting with the various mass flow rate of rate 0.01, 0.02 and 0.03 kg/s·m^2. The novel and conventional solar collectors were predicted the energy production in the whole year.

Conclusion

The novel solar collector was integrated with phase change material riser in different outside diameter of 16 and 10 mm (RT42 a melting point 38 – 43 $^\circ$C) were arrange as PCM1, PCM2 which were study the thermal performance following to the ASHRAE Standard 93-2003. The thermal performance of the novel solar collector had been conducted as using the various mass flow rate 0.01, 0.02 and 0.03 kg/s·m^2 and such as main condition as the solar radiation higher than 790 W/m^2, ambient temperature not over than 30°C, air velocity not over than 2.2-4.4 m/s and the various inlet temperature of 35 to 65 $^\circ$C. Both novel solar collector and the conventional solar collector were showed that the novel solar collector integrated with phase change material with riser 16 mm outside diameter was given the highest thermal performance with the mass flow rate 0.03 kg/s·m^2 which represented as $F_R(\tau\alpha)_e$ 0.835 and F_RU_L 9.68 W/m^2·Kwhile the novel collector integrated with the PCM riser 10 mm and conventional solar collector were given highest thermal energy with the mass flow rate 0.02 kg/s·m^2 were $F_R(\tau\alpha)_e$ 0.828, 0.713 and F_RU_L 11.304 W/m^2·K, 10.642 W/m^2·K. The convective heat transfer coefficient of the novel solar collectors also were studied with using the standard condition which seen that the collected energy was changing following to the change of flow rate and various of inlet temperature, otherwise, the riser inserted into the absorber plate tube in difference diameter were effected the velocity flow rate inner of each collector integrated which the volume of the riser inner collector was effected to the Reynold Number (Re) of each collector were bigger riser inserted into the collector was increased the values of the number while the Prandtl

Number (Pr) was effected on the fluid temperature circulating inside. The heat transfers (hi) were calculated following to the energy collector, average temperature of the fluid and the average wall temperature of the collector which the convective heat transfer efficiency could calculated from the new correlation of novel solar collector:

Nusselt number (N_u) relates to the Reynold number (R_e) and Prandtl number (P_r) as:

Correlation: $Nu = 0.143 \text{Re}^{0.193} \text{Pr}^{1.821}$ which 2 < Pr < 5 .

The thermal energy of each solar collector were predicted of energy production in the whole year which seen the novel solar collector integrated with Phase Change Material riser 16 mm outside diameter was given highest energy production **Figure 99**:
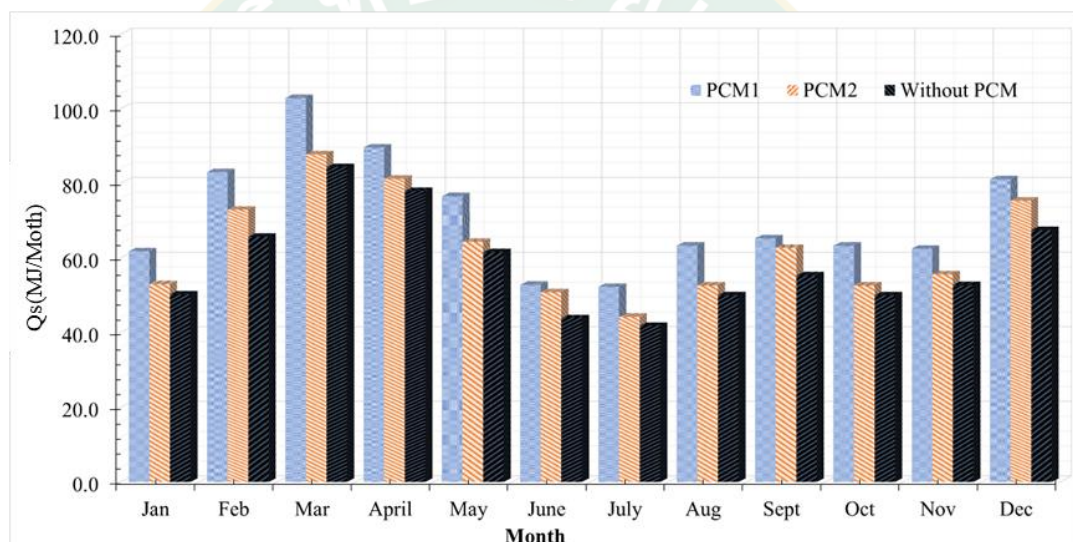
Figure 99 Energy consumption in a whole year.

Future work

The development never ends of integrated of the solar collector to get better performance, the future study, it should be study the phenomena of the phase change material inside the solar collector and selected the PCM in difference type, characteristic such the melting point and riser side. The phenomena of energy store of PCM in different type should be studied.

REFERENCES

Al-Madani, H. 2006. The performance of a cylindrical solar water heater. **Renewable Energy**, 31(11), 1751-1763.

Balaji, K., Iniyan, S. & Muthusamyswami, V. 2017. Experimental investigation on heat transfer and pumping power of forced circulation flat plate solar collector using heat transfer enhancer in absorber tube. **Applied Thermal Engineering**, 112(237-247.

Bellan, S., Alam, T. E., González-Aguilar, J., Romero, M., Rahman, M. M., Goswami, D. Y. & Stefanakos, E. K. 2015. Numerical and experimental studies on heat transfer characteristics of thermal energy storage system packed with molten salt PCM capsules. **Applied Thermal Engineering**, 90(970-979.

Bhowmik, H. & Amin, R. 2017. Efficiency improvement of flat plate solar collector using reflector. **Energy Reports**, 3(119-123.

Bliss, R. W. 1959. The derivations of several "Plate-efficiency factors" useful in the design of flat-plate solar heat collectors. **Solar Energy**, 3(4), 55-64.

Cabeza, L. F., Castell, A., Barreneche, C., de Gracia, A. & Fernández, A. I. 2011. Materials used as PCM in thermal energy storage in buildings: A review. **Renewable and Sustainable Energy Reviews**, 15(3), 1675-1695.

Cengel, Y. & Cimbala, J. 2013. **Fluid Mechanics Fundamentals and Applications: Third Edition**. McGraw-Hill Higher Education.

Duffie, J. A. & Beckman, W. A. 2013. **Solar engineering of thermal processes**. Available

EnergyOutlook2017. 16 Oct 2018. Southeast Asia Energy Outlook 2017.

Gary. 2006. Measuring Collector Performance and Efficiency.

Gond, B. K., , M. K. G. & , C. S. M. 2012. Manufacturing and performance analysis of solar flat plate collector with phase change material. **International Journal of Emerging Technology and Advanced Engineering**, 2(3), 2250.

Gupta, A., Gaur, M. K., Crook, R. & Dixon-Hardy, D. W. 2017. Experimental investigation of heat removal factor in solar flat plate collector for various flow configurations AU - Malvi, C. S. **International Journal of Green Energy**, 14(4), 442-448.

Hollands, K. G. T. 1965. Honeycomb devices in flat-plate solar collectors. **Solar Energy**, 9(3), 159-164.

ICNQT. 2018. **Nano PCM**. [Online]. Available http://icnqt.com/nano-products/nano-pcm/.

IEA. 2019. **Shaping a secure and sustainable energy future**. [Online]. Available https://www.iea.org/.

Jafarkazemi, F. & Ahmadifard, E. 2013. Energetic and exergetic evaluation of flat plate solar collectors. **Renewable Energy**, 56(55-63.

Jaisankar, S., Radhakrishnan, T. K. & Sheeba, K. N. 2009. Experimental studies on heat transfer and friction factor characteristics of thermosyphon solar water heater system fitted with spacer at the trailing edge of twisted tapes. **Applied Thermal Engineering**, 29(5), 1224-1231.

Khalifa, A. J. N. & Abdul Jabbar, R. A. 2010. Conventional versus storage domestic solar hot water systems: A comparative performance study. **Energy Conversion and Management**, 51(2), 265-270.

Khalifa, A. J. N., Suffer, K. H. & Mahmoud, M. S. 2013. A storage domestic solar hot water system with a back layer of phase change material. **Experimental Thermal and Fluid Science**, 44(174-181.

Koca, A., Oztop, H. F., Koyun, T. & Varol, Y. 2008. Energy and exergy analysis of a latent heat storage system with phase change material for a solar collector. **Renewable Energy**, 33(4), 567-574.

Koyuncu, T. & Lüle, F. 2015. Thermal Performance of a Domestic Chromium Solar Water Collector with Phase Change Material. **Procedia - Social and Behavioral Sciences**, 195(2430-2442.

Lin, S. C., Al-Kayiem, H. H. & Aris, M. 2012. Experimental investigation on the performance enhancement of integrated PCM-flat plate solar collector. **Journal of Applied Sciences**, 12(24), 2390-2396.

Liu, Z.-H., Hu, R.-L., Lu, L., Zhao, F. & Xiao, H.-s. 2013. Thermal performance of an open thermosyphon using nanofluid for evacuated tubular high temperature air solar collector. **Energy Conversion and Management**, 73(135-143.

Loem, S., Deethayat, T., Asanakham, A. & Kiatsiriroat, T. 2019. Thermal characteristics on melting/solidification of low temperature PCM balls packed bed with air charging/discharging. **Case Studies in Thermal Engineering**, 14(100431.

Ministry of Energy, T. 2019. RENEWABLE ENERGY OUTLOOK THAILAND.

Murugan, M., Vijayan, R., Saravanan, A. & Jaisankar, S. 2019. Performance enhancement of centrally finned twist inserted solar collector using corrugated booster reflectors. **Energy**, 168(858-869.

Naghavi, M. S., Ong, K. S., Badruddin, I. A., Mehrali, M., Silakhori, M. & Metselaar, H. S. C. 2015. Theoretical model of an evacuated tube heat pipe solar collector integrated with phase change material. **Energy**, 91(911-924.

Papadimitratos, A., Sobhansarbandi, S., Pozdin, V., Zakhidov, A. & Hassanipour, F. 2016. Evacuated tube solar collectors integrated with phase change materials. **Solar Energy**, 129(10-19.

Polvongsri, S. (2013). **ASHRAE STANDARD 93-2003 METHODS OF TESTING TO DETERMINE THE THERMAL PERFORMANCE OF FLAT-PLATE SOLAR COLLECTORS**: CHING MAI: THERMAL SYSTEM RESEARCH UNIT.

Reddy, K. S. 2007. Thermal Modeling of PCM-Based Solar Integrated Collector Storage Water Heating System. **Journal of Solar Energy Engineering**, 129(4), 458-464.

RUBITHERM. 2018. **Phase Change Material** [Online]. Available https://www.rubitherm.eu/en/.

Sarawut , P. & Kiatsiriroat, T. 2014. Performance Analysis of Flat-Plate Solar Collector Having Silver Nanofluid as a Working Fluid AU. **Heat Transfer Engineering**, 35(13), 1183-1191.

Struckmann, F. 2008. Analysis of a Flat-plate Solar Collector. **Heat and Mass Transport**.

Syam Sundar, L., Kirubeil, A., Punnaiah, V., Singh, M. K. & Sousa, A. C. M. 2018. Effectiveness analysis of solar flat plate collector with Al2O3 water nanofluids and with longitudinal strip inserts. **International Journal of Heat and Mass Transfer**, 127(422-435.

Taheri, Y., Ziapour, B. M. & Alimardani, K. 2013. Study of an efficient compact solar water heater. **Energy Conversion and Management**, 70(187-193.

UN. 16 Oct 2018. **The 2017 Revision of World Population Prospects**. [Online]. Available https://population.un.org/wpp/.

Weather, T. 2019. Thai Meteorological Department.

Wongcharee, K. & Eiamsa-ard, S. 2011. Heat transfer enhancement by twisted tapes with alternate-axes and triangular, rectangular and trapezoidal wings. **Chemical Engineering and Processing: Process Intensification**, 50(2), 211-219.

Wu, W., Dai, S., Liu, Z., Dou, Y., Hua, J., Li, M., Wang, X. & Wang, X. 2018. Experimental study on the performance of a novel solar water heating system with and without PCM. **Solar Energy**, 171(604-612.

Zambolin, E. & Del Col, D. 2010. Experimental analysis of thermal performance of flat plate and evacuated tube solar collectors in stationary standard and daily conditions. **Solar Energy**, 84(8), 1382-1396.

APPENDIX

APPENDIX A

Uncertainty Analysis

The uncertainty analysis uses the Taylor's expansion:

$$f(x_1 + \Delta x_1, x_2 + \Delta x_2, ..., x_n + \Delta x_n) = f(x_1, x_2, ..., x_n) + \Delta x_1 \frac{\partial f}{\partial x_1} + \Delta x_2 \frac{\partial f}{\partial x_2} + ... + \Delta x_n \frac{\partial f}{\partial x_n} + \frac{1}{2}\left[(\Delta x_1)^2 \frac{\partial^2 f}{\partial x_1^2} + ...\right] + ...$$

The first order term,

$$f(x_1 + \Delta x_1, x_2 + \Delta x_2, ..., x_n + \Delta x_n) = f(x_1, x_2, ..., x_n) + \Delta x_1 \frac{\partial f}{\partial x_1} + \Delta x_2 \frac{\partial f}{\partial x_2} + ... + \Delta x_n \frac{\partial f}{\partial x_n}$$

The root-sum square,

$$\Delta R = \sqrt{\left(\Delta x_1 \frac{\partial f}{\partial x_1}\right)^2 + \left(\Delta x_2 \frac{\partial f}{\partial x_2}\right)^2 + ... + \left(\Delta x_n \frac{\partial f}{\partial x_n}\right)^2}$$

Or

$$\omega_R = \left[\left(\frac{\partial R}{\partial x_1} \omega_1\right)^2 + \left(\frac{\partial R}{\partial x_2} \omega_2\right)^2 + ... \left(\frac{\partial R}{\partial x_n} \omega_n\right)^2\right]^{1/2}$$

Which ω_R is uncertainty in the output result and ω_1, ω_2, ..., ω_n are errors in the parameters related.

Thermal energy

The collected thermal energy was calculated as:

$$Q_{coll} = \dot{m}C_p(T_o - T_i)$$

The solar collector was tested with mass flow rate 0.03 kg/s·m^2 and the collector area 0.128 m^2 the water temperature inlet and outlet temperature difference was 36.4 and 41.3 °C the specific heat of water is 4187 J/kg·K.

The thermal energy collected of the solar collector was:

$$Q_{coll} = \dot{m}C_p(T_o - T_i) 0.03 \times 0.128 \times 4187(41.3 - 36.4) = 78.57\ W$$

So, the energy collected of solar collector when the inlet temperature 36.4 was Q $_{coll}$ = 78.57 W

The variable of the accuracy of equipment measurement as Uncertainty were:

- Mass flow rate: $\dot{m}$ is ± 1.6%

- Specific heat of water is 0.01%

- Temperature difference $(T_o - T_i)$ is ± (0.4%+0.5°C)

$$\frac{\partial Q}{\partial \dot{m}} = \frac{\partial}{\partial \dot{m}} \left(\dot{m} C_p \Delta T \right) = C_p \Delta T = 4.187 kJ / kg \cdot K \times (41.3 - 36.4)°C = 20.52 kJ / kg$$

$$\frac{\partial Q}{\partial C_p} = \frac{\partial}{\partial C_p} \left(\dot{m} C_p \Delta T \right) = \dot{m} \Delta T = 0.00383 kg / s \times (41.3 - 36.4)°C = 0.0187 kg \cdot °C / s$$

$$\frac{\partial Q}{\partial \Delta T} = \frac{\partial}{\partial \Delta T} \left(\dot{m} C_p \Delta T \right) = \dot{m} C_p = 0.00383 kg / s \times 4.187 kJ / kg \cdot K = 0.016 kJ / s \cdot K$$

$$\omega_{\dot{m}} = 0.00383 kg / s \times 1.6\% = 6.1 \times 10^{-5} kg / s$$

$$\omega_{A_C} = 4.187 \times 0.01\% = 4.2 \times 10^{-4} kJ / kg \cdot K$$

$$\omega_{\Delta T} = 0.5°C$$

The uncertainty of the collected energy ω_{Qcoll} =0.0081 W

So, the Collected Energy of solar collector was Q_{coll}= 78.57 ± 0.0081W = 78.57 W ± 0.0103%

Thermal efficiency of the solar collector (η_{coll})

The thermal efficiency of the solar collector was calculated as:

$$\eta_{coll} = \frac{Q_{coll}}{I_T A_C} = F_R (\tau\alpha)_e - F_R \left(\frac{T_i - T_a}{I_T} \right)$$

The intersection of the vertical line of efficiency axis is equal to $F_R(\tau\alpha)_e$. At this axis the temperature of working fluid that entered the collector near ambient temperature means that the collector efficient is nearly maximum. So, the slope of the linear line is equal to $F_R U_L$ shows that the way energy has removed from the solar collector. At the intersection of the line with the horizontal axis collector efficiency is zero and this point normally calls the stagnation, usually occurs when no fluid flows in the collector which presented in the graphic below:
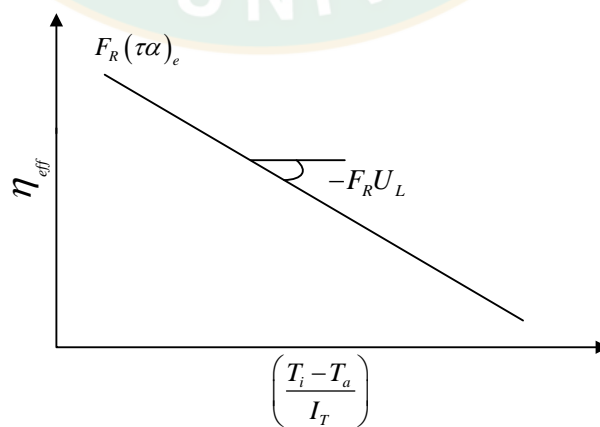
The thermal efficiency of the solar collector which has the energy collected Q_{coll} = 78.57 W, Solar radiation intensity 802.6 W/m² and the solar collector area 0.128 m² was calculated as:

$$\eta_{coll} = \frac{Q_{coll}}{I_T A_C} = \frac{78.57\ W}{802.6\ W/m^2 \times 0.128\ m^2} = 0.75$$

So, the thermal performance of the solar collector was 75% when the inlet temperature at 36.4 °C with the mass flow rate 0.03 kg/s·m².

The variable accuracy of the instrument measurement:

- Surface area of the copper tube is ± 0.01%

- The solar radiation intensity value is ± 5%

- The collected energy is ± 0.0103%

$$\frac{\partial \eta}{\partial Q_{coll}} = \frac{\partial}{\partial Q_{coll}}\left(\frac{Q_{coll}}{I_T A_C}\right) = \frac{1}{I_T A_C} = \frac{1}{802.6 \times 0.128} = 0.0097\ /W$$

$$\frac{\partial \eta}{\partial I_T} = \frac{\partial}{\partial I_T}\left(\frac{Q_{coll}}{I_T A_C}\right) = \frac{Q_{coll}}{A_C}\left(-\frac{1}{I_T^2}\right) = \frac{78.57\ W}{0.128\ m^2}\left(-\frac{1}{\left(802.6\ W/m^2\right)^2}\right) = -9.5 \times 10^{-4}\ m^2/W$$

$$\frac{\partial \eta}{\partial A_c} = \frac{\partial}{\partial A_c}\left(\frac{Q_{coll}}{I_T A_C}\right) = \frac{Q_{coll}}{I_T}\left(-\frac{1}{A_c^2}\right) = \frac{78.57\ W}{802.6\ W/m^2}\left(-\frac{1}{\left(0.128\ m^2\right)^2}\right) = -5.97\ /m^2$$

$$\omega_{Q_{coll}} = 78.57\ W \times 0.0103\% = 8.1 \times 10^{-3}\ W$$

$$\omega_{A_c} = 0.128\ m^2 \times 0.01\% = 1.28 \times 10^{-5}\ m^2$$

$$\omega_{I_T} = 802.6\ W/m^2 \times 5\% = 40\ W/m^2$$

The uncertainty of the thermal efficiency of the solar collector was $\omega\eta_{coll}$ = 0.038

So, the thermal efficiency of the solar collector was η_{coll} = 0.75 ± 0.038 = 0.75 ± 5.1%

Heat transfer

The heat transfer of solar collector was calculated as:

$$h_i = \frac{Q_{coll}}{A_{tube}\left(\Delta T\right)} = \frac{Q_{coll}}{A_{tube}\left(T_s - T_{av}\right)}$$

The heat transfers of the solar collector with collected energy 78.57 W, inner tube surface area was A_{tube} = 0.086 m² and the average surface of absorber plate

temperature was 40.73 °C and average temperature of the water circulating in the collector was 38.8 °C:

So, $h_i = \dfrac{Q_{coll}}{A_{tube}(T_s - T_{av})} = \dfrac{78.57\ W}{0.086\ m^2 \times (40.73 - 38.88)°C} = 157.73\ \text{W/ m}^2 \cdot \text{K}$

The variable of the accuracy of equipment measurement as Uncertainty were:

- Surface area of the copper tube is ± 0.01%

- Temperature difference $(T_w - T_{av})$ is ± (0.75% +0.1%)

$\dfrac{\partial h_i}{\partial Q_{coll}} = \dfrac{\partial}{\partial Q_{coll}}\left(\dfrac{Q_{coll}}{A \times \Delta T}\right) = \dfrac{1}{A \times \Delta T} = \dfrac{1}{0.086\ m^2 \times 1.89°C} = 6.46/m^2 \cdot °C$

$\dfrac{\partial h_i}{\partial A} = \dfrac{\partial}{\partial A}\left(\dfrac{Q_{coll}}{A \times \Delta T}\right) = \dfrac{Q_{coll}}{\Delta T}\left(-\dfrac{1}{A^{-2}}\right) = \dfrac{78.57W}{1.89°C}\left(-\dfrac{1}{(0.086m^2)^2}\right) = -135.21\ W/m^4 \cdot °C$

$\dfrac{\partial h_i}{\partial \Delta T} = \dfrac{\partial}{\partial \Delta T}\left(\dfrac{Q_{coll}}{A \times \Delta T}\right) = \dfrac{Q_{coll}}{A}\left(-\dfrac{1}{\Delta T^{-2}}\right) = \dfrac{78.57W}{0.086m^2}\left(-\dfrac{1}{(1.86°C)^2}\right) = -264.1\ W/m^2 \cdot °C^2$

$\omega_{Q_{coll}} = 0.0081\ \text{W}$

$\omega_A = 0.086\,m^2 \times 0.01\% = 0.0000086\,m^2$

$\omega_{\Delta T} = 1.86°C \times 0.85\% = 0.016°C$

The uncertainty of the heat transfer of the solar collector was $\omega_{hi} = 4.23\ \text{W/m}^2 \cdot \text{K}$

The heat transfers of the solar collector $h_i = 157.73 \pm 4.23\ \text{W/m}^2 \cdot \text{K} = 157.73 \pm 2.7\%$ W/m²·K

APPENDIX B

Data Analysis

PCM1

Mass flow rate 0.03 kg/s·m^2

Set T$_i$	T$_s$	T$_i$	T$_o$	ΔT	Q$_{coll}$	(T$_i$-T$_a$)I$_T$	η$_{coll}$	T$_a$	I$_T$	F$_R$(τα)$_e$	F$_R$U$_L$
	38.3	36.4	41.3	4.9	78.58	0.0072	0.75	30.66	802.06	8.11	9.75
	38.7	36.3	41.3	5	80.18	0.0069	0.77	30.76	799.58	8.11	9.75
35	39.1	36.5	41.4	4.9	78.58	0.0070	0.75	30.85	804.30	8.11	9.75
	39.4	36.4	41.3	4.9	78.58	0.0072	0.76	30.66	798.73	8.11	9.75
	39.7	36.5	41.4	4.9	78.58	0.0074	0.76	30.55	800.20	8.11	9.75
	39.04	36.42	41.34	4.92	78.90	0.0071	0.76	30.70	800.97	8.11	9.75
	41.8	40.5	44.8	4.3	68.96	0.0133	0.66	29.86	802.06	8.11	9.75
	41.9	40.6	44.9	4.3	68.96	0.0128	0.66	30.26	805.62	8.11	9.75
40	42	40.6	45	4.4	70.56	0.0134	0.68	29.86	802.99	8.11	9.75
	42.1	40.7	45.1	4.4	70.56	0.0130	0.68	30.26	803.53	8.11	9.75
	42.1	40.7	45	4.3	68.96	0.0136	0.67	29.94	787.97	8.11	9.75
	41.98	40.62	44.96	4.34	69.60	0.0132	0.67	30.04	800.43	8.11	9.75
	47.7	46.1	50	3.9	62.54	0.0185	0.59	30.85	808.41	8.11	9.75
	47.7	46.1	50	3.9	62.54	0.0189	0.60	30.85	809.03	8.11	9.75
45	47.8	46.1	50.1	4	64.14	0.0189	0.61	30.76	810.81	8.11	9.75
	47.9	46.1	50.2	4.1	65.75	0.0189	0.62	30.76	810.50	8.11	9.75
	48.1	46.2	50.3	4.1	65.75	0.0190	0.62	31.06	810.50	8.11	9.75
	47.84	46.12	50.12	4	64.14	0.0188	0.61	30.86	809.85	8.11	9.75
	52.3	50.3	54.1	3.8	60.94	0.0255	0.57	29.15	829.00	8.11	9.75
	52.4	50.3	54.1	3.8	60.94	0.0252	0.57	29.44	826.83	8.11	9.75
50	52.4	50.2	54	3.8	60.94	0.0257	0.57	28.96	827.53	8.11	9.75
	52.4	50.2	54	3.8	60.94	0.0257	0.56	28.85	830.62	8.11	9.75
	52.5	50.3	54.1	3.8	60.94	0.0261	0.56	28.64	829.93	8.11	9.75
	52.4	50.26	54.06	3.8	60.94	0.0256	0.57	29.01	828.78	8.11	9.75
	56.4	54.2	57.8	3.6	57.73	0.0299	0.54	29.76	818.86	8.11	9.75
	56.4	54.2	57.7	3.5	56.13	0.0296	0.53	30.05	816.22	8.11	9.75
55	56.4	54.2	57.7	3.5	56.13	0.0294	0.53	30.26	814.29	8.11	9.75
	56.5	54.2	57.7	3.5	56.13	0.0295	0.53	30.15	815.60	8.11	9.75
	56.4	54	57.6	3.6	57.73	0.0295	0.55	29.94	814.29	8.11	9.75
	56.42	54.16	57.7	3.54	56.77	0.0296	0.54	30.03	815.85	8.11	9.75
	62.8	60.7	63.5	2.8	44.90	0.0364	0.43	31.66	797.41	8.11	9.75
	62.7	60.7	63.4	2.7	43.30	0.0368	0.42	31.46	795.17	8.11	9.75
60	62.6	60.5	63.4	2.9	46.51	0.0364	0.45	31.56	794.16	8.11	9.75
	62.7	60.4	63.4	3	48.11	0.0365	0.47	31.46	792.07	8.11	9.75
	62.7	60.4	63.3	2.9	46.51	0.0363	0.45	31.66	792.23	8.11	9.75
	62.7	60.54	63.4	2.86	45.86	0.0365	0.44	31.56	794.21	8.11	9.75
	67.1	64.7	67.4	2.7	44.09	0.0416	0.42	31.46	799.74	8.11	9.75
	67.1	64.8	67.4	2.6	42.46	0.0411	0.41	31.96	799.58	8.11	9.75
65	67	64.8	67.4	2.6	42.46	0.0408	0.41	32.36	795.32	8.11	9.75
	66.8	64.6	67.3	2.7	44.09	0.0404	0.43	32.57	793.54	8.11	9.75
	66.9	64.6	67.2	2.6	42.46	0.0412	0.41	31.96	791.38	8.11	9.75
	66.98	64.7	67.34	2.64	43.11	0.0410	0.42	32.06	795.91	8.11	9.75

q"	h_i	$F'U_L$	$1T_{PCM}$	$2T_{PCM}$	$3T_{PCM}$	T_{PCM}av	$1T_P$	$2T_P$	$3T_P$	$T_{P\ av}$	F'
290.84	153.88	10.15	39.79	37.38	41.52	39.56	38.07	41.12	43.03	40.74	0.88
296.77	159.08	10.15	39.70	37.46	41.52	39.56	38.07	40.91	43.02	40.67	0.88
290.84	156.66	10.15	39.79	37.46	41.41	39.55	38.18	41.01	43.23	40.81	0.88
290.84	159.25	10.15	40.00	37.67	41.41	39.69	38.07	40.91	43.05	40.68	0.88
290.84	159.80	10.15	40.00	37.46	41.71	39.72	38.18	41.01	43.12	40.77	0.88
292.02	157.73	10.15	39.85	37.49	41.51	39.62	38.12	40.99	43.09	40.73	0.88
255.22	141.83	10.15	43.63	41.71	45.45	43.60	41.62	44.76	46.97	44.45	0.87
255.22	137.96	10.15	43.74	41.92	45.55	43.74	41.66	44.96	47.18	44.60	0.87
261.16	141.17	10.15	44.14	42.02	45.85	44.00	41.82	45.05	47.08	44.65	0.87
261.16	140.41	10.15	43.74	41.71	45.45	43.63	41.86	45.21	47.21	44.76	0.87
255.22	146.84	10.15	43.74	41.81	45.66	43.74	41.74	44.95	47.08	44.59	0.87
257.60	141.64	10.15	43.80	41.83	45.59	43.74	41.74	44.98	47.10	44.61	0.87
231.48	123.32	10.15	50.20	48.28	51.62	50.03	47.50	50.19	52.09	49.93	0.86
231.48	127.65	10.15	50.31	48.17	51.91	50.13	47.30	50.20	52.09	49.86	0.86
237.42	127.80	10.15	49.69	47.69	51.11	49.50	47.59	50.19	52.09	49.96	0.86
243.35	134.91	10.15	49.69	47.48	51.11	49.43	47.79	49.99	52.08	49.95	0.86
243.35	137.12	10.15	49.29	47.37	50.92	49.19	48.00	49.98	52.09	50.02	0.87
237.42	130.16	10.15	49.84	47.80	51.33	49.66	47.63	50.11	52.09	49.95	0.86
225.55	114.35	10.15	52.93	50.78	54.44	52.72	52.00	53.82	56.69	54.17	0.85
225.55	114.21	10.15	52.72	50.78	54.25	52.58	52.11	53.73	56.68	54.17	0.85
225.55	110.34	10.15	52.61	50.89	54.25	52.58	52.01	53.63	56.79	54.14	0.84
225.55	118.17	10.15	52.20	50.48	53.74	52.14	51.91	53.54	56.58	54.01	0.85
225.55	120.13	10.15	52.10	50.37	53.74	52.07	51.50	53.94	56.79	54.08	0.85
225.55	115.44	10.15	52.51	50.66	54.08	52.42	51.91	53.73	56.71	54.12	0.85
213.68	102.88	10.15	55.89	55.27	58.63	56.60	55.78	58.21	60.25	58.08	0.83
207.74	98.37	10.15	56.10	55.27	58.63	56.67	55.63	58.32	60.24	58.06	0.83
207.74	100.89	10.15	55.89	55.38	58.72	56.66	55.57	58.21	60.25	58.01	0.83
207.74	100.89	10.15	55.89	55.27	58.42	56.53	55.47	58.32	60.24	58.01	0.83
213.68	93.97	10.15	55.89	55.17	58.53	56.53	55.77	58.21	60.24	58.07	0.82
210.11	99.40	10.15	55.93	55.27	58.59	56.60	55.64	58.25	60.24	58.05	0.83
166.19	101.44	10.15	64.86	63.34	65.96	64.72	61.18	63.87	66.16	63.74	0.83
160.26	88.03	10.15	64.36	62.94	65.67	64.32	61.37	64.37	65.87	63.87	0.81
172.13	92.77	10.15	64.25	62.73	65.46	64.15	61.17	64.48	65.77	63.81	0.82
178.06	80.58	10.15	63.96	62.54	65.37	63.96	61.48	65.07	65.78	64.11	0.80
172.13	76.38	10.15	63.85	62.63	65.05	63.84	61.57	65.07	65.67	64.10	0.79
169.75	87.84	10.15	64.26	62.84	65.50	64.20	61.35	64.57	65.85	63.93	0.81
163.19	80.15	10.15	68.10	66.58	68.90	67.86	66.26	67.89	70.10	68.09	0.80
157.14	76.43	10.15	68.39	66.79	69.20	68.13	66.26	68.10	70.10	68.16	0.79
157.14	73.88	10.15	68.50	67.08	69.30	68.29	66.37	67.89	70.42	68.23	0.79
163.19	60.79	10.15	68.69	67.08	69.41	68.39	66.48	69.11	70.32	68.63	0.76
157.14	70.56	10.15	67.99	66.47	68.79	67.75	66.07	68.50	69.81	68.13	0.78
159.56	72.36	10.15	68.33	66.80	69.12	68.08	66.29	68.30	70.15	68.25	0.78

F_R	U_L	k	ρ	C_p	ν	μ	Re	Pr	Nu
0.84	11.57	0.63	992.41	4186.37	6.74837E-07	0.00066972	567.98	4.44	6.99
0.85	11.53	0.63	992.43	4186.31	6.75444E-07	0.00067033	567.46	4.44	7.23
0.84	11.55	0.63	992.38	4186.49	6.73626E-07	0.00066849	569.02	4.43	7.12
0.85	11.53	0.63	992.41	4186.37	6.74837E-07	0.00066972	567.98	4.44	7.24
0.85	11.53	0.63	992.38	4186.49	6.73626E-07	0.00066849	569.02	4.43	7.26
0.84	11.54	0.63	992.40	4186.41	6.74473E-07	0.00066935	568.29	4.44	7.17
0.84	11.67	0.64	991.02	4191.77	6.31270E-07	0.00062560	608.03	4.11	6.38
0.83	11.70	0.64	990.98	4191.94	6.30188E-07	0.00062450	609.10	4.10	6.21
0.83	11.68	0.64	990.96	4192.02	6.29648E-07	0.00062396	609.63	4.10	6.35
0.83	11.68	0.64	990.92	4192.18	6.28570E-07	0.00062286	610.70	4.09	6.31
0.84	11.63	0.64	990.94	4192.10	6.29109E-07	0.00062341	610.16	4.10	6.60
0.84	11.67	0.64	990.96	4192.00	6.29756E-07	0.00062407	609.52	4.10	6.37
0.82	11.87	0.65	988.87	4202.29	5.76981E-07	0.00057056	666.69	3.71	5.48
0.82	11.82	0.65	988.87	4202.29	5.76981E-07	0.00057056	666.69	3.71	5.67
0.82	11.82	0.65	988.85	4202.40	5.76515E-07	0.00057008	667.24	3.71	5.67
0.83	11.75	0.65	988.83	4202.52	5.76049E-07	0.00056961	667.79	3.70	5.99
0.83	11.73	0.65	988.78	4202.74	5.75120E-07	0.00056867	668.90	3.70	6.09
0.83	11.80	0.65	988.84	4202.45	5.76328E-07	0.00056990	667.46	3.71	5.78
0.81	11.99	0.65	987.08	4212.64	5.40310E-07	0.00053333	713.22	3.44	5.03
0.81	12.00	0.65	987.08	4212.64	5.40310E-07	0.00053333	713.22	3.44	5.02
0.81	12.05	0.65	987.12	4212.37	5.41148E-07	0.00053418	712.09	3.45	4.85
0.82	11.95	0.65	987.12	4212.37	5.41148E-07	0.00053418	712.09	3.45	5.20
0.82	11.92	0.65	987.08	4212.64	5.40310E-07	0.00053333	713.22	3.44	5.28
0.81	11.98	0.65	987.10	4212.53	5.40645E-07	0.00053367	712.77	3.45	5.08
0.80	12.18	0.66	985.34	4223.85	5.09961E-07	0.00050248	757.00	3.23	4.49
0.80	12.25	0.66	985.36	4223.69	5.10342E-07	0.00050287	756.42	3.23	4.29
0.80	12.21	0.66	985.36	4223.69	5.10342E-07	0.00050287	756.42	3.23	4.40
0.80	12.21	0.66	985.36	4223.69	5.10342E-07	0.00050287	756.42	3.23	4.40
0.79	12.33	0.66	985.43	4223.22	5.11489E-07	0.00050404	754.67	3.24	4.10
0.80	12.23	0.66	985.37	4223.63	5.10495E-07	0.00050303	756.19	3.23	4.34
0.80	12.22	0.67	982.34	4245.30	4.66675E-07	0.00045843	829.75	2.92	4.37
0.78	12.48	0.67	982.36	4245.11	4.67006E-07	0.00045877	829.14	2.92	3.79
0.79	12.38	0.67	982.41	4244.72	4.67668E-07	0.00045944	827.92	2.93	4.00
0.77	12.67	0.67	982.44	4244.53	4.68000E-07	0.00045978	827.31	2.93	3.47
0.76	12.78	0.67	982.47	4244.34	4.68332E-07	0.00046012	826.70	2.93	3.29
0.78	12.49	0.67	982.40	4244.80	4.67536E-07	0.00045931	828.16	2.93	3.79
0.77	12.70	0.67	980.26	4261.46	4.41684E-07	0.00043297	878.55	2.75	3.43
0.76	12.80	0.67	980.23	4261.68	4.41381E-07	0.00043266	879.18	2.75	3.27
0.76	12.88	0.67	980.23	4261.68	4.41381E-07	0.00043266	879.18	2.75	3.16
0.73	13.39	0.67	980.31	4261.03	4.42291E-07	0.00043358	877.30	2.75	2.60
0.75	12.99	0.67	980.34	4260.82	4.42594E-07	0.00043389	876.67	2.75	3.02
0.75	12.93	0.67	980.28	4261.33	4.41866E-07	0.00043315	878.18	2.75	3.09

Mass flow rate 0.02 kg/s·m^2

Set T$_i$	T$_s$	T$_i$	T$_o$	ΔT	Q$_{coll}$	(T$_i$-T$_a$)I$_T$	η$_{coll}$	T$_a$	I$_T$	F$_R$(τα)$_e$	F$_R$U$_L$
	38.00	35.00	41.00	6.00	67.08	0.0143	0.627	23.233	823.113	0.789	11.045
	38.10	35.00	41.00	6.00	67.08	0.0135	0.625	23.842	825.203	0.789	11.045
35	38.30	35.00	41.00	6.00	67.08	0.0135	0.625	23.842	825.203	0.789	11.045
	38.40	35.00	41.10	6.10	68.19	0.0138	0.637	23.632	823.268	0.789	11.045
	38.50	35.00	41.10	6.10	68.19	0.0140	0.635	23.422	826.055	0.789	11.045
	38.26	35.00	41.04	6.04	67.52	0.0138	0.630	23.594	824.569	0.789	11.045
	43.00	39.80	45.20	5.40	60.37	0.0195	0.577	24.135	804.613	0.789	11.045
	43.00	39.70	45.20	5.50	61.49	0.0191	0.589	24.345	803.142	0.789	11.045
40	43.20	39.90	45.30	5.40	60.37	0.0202	0.577	23.632	804.458	0.789	11.045
	43.20	39.90	45.20	5.30	59.25	0.0194	0.569	24.345	800.588	0.789	11.045
	43.30	40.00	45.30	5.30	59.25	0.0204	0.571	23.737	798.575	0.789	11.045
	43.14	39.86	45.24	5.38	60.14	0.0197	0.577	24.039	802.275	0.789	11.045
	47.00	45.20	49.90	4.70	52.54	0.0244	0.491	25.142	822.417	0.789	11.045
	47.00	45.20	50.00	4.80	53.66	0.0245	0.503	25.142	819.862	0.789	11.045
45	47.10	45.30	50.10	4.80	53.66	0.0246	0.502	25.037	822.726	0.789	11.045
	47.10	45.30	50.10	4.80	53.66	0.0245	0.502	25.142	822.262	0.789	11.045
	47.10	45.30	50.10	4.80	53.66	0.0252	0.503	24.639	821.101	0.789	11.045
	47.06	45.26	50.04	4.78	53.44	0.0246	0.500	25.020	821.674	0.789	11.045
	54.00	51.40	55.70	4.30	48.07	0.0320	0.463	25.834	799.427	0.789	11.045
	53.90	51.20	55.60	4.40	49.19	0.0316	0.474	25.939	798.420	0.789	11.045
50	53.90	51.30	55.50	4.20	46.95	0.0315	0.454	26.233	795.789	0.789	11.045
	53.80	51.20	55.40	4.20	46.95	0.0319	0.456	25.939	791.763	0.789	11.045
	53.90	51.20	55.40	4.20	46.95	0.0318	0.456	26.044	791.221	0.789	11.045
	53.90	51.26	55.52	4.26	47.62	0.0318	0.461	25.998	795.324	0.789	11.045
	58.20	55.60	59.00	3.40	38.01	0.0382	0.369	25.331	793.234	0.789	11.045
	58.20	55.60	59.00	3.40	38.01	0.0377	0.368	25.645	795.479	0.789	11.045
55	58.40	55.60	59.00	3.40	38.01	0.0381	0.367	25.247	795.943	0.789	11.045
	59.20	55.60	59.10	3.50	39.13	0.0378	0.378	25.540	795.324	0.789	11.045
	59.90	55.60	59.10	3.50	39.13	0.0382	0.380	25.331	793.002	0.789	11.045
	58.78	55.60	59.04	3.44	38.46	0.0380	0.372	25.419	794.596	0.789	11.045
	64.10	60.10	63.30	3.20	35.77	0.0414	0.347	27.239	793.544	0.789	11.045
	64.10	60.30	63.30	3.00	33.54	0.0421	0.325	26.841	794.473	0.789	11.045
60	64.00	60.30	63.20	2.90	32.42	0.0415	0.314	27.344	793.853	0.789	11.045
	64.40	60.40	63.30	2.90	32.42	0.0414	0.315	27.638	792.073	0.789	11.045
	65.10	60.60	63.50	2.90	32.42	0.0421	0.316	27.344	789.906	0.789	11.045
	64.34	60.34	63.32	2.98	33.31	0.0417	0.323	27.281	792.770	0.789	11.045
	69.40	65.00	67.40	2.40	26.83	0.0459	0.260	28.645	792.847	0.789	11.045
	69.30	65.10	67.60	2.50	27.95	0.0463	0.272	28.456	791.221	0.789	11.045
65	69.50	65.00	67.50	2.50	27.95	0.0466	0.272	28.141	790.447	0.789	11.045
	69.70	65.10	67.60	2.50	27.95	0.0461	0.272	28.593	791.469	0.789	11.045
	69.60	65.20	67.70	2.50	27.95	0.0462	0.272	28.678	791.348	0.789	11.045
	69.50	65.08	67.56	2.48	27.72	0.0462	0.269	28.502	791.467	0.789	11.045

q"	h_i	$F'U_L$	$1T_{PCM}$	$2T_{PCM}$	$3T_{PCM}$	$T_{PCM}av$	$1T_P$	$2T_P$	$3T_P$	$T_{P\ av}$	F'
248.266	142.448	11.809	37.561	35.114	40.497	37.724	37.162	39.608	42.459	39.743	0.906
248.266	139.607	11.809	37.455	35.114	40.497	37.689	37.162	39.608	42.565	39.778	0.905
248.266	145.406	11.809	37.455	35.114	40.391	37.653	37.055	39.608	42.459	39.707	0.908
252.404	144.412	11.809	37.455	35.008	40.391	37.618	37.326	39.502	42.565	39.798	0.907
252.404	141.836	11.809	37.242	34.795	40.199	37.412	37.438	39.503	42.547	39.830	0.906
249.921	142.715	11.809	37.433	35.029	40.395	37.619	37.229	39.566	42.519	39.771	0.906
223.439	132.971	11.808	41.816	39.688	44.773	42.093	41.544	44.094	46.903	44.180	0.900
227.577	131.263	11.808	41.922	39.795	44.667	42.128	41.544	44.084	46.923	44.184	0.899
223.439	134.784	11.808	41.922	39.795	44.773	42.163	41.736	44.104	46.933	44.258	0.901
219.302	129.110	11.808	42.241	39.901	44.986	42.376	41.743	44.076	46.927	44.249	0.898
219.302	139.753	11.808	41.922	39.901	44.880	42.234	41.651	44.094	46.913	44.219	0.904
222.612	133.466	11.808	41.965	39.816	44.816	42.199	41.644	44.090	46.920	44.218	0.900
194.475	120.894	11.806	47.687	45.553	50.202	47.814	46.971	48.995	51.509	49.159	0.891
198.613	122.261	11.806	47.687	45.553	50.202	47.814	46.967	49.096	51.611	49.225	0.892
198.613	122.066	11.806	47.772	45.659	50.096	47.842	47.275	49.096	51.611	49.327	0.892
198.613	119.522	11.806	47.476	45.553	50.096	47.708	47.367	49.092	51.627	49.362	0.890
198.613	124.573	11.806	47.476	45.448	50.011	47.645	47.164	49.092	51.627	49.294	0.894
197.785	121.844	11.806	47.620	45.553	50.121	47.765	47.149	49.074	51.597	49.273	0.892
177.924	109.537	11.803	54.237	52.336	56.477	54.350	52.854	55.274	57.395	55.174	0.881
182.062	104.471	11.803	54.237	52.336	56.667	54.413	52.854	55.178	57.396	55.143	0.877
173.786	108.492	11.803	54.047	52.336	56.477	54.286	52.748	54.967	57.291	55.002	0.880
173.786	106.067	11.803	53.836	52.230	56.371	54.146	52.642	54.882	57.291	54.938	0.878
173.786	103.836	11.803	54.153	52.336	56.265	54.251	52.748	54.967	57.206	54.974	0.876
176.269	106.430	11.803	54.102	52.314	56.451	54.289	52.769	55.054	57.316	55.046	0.878
140.684	86.773	11.800	57.977	56.265	59.815	58.019	57.268	58.683	60.812	58.921	0.856
140.684	92.261	11.800	57.681	55.970	59.604	57.752	56.973	58.790	60.712	58.825	0.863
140.684	96.729	11.800	57.575	55.970	59.604	57.716	56.867	58.790	60.607	58.754	0.868
144.822	98.194	11.800	57.787	56.075	59.604	57.822	56.973	58.790	60.712	58.825	0.869
144.822	98.275	11.800	57.787	55.864	59.498	57.716	56.877	58.886	60.708	58.824	0.870
142.339	94.276	11.800	57.761	56.029	59.625	57.805	56.992	58.788	60.710	58.830	0.865
132.409	82.682	11.797	62.139	60.407	63.745	62.097	61.720	63.234	64.950	63.301	0.850
124.133	81.940	11.797	61.928	60.301	63.639	61.956	61.934	63.145	64.866	63.315	0.849
119.995	82.616	11.797	62.329	60.724	63.851	62.301	61.515	63.243	64.849	63.202	0.850
119.995	84.570	11.797	62.435	60.808	63.956	62.400	61.515	63.332	64.959	63.269	0.852
119.995	86.815	11.797	62.435	60.808	63.956	62.400	61.818	63.519	64.959	63.432	0.855
123.305	83.655	11.797	62.253	60.610	63.830	62.231	61.701	63.295	64.917	63.304	0.851
99.306	60.601	11.794	67.069	65.835	68.580	67.161	66.142	67.871	69.503	67.839	0.808
103.444	72.709	11.794	67.261	65.835	68.495	67.197	66.142	67.780	69.397	67.773	0.833
103.444	74.529	11.794	66.963	65.537	68.495	66.998	66.035	67.673	69.205	67.638	0.836
103.444	66.208	11.794	67.547	66.010	68.937	67.498	66.022	67.915	69.799	67.912	0.820
103.444	66.819	11.794	67.722	66.151	69.126	67.666	66.048	67.968	69.978	67.998	0.822
102.617	67.869	11.794	67.312	65.874	68.726	67.304	66.078	67.842	69.576	67.832	0.824

F_R	U_L	k	ρ	C_p	ν	μ	Re	Pr	Nu
0.848	13.032	0.630	992.710	4185.38761	6.853E-07	6.803E-04	389.800	4.517	6.486
0.846	13.053	0.630	992.710	4185.38761	6.853E-07	6.803E-04	389.800	4.517	6.357
0.849	13.011	0.630	992.710	4185.38761	6.853E-07	6.803E-04	389.800	4.517	6.621
0.848	13.018	0.630	992.692	4185.44308	6.847E-07	6.797E-04	390.161	4.513	6.575
0.847	13.037	0.630	992.692	4185.44308	6.847E-07	6.797E-04	390.161	4.513	6.457
0.848	13.030	0.630	992.703	4185.40977	6.850E-07	6.800E-04	389.944	4.515	6.498
0.842	13.120	0.638	991.074	4191.52607	6.329E-07	6.272E-04	422.759	4.123	5.985
0.841	13.135	0.638	991.093	4191.44513	6.334E-07	6.278E-04	422.388	4.127	5.909
0.843	13.106	0.638	991.037	4191.68881	6.318E-07	6.261E-04	423.502	4.115	6.065
0.840	13.154	0.638	991.055	4191.6073	6.324E-07	6.267E-04	423.131	4.119	5.811
0.845	13.066	0.638	991.018	4191.77061	6.313E-07	6.256E-04	423.874	4.111	6.288
0.842	13.116	0.638	991.055	4191.6073	6.324E-07	6.267E-04	423.131	4.119	6.007
0.834	13.249	0.646	989.075	4201.1755	5.817E-07	5.753E-04	460.918	3.744	5.375
0.835	13.235	0.646	989.054	4201.28563	5.812E-07	5.748E-04	461.302	3.741	5.435
0.834	13.237	0.646	989.012	4201.50676	5.803E-07	5.739E-04	462.071	3.734	5.425
0.833	13.264	0.646	989.012	4201.50676	5.803E-07	5.739E-04	462.071	3.734	5.312
0.836	13.212	0.646	989.012	4201.50676	5.803E-07	5.739E-04	462.071	3.734	5.537
0.834	13.239	0.646	989.033	4201.39605	5.807E-07	5.744E-04	461.686	3.737	5.416
0.824	13.398	0.654	986.472	4216.4354	5.292E-07	5.220E-04	507.960	3.364	4.804
0.820	13.466	0.654	986.540	4216.00367	5.304E-07	5.233E-04	506.761	3.372	4.583
0.824	13.411	0.654	986.540	4216.00367	5.304E-07	5.233E-04	506.761	3.372	4.760
0.822	13.443	0.654	986.585	4215.71729	5.312E-07	5.241E-04	505.962	3.378	4.654
0.820	13.474	0.654	986.585	4215.71729	5.312E-07	5.241E-04	505.962	3.378	4.556
0.822	13.438	0.654	986.544	4215.97498	5.305E-07	5.234E-04	506.681	3.373	4.669
0.802	13.779	0.660	984.720	4228.06581	5.002E-07	4.926E-04	538.355	3.157	3.775
0.808	13.673	0.660	984.720	4228.06581	5.002E-07	4.926E-04	538.355	3.157	4.014
0.812	13.595	0.660	984.720	4228.06581	5.002E-07	4.926E-04	538.355	3.157	4.208
0.814	13.572	0.660	984.696	4228.23176	4.998E-07	4.922E-04	538.766	3.154	4.271
0.814	13.571	0.660	984.696	4228.23176	4.998E-07	4.922E-04	538.766	3.154	4.275
0.810	13.637	0.660	984.711	4228.13216	5.001E-07	4.924E-04	538.520	3.156	4.101
0.795	13.884	0.666	982.543	4243.76491	4.693E-07	4.611E-04	575.047	2.940	3.565
0.795	13.901	0.666	982.491	4244.14746	4.687E-07	4.605E-04	575.894	2.935	3.532
0.795	13.885	0.666	982.517	4243.95604	4.690E-07	4.608E-04	575.470	2.938	3.562
0.798	13.842	0.666	982.466	4244.33917	4.683E-07	4.601E-04	576.318	2.933	3.645
0.801	13.795	0.666	982.364	4245.10887	4.670E-07	4.588E-04	578.014	2.924	3.740
0.797	13.862	0.666	982.476	4244.26246	4.685E-07	4.603E-04	576.148	2.934	3.606
0.757	14.594	0.671	980.178	4262.1134	4.408E-07	4.320E-04	613.775	2.742	2.590
0.780	14.162	0.672	980.097	4262.76495	4.399E-07	4.311E-04	615.088	2.736	3.107
0.783	14.109	0.672	980.151	4262.3303	4.405E-07	4.317E-04	614.213	2.740	3.185
0.768	14.375	0.672	980.097	4262.76495	4.399E-07	4.311E-04	615.088	2.736	2.829
0.769	14.354	0.672	980.043	4263.20074	4.393E-07	4.305E-04	615.964	2.732	2.855
0.771	14.317	0.672	980.113	4262.63443	4.401E-07	4.313E-04	614.825	2.737	2.900

Mass flow rate 0.01 kg/s·m²

Set T_i	T_s	T_i	T_o	ΔT	Q_{coll}	$(T_i-T_a)I_T$	η_{coll}	T_a	I_T	$F_R(\tau\alpha)_e$	$F_R U_L$
35	35.9	35.2	45.3	10.1	70.622	0.00795	0.681	28.854	797.956	0.734	10.304
	36.1	35.2	45.2	10.0	69.923	0.00855	0.671	28.351	801.362	0.734	10.304
	36.2	35.1	45.2	10.1	70.622	0.00766	0.678	28.959	801.207	0.734	10.304
	36.4	35.1	45.2	10.1	70.622	0.00715	0.676	29.358	803.684	0.734	10.304
	36.5	35.0	45.1	10.1	70.622	0.00690	0.674	29.442	805.464	0.734	10.304
	36.2	35.1	45.2	10.1	70.482	0.00764	0.676	28.993	801.935	0.734	10.304
40	41.8	39.6	48.1	8.5	59.434	0.01218	0.577	29.546	791.763	0.734	10.304
	41.9	39.6	48.2	8.6	60.134	0.01225	0.582	29.148	792.383	0.734	10.304
	42.0	39.6	48.2	8.6	60.134	0.01206	0.584	29.756	791.067	0.734	10.304
	42.1	39.7	48.3	8.6	60.134	0.01190	0.583	29.861	793.699	0.734	10.304
	42.2	39.6	48.3	8.7	60.833	0.01235	0.593	30.155	793.079	0.734	10.304
	42.0	39.6	48.2	8.6	60.134	0.01215	0.584	29.693	792.398	0.734	10.304
45	51.3	46.2	53.9	7.7	53.841	0.02178	0.508	28.456	814.599	0.734	10.304
	51.3	46.3	54.0	7.7	53.841	0.02154	0.508	28.749	814.753	0.734	10.304
	51.3	46.2	53.9	7.7	53.841	0.02160	0.506	28.540	817.695	0.734	10.304
	51.3	46.3	54.0	7.7	53.841	0.02174	0.507	28.540	816.921	0.734	10.304
	51.4	46.4	54.0	7.6	53.141	0.02176	0.501	28.645	816.069	0.734	10.304
	51.3	46.3	54.0	7.7	53.701	0.02168	0.506	28.586	816.007	0.734	10.304
50	54.9	51.1	58.1	7.0	48.946	0.02663	0.472	29.861	797.414	0.734	10.304
	55.2	51.2	58.2	7.0	48.946	0.02630	0.471	30.155	800.201	0.734	10.304
	56.4	51.1	58.1	7.0	48.946	0.02580	0.470	30.448	800.433	0.734	10.304
	57.9	51.1	58.2	7.1	49.645	0.02636	0.478	30.050	798.575	0.734	10.304
	57.8	51.1	58.0	6.9	48.247	0.02602	0.463	30.260	801.052	0.734	10.304
	56.4	51.1	58.1	7.0	48.946	0.02622	0.471	30.155	799.535	0.734	10.304
55	62.3	55.1	61.4	6.3	44.051	0.03054	0.422	30.553	803.684	0.734	10.304
	63.1	55.0	61.4	6.4	44.751	0.03043	0.429	30.553	803.297	0.734	10.304
	63.5	55.0	61.5	6.5	45.450	0.03065	0.433	30.260	807.090	0.734	10.304
	64.2	55.0	61.6	6.6	46.149	0.03055	0.442	30.448	803.684	0.734	10.304
	64.8	55.3	61.6	6.3	44.051	0.03100	0.423	30.448	801.672	0.734	10.304
	63.6	55.1	61.5	6.4	44.891	0.03064	0.430	30.453	803.885	0.734	10.304
60	67.5	62.4	66.6	4.2	29.368	0.03964	0.285	30.952	793.389	0.734	10.304
	67.4	62.4	66.7	4.3	30.067	0.03967	0.291	30.847	795.324	0.734	10.304
	67.3	62.4	66.8	4.4	30.766	0.03953	0.298	31.057	793.002	0.734	10.304
	67.3	62.2	67.0	4.8	33.563	0.03942	0.326	30.952	792.692	0.734	10.304
	67.2	62.3	67.0	4.7	32.864	0.03996	0.319	30.658	791.763	0.734	10.304
	67.3	62.3	66.8	4.5	31.325	0.03964	0.304	30.893	793.234	0.734	10.304
65	70.5	65.3	69.5	4.2	29.368	0.04545	0.283	29.043	797.777	0.734	10.304
	70.5	65.3	69.5	4.2	29.368	0.04505	0.283	29.358	797.777	0.734	10.304
	70.4	65.2	69.4	4.2	29.368	0.04493	0.283	29.358	797.777	0.734	10.304
	70.2	65.2	69.4	4.2	29.368	0.04469	0.283	29.546	797.777	0.734	10.304
	70.1	65.0	69.3	4.3	30.067	0.04457	0.290	29.442	797.777	0.734	10.304
	70.3	65.2	69.4	4.2	29.507	0.04494	0.285	29.349	797.777	0.734	10.304

q"	h_i	$F'U_L$	$1T_{PCM}$	$2T_{PCM}$	$3T_{PCM}$	T_{PCM}av	$1T_P$	$2T_P$	$3T_P$	$T_{P\ av}$	F'
260.786	132.343	11.418	40.434	36.175	44.611	40.407	37.901	42.419	46.341	42.221	0.864
258.204	131.983	11.418	40.434	36.277	44.611	40.441	37.802	42.223	46.443	42.156	0.864
260.786	131.679	11.418	40.637	36.459	44.793	40.630	37.811	42.428	46.152	42.130	0.864
260.786	134.755	11.418	40.434	36.561	44.712	40.569	37.906	42.097	46.253	42.085	0.866
260.786	130.507	11.418	40.637	36.561	44.895	40.697	37.998	41.995	46.152	42.048	0.863
260.269	132.254	11.418	40.515	36.407	44.725	0.000	37.884	42.232	46.268	42.128	0.864
219.473	119.976	11.416	45.475	41.570	49.107	45.384	41.357	45.378	50.303	45.679	0.854
222.055	124.415	11.416	45.181	41.570	49.107	45.286	41.462	45.289	50.303	45.685	0.858
222.055	120.198	11.416	45.580	42.073	49.506	45.720	41.258	45.387	50.597	45.747	0.854
222.055	113.589	11.416	45.895	42.367	49.611	45.958	41.468	45.379	51.017	45.955	0.848
224.637	113.826	11.416	46.188	42.472	50.009	46.223	41.360	45.393	51.017	45.924	0.849
222.055	118.401	11.416	45.664	42.010	49.468	0.000	41.381	45.365	50.648	45.798	0.853
198.817	96.480	11.412	51.156	47.829	54.716	51.234	48.023	52.385	55.924	52.111	0.828
198.817	97.875	11.412	51.474	47.829	54.822	51.375	48.023	52.491	56.030	52.181	0.830
198.817	101.710	11.412	51.156	47.617	54.822	51.198	47.917	52.279	55.818	52.005	0.834
198.817	97.931	11.412	51.071	47.511	54.610	51.064	48.740	52.067	55.733	52.180	0.830
196.235	104.638	11.412	51.262	47.829	54.907	51.333	47.917	52.279	56.030	52.075	0.838
198.300	99.727	11.412	51.224	47.723	54.775	0.000	48.124	52.300	55.907	52.110	0.832
180.743	93.259	11.409	56.160	52.230	58.885	55.758	53.226	56.477	59.912	56.538	0.823
180.743	94.704	11.408	56.075	52.336	58.991	55.801	53.534	56.477	59.815	56.608	0.824
180.743	98.472	11.409	56.075	52.230	58.885	55.730	52.927	56.371	60.008	56.435	0.829
183.325	86.386	11.408	55.357	51.617	58.188	55.054	53.642	56.567	60.107	56.772	0.813
178.160	83.957	11.409	55.251	51.617	58.188	55.019	53.536	56.579	59.901	56.672	0.809
180.743	91.356	11.408	55.784	52.006	58.628	0.000	53.373	56.494	59.949	56.605	0.820
162.668	73.078	11.405	60.217	56.477	62.625	59.773	57.783	60.301	63.344	60.476	0.789
165.250	74.842	11.405	59.709	56.075	62.435	59.407	57.981	60.005	63.238	60.408	0.792
167.832	76.485	11.405	58.885	55.061	61.527	58.491	57.991	60.002	63.340	60.444	0.795
170.414	74.574	11.405	58.885	55.167	61.527	58.526	58.097	60.213	63.446	60.585	0.792
162.668	77.463	11.405	58.801	55.251	61.527	58.526	58.097	60.213	63.340	60.550	0.797
165.767	75.288	11.405	59.300	55.606	61.928	0.000	57.990	60.147	63.341	60.493	0.793
108.446	54.969	11.398	65.963	62.942	67.590	65.499	64.249	66.671	68.499	66.473	0.742
111.028	56.632	11.398	65.963	62.942	67.781	65.562	64.143	66.784	68.605	66.511	0.747
113.610	54.697	11.398	65.963	63.132	67.886	65.661	64.566	66.777	68.689	66.677	0.741
123.938	63.778	11.398	65.963	62.942	67.992	65.632	64.354	66.671	68.605	66.543	0.766
121.356	60.868	11.398	65.562	62.731	67.781	65.358	64.648	66.784	68.499	66.644	0.759
115.675	58.189	11.398	65.883	62.938	67.806	0.000	64.392	66.737	68.579	66.569	0.751
108.446	52.073	11.394	68.569	66.122	70.590	68.427	68.261	69.172	71.015	69.483	0.731
108.446	51.397	11.394	68.866	66.335	70.696	68.632	68.249	69.075	71.207	69.510	0.729
108.446	46.736	11.394	68.973	66.526	71.015	68.838	68.265	69.283	71.313	69.620	0.711
108.446	49.596	11.394	68.675	66.228	70.505	68.469	68.261	69.184	71.015	69.487	0.722
111.028	46.917	11.395	68.675	66.228	70.590	68.498	68.261	69.273	71.015	69.516	0.712
108.962	49.344	11.394	68.751	66.288	70.679	68.573	68.259	69.197	71.113	69.523	0.721

F_R	U_L	k	ρ	C_p	ν	μ	Re	Pr	Nu
0.780	13.209	0.634	991.909	4188.167	6.582E-07	6.529E-04	254.040	4.313	5.991
0.780	13.213	0.634	991.928	4188.099	6.588E-07	6.535E-04	253.811	4.317	5.975
0.780	13.216	0.634	991.946	4188.031	6.594E-07	6.541E-04	253.582	4.322	5.962
0.782	13.184	0.634	991.946	4188.031	6.594E-07	6.541E-04	253.582	4.322	6.102
0.779	13.228	0.634	991.982	4187.897	6.605E-07	6.552E-04	253.124	4.330	5.911
0.780	13.210	0.634	991.942	4188.045	6.593E-07	6.539E-04	253.628	4.321	5.988
0.771	13.368	0.640	990.557	4193.820	6.185E-07	6.126E-04	270.725	4.016	5.382
0.774	13.313	0.640	990.537	4193.909	6.180E-07	6.121E-04	270.960	4.012	5.581
0.771	13.366	0.640	990.537	4193.909	6.180E-07	6.121E-04	270.960	4.012	5.391
0.766	13.457	0.640	990.499	4194.087	6.169E-07	6.111E-04	271.429	4.004	5.094
0.766	13.453	0.640	990.518	4193.998	6.174E-07	6.116E-04	271.194	4.008	5.105
0.770	13.389	0.640	990.530	4193.944	6.178E-07	6.119E-04	271.053	4.011	5.311
0.748	13.779	0.649	988.020	4207.033	5.588E-07	5.521E-04	300.404	3.578	4.265
0.749	13.751	0.649	987.977	4207.282	5.579E-07	5.512E-04	300.893	3.571	4.325
0.753	13.678	0.649	988.020	4207.033	5.588E-07	5.521E-04	300.404	3.578	4.496
0.749	13.750	0.649	987.977	4207.282	5.579E-07	5.512E-04	300.893	3.571	4.328
0.756	13.626	0.649	987.955	4207.407	5.575E-07	5.508E-04	301.138	3.568	4.624
0.751	13.715	0.649	987.990	4207.207	5.582E-07	5.515E-04	300.747	3.573	4.408
0.743	13.869	0.656	985.991	4219.530	5.208E-07	5.135E-04	322.987	3.304	4.081
0.745	13.838	0.656	985.945	4219.831	5.200E-07	5.127E-04	323.491	3.298	4.143
0.749	13.760	0.656	985.991	4219.530	5.208E-07	5.135E-04	322.987	3.304	4.309
0.734	14.032	0.656	985.968	4219.680	5.204E-07	5.131E-04	323.239	3.301	3.780
0.731	14.096	0.656	986.014	4219.379	5.212E-07	5.139E-04	322.735	3.306	3.674
0.741	13.911	0.656	985.982	4219.590	5.207E-07	5.134E-04	323.087	3.302	3.997
0.713	14.457	0.661	984.261	4231.268	4.933E-07	4.855E-04	341.619	3.108	3.173
0.716	14.394	0.661	984.286	4231.097	4.936E-07	4.859E-04	341.361	3.110	3.250
0.719	14.339	0.661	984.261	4231.268	4.933E-07	4.855E-04	341.619	3.108	3.321
0.715	14.405	0.661	984.237	4231.439	4.929E-07	4.851E-04	341.878	3.105	3.238
0.720	14.308	0.661	984.164	4231.955	4.918E-07	4.840E-04	342.654	3.098	3.362
0.717	14.380	0.661	984.242	4231.405	4.930E-07	4.852E-04	341.826	3.106	3.269
0.670	15.368	0.669	981.088	4254.909	4.512E-07	4.427E-04	374.654	2.814	2.357
0.675	15.265	0.669	981.061	4255.116	4.509E-07	4.424E-04	374.924	2.812	2.428
0.670	15.388	0.669	981.035	4255.324	4.506E-07	4.421E-04	375.194	2.810	2.345
0.692	14.880	0.669	981.035	4255.324	4.506E-07	4.421E-04	375.194	2.810	2.734
0.686	15.026	0.670	981.008	4255.532	4.503E-07	4.417E-04	375.465	2.808	2.609
0.679	15.173	0.669	981.045	4255.241	4.507E-07	4.422E-04	375.086	2.811	2.495
0.661	15.589	0.673	979.525	4267.398	4.336E-07	4.247E-04	390.490	2.693	2.221
0.659	15.639	0.673	979.525	4267.398	4.336E-07	4.247E-04	390.490	2.693	2.192
0.643	16.021	0.673	979.579	4266.951	4.342E-07	4.253E-04	389.938	2.697	1.993
0.653	15.777	0.673	979.579	4266.951	4.342E-07	4.253E-04	389.938	2.697	2.115
0.644	16.004	0.673	979.662	4266.283	4.351E-07	4.262E-04	389.112	2.703	2.002
0.652	15.798	0.673	979.574	4266.996	4.342E-07	4.253E-04	389.993	2.697	2.105

PCM2

Mass flow rate 0.03 kg/s·m²

Set T_i	T_s	T_i	T_o	ΔT	Q_{coll}	$(T_i\text{-}T_a)I_T$	η_{coll}	T_a	I_T	$F_R(\tau\alpha)_e$	$F_R U_L$
35	37.4	37	41.1	4.1	65.75	0.0117	0.63	27.55	805.62	0.74	8.61
	37.6	37.1	41.3	4.2	67.35	0.0121	0.64	27.34	805.93	0.74	8.61
	37.7	37.1	41.3	4.2	67.35	0.0115	0.64	27.74	810.50	0.74	8.61
	37.7	37.1	41.3	4.2	67.35	0.0117	0.64	27.64	808.10	0.74	8.61
	37.8	37.2	41.3	4.1	65.75	0.0117	0.63	27.74	805.15	0.74	8.61
	37.64	37.1	41.26	4.16	66.71	0.0118	0.64	27.60	807.06	0.74	8.61
40	41	40	44	4	64.14	0.0136	0.60	28.90	817.54	0.74	8.61
	41.2	40.2	44.2	4	64.14	0.0138	0.60	28.90	816.07	0.74	8.61
	41.2	40.2	44.2	4	64.14	0.0139	0.61	28.90	814.44	0.74	8.61
	41.4	40.4	44.3	3.9	62.54	0.0141	0.59	28.90	818.39	0.74	8.61
	41.4	40.4	44.4	4	64.14	0.0140	0.60	28.90	820.48	0.74	8.61
	41.24	40.24	44.22	3.98	63.82	0.0139	0.60	28.90	817.39	0.74	8.61
45	51.3	46	49.8	3.8	60.94	0.0176	0.58	31.66	812.35	0.74	8.61
	52.4	45.9	49.7	3.8	60.94	0.0176	0.58	31.66	808.72	0.74	8.61
	53.7	46	49.8	3.8	60.94	0.0178	0.58	31.56	809.41	0.74	8.61
	53.8	46.1	49.9	3.8	60.94	0.0183	0.58	31.35	807.71	0.74	8.61
	53.4	46.1	49.8	3.7	59.33	0.0188	0.57	30.95	806.63	0.74	8.61
	52.92	46.02	49.8	3.78	60.62	0.0180	0.58	31.44	808.96	0.74	8.61
50	52.7	50.3	53.7	3.4	54.52	0.0261	0.51	28.85	820.64	0.74	8.61
	52.7	50.3	53.7	3.4	54.52	0.0258	0.51	29.04	823.73	0.74	8.61
	52.7	50.2	53.8	3.6	57.73	0.0256	0.54	29.15	822.26	0.74	8.61
	52.7	50.2	53.8	3.6	57.73	0.0259	0.54	29.04	816.07	0.74	8.61
	52.7	50.1	53.8	3.7	59.33	0.0256	0.56	29.25	814.91	0.74	8.61
	52.7	50.22	53.76	3.54	56.77	0.0258	0.53	29.07	819.52	0.74	8.61
55	57.5	54.9	57.9	3	48.11	0.0304	0.47	30.76	792.85	0.74	8.61
	57.4	54.8	57.9	3.1	49.71	0.0306	0.48	30.55	792.54	0.74	8.61
	57.3	54.7	57.9	3.2	51.32	0.0302	0.50	30.76	791.76	0.74	8.61
	57.2	54.7	57.9	3.2	51.32	0.0301	0.50	30.95	788.59	0.74	8.61
	57.2	54.6	57.8	3.2	51.32	0.0299	0.50	30.95	791.38	0.74	8.61
	57.32	54.74	57.88	3.14	50.35	0.0303	0.49	30.80	791.42	0.74	8.61
60	62	59.1	61.9	2.8	44.90	0.0392	0.44	28.04	791.61	0.74	8.61
	61.9	59	61.8	2.8	44.90	0.0392	0.44	28.04	789.29	0.74	8.61
	61.8	58.9	61.7	2.8	44.90	0.0390	0.44	28.14	788.67	0.74	8.61
	63	58.9	61.6	2.7	43.30	0.0387	0.42	28.35	789.29	0.74	8.61
	63.5	59	61.6	2.6	41.69	0.0389	0.41	28.35	787.97	0.74	8.61
	62.44	58.98	61.72	2.74	43.94	0.0390	0.43	28.18	789.36	0.74	8.61
65	70.1	65.2	67.2	2	32.07	0.0462	0.31	28.85	786.04	0.74	8.61
	69.8	65.1	67.1	2	32.07	0.0451	0.31	29.25	794.16	0.74	8.61
	69.7	65.1	67.2	2.1	33.68	0.0453	0.33	29.36	788.28	0.74	8.61
	69.4	65.1	67.1	2	32.07	0.0451	0.31	29.36	792.54	0.74	8.61
	43.9	65.2	67.1	1.9	30.47	0.0456	0.30	29.04	792.23	0.74	8.61
	64.58	65.14	67.14	2	32.07	0.0455	0.31	29.17	790.65	0.74	8.61

q"	h_i	$F'U_L$	$1T_{PCM}$	$2T_{PCM}$	$3T_{PCM}$	$T_{PCM}av$	$1T_P$	$2T_P$	$3T_P$	$T_{P\,av}$	F'
243.35	137.44	8.92	38.89	41.19	42.39	40.82	38.30	40.18	41.79	40.09	0.87
249.29	141.73	8.92	38.90	41.58	42.40	40.96	38.09	39.89	41.68	39.89	0.87
249.29	137.38	8.92	38.98	41.58	42.48	41.01	38.19	39.99	41.68	39.96	0.87
249.29	142.25	8.92	38.78	41.48	42.59	40.95	38.38	40.10	41.89	40.12	0.87
243.35	140.12	8.92	39.00	41.48	42.48	40.99	38.19	39.99	41.79	39.99	0.87
246.91	139.76	8.92	38.91	41.46	42.47	40.95	38.23	40.03	41.77	40.01	0.87
237.42	114.42	8.92	41.83	44.25	46.14	44.08	41.44	42.74	44.73	42.97	0.85
237.42	129.03	8.92	41.83	44.15	46.14	44.04	41.02	42.63	44.65	42.77	0.86
237.42	131.02	8.92	41.73	44.25	46.06	44.01	41.33	42.63	44.73	42.90	0.86
231.48	132.23	8.92	42.02	44.14	46.14	44.10	41.44	42.84	44.84	43.04	0.86
237.42	136.08	8.92	41.74	44.65	46.05	44.14	41.52	43.03	44.84	43.13	0.87
236.23	128.07	8.92	41.83	44.29	46.11	44.07	41.35	42.78	44.76	42.96	0.86
225.55	115.28	8.92	48.05	49.86	51.66	49.86	46.96	48.66	50.36	48.66	0.85
225.55	102.68	8.92	48.16	50.07	51.77	50.00	47.15	48.87	50.47	48.83	0.84
225.55	104.11	8.92	48.26	50.07	51.87	50.07	47.25	48.87	50.36	48.83	0.84
225.55	104.35	8.92	48.60	50.41	51.47	50.16	46.75	48.76	50.17	48.56	0.84
219.61	117.09	8.92	48.29	50.01	51.18	49.83	46.56	48.26	49.86	48.23	0.85
224.36	108.32	8.92	48.27	50.08	51.59	49.98	46.93	48.69	50.24	48.62	0.84
201.81	97.11	8.92	52.17	54.18	55.88	54.08	51.37	52.88	54.39	52.88	0.83
201.81	95.51	8.92	52.17	54.29	55.88	54.11	51.47	52.98	54.48	52.98	0.83
213.68	99.69	8.92	52.17	54.38	55.88	54.14	51.37	52.98	54.29	52.88	0.83
213.68	100.89	8.92	52.08	54.38	55.89	54.12	51.18	52.67	54.29	52.71	0.83
219.61	97.96	8.92	52.08	54.49	56.00	54.19	51.18	52.77	54.39	52.78	0.83
210.11	98.24	8.92	52.13	54.34	55.91	54.13	51.31	52.86	54.37	52.85	0.83
178.06	83.43	8.92	56.78	58.61	60.21	58.53	56.20	57.50	58.70	57.46	0.81
184.00	88.19	8.92	56.70	58.51	60.10	58.44	56.30	57.39	58.80	57.50	0.82
189.93	87.47	8.92	56.70	58.61	60.10	58.47	56.30	57.50	58.80	57.53	0.81
189.93	87.75	8.92	56.78	58.51	60.10	58.46	56.30	57.39	58.70	57.46	0.81
189.93	93.40	8.92	56.49	58.30	59.91	58.23	56.09	57.20	58.61	57.30	0.82
186.37	87.99	8.92	56.69	58.51	60.09	58.43	56.24	57.40	58.72	57.45	0.81
166.19	71.72	8.92	61.32	62.81	64.32	62.82	60.82	62.01	63.23	62.02	0.79
166.19	68.75	8.92	61.32	62.81	64.32	62.82	60.92	61.91	63.13	61.98	0.78
166.19	66.02	8.92	61.32	62.81	64.32	62.82	60.71	61.91	63.02	61.88	0.77
160.26	65.64	8.92	61.21	62.73	64.13	62.69	60.71	61.72	63.02	61.82	0.77
154.32	68.55	8.92	61.11	62.52	64.03	62.55	60.71	61.61	62.92	61.75	0.78
162.63	68.08	8.92	61.26	62.73	64.23	62.74	60.77	61.83	63.06	61.89	0.78
118.71	56.24	8.91	66.95	68.44	69.55	68.31	66.95	67.74	68.84	67.84	0.74
118.71	52.04	8.91	66.95	68.54	69.65	68.38	66.95	67.85	68.84	67.88	0.73
124.64	57.68	8.91	66.84	68.54	69.55	68.31	66.84	67.74	68.75	67.78	0.75
118.71	57.13	8.91	66.63	68.35	69.55	68.18	66.74	67.64	68.75	67.71	0.75
112.77	57.60	8.91	66.74	68.25	69.34	68.11	66.53	67.35	68.44	67.44	0.75
118.71	56.05	8.91	66.82	68.42	69.53	68.26	66.80	67.66	68.72	67.73	0.74

F_R	U_L	k	ρ	C_p	ν	μ	Re	Pr	Nu
0.84	10.27	0.63	992.34	4186.61	6.72418E-07	0.00066727	381.031	4.420	6.241
0.84	10.24	0.63	992.29	4186.80	6.70614E-07	0.00066544	382.077	4.406	6.433
0.84	10.27	0.63	992.29	4186.80	6.70614E-07	0.00066544	382.077	4.406	6.236
0.84	10.24	0.63	992.29	4186.80	6.70614E-07	0.00066544	382.077	4.406	6.457
0.84	10.25	0.63	992.27	4186.86	6.70014E-07	0.00066483	382.425	4.402	6.359
0.84	10.26	0.63	992.29	4186.77	6.70854E-07	0.00066568	381.937	4.408	6.344
0.82	10.50	0.64	991.26	4190.73	6.3838E-07	0.0006328	401.783	4.164	5.156
0.83	10.35	0.64	991.19	4191.04	6.36178E-07	0.0006306	403.205	4.148	5.812
0.83	10.34	0.64	991.19	4191.04	6.36178E-07	0.0006306	403.205	4.148	5.902
0.83	10.33	0.64	991.13	4191.28	6.34535E-07	0.0006289	404.272	4.136	5.954
0.84	10.30	0.64	991.11	4191.36	6.33989E-07	0.0006284	404.628	4.131	6.127
0.83	10.36	0.64	991.18	4191.09	6.35849E-07	0.0006302	403.418	4.145	5.769
0.82	10.51	0.65	988.93	4201.95	5.78383E-07	0.0005720	444.508	3.720	5.121
0.81	10.67	0.65	988.97	4201.73	5.7932E-07	0.0005729	443.770	3.727	4.563
0.81	10.65	0.65	988.93	4201.95	5.78383E-07	0.0005720	444.508	3.720	4.625
0.81	10.64	0.65	988.89	4202.18	5.77447E-07	0.0005710	445.247	3.713	4.635
0.82	10.49	0.65	988.91	4202.06	5.77915E-07	0.0005715	444.877	3.717	5.201
0.81	10.59	0.65	988.93	4201.97	5.78289E-07	0.0005719	444.582	3.720	4.812
0.80	10.77	0.65	987.17	4212.10	5.41989E-07	0.0005350	475.203	3.456	4.274
0.80	10.79	0.65	987.17	4212.10	5.41989E-07	0.0005350	475.203	3.456	4.203
0.80	10.73	0.65	987.17	4212.10	5.41989E-07	0.0005350	475.203	3.456	4.387
0.80	10.71	0.65	987.17	4212.10	5.41989E-07	0.0005350	475.203	3.456	4.440
0.80	10.75	0.65	987.19	4211.96	5.4241E-07	0.0005355	474.823	3.459	4.312
0.80	10.75	0.65	987.17	4212.07	5.42073E-07	0.0005351	475.127	3.456	4.323
0.78	11.04	0.66	985.15	4225.13	5.06928E-07	0.0004994	509.111	3.205	3.636
0.79	10.94	0.66	985.17	4224.97	5.07305E-07	0.0004998	508.719	3.207	3.844
0.79	10.95	0.66	985.20	4224.81	5.07683E-07	0.0005002	508.328	3.210	3.813
0.79	10.95	0.66	985.20	4224.81	5.07683E-07	0.0005002	508.328	3.210	3.826
0.79	10.85	0.66	985.24	4224.49	5.08441E-07	0.0005009	507.547	3.215	4.073
0.79	10.94	0.66	985.19	4224.84	5.07608E-07	0.0005001	508.407	3.209	3.836
0.76	11.35	0.66	983.15	4239.26	4.77443E-07	0.0004694	541.651	2.997	3.100
0.75	11.44	0.66	983.20	4238.90	4.78129E-07	0.0004701	540.846	3.001	2.972
0.75	11.54	0.66	983.25	4238.53	4.78817E-07	0.0004708	540.041	3.006	2.854
0.75	11.55	0.66	983.27	4238.35	4.79161E-07	0.0004711	539.640	3.009	2.838
0.75	11.45	0.66	983.25	4238.53	4.78817E-07	0.0004708	540.041	3.006	2.964
0.75	11.47	0.66	983.22	4238.71	4.78473E-07	0.0004704	540.444	3.004	2.943
0.72	11.97	0.67	980.18	4262.11	4.40777E-07	0.0004320	588.486	2.742	2.404
0.71	12.19	0.67	980.23	4261.68	4.41381E-07	0.0004327	587.648	2.746	2.225
0.72	11.90	0.67	980.21	4261.90	4.41079E-07	0.0004323	588.067	2.744	2.466
0.72	11.93	0.67	980.23	4261.68	4.41381E-07	0.0004327	587.648	2.746	2.442
0.72	11.90	0.67	980.21	4261.90	4.41079E-07	0.0004323	588.067	2.744	2.462
0.72	11.98	0.67	980.21	4261.85	4.4114E-07	0.0004324	587.983	2.745	2.396

Mass flow rate 0.02 kg/s·m^2

Set T_i	T_s	T_i	T_o	ΔT	Q_{coll}	$(T_i-T_a)I_T$	η_{coll}	T_a	I_T	$F_R(\tau\alpha)_e$	$F_R U_L$
35	39.4	34.9	41.1	6.2	69.312	0.0138	0.6428	23.4221	829.4608	0.8150	11.1380
	39.4	34.9	41.1	6.2	69.312	0.0137	0.6437	23.5269	828.2997	0.8150	11.1380
	39.5	34.9	41	6.1	68.194	0.0144	0.6334	22.9397	828.1449	0.8150	11.1380
	39.5	35	41	6	67.076	0.0144	0.6224	23.0236	828.9963	0.8150	11.1380
	39.5	35	41	6	67.076	0.0146	0.6251	22.9397	825.3582	0.8150	11.1380
	39.46	34.94	41.04	6.1	68.194	0.0142	0.6335	23.1704	828.0520	0.8150	11.1380
40	41.4	39.1	45	5.9	65.958	0.0187	0.6249	23.9254	811.9667	0.8150	11.1380
	41.4	39.1	45	5.9	65.958	0.0183	0.6244	24.2401	812.5086	0.8150	11.1380
	41.5	39.2	45.1	5.9	65.958	0.0187	0.6243	24.0303	812.6634	0.8150	11.1380
	41.6	39.2	45	5.8	64.840	0.0192	0.6161	23.6318	809.5671	0.8150	11.1380
	41.6	39.2	45	5.8	64.840	0.0189	0.6171	23.9254	808.2511	0.8150	11.1380
	41.5	39.16	45.02	5.86	65.511	0.0188	0.6214	23.9506	810.9914	0.8150	11.1380
45	47	44.6	50	5.4	60.368	0.0240	0.5675	24.9322	818.3141	0.8150	11.1380
	47.1	44.7	50.1	5.4	60.368	0.0241	0.5682	25.0371	817.2304	0.8150	11.1380
	47.1	44.7	50.1	5.4	60.368	0.0242	0.5680	24.9322	817.5400	0.8150	11.1380
	47.1	44.7	50	5.3	59.250	0.0246	0.5578	24.6386	817.0756	0.8150	11.1380
	47.9	44.7	50	5.3	59.250	0.0243	0.5583	24.8273	816.3789	0.8150	11.1380
	47.24	44.68	50.04	5.36	59.921	0.0242	0.5640	24.8735	817.3078	0.8150	11.1380
50	54.3	51.1	55.3	4.2	46.953	0.0316	0.4518	25.8341	799.4267	0.8150	11.1380
	54.2	51.1	55.3	4.2	46.953	0.0315	0.4524	25.9389	798.4204	0.8150	11.1380
	54.2	51.1	55.5	4.4	49.189	0.0312	0.4755	26.2326	795.7885	0.8150	11.1380
	54.1	51	55.3	4.3	48.071	0.0317	0.4670	25.9389	791.7633	0.8150	11.1380
	54.1	51	55.4	4.4	49.189	0.0315	0.4782	26.0438	791.2215	0.8150	11.1380
	54.18	51.06	55.36	4.3	48.071	0.0315	0.4650	25.9977	795.3241	0.8150	11.1380
55	58.8	54.8	58.4	3.6	40.245	0.0371	0.3889	25.2468	795.9433	0.8150	11.1380
	59.1	54.8	58.4	3.6	40.245	0.0368	0.3893	25.5404	795.3241	0.8150	11.1380
	59.9	54.8	58.5	3.7	41.363	0.0372	0.4012	25.3307	793.0019	0.8150	11.1380
	60.5	54.9	58.6	3.7	41.363	0.0368	0.4006	25.6453	794.3178	0.8150	11.1380
	61.2	55.1	58.7	3.6	40.245	0.0377	0.3897	25.1419	794.3178	0.8150	11.1380
	59.9	54.88	58.52	3.64	40.693	0.0371	0.3939	25.3810	794.5810	0.8150	11.1380
60	63.8	59.5	62.9	3.4	38.010	0.0402	0.3699	27.7427	790.4474	0.8150	11.1380
	63.7	59.5	62.8	3.3	36.892	0.0398	0.3589	28.0363	790.6022	0.8150	11.1380
	63.5	59.5	62.8	3.3	36.892	0.0396	0.3585	28.1412	791.5311	0.8150	11.1380
	63.4	59.4	62.8	3.4	38.010	0.0403	0.3700	27.5539	790.2926	0.8150	11.1380
	63.3	59.4	62.7	3.3	36.892	0.0402	0.3589	27.6378	790.6022	0.8150	11.1380
	63.54	59.46	62.8	3.34	37.339	0.0400	0.3633	27.8224	790.6951	0.8150	11.1380
65	69.2	63.9	66.7	2.8	31.302	0.0445	0.3037	28.6446	792.8470	0.8150	11.1380
	68.9	63.8	66.8	3	33.538	0.0447	0.3261	28.4558	791.2215	0.8150	11.1380
	69.3	63.8	66.8	3	33.538	0.0451	0.3264	28.1412	790.4474	0.8150	11.1380
	69.9	63.8	66.8	3	33.538	0.0445	0.3260	28.5928	791.4692	0.8150	11.1380
	70.5	63.9	66.8	2.9	32.420	0.0445	0.3151	28.6780	791.3482	0.8150	11.1380
	69.56	63.84	66.78	2.94	32.867	0.0446	0.3194	28.5025	791.4667	0.8150	11.1380

q"	h_i	F'U$_L$	1T$_{PCM}$	2T$_{PCM}$	3T$_{PCM}$	T$_{PCM}$av	1T$_P$	2T$_P$	3T$_P$	T$_{P\ av}$	F'
256.5415	137.2747	11.9153	35.7345	38.3350	41.3339	38.4678	37.1867	39.8333	42.5864	39.8688	0.8684
256.5415	137.6847	11.9153	35.8184	38.3350	41.2500	38.4678	37.0681	39.9352	42.5864	39.8633	0.8687
252.4037	135.1216	11.9154	35.5248	38.0414	41.0403	38.2021	37.1867	39.8241	42.4431	39.8180	0.8671
248.2659	135.5333	11.9153	35.8184	38.2301	41.0403	38.3629	37.1867	39.8287	42.4799	39.8318	0.8673
248.2659	135.7078	11.9153	35.5248	38.0414	40.8306	38.1322	37.1775	40.0318	42.2789	39.8294	0.8674
252.4037	136.2690	11.9153	35.6841	38.1966	41.0990	38.3266	37.1612	39.8906	42.4750	39.8422	0.8678
244.1282	108.7126	11.9142	39.3416	41.7534	44.6475	41.9141	41.9365	43.8793	47.0711	44.2956	0.8444
244.1282	133.7339	11.9142	39.5304	41.9421	44.8572	42.1099	41.4262	43.6726	46.5276	43.8755	0.8648
244.1282	130.9388	11.9142	39.7401	42.1518	44.8572	42.2497	41.6347	43.6726	46.7361	44.0144	0.8629
239.9904	127.4655	11.9142	39.5304	41.8373	44.6475	42.0050	41.6354	43.7799	46.5330	43.9828	0.8604
239.9904	137.8968	11.9142	39.8449	42.0470	44.8572	42.2497	41.3374	43.6643	46.5194	43.8404	0.8676
242.4731	126.8337	11.9142	39.5975	41.9463	44.7733	42.1057	41.5940	43.7337	46.6774	44.0017	0.8599
223.4393	101.8559	11.9123	44.9103	47.2197	49.6131	47.2477	47.0496	49.2868	52.1447	49.4937	0.8354
223.4393	108.7245	11.9122	44.7003	47.0097	49.5291	47.0797	47.0404	49.3841	51.9408	49.4551	0.8426
223.4393	108.4615	11.9122	44.4064	46.8208	49.3192	46.8488	47.2563	49.0904	52.0335	49.4601	0.8423
219.3016	107.1466	11.9122	44.5954	46.8208	49.3192	46.9118	47.2609	49.0950	51.8343	49.3967	0.8410
219.3016	110.8257	11.9122	44.5954	46.9048	49.4241	46.9748	47.0571	49.0950	51.8343	49.3288	0.8447
221.7842	107.3039	11.9122	44.6415	46.9552	49.4409	47.0125	47.1329	49.1903	51.9575	49.4269	0.8412
173.7862	92.5228	11.9093	51.0197	53.2452	55.4496	53.2382	53.1394	54.9718	57.1237	55.0783	0.8222
173.7862	89.1519	11.9093	51.0197	53.4341	55.5546	53.3362	53.1394	55.0783	57.2302	55.1493	0.8176
182.0617	100.3749	11.9092	51.0197	53.3292	55.4496	53.2662	53.0329	55.0783	57.2302	55.1138	0.8318
177.9239	92.2695	11.9093	50.9358	53.2452	55.5546	53.2452	53.1394	54.9718	57.1237	55.0783	0.8218
182.0617	98.7964	11.9093	50.9358	53.2452	55.4496	53.2102	53.0329	54.9718	57.1237	55.0428	0.8300
177.9239	94.5142	11.9093	50.9862	53.2998	55.4916	53.2592	53.0968	55.0144	57.1663	55.0925	0.8247
148.9596	84.7433	11.9072	54.3849	56.1885	58.0130	56.1955	56.6533	58.2939	60.1262	58.3578	0.8099
148.9596	73.6993	11.9072	54.5946	56.6079	58.5164	56.5730	56.9522	58.4862	60.4251	58.6212	0.7909
153.0973	78.8291	11.9072	54.3849	56.3982	58.3066	56.3633	56.8663	58.4856	60.4245	58.5921	0.8002
153.0973	80.0232	11.9071	54.6995	56.6079	58.5164	56.6079	56.8663	58.5921	60.5310	58.6632	0.8023
148.9596	75.6477	11.9070	54.8882	56.7967	58.8100	56.8316	57.1646	58.8052	60.6375	58.8691	0.7944
150.6147	78.4175	11.9071	54.5904	56.5198	58.4325	56.5143	56.9006	58.5326	60.4289	58.6207	0.7995
140.6840	59.1896	11.9040	59.0048	61.2302	63.3297	61.1882	61.9753	63.9141	64.8411	63.5768	0.7553
136.5463	65.2383	11.9041	58.9208	60.9153	63.1197	60.9853	61.7835	63.5093	64.4363	63.2430	0.7709
136.5463	63.4909	11.9041	58.8158	60.8103	62.9308	60.8523	61.5705	63.4028	64.9287	63.3006	0.7666
140.6840	68.8144	11.9041	58.3119	60.3274	62.4269	60.3554	61.4852	63.2110	64.7369	63.1444	0.7790
136.5463	71.3412	11.9041	60.1020	62.0125	64.0280	62.0475	61.1656	62.8062	64.9201	62.9640	0.7844
138.2014	65.3193	11.9041	59.0311	61.0591	63.1670	61.0857	61.5960	63.3687	64.7726	63.2458	0.7711
115.8574	48.4262	11.9008	63.6134	65.3331	67.0318	65.3261	66.2578	67.6001	69.2194	67.6925	0.7187
124.1330	52.5087	11.9008	63.6134	65.3331	67.0318	65.3261	66.1726	67.6001	69.2194	67.6640	0.7332
124.1330	57.5199	11.9008	63.3198	65.1234	66.8430	65.0954	66.0661	67.3871	68.9211	67.4581	0.7489
124.1330	46.1171	11.9008	63.8776	65.6980	67.4428	65.6728	66.4950	67.9424	69.5376	67.9917	0.7095
119.9952	43.0115	11.9008	64.0084	65.8513	67.6304	65.8300	66.6164	68.0988	69.7043	68.1398	0.6962
121.6503	49.0679	11.9008	63.6865	65.4678	67.1960	65.4501	66.3216	67.7257	69.3204	67.7892	0.7210

F_R	U_L	k	ρ	C_p	ν	μ	Re	Pr	Nu
0.8118	13.7203	0.6303	992.7097	4185.3876	6.853E-07	6.803E-04	260.544	4.517	6.251
0.8120	13.7162	0.6303	992.7097	4185.3876	6.853E-07	6.803E-04	260.544	4.517	6.269
0.8105	13.7422	0.6302	992.7271	4185.3324	6.859E-07	6.809E-04	260.303	4.522	6.153
0.8107	13.7380	0.6303	992.7097	4185.3876	6.853E-07	6.803E-04	260.544	4.517	6.171
0.8109	13.7361	0.6303	992.7097	4185.3876	6.853E-07	6.803E-04	260.544	4.517	6.179
0.8112	13.7304	0.6303	992.7132	4185.3766	6.854E-07	6.804E-04	260.496	4.518	6.205
0.7894	14.1102	0.6369	991.2442	4190.8079	6.378E-07	6.322E-04	280.342	4.160	4.899
0.8085	13.7766	0.6369	991.2442	4190.8079	6.378E-07	6.322E-04	280.342	4.160	6.026
0.8066	13.8080	0.6371	991.2066	4190.9655	6.367E-07	6.311E-04	280.838	4.152	5.899
0.8043	13.8479	0.6370	991.2254	4190.8866	6.373E-07	6.317E-04	280.590	4.156	5.743
0.8110	13.7329	0.6370	991.2254	4190.8866	6.373E-07	6.317E-04	280.590	4.156	6.213
0.8039	13.8555	0.6370	991.2292	4190.8708	6.374E-07	6.318E-04	280.540	4.157	5.715
0.7811	14.2592	0.6451	989.1776	4200.6291	5.840E-07	5.777E-04	306.797	3.762	4.531
0.7878	14.1378	0.6453	989.1365	4200.8468	5.831E-07	5.768E-04	307.310	3.755	4.836
0.7876	14.1422	0.6453	989.1365	4200.8468	5.831E-07	5.768E-04	307.310	3.755	4.824
0.7864	14.1640	0.6452	989.1571	4200.7378	5.836E-07	5.772E-04	307.053	3.758	4.766
0.7898	14.1031	0.6452	989.1571	4200.7378	5.836E-07	5.772E-04	307.053	3.758	4.930
0.7865	14.1615	0.6452	989.1529	4200.7596	5.835E-07	5.771E-04	307.104	3.758	4.773
0.7689	14.4850	0.6539	986.6304	4215.4320	5.320E-07	5.249E-04	337.653	3.384	4.061
0.7646	14.5664	0.6539	986.6304	4215.4320	5.320E-07	5.249E-04	337.653	3.384	3.913
0.7779	14.3178	0.6540	986.5852	4215.7173	5.312E-07	5.241E-04	338.187	3.378	4.405
0.7686	14.4910	0.6538	986.6530	4215.2899	5.325E-07	5.253E-04	337.387	3.387	4.050
0.7762	14.3489	0.6539	986.6304	4215.4320	5.320E-07	5.249E-04	337.653	3.384	4.336
0.7713	14.4400	0.6539	986.6259	4215.4605	5.320E-07	5.248E-04	337.707	3.383	4.148
0.7576	14.7012	0.6587	985.0545	4225.7726	5.054E-07	4.979E-04	356.007	3.194	3.692
0.7398	15.0561	0.6587	985.0545	4225.7726	5.054E-07	4.979E-04	356.007	3.194	3.211
0.7485	14.8795	0.6588	985.0308	4225.9345	5.050E-07	4.975E-04	356.280	3.191	3.434
0.7504	14.8421	0.6589	984.9832	4226.2593	5.043E-07	4.967E-04	356.826	3.186	3.485
0.7431	14.9879	0.6591	984.9117	4226.7485	5.032E-07	4.956E-04	357.647	3.178	3.294
0.7479	14.8930	0.6589	985.0070	4226.0968	5.047E-07	4.971E-04	356.553	3.189	3.416
0.7067	15.7611	0.6650	982.7966	4241.8693	4.727E-07	4.646E-04	381.538	2.963	2.554
0.7213	15.4420	0.6649	982.8220	4241.6813	4.730E-07	4.649E-04	381.256	2.966	2.816
0.7173	15.5276	0.6649	982.8220	4241.6813	4.730E-07	4.649E-04	381.256	2.966	2.740
0.7289	15.2804	0.6649	982.8473	4241.4936	4.734E-07	4.652E-04	380.975	2.968	2.970
0.7340	15.1752	0.6648	982.8726	4241.3062	4.737E-07	4.656E-04	380.693	2.970	3.080
0.7215	15.4382	0.6649	982.8321	4241.6062	4.732E-07	4.650E-04	381.144	2.967	2.819
0.6726	16.5592	0.6703	980.6623	4258.2582	4.463E-07	4.376E-04	405.006	2.780	2.073
0.6862	16.2316	0.6703	980.6623	4258.2582	4.463E-07	4.376E-04	405.006	2.780	2.248
0.7009	15.8914	0.6703	980.6623	4258.2582	4.463E-07	4.376E-04	405.006	2.780	2.463
0.6640	16.7733	0.6703	980.6623	4258.2582	4.463E-07	4.376E-04	405.006	2.780	1.974
0.6516	17.0944	0.6704	980.6356	4258.4700	4.460E-07	4.373E-04	405.296	2.778	1.841
0.6748	16.5051	0.6704	980.6570	4258.3006	4.462E-07	4.376E-04	405.064	2.780	2.101

Mass flow rate 0.01 kg/s·m^2

Set T$_i$	T$_s$	T$_i$	T$_o$	ΔT	Q$_{coll}$	(T$_i$-T$_a$)I$_T$	η$_{coll}$	T$_a$	I$_T$	F$_R$(τα)$_e$	F$_R$U$_L$
	40.3	35.5	44.7	9.2	64.329	0.00857	0.628	28.749	787.970	0.699	9.475
	40.3	35.5	44.7	9.2	64.329	0.00833	0.620	28.854	797.956	0.699	9.475
35	38.5	35.5	44.7	9.2	64.329	0.00892	0.617	28.351	801.362	0.699	9.475
	39.5	35.6	44.9	9.3	65.028	0.00829	0.624	28.959	801.207	0.699	9.475
	40.5	35.8	45.0	9.2	64.329	0.00802	0.616	29.358	803.684	0.699	9.475
	39.8	35.6	44.8	9.2	64.469	0.00842	0.621	28.854	798.436	0.699	9.475
	45.6	39.3	47.7	8.4	58.735	0.01232	0.571	29.546	791.763	0.699	9.475
	45.7	39.3	47.7	8.4	58.735	0.01281	0.570	29.148	792.383	0.699	9.475
40	45.8	39.4	47.8	8.4	58.735	0.01219	0.571	29.756	791.067	0.699	9.475
	45.8	39.5	47.8	8.3	58.036	0.01214	0.562	29.861	793.699	0.699	9.475
	45.9	39.5	47.9	8.4	58.735	0.01178	0.570	30.155	793.079	0.699	9.475
	45.8	39.4	47.8	8.4	58.595	0.01225	0.569	29.693	792.398	0.699	9.475
	51.7	47.6	55.1	7.5	52.442	0.02264	0.495	29.148	815.063	0.699	9.475
	51.7	47.6	55.1	7.5	52.442	0.02277	0.498	29.148	810.496	0.699	9.475
45	51.8	47.6	55.0	7.4	51.743	0.02379	0.492	28.351	809.180	0.699	9.475
	51.8	47.6	55.0	7.4	51.743	0.02381	0.492	28.351	808.406	0.699	9.475
	51.8	47.6	55.0	7.4	51.743	0.02466	0.492	27.638	809.412	0.699	9.475
	51.8	47.6	55.0	7.4	52.023	0.02353	0.494	28.527	810.511	0.699	9.475
	55.0	51.2	57.9	6.7	46.848	0.02683	0.449	29.651	803.142	0.699	9.475
	54.9	51.2	58.0	6.8	47.548	0.02652	0.456	29.945	801.517	0.699	9.475
50	54.9	51.2	58.1	6.9	48.247	0.02617	0.462	30.155	804.149	0.699	9.475
	54.9	51.2	58.2	7.0	48.946	0.02588	0.470	30.448	801.826	0.699	9.475
	54.9	51.1	58.3	7.2	50.344	0.02604	0.484	30.260	800.201	0.699	9.475
	54.9	51.2	58.1	6.9	48.387	0.02629	0.464	30.092	802.167	0.699	9.475
	63.5	54.9	60.9	6.0	41.954	0.03029	0.402	30.553	803.684	0.699	9.475
	64.5	54.9	60.9	6.0	41.954	0.03031	0.402	30.553	803.297	0.699	9.475
55	64.8	54.9	61.0	6.1	42.653	0.03053	0.407	30.260	807.090	0.699	9.475
	64.6	54.8	61.1	6.3	44.051	0.03030	0.422	30.448	803.684	0.699	9.475
	65.2	54.9	61.1	6.2	43.352	0.03050	0.416	30.448	801.672	0.699	9.475
	64.5	54.9	61.0	6.1	42.793	0.03039	0.409	30.453	803.885	0.699	9.475
	66.5	61.2	65.5	4.3	30.067	0.03813	0.292	30.952	793.389	0.699	9.475
	66.3	61.1	65.6	4.5	31.465	0.03804	0.304	30.847	795.324	0.699	9.475
60	66.2	61.1	65.7	4.6	32.165	0.03789	0.312	31.057	793.002	0.699	9.475
	66.0	61.0	65.7	4.7	32.864	0.03791	0.319	30.952	792.692	0.699	9.475
	65.9	61.0	65.6	4.6	32.165	0.03832	0.312	30.658	791.763	0.699	9.475
	66.2	61.1	65.6	4.5	31.745	0.03806	0.308	30.893	793.234	0.699	9.475
	71.7	65.7	69.8	4.1	28.668	0.04545	0.276	29.442	797.777	0.699	9.475
	71.5	65.5	69.7	4.2	29.368	0.04520	0.283	29.442	797.777	0.699	9.475
65	71.4	65.5	69.6	4.1	28.668	0.04607	0.276	28.749	797.777	0.699	9.475
	71.2	65.3	69.5	4.2	29.368	0.04595	0.283	28.645	797.777	0.699	9.475
	71.1	65.4	69.5	4.1	28.668	0.04568	0.276	28.959	797.777	0.699	9.475
	71.4	65.5	69.6	4.1	28.948	0.04567	0.279	29.047	797.777	0.699	9.475

q"	h_i	$F'U_L$	$1T_{PCM}$	$2T_{PCM}$	$3T_{PCM}$	$T_{PCM}av$	$1T_P$	$2T_P$	$3T_P$	$T_{P\,av}$	F'
237.547	126.644	10.405	36.476	41.279	45.494	41.083	37.797	41.906	46.224	41.976	0.860
237.547	126.644	10.405	36.267	41.279	45.305	40.950	37.692	42.011	46.224	41.976	0.860
237.547	126.644	10.405	36.267	41.279	45.305	40.950	37.797	41.906	46.224	41.976	0.860
240.129	129.208	10.405	36.372	41.279	45.305	40.985	37.797	42.115	46.413	42.108	0.862
237.547	127.086	10.405	36.476	41.593	45.704	41.258	38.090	42.199	46.518	42.269	0.861
238.064	127.242	10.405	36.372	41.342	45.423	41.045	37.835	42.027	46.321	42.061	0.861
216.891	119.480	10.404	38.577	44.299	48.221	43.699	41.904	45.113	48.929	45.315	0.854
216.891	119.941	10.404	39.391	44.194	47.801	43.796	41.799	45.008	49.117	45.308	0.854
216.891	121.354	10.404	38.577	44.592	48.116	43.762	41.407	45.323	49.432	45.387	0.855
214.309	113.060	10.404	39.080	44.907	48.514	44.167	41.400	45.616	49.620	45.546	0.848
216.891	115.026	10.404	39.185	45.201	48.703	44.363	41.313	45.509	49.935	45.586	0.850
216.375	117.698	10.404	38.962	44.639	48.271	43.957	41.565	45.314	49.407	45.428	0.852
193.653	94.258	10.400	48.221	51.723	55.225	51.723	50.033	52.828	57.352	53.405	0.825
193.653	95.629	10.400	48.221	51.618	55.036	51.625	50.134	52.744	57.248	53.375	0.827
191.071	84.196	10.400	47.508	51.010	54.533	51.017	49.927	53.139	57.642	53.569	0.811
191.071	85.419	10.400	47.612	50.926	54.323	50.954	50.123	53.034	57.454	53.537	0.813
191.071	86.604	10.400	47.004	50.423	53.820	50.416	50.025	53.037	57.457	53.506	0.815
192.103	89.003	10.400	47.713	51.140	54.588	51.147	50.048	52.956	57.431	53.478	0.818
172.996	78.270	10.397	51.321	54.329	58.433	54.694	53.522	56.696	60.063	56.760	0.800
175.578	78.941	10.397	51.530	54.317	58.438	54.762	53.522	56.888	60.063	56.824	0.801
178.160	78.360	10.397	51.434	54.322	58.438	54.731	53.628	56.888	60.254	56.924	0.800
180.743	85.150	10.397	51.625	54.317	58.438	54.793	53.522	56.798	60.148	56.823	0.811
185.907	88.796	10.397	51.816	54.329	58.529	54.891	53.534	56.891	59.956	56.794	0.816
178.677	81.779	10.397	51.545	54.323	58.455	54.774	53.545	56.832	60.097	56.825	0.806
154.922	67.488	10.395	54.329	59.220	61.226	58.259	57.341	60.196	63.051	60.196	0.777
154.922	70.772	10.395	54.436	59.236	61.038	58.237	57.234	59.982	63.051	60.089	0.784
157.504	69.154	10.395	54.518	58.926	61.132	58.192	57.230	60.192	63.260	60.228	0.781
162.668	69.472	10.395	54.435	58.930	61.020	58.128	57.230	60.299	63.345	60.291	0.782
160.086	69.552	10.395	54.435	58.930	61.025	58.130	57.145	60.405	63.355	60.302	0.782
158.021	69.275	10.395	54.431	59.048	61.088	58.189	57.236	60.215	63.212	60.221	0.781
111.028	55.226	10.390	60.934	62.526	65.827	63.096	62.981	65.325	67.775	65.360	0.743
116.192	53.452	10.390	60.934	62.631	66.036	63.200	63.173	65.431	67.967	65.524	0.737
118.774	58.673	10.390	60.934	63.422	66.036	63.464	62.981	65.431	67.860	65.424	0.753
121.356	57.713	10.390	60.829	63.631	66.120	63.527	63.066	65.431	67.860	65.453	0.750
118.774	60.788	10.390	60.536	63.234	65.932	63.234	62.768	65.218	67.775	65.254	0.759
117.224	57.098	10.390	60.833	63.089	65.990	63.304	62.994	65.368	67.848	65.403	0.749
105.863	37.254	10.385	65.414	68.227	70.328	67.989	68.440	70.484	72.851	70.592	0.666
108.446	38.944	10.385	65.414	68.439	70.340	68.064	68.529	70.183	72.442	70.385	0.675
105.863	33.262	10.385	65.015	68.430	70.431	67.959	68.953	70.997	72.248	70.733	0.642
108.446	36.818	10.386	64.931	68.342	70.443	67.905	68.523	70.696	71.818	70.345	0.664
105.863	36.562	10.386	64.826	68.241	70.338	67.802	68.630	70.588	71.818	70.345	0.663
106.896	36.484	10.385	65.120	68.336	70.376	67.944	68.615	70.590	72.235	70.480	0.662

F_R	U_L	k	ρ	C_p	ν	μ	Re	Pr	Nu
0.783	12.093	0.634	991.964	4187.964	6.600E-07	6.547E-04	169.342	4.326	5.735
0.783	12.093	0.634	991.964	4187.964	6.600E-07	6.547E-04	169.342	4.326	5.735
0.783	12.093	0.634	991.964	4187.964	6.600E-07	6.547E-04	169.342	4.326	5.735
0.785	12.068	0.634	991.909	4188.167	6.582E-07	6.529E-04	169.801	4.313	5.849
0.783	12.090	0.634	991.855	4188.373	6.565E-07	6.511E-04	170.261	4.300	5.751
0.783	12.087	0.634	991.931	4188.085	6.589E-07	6.536E-04	169.618	4.318	5.761
0.777	12.187	0.639	990.692	4193.205	6.222E-07	6.164E-04	179.858	4.043	5.364
0.777	12.182	0.639	990.692	4193.205	6.222E-07	6.164E-04	179.858	4.043	5.385
0.778	12.165	0.639	990.654	4193.379	6.211E-07	6.153E-04	180.171	4.036	5.447
0.772	12.268	0.639	990.634	4193.467	6.206E-07	6.148E-04	180.327	4.032	5.074
0.773	12.243	0.640	990.615	4193.555	6.201E-07	6.142E-04	180.484	4.028	5.162
0.776	12.209	0.639	990.658	4193.362	6.212E-07	6.154E-04	180.140	4.036	5.283
0.751	12.605	0.651	987.455	4210.362	5.475E-07	5.406E-04	205.057	3.496	4.154
0.753	12.579	0.651	987.455	4210.362	5.475E-07	5.406E-04	205.057	3.496	4.215
0.738	12.825	0.651	987.477	4210.230	5.479E-07	5.411E-04	204.892	3.499	3.711
0.740	12.795	0.651	987.477	4210.230	5.479E-07	5.411E-04	204.892	3.499	3.765
0.742	12.767	0.651	987.477	4210.230	5.479E-07	5.411E-04	204.892	3.499	3.817
0.745	12.714	0.651	987.468	4210.283	5.478E-07	5.409E-04	204.958	3.497	3.923
0.729	12.997	0.656	986.014	4219.379	5.212E-07	5.139E-04	215.717	3.306	3.425
0.730	12.979	0.656	985.991	4219.530	5.208E-07	5.135E-04	215.886	3.304	3.454
0.729	12.995	0.656	985.968	4219.680	5.204E-07	5.131E-04	216.054	3.301	3.428
0.739	12.818	0.656	985.945	4219.831	5.200E-07	5.127E-04	216.223	3.298	3.725
0.744	12.734	0.656	985.945	4219.831	5.200E-07	5.127E-04	216.223	3.298	3.885
0.734	12.902	0.656	985.973	4219.650	5.205E-07	5.132E-04	216.021	3.301	3.578
0.708	13.373	0.661	984.431	4230.076	4.958E-07	4.881E-04	227.132	3.126	2.932
0.715	13.251	0.661	984.431	4230.076	4.958E-07	4.881E-04	227.132	3.126	3.075
0.711	13.310	0.661	984.407	4230.245	4.954E-07	4.877E-04	227.304	3.123	3.004
0.712	13.299	0.661	984.407	4230.245	4.954E-07	4.877E-04	227.304	3.123	3.018
0.712	13.296	0.661	984.383	4230.415	4.951E-07	4.873E-04	227.477	3.121	3.021
0.712	13.306	0.661	984.412	4230.212	4.955E-07	4.878E-04	227.270	3.124	3.010
0.677	13.985	0.668	981.692	4250.224	4.585E-07	4.501E-04	246.284	2.865	2.373
0.672	14.093	0.668	981.692	4250.224	4.585E-07	4.501E-04	246.284	2.865	2.297
0.686	13.797	0.668	981.666	4250.424	4.582E-07	4.498E-04	246.463	2.863	2.521
0.684	13.847	0.668	981.692	4250.224	4.585E-07	4.501E-04	246.284	2.865	2.480
0.692	13.691	0.668	981.718	4250.023	4.589E-07	4.505E-04	246.104	2.867	2.613
0.682	13.880	0.668	981.692	4250.224	4.585E-07	4.501E-04	246.284	2.865	2.454
0.608	15.586	0.673	979.332	4268.970	4.316E-07	4.227E-04	262.298	2.679	1.588
0.616	15.375	0.673	979.415	4268.295	4.324E-07	4.235E-04	261.744	2.685	1.660
0.586	16.165	0.673	979.442	4268.070	4.327E-07	4.238E-04	261.559	2.687	1.418
0.605	15.641	0.673	979.525	4267.398	4.336E-07	4.247E-04	261.005	2.693	1.570
0.604	15.675	0.673	979.497	4267.622	4.333E-07	4.244E-04	261.190	2.691	1.559
0.604	15.687	0.673	979.442	4268.070	4.327E-07	4.238E-04	261.559	2.687	1.555

Without PCM

Mass flow rate 0.03 kg/s·m^2

Set T$_i$	T$_s$	T$_i$	T$_o$	ΔT	Q$_{coll}$	(T$_i$-T$_a$)I$_T$	η$_{coll}$	T$_a$	I$_T$	F$_R$(τα)$_e$	F$_R$U$_L$
	39.60	36.20	40.40	4.20	67.35	0.00680	0.65	30.76	799.58	0.70	8.70
	39.80	36.30	40.50	4.20	67.35	0.00678	0.64	30.85	804.30	0.70	8.70
35	39.90	36.30	40.40	4.10	65.75	0.00706	0.63	30.66	798.73	0.70	8.70
	40.00	36.30	40.50	4.20	67.35	0.00718	0.65	30.55	800.20	0.70	8.70
	40.00	36.40	40.50	4.10	65.75	0.00703	0.63	30.76	801.83	0.70	8.70
	39.93	36.33	40.48	4.15	66.55	0.00701	0.64	30.71	801.27	0.70	8.70
	42.90	40.50	44.40	3.90	62.54	0.01274	0.60	30.26	803.53	0.70	8.70
	42.90	40.50	44.30	3.80	60.94	0.01340	0.59	29.94	787.97	0.70	8.70
40	43.00	40.50	44.30	3.80	60.94	0.01290	0.58	30.15	801.67	0.70	8.70
	43.10	40.50	44.20	3.70	59.33	0.01327	0.57	29.94	795.17	0.70	8.70
	43.20	40.50	44.30	3.80	60.94	0.01373	0.58	29.44	805.31	0.70	8.70
	43.05	40.50	44.28	3.78	60.54	0.01333	0.58	29.87	797.53	0.70	8.70
	48.00	46.00	49.70	3.70	59.33	0.01874	0.56	30.85	808.41	0.70	8.70
	48.10	46.00	49.60	3.60	57.73	0.01873	0.55	30.85	809.03	0.70	8.70
45	48.20	46.00	49.70	3.70	59.33	0.01879	0.56	30.76	810.81	0.70	8.70
	48.30	46.10	49.80	3.70	59.33	0.01892	0.56	30.76	810.50	0.70	8.70
	48.00	46.10	49.70	3.60	57.73	0.01856	0.55	31.06	810.50	0.70	8.70
	48.17	46.07	49.73	3.67	58.80	0.01876	0.56	30.86	810.60	0.70	8.70
	52.50	50.10	53.20	3.10	49.71	0.02512	0.46	29.15	834.18	0.70	8.70
	52.50	50.10	53.30	3.20	51.32	0.02524	0.47	29.04	834.34	0.70	8.70
50	52.70	50.10	53.30	3.20	51.32	0.02480	0.47	29.44	832.87	0.70	8.70
	54.80	50.20	53.40	3.20	51.32	0.02481	0.47	29.55	832.56	0.70	8.70
	56.40	50.30	53.40	3.10	49.71	0.02560	0.46	29.04	830.47	0.70	8.70
	54.10	50.18	53.35	3.18	50.91	0.02511	0.47	29.27	832.56	0.70	8.70
	56.40	54.00	57.10	3.10	49.71	0.02915	0.47	30.26	814.29	0.70	8.70
	58.10	53.70	56.70	3.00	48.11	0.02852	0.45	29.65	814.75	0.70	8.70
55	59.10	53.80	56.70	2.90	46.51	0.02934	0.44	30.15	811.66	0.70	8.70
	60.30	53.70	56.60	2.90	46.51	0.02892	0.44	30.05	811.04	0.70	8.70
	60.20	53.70	56.60	2.90	46.51	0.02847	0.44	30.45	815.37	0.70	8.70
	59.43	53.73	56.65	2.93	46.91	0.02881	0.44	30.08	813.21	0.70	8.70
	62.50	60.20	62.60	2.40	38.49	0.03553	0.37	31.75	800.74	0.70	8.70
	62.40	60.20	62.60	2.40	38.49	0.03596	0.37	31.46	799.43	0.70	8.70
60	62.50	60.30	62.70	2.40	38.49	0.03550	0.37	31.96	798.27	0.70	8.70
	62.40	60.10	62.60	2.50	40.09	0.03566	0.39	31.66	797.41	0.70	8.70
	62.30	60.10	62.60	2.50	40.09	0.03602	0.39	31.46	795.17	0.70	8.70
	62.40	60.18	62.63	2.45	39.29	0.03579	0.38	31.63	797.57	0.70	8.70
	66.20	63.50	66.00	2.50	40.09	0.03949	0.39	31.96	798.73	0.70	8.70
	66.00	63.20	65.70	2.50	40.09	0.03907	0.39	31.96	799.58	0.70	8.70
65	65.90	63.10	65.60	2.50	40.09	0.03865	0.39	32.36	795.32	0.70	8.70
	65.80	63.00	65.40	2.40	38.49	0.03835	0.37	32.57	793.54	0.70	8.70
	65.80	63.00	65.40	2.40	38.49	0.03922	0.37	31.96	791.38	0.70	8.70
	65.88	63.08	65.53	2.45	39.29	0.03883	0.38	32.21	794.96	0.70	8.70

q"	h_i	$F'U_L$	$1T_P$	$2T_P$	$3T_P$	$T_{P\,av}$	F'	F_R	U_L
249.29	128.13	9.01	38.47	40.68	41.59	40.25	0.86	0.83	10.45
249.29	137.34	9.01	38.38	40.58	41.69	40.22	0.87	0.84	10.38
243.35	128.38	9.01	38.58	40.68	41.48	40.25	0.86	0.83	10.45
249.29	127.81	9.01	38.58	40.89	41.59	40.35	0.86	0.83	10.46
243.35	145.55	9.01	38.68	39.99	41.69	40.12	0.87	0.84	10.32
246.32	134.77	9.01	38.56	40.53	41.61	40.23	0.87	0.84	10.40
231.48	122.10	9.01	42.31	44.61	46.12	44.35	0.86	0.83	10.53
225.55	118.52	9.01	42.29	44.50	46.12	44.30	0.85	0.82	10.56
225.55	118.52	9.01	42.29	44.40	46.22	44.30	0.85	0.82	10.56
219.61	116.28	9.01	42.31	44.40	46.01	44.24	0.85	0.82	10.59
225.55	122.69	9.01	42.49	44.11	46.11	44.24	0.86	0.83	10.52
224.06	119.00	9.01	42.35	44.35	46.12	44.27	0.85	0.82	10.56
219.61	87.74	9.01	48.61	50.12	52.32	50.35	0.82	0.79	11.02
213.68	93.44	9.01	48.32	50.02	51.93	50.09	0.83	0.80	10.92
219.61	95.58	9.01	48.71	49.91	51.82	50.15	0.83	0.80	10.88
219.61	95.40	9.01	48.91	49.91	51.93	50.25	0.83	0.80	10.89
213.68	94.57	9.01	48.92	49.83	51.73	50.16	0.83	0.80	10.90
217.63	95.18	9.01	48.85	49.88	51.83	50.19	0.83	0.80	10.89
184.00	77.57	9.01	51.90	53.88	56.29	54.02	0.80	0.77	11.26
189.93	79.59	9.01	51.99	53.29	56.98	54.09	0.80	0.78	11.22
189.93	76.23	9.01	51.89	53.90	56.79	54.19	0.80	0.77	11.30
189.93	80.73	9.01	51.89	53.88	56.69	54.15	0.81	0.78	11.19
184.00	79.66	9.01	51.89	54.00	56.60	54.16	0.80	0.78	11.22
188.45	79.05	9.01	51.91	53.76	56.77	54.15	0.80	0.77	11.23
184.00	65.64	9.01	56.89	58.89	59.29	58.35	0.77	0.75	11.64
178.06	63.85	9.01	56.09	58.78	59.10	57.99	0.77	0.74	11.70
172.13	63.49	9.01	56.09	58.70	59.10	57.96	0.77	0.74	11.72
172.13	59.93	9.01	56.09	58.59	59.39	58.02	0.76	0.73	11.86
172.13	66.87	9.01	55.80	58.49	58.89	57.72	0.78	0.75	11.60
173.61	63.53	9.01	56.01	58.64	59.12	57.92	0.77	0.74	11.72
142.45	43.20	9.01	63.09	64.89	66.11	64.70	0.70	0.67	12.89
142.45	42.75	9.01	63.09	64.89	66.21	64.73	0.70	0.67	12.93
142.45	42.33	9.01	63.30	65.00	66.30	64.87	0.69	0.67	12.97
148.39	43.87	9.01	63.09	64.89	66.21	64.73	0.70	0.68	12.84
148.39	45.27	9.01	62.99	64.90	66.00	64.63	0.71	0.68	12.73
145.42	43.56	9.01	63.12	64.92	66.18	64.74	0.70	0.68	12.86
148.39	38.98	9.01	66.99	68.69	70.00	68.56	0.68	0.65	13.31
148.39	31.94	9.01	67.73	68.76	70.79	69.10	0.63	0.61	14.19
148.39	31.28	9.01	67.64	68.87	70.78	69.09	0.63	0.61	14.30
142.45	29.10	9.01	67.74	68.77	70.78	69.10	0.61	0.59	14.67
142.45	48.83	9.01	66.18	66.79	68.38	67.12	0.72	0.70	12.50
145.42	35.29	9.01	67.32	68.30	70.18	68.60	0.66	0.63	13.73

k	ρ	C_p	ν	μ	Re	Pr	Nu
0.631	992.605	4185.725	6.816E-07	6.765E-04	251.156	4.489	5.830
0.631	992.570	4185.839	6.803E-07	6.753E-04	251.620	4.480	6.247
0.631	992.587	4185.782	6.809E-07	6.759E-04	251.388	4.484	5.840
0.631	992.570	4185.839	6.803E-07	6.753E-04	251.620	4.480	5.814
0.631	992.552	4185.897	6.797E-07	6.747E-04	251.851	4.475	6.619
0.631	992.570	4185.839	6.803E-07	6.753E-04	251.620	4.480	6.130
0.638	991.093	4191.445	6.334E-07	6.278E-04	270.648	4.127	5.496
0.637	991.112	4191.364	6.340E-07	6.284E-04	270.410	4.131	5.336
0.637	991.112	4191.364	6.340E-07	6.284E-04	270.410	4.131	5.336
0.637	991.131	4191.284	6.345E-07	6.289E-04	270.172	4.136	5.236
0.637	991.112	4191.364	6.340E-07	6.284E-04	270.410	4.131	5.524
0.637	991.117	4191.344	6.341E-07	6.285E-04	270.350	4.132	5.358
0.646	988.950	4201.841	5.789E-07	5.725E-04	296.815	3.724	3.898
0.646	988.971	4201.729	5.793E-07	5.729E-04	296.568	3.727	4.152
0.646	988.950	4201.841	5.789E-07	5.725E-04	296.815	3.724	4.247
0.646	988.909	4202.065	5.779E-07	5.715E-04	297.308	3.717	4.238
0.646	988.929	4201.952	5.784E-07	5.720E-04	297.062	3.720	4.201
0.646	988.929	4201.952	5.784E-07	5.720E-04	297.062	3.720	4.228
0.652	987.323	4211.157	5.449E-07	5.380E-04	315.801	3.477	3.417
0.652	987.301	4211.291	5.445E-07	5.376E-04	316.054	3.474	3.505
0.652	987.301	4211.291	5.445E-07	5.376E-04	316.054	3.474	3.357
0.652	987.256	4211.559	5.437E-07	5.367E-04	316.561	3.468	3.554
0.652	987.234	4211.693	5.433E-07	5.363E-04	316.814	3.465	3.507
0.652	987.273	4211.458	5.440E-07	5.371E-04	316.371	3.470	3.481
0.657	985.550	4222.438	5.134E-07	5.060E-04	335.804	3.251	2.866
0.657	985.713	4221.354	5.161E-07	5.087E-04	333.987	3.270	2.790
0.657	985.690	4221.508	5.157E-07	5.083E-04	334.246	3.267	2.774
0.657	985.736	4221.201	5.165E-07	5.091E-04	333.727	3.273	2.619
0.657	985.736	4221.201	5.165E-07	5.091E-04	333.727	3.273	2.922
0.657	985.719	4221.316	5.162E-07	5.088E-04	333.922	3.271	2.776
0.665	982.695	4242.624	4.713E-07	4.632E-04	366.839	2.954	1.864
0.665	982.695	4242.624	4.713E-07	4.632E-04	366.839	2.954	1.844
0.665	982.644	4243.003	4.707E-07	4.625E-04	367.381	2.949	1.826
0.665	982.721	4242.435	4.717E-07	4.635E-04	366.568	2.956	1.893
0.665	982.721	4242.435	4.717E-07	4.635E-04	366.568	2.956	1.953
0.665	982.695	4242.624	4.713E-07	4.632E-04	366.839	2.954	1.879
0.670	980.955	4255.948	4.497E-07	4.411E-04	385.197	2.804	1.670
0.669	981.114	4254.702	4.515E-07	4.430E-04	383.535	2.816	1.370
0.669	981.167	4254.289	4.522E-07	4.437E-04	382.982	2.821	1.342
0.669	981.246	4253.672	4.531E-07	4.446E-04	382.153	2.827	1.248
0.669	981.246	4253.672	4.531E-07	4.446E-04	382.153	2.827	2.095
0.669	981.193	4254.083	4.525E-07	4.440E-04	382.706	2.823	1.514

Mass flow rate 0.02 kg/s·m²

Set T_i	T_s	T_i	T_o	ΔT	Q_{coll}	$(T_i-T_a)I_T$	η_{coll}	T_a	I_T	$F_R(\tau\alpha)_e$	F_RU_L
35	37.4	35.2	40.7	5.5	59.874	0.0142	0.562	23.527	820.172	0.714	10.642
	37.4	35.2	40.7	5.5	59.874	0.0141	0.562	23.632	818.856	0.714	10.642
	37.4	35.2	40.7	5.5	59.874	0.0141	0.560	23.632	821.952	0.714	10.642
	37.4	35.2	40.7	5.5	59.874	0.0138	0.562	23.925	819.475	0.714	10.642
	37.5	35.3	40.8	5.5	59.874	0.0146	0.566	23.422	814.444	0.714	10.642
	37.4	35.2	40.7	5.5	59.874	0.0141	0.563	23.653	818.682	0.714	10.642
40	41.3	38.9	43.7	4.8	52.254	0.0186	0.506	24.135	794.473	0.714	10.642
	41.3	38.9	43.7	4.8	52.254	0.0187	0.508	24.135	791.067	0.714	10.642
	41.3	38.9	43.8	4.9	53.342	0.0187	0.519	24.135	790.912	0.714	10.642
	41.3	38.9	43.9	5.0	54.431	0.0190	0.529	23.842	790.757	0.714	10.642
	41.2	38.9	43.8	4.9	53.342	0.0196	0.519	23.422	790.757	0.714	10.642
	41.3	38.9	43.8	4.9	53.342	0.0190	0.519	23.883	790.873	0.714	10.642
45	46.1	44.1	48.5	4.4	47.899	0.0232	0.446	24.932	825.513	0.714	10.642
	46.1	44.1	48.6	4.5	48.988	0.0232	0.458	25.037	822.959	0.714	10.642
	46.0	44.0	48.5	4.5	48.988	0.0226	0.459	25.436	821.643	0.714	10.642
	46.0	44.0	48.5	4.5	48.988	0.0225	0.460	25.540	819.862	0.714	10.642
	46.0	44.1	48.5	4.4	47.899	0.0229	0.449	25.331	819.785	0.714	10.642
	46.0	44.0	48.5	4.5	48.625	0.0227	0.456	25.436	820.430	0.714	10.642
50	52.2	49.4	53.4	4.0	43.545	0.0295	0.419	25.834	799.427	0.714	10.642
	52.0	49.4	53.4	4.0	43.545	0.0294	0.420	25.939	798.420	0.714	10.642
	52.1	49.4	53.4	4.0	43.545	0.0291	0.421	26.233	795.789	0.714	10.642
	51.9	49.2	53.2	4.0	43.545	0.0294	0.423	25.939	791.763	0.714	10.642
	51.7	49.2	53.1	3.9	42.456	0.0293	0.413	26.044	791.221	0.714	10.642
	51.9	49.3	53.3	4.0	43.273	0.0293	0.419	26.039	794.298	0.714	10.642
55	58.1	54.9	57.7	2.8	30.481	0.0368	0.295	25.645	795.479	0.714	10.642
	58.6	54.8	57.9	3.1	33.747	0.0371	0.326	25.247	795.943	0.714	10.642
	59.4	54.7	58.0	3.3	35.924	0.0367	0.347	25.540	795.324	0.714	10.642
	60.0	54.9	58.0	3.1	33.747	0.0373	0.327	25.331	793.002	0.714	10.642
	60.7	55.2	58.0	2.8	30.481	0.0372	0.295	25.645	794.318	0.714	10.642
	59.7	54.9	58.0	3.1	33.475	0.0371	0.324	25.441	794.647	0.714	10.642
60	63.8	59.4	62.0	2.6	28.304	0.0391	0.275	28.456	790.447	0.714	10.642
	63.6	59.3	61.9	2.6	28.304	0.0399	0.275	27.743	790.447	0.714	10.642
	63.5	59.3	62.0	2.7	29.393	0.0395	0.286	28.036	790.602	0.714	10.642
	63.3	59.2	62.1	2.9	31.570	0.0392	0.307	28.141	791.531	0.714	10.642
	63.1	59.1	62.2	3.1	33.747	0.0399	0.328	27.554	790.293	0.714	10.642
	63.4	59.2	62.1	2.8	30.754	0.0397	0.299	27.869	790.718	0.714	10.642
65	69.6	63.6	65.7	2.1	22.861	0.0445	0.222	28.246	793.853	0.714	10.642
	69.1	63.8	65.8	2.0	21.772	0.0451	0.212	28.141	791.376	0.714	10.642
	68.9	63.8	65.9	2.1	22.861	0.0448	0.222	28.246	792.847	0.714	10.642
	68.7	63.6	65.9	2.3	25.038	0.0441	0.243	28.645	792.847	0.714	10.642
	68.4	63.6	66.1	2.5	27.215	0.0444	0.265	28.456	791.221	0.714	10.642
	68.8	63.7	65.9	2.2	24.222	0.0446	0.235	28.372	792.073	0.714	10.642

q"	h_i	$F'U_L$	$1T_P$	$2T_P$	$3T_P$	$T_{P\,av}$	F'
221.611	131.064	11.349	36.811	38.980	43.131	39.641	0.865
221.611	132.887	11.349	36.816	39.003	43.034	39.618	0.866
221.611	136.059	11.349	36.924	38.992	42.821	39.579	0.868
221.611	133.384	11.349	36.816	38.985	43.034	39.611	0.866
221.611	136.263	11.349	36.816	38.980	43.233	39.676	0.868
221.611	133.931	11.349	36.843	38.990	43.030	39.621	0.866
193.406	114.778	11.348	40.285	43.437	45.233	42.985	0.851
193.406	114.470	11.348	40.285	43.341	45.343	42.990	0.850
197.435	115.801	11.348	40.285	43.337	45.543	43.055	0.852
201.464	119.752	11.348	40.381	43.332	45.534	43.082	0.855
197.435	116.332	11.348	40.078	42.929	46.134	43.047	0.852
197.435	116.227	11.348	40.257	43.235	45.639	43.044	0.852
177.289	95.991	11.346	46.205	48.209	50.027	48.147	0.829
181.318	97.253	11.346	46.310	48.118	50.215	48.214	0.831
181.318	90.688	11.346	46.415	48.223	50.111	48.249	0.822
181.318	90.688	11.346	46.415	48.118	50.215	48.249	0.822
177.289	96.148	11.346	46.305	48.310	49.817	48.144	0.829
179.975	94.154	11.346	46.378	48.217	50.048	48.214	0.827
161.171	77.838	11.344	51.527	53.541	55.344	53.471	0.801
161.171	78.102	11.344	51.422	53.541	55.428	53.464	0.801
161.171	79.175	11.344	51.422	53.541	55.344	53.436	0.803
161.171	78.206	11.344	51.317	53.226	55.239	53.261	0.801
157.142	73.232	11.344	51.422	53.331	55.135	53.296	0.792
160.164	77.310	11.344	51.396	53.409	55.287	53.364	0.800
112.820	56.004	11.341	56.276	58.388	60.279	58.314	0.749
124.908	64.237	11.341	56.372	58.421	60.090	58.294	0.771
132.966	65.535	11.341	56.381	58.472	60.283	58.379	0.774
124.908	63.621	11.341	56.468	58.489	60.283	58.413	0.769
112.820	63.549	11.341	56.368	58.480	60.279	58.375	0.769
123.901	62.589	11.341	56.397	58.465	60.234	58.366	0.767
104.761	35.677	11.339	61.815	63.593	65.501	63.636	0.661
104.761	36.542	11.339	61.894	63.404	65.103	63.467	0.666
108.791	42.181	11.339	61.684	63.194	64.809	63.229	0.695
116.849	47.225	11.339	61.684	63.089	64.599	63.124	0.716
124.908	53.829	11.339	61.600	63.005	64.306	62.970	0.740
113.827	44.944	11.339	61.716	63.173	64.704	63.198	0.707
84.615	30.876	11.336	66.067	67.502	68.603	67.391	0.628
80.586	30.941	11.336	66.003	67.502	68.709	67.404	0.629
84.615	30.709	11.336	66.013	67.798	69.005	67.605	0.627
92.674	31.483	11.336	66.174	67.989	68.918	67.694	0.632
100.732	38.110	11.336	66.170	67.492	68.818	67.493	0.673
89.652	32.811	11.336	66.090	67.695	68.862	67.549	0.641

F_R	U_L	k	ρ	C_p	ν	μ	Re	Pr	Nu
0.811	13.127	0.630	992.727	4185.332	6.859E-07	6.809E-04	173.958	4.522	5.969
0.812	13.108	0.630	992.727	4185.332	6.859E-07	6.809E-04	173.958	4.522	6.052
0.814	13.076	0.630	992.727	4185.332	6.859E-07	6.809E-04	173.958	4.522	6.196
0.812	13.103	0.630	992.727	4185.332	6.859E-07	6.809E-04	173.958	4.522	6.074
0.814	13.074	0.630	992.692	4185.443	6.847E-07	6.797E-04	174.281	4.513	6.204
0.813	13.097	0.630	992.718	4185.360	6.856E-07	6.806E-04	174.039	4.520	6.099
0.798	13.340	0.636	991.524	4189.662	6.462E-07	6.407E-04	184.874	4.223	5.182
0.797	13.345	0.636	991.524	4189.662	6.462E-07	6.407E-04	184.874	4.223	5.168
0.799	13.327	0.636	991.506	4189.737	6.456E-07	6.401E-04	185.039	4.218	5.227
0.802	13.275	0.636	991.487	4189.811	6.451E-07	6.396E-04	185.204	4.214	5.405
0.799	13.320	0.636	991.506	4189.737	6.456E-07	6.401E-04	185.039	4.218	5.251
0.799	13.321	0.636	991.506	4189.737	6.456E-07	6.401E-04	185.039	4.218	5.247
0.778	13.682	0.644	989.586	4198.515	5.937E-07	5.875E-04	201.615	3.833	4.281
0.779	13.657	0.644	989.566	4198.618	5.932E-07	5.870E-04	201.785	3.829	4.336
0.771	13.795	0.644	989.606	4198.412	5.942E-07	5.880E-04	201.445	3.836	4.045
0.771	13.795	0.644	989.606	4198.412	5.942E-07	5.880E-04	201.445	3.836	4.045
0.778	13.679	0.644	989.586	4198.515	5.937E-07	5.875E-04	201.615	3.833	4.288
0.776	13.720	0.644	989.599	4198.447	5.940E-07	5.878E-04	201.502	3.835	4.199
0.751	14.167	0.651	987.433	4210.493	5.471E-07	5.402E-04	219.273	3.492	3.430
0.752	14.159	0.651	987.433	4210.493	5.471E-07	5.402E-04	219.273	3.492	3.442
0.753	14.126	0.651	987.433	4210.493	5.471E-07	5.402E-04	219.273	3.492	3.489
0.752	14.155	0.651	987.521	4209.968	5.488E-07	5.419E-04	218.569	3.505	3.448
0.743	14.318	0.651	987.542	4209.837	5.492E-07	5.424E-04	218.393	3.508	3.229
0.750	14.183	0.651	987.482	4210.197	5.480E-07	5.412E-04	218.877	3.499	3.408
0.703	15.149	0.658	985.197	4224.807	5.077E-07	5.002E-04	236.823	3.210	2.442
0.723	14.714	0.658	985.173	4224.967	5.073E-07	4.998E-04	237.005	3.207	2.800
0.726	14.656	0.658	985.173	4224.967	5.073E-07	4.998E-04	237.005	3.207	2.857
0.722	14.743	0.659	985.126	4225.288	5.066E-07	4.990E-04	237.369	3.202	2.773
0.722	14.746	0.659	985.055	4225.773	5.054E-07	4.979E-04	237.917	3.194	2.769
0.719	14.792	0.658	985.132	4225.248	5.066E-07	4.991E-04	237.324	3.203	2.728
0.621	17.149	0.664	983.049	4240.002	4.761E-07	4.680E-04	253.098	2.987	1.541
0.625	17.019	0.664	983.099	4239.632	4.768E-07	4.687E-04	252.722	2.992	1.579
0.652	16.313	0.664	983.074	4239.817	4.764E-07	4.684E-04	252.910	2.989	1.822
0.672	15.826	0.664	983.074	4239.817	4.764E-07	4.684E-04	252.910	2.989	2.040
0.694	15.326	0.664	983.074	4239.817	4.764E-07	4.684E-04	252.910	2.989	2.326
0.664	16.033	0.664	983.081	4239.771	4.765E-07	4.684E-04	252.863	2.990	1.942
0.590	18.040	0.670	981.008	4255.532	4.503E-07	4.417E-04	268.145	2.808	1.324
0.590	18.027	0.670	980.929	4256.157	4.494E-07	4.408E-04	268.725	2.801	1.326
0.589	18.077	0.670	980.902	4256.365	4.490E-07	4.405E-04	268.919	2.799	1.316
0.594	17.923	0.670	980.955	4255.948	4.497E-07	4.411E-04	268.532	2.804	1.349
0.632	16.849	0.670	980.902	4256.365	4.490E-07	4.405E-04	268.919	2.799	1.633
0.602	17.672	0.670	980.922	4256.209	4.493E-07	4.407E-04	268.773	2.801	1.406

Mass flow rate 0.01 kg/s·m^2

Set T_i	T_s	T_i	T_o	ΔT	Q_{coll}	$(T_i-T_a)I_T$	η_{coll}	T_a	I_T	$F_R(\tau\alpha)_e$	$F_R U_L$
	36.5	35.9	44.2	8.3	58.036	0.00896	0.559	28.749	798.266	0.637	8.774
	37.8	36.0	44.4	8.4	58.735	0.00882	0.566	28.959	798.575	0.637	8.774
35	38.5	36.0	44.5	8.5	59.434	0.00885	0.575	28.959	795.634	0.637	8.774
	39.2	36.1	44.5	8.4	58.735	0.00838	0.569	29.442	794.473	0.637	8.774
	39.9	36.4	44.7	8.3	58.036	0.00863	0.562	29.546	794.008	0.637	8.774
	38.9	36.1	44.5	8.4	58.735	0.00867	0.568	29.227	795.672	0.637	8.774
	44.0	40.0	47.4	7.4	51.743	0.01283	0.504	29.861	790.138	0.637	8.774
	44.2	40.0	47.5	7.5	52.442	0.01317	0.508	29.546	793.544	0.637	8.774
40	44.2	40.1	47.5	7.4	51.743	0.01333	0.503	29.546	791.763	0.637	8.774
	44.3	40.1	47.5	7.4	51.743	0.01382	0.502	29.148	792.383	0.637	8.774
	44.4	40.1	47.6	7.5	52.442	0.01308	0.510	29.756	791.067	0.637	8.774
	44.3	40.1	47.5	7.5	52.093	0.01335	0.506	29.499	792.189	0.637	8.774
	52.3	46.2	53.2	7.0	48.946	0.02066	0.462	29.358	815.218	0.637	8.774
	52.2	46.2	53.1	6.9	48.247	0.02103	0.455	29.043	815.914	0.637	8.774
45	52.3	46.3	53.2	6.9	48.247	0.02052	0.455	29.546	816.534	0.637	8.774
	52.2	46.2	53.2	7.0	48.946	0.02081	0.462	29.253	814.289	0.637	8.774
	52.3	46.3	53.3	7.0	48.946	0.02079	0.464	29.442	811.038	0.637	8.774
	52.3	46.3	53.2	7.0	48.713	0.02071	0.460	29.414	813.953	0.637	8.774
	54.2	50.8	57.3	6.5	45.450	0.02633	0.435	29.651	803.142	0.637	8.774
	54.0	50.8	57.3	6.5	45.450	0.02602	0.436	29.945	801.517	0.637	8.774
50	54.0	50.9	57.3	6.4	44.751	0.02580	0.428	30.155	804.149	0.637	8.774
	53.9	50.9	57.3	6.4	44.751	0.02551	0.429	30.448	801.826	0.637	8.774
	53.9	50.8	57.3	6.5	45.450	0.02567	0.437	30.260	800.201	0.637	8.774
	54.0	50.9	57.3	6.5	45.100	0.02575	0.433	30.202	801.923	0.637	8.774
	59.2	54.7	60.1	5.4	37.758	0.02973	0.361	30.763	805.155	0.637	8.774
	59.8	54.8	60.2	5.4	37.758	0.02981	0.360	30.763	806.471	0.637	8.774
55	60.8	54.8	60.2	5.4	37.758	0.02990	0.361	30.763	803.839	0.637	8.774
	61.6	54.8	60.2	5.4	37.758	0.03017	0.361	30.553	803.684	0.637	8.774
	62.3	54.7	60.1	5.4	37.758	0.03006	0.362	30.553	803.297	0.637	8.774
	61.1	54.8	60.2	5.4	37.758	0.02998	0.361	30.658	804.323	0.637	8.774
	65.3	61.0	64.9	3.9	27.270	0.03787	0.264	30.952	793.389	0.637	8.774
	65.2	61.1	65.2	4.1	28.668	0.03804	0.277	30.847	795.324	0.637	8.774
60	65.0	60.9	65.2	4.3	30.067	0.03763	0.292	31.057	793.002	0.637	8.774
	64.8	60.8	65.2	4.4	30.766	0.03765	0.299	30.952	792.692	0.637	8.774
	64.6	60.5	65.1	4.6	32.165	0.03769	0.312	30.658	791.763	0.637	8.774
	64.9	60.8	65.2	4.4	30.416	0.03775	0.295	30.878	793.195	0.637	8.774
	70.7	64.8	68.0	3.2	22.375	0.04432	0.216	29.442	797.777	0.637	8.774
	70.4	64.5	68.2	3.7	25.871	0.04381	0.249	29.546	797.777	0.637	8.774
65	70.3	64.4	68.4	4.0	27.969	0.04343	0.270	29.756	797.777	0.637	8.774
	70.8	64.1	68.4	4.3	30.067	0.04281	0.290	29.945	797.777	0.637	8.774
	71.3	63.9	68.3	4.4	30.766	0.04306	0.297	29.546	797.777	0.637	8.774
	70.7	64.2	68.3	4.1	28.668	0.04328	0.276	29.698	797.777	0.637	8.774

q"	h_i	$F'U_L$	$1T_P$	$2T_P$	$3T_P$	$T_{P\ av}$	F'
214.309	122.534	9.565	38.413	41.781	45.203	41.799	0.857
216.891	121.620	9.565	38.597	41.863	45.490	41.983	0.857
219.473	118.944	9.564	38.802	41.537	45.947	42.095	0.854
216.891	116.759	9.564	38.904	41.669	45.899	42.158	0.852
214.309	121.409	9.564	38.986	41.726	46.234	42.315	0.856
216.891	119.683	9.564	38.822	41.699	45.892	42.138	0.855
191.071	103.796	9.563	41.400	45.310	49.912	45.541	0.839
193.653	112.567	9.563	41.386	45.196	49.828	45.470	0.848
191.071	108.001	9.563	41.788	45.196	49.723	45.569	0.843
191.071	109.868	9.563	41.900	45.309	49.409	45.539	0.845
193.653	107.457	9.563	42.329	45.301	49.326	45.652	0.843
192.362	109.473	9.563	41.851	45.251	49.572	45.558	0.845
180.743	83.234	9.561	49.456	51.632	54.526	51.872	0.810
178.160	84.172	9.561	49.351	51.422	54.526	51.767	0.812
178.160	79.030	9.561	49.561	51.716	54.736	52.004	0.803
180.743	93.465	9.561	49.142	51.317	54.442	51.634	0.825
180.743	91.904	9.561	49.351	51.422	54.526	51.767	0.823
179.882	88.133	9.561	49.351	51.485	54.568	51.802	0.817
167.832	74.743	9.558	52.323	56.881	59.682	56.295	0.794
167.832	73.601	9.558	52.323	56.881	59.787	56.330	0.792
165.250	74.094	9.558	52.323	56.881	59.787	56.330	0.793
165.250	72.954	9.558	52.323	56.881	59.891	56.365	0.790
167.832	79.426	9.558	52.323	56.588	59.578	56.163	0.802
166.541	75.019	9.558	52.323	56.808	59.761	56.297	0.794
139.430	55.942	9.556	56.882	59.997	62.798	59.892	0.748
139.430	61.694	9.556	56.799	59.892	62.589	59.760	0.764
139.430	59.316	9.556	56.882	60.081	62.589	59.851	0.757
139.430	62.857	9.556	56.882	59.892	62.380	59.718	0.767
139.430	62.788	9.556	56.694	59.788	62.380	59.621	0.766
139.430	61.664	9.556	56.814	59.913	62.485	59.737	0.764
100.699	36.738	9.552	63.390	65.931	67.752	65.691	0.666
105.863	38.164	9.552	63.602	66.016	68.154	65.924	0.674
111.028	39.016	9.552	63.602	65.931	68.154	65.896	0.678
113.610	42.329	9.552	63.179	65.825	68.048	65.684	0.694
118.774	41.184	9.552	63.179	65.931	67.942	65.684	0.689
112.319	40.173	9.552	63.390	65.926	68.075	65.797	0.684
82.625	25.415	9.549	67.957	70.096	70.900	69.651	0.583
95.535	28.879	9.549	67.873	69.990	71.112	69.658	0.612
103.281	31.428	9.549	67.767	69.884	71.408	69.686	0.631
111.028	33.337	9.549	67.449	69.778	71.514	69.580	0.644
113.610	34.607	9.549	67.259	69.482	71.408	69.383	0.652
105.863	32.063	9.549	67.587	69.783	71.361	69.577	0.635

F_R	U_L	k	ρ	C_p	ν	μ	Re	Pr	Nu
0.786	11.156	0.634	991.982	4187.897	6.605E-07	6.552E-04	113.068	4.330	5.550
0.785	11.166	0.634	991.928	4188.099	6.588E-07	6.535E-04	113.375	4.317	5.506
0.783	11.195	0.634	991.909	4188.167	6.582E-07	6.529E-04	113.477	4.313	5.384
0.782	11.220	0.634	991.891	4188.235	6.576E-07	6.523E-04	113.579	4.309	5.285
0.785	11.170	0.634	991.800	4188.581	6.547E-07	6.494E-04	114.092	4.287	5.492
0.784	11.187	0.634	991.882	4188.270	6.573E-07	6.520E-04	113.631	4.306	5.417
0.769	11.400	0.640	990.615	4193.555	6.201E-07	6.142E-04	120.616	4.028	4.658
0.777	11.283	0.640	990.596	4193.643	6.195E-07	6.137E-04	120.721	4.024	5.051
0.773	11.341	0.640	990.576	4193.731	6.190E-07	6.132E-04	120.825	4.020	4.846
0.775	11.317	0.640	990.576	4193.731	6.190E-07	6.132E-04	120.825	4.020	4.929
0.773	11.349	0.640	990.557	4193.820	6.185E-07	6.126E-04	120.930	4.016	4.821
0.775	11.322	0.640	990.576	4193.731	6.190E-07	6.132E-04	120.825	4.020	4.912
0.743	11.802	0.649	988.170	4206.170	5.619E-07	5.553E-04	133.425	3.600	3.682
0.744	11.781	0.649	988.192	4206.048	5.624E-07	5.557E-04	133.316	3.603	3.724
0.737	11.904	0.649	988.149	4206.292	5.615E-07	5.548E-04	133.533	3.597	3.496
0.756	11.594	0.649	988.170	4206.170	5.619E-07	5.553E-04	133.425	3.600	4.135
0.755	11.623	0.649	988.127	4206.415	5.610E-07	5.544E-04	133.642	3.594	4.065
0.750	11.696	0.649	988.149	4206.292	5.615E-07	5.548E-04	133.533	3.597	3.898
0.728	12.042	0.655	986.244	4217.893	5.252E-07	5.180E-04	143.039	3.335	3.274
0.726	12.075	0.655	986.244	4217.893	5.252E-07	5.180E-04	143.039	3.335	3.224
0.727	12.060	0.655	986.221	4218.040	5.248E-07	5.175E-04	143.151	3.332	3.246
0.725	12.094	0.655	986.221	4218.040	5.248E-07	5.175E-04	143.151	3.332	3.196
0.736	11.915	0.655	986.244	4217.893	5.252E-07	5.180E-04	143.039	3.335	3.480
0.729	12.034	0.655	986.232	4217.967	5.250E-07	5.178E-04	143.095	3.333	3.286
0.686	12.783	0.660	984.672	4228.398	4.995E-07	4.918E-04	150.641	3.152	2.433
0.701	12.514	0.660	984.624	4228.731	4.987E-07	4.911E-04	150.870	3.146	2.683
0.695	12.619	0.660	984.624	4228.731	4.987E-07	4.911E-04	150.870	3.146	2.579
0.704	12.466	0.660	984.624	4228.731	4.987E-07	4.911E-04	150.870	3.146	2.733
0.703	12.468	0.660	984.672	4228.398	4.995E-07	4.918E-04	150.641	3.152	2.731
0.701	12.515	0.660	984.636	4228.648	4.989E-07	4.913E-04	150.813	3.148	2.682
0.611	14.344	0.667	981.900	4248.629	4.611E-07	4.528E-04	163.633	2.883	1.580
0.618	14.180	0.668	981.796	4249.424	4.598E-07	4.514E-04	164.111	2.874	1.641
0.623	14.087	0.667	981.848	4249.026	4.605E-07	4.521E-04	163.872	2.878	1.678
0.637	13.758	0.667	981.874	4248.827	4.608E-07	4.524E-04	163.753	2.880	1.820
0.633	13.865	0.667	981.977	4248.036	4.621E-07	4.538E-04	163.275	2.889	1.772
0.628	13.966	0.667	981.874	4248.827	4.608E-07	4.524E-04	163.753	2.880	1.728
0.536	16.375	0.672	980.070	4262.983	4.396E-07	4.308E-04	171.972	2.734	1.086
0.562	15.600	0.672	980.097	4262.765	4.399E-07	4.311E-04	171.850	2.736	1.234
0.579	15.139	0.672	980.070	4262.983	4.396E-07	4.308E-04	171.972	2.734	1.343
0.591	14.839	0.672	980.151	4262.330	4.405E-07	4.317E-04	171.605	2.740	1.425
0.598	14.656	0.671	980.232	4261.680	4.414E-07	4.327E-04	171.239	2.746	1.479
0.583	15.034	0.672	980.138	4262.439	4.403E-07	4.316E-04	171.666	2.739	1.370

APPENDIX C

Publication of the research

The Thermal Performance of the Novel Solar Collector Integrated with Phase
Change Material

The 1st International Conference on Smart Community Development in the Asia Pacific
(iSCAP2020) at Asian Development College for Community Economy and Technology,
Chiang Mai Rajabhat University on 20th - 21st February 2020

Agenda The 1st International Conference on Smart Community Development in the Asia Pacific (iSCAP2020)

Asian Development College for Community Economy and Technology, Chiang Mai Rajabhat University

20th - 21st February 2020

Session 1: WEF Nexus; Renewable Energy & Environment
Session Chairs: Assistant Professor Dr. Saoharit Nitayavardhana
Assistant Professor Dr. Rotjapun Nirunsin

Room 1: AREC

Time	Topic
09:00-09:12	Experimental Study on Strength of Concrete with Partial Replacement of Fine Aggregate with Brick Waste by Pyae Su Htike
09:12-09:24	Estimation of Runoff Potential in Sittaung River Basin Using GIS Application by Thet Hnin Aung
09:24-09:36	Statistical Analysis for Initial Wind Characteristics in Southern Region of Myanmar by Ni Ni Moe Kyaw
09:36-09:48	Application of Support Vector Regression for Solar Power Predication by Narakorn Songkittirote
09:48-10:00	Semi-Transparent Photovoltaic Window Louvers for Building Integration Application by Phetdavanh Ladthavong
10:00-10:12	Comparison of Biodiesel Synthesis via Transesterification by Using Homogeneous and Heterogeneous Catalyst by Ying Chusree
10:12-10:24	The Thermal Performance of the Novel Solar Collector Integrated with Phase Change Material by Bundarith Nhel
10:24-10:36	Development of Biogas Fermentation Tank for Organic Food Waste in Chiangmai Community by Chakriya Chanracha
10:36-10:48	The Combustion Characteristic of a Community-Scale Biomass Stove by Paitoon Laodee
10:48-11:00	Modelling of Cooling Load in Close-System Solar Greenhouse Under Thailand Climates Using TRNSYS by Thiri Shoon Wai

The Thermal Performance of the Novel Solar Collector Integrated with Phase Change Material

Bundarith Nhel, and Sarawut Polvongsri[*]

School of Renewable Energy Engineering, Maejo University, Chiang Mai, Thailand
[*]saravooth@hotmail.com

Abstract: The objective of this research is demonstrated the thermal performance of the two novel solar collectors integrated with phase change material (PCM) riser comparing with the conventional flat plate solar collector without PCM riser. The two novel solar collectors and a conventional solar collector had a similar area of 0.22×1.09 m^2 installed at 18° facing to the south. Each novel collectors had two single copper tubes, the outside tube was water tube with 28.7 mm of diameter and inner tube was a riser tube filled RT42 PCM with a melting point between 38-42 °C. In this study, the PCM risers investigated with diameter of 10 and 16 mm. The water in system was circulated by pump though a gap between outside tube and riser tube for heat receiving from solar radiation. The experiment was conducted in outdoor testing following ASHRAE standard 93-2003 that the water mass flow rate per collector is equal to 0.02 kg/s·m^2 and the inlet water temperature is controlled by electric heater at 35, 40, 45, 50, 55, 60, and 65 °C, respectively. The solar radiation, ambient temperature, inlet water temperature, outlet water temperature, and hot water temperature in a storage tank were collected during the day at School of Renewable Energy, Chiangmai. From the experiment showed that inlet water temperature increased, the heat loss from collector would increase too. The thermal performance of the novel solar collector with PCM riser provided the higher values than the conventional flat plate solar collector. The novel solar collector that integrates with PCM in 10 mm diameter riser (PCM2) gave the highest $F_R(\tau\alpha)_e$ and $F_R U_L$ of 0.815 and 11.140 W/m^2·K following by 16 mm diameter riser (PCM1) let the values of 0.788 and 11.050 W/m^2·K and the conventional solar collector gave the values of 0.713 and 10.642 W/m^2·K, respectively.

Keywords: The Novel solar collector, Thermal performance, Riser phase change materials, Solar water heater.

1   INTRODUCTION

Presently, human attempts to seek the alternative energy instead of the conventional fuel like fossil fuel. Many renewable energies such as wind, hydro, especially solar energy that are reliable and in abundant on earth can compensate. Heating system is an important system for buildings facility from fossil fuel production in households and industrial sector. By the ways, most building heating systems use in the range of low temperature for daily usage that is generated from fossil fuel but can be replaced to solar energy. Solar energy is free, clean, and can transform to electricity and thermal energy during daytime. The conventional of the solar collector system is built from a metal absorber plate. Its temperature is in a range of 40-70 °C (Kiatsiriroat, 2014, Gautam et al., 2017, Kalogirou, 2014). Many researchers try to find the newly technique will enhance the solar collector performance. The using nano-particle as a working fluid in solar collector is the alternative option gives the heat transfer enhancement higher than normal style (Kiatsiriroat, 2014, Syam Sundar et al., 2018, Sharafeldin et al., 2017, Mirzaei, 2017, Sharafeldin and Gróf, 2018, Muhammad et al., 2016). However, the modern technique with the nano-fluid is given a dropping heat transfer when using in a long time. There is a new option, the twist-tap or helical coil inserted into the absorber tube of the collector which is directly contacted to the water or working fluid during operation (Jaisankar et al., 2009, Saravanan et al., 2016, Eiamsa-ard and Seemawute, 2012, Murugan et al., 2019). Due to the fluctuation of solar radiation during daytime, the thermal energy storage has been designed and integrated on solar collector while the energy stored as phase change materials (PCM) is chemical composite materials which stores thermal energy by its latent heat during a melting point or freezing point. The capable of thermal is from more sensible thermal storing and the most command applications that benefit from PCM including those with known duty cycles (ICNQT, 2018, Bellan et al., 2015, Loem et al., 2019). The solar collector integrated with phase change materials (PCM) was studied by various researchers to investigate the abilities of the system during in sunny day and cloudy day operation. Khalifa et al. (Khalifa and Abdul Jabbar, 2010) studied the performance between a solar hot water system storage to the conventional which built from 6 copper tubes of 80 mm outside diameter and PCM was installed at a back of the copper plate. The result showed that the system could reduce heat loss by the PCM heat storage and an acceptable of mathematical analysis and experimental data were analyzed. Guta et al. (Gupta et al., 2017) studied the investigation of heat removal and the performance of solar collector with various flow configurations. The working fluid was flown in riser tube by using PCM filled in external tube. The result showed that the parallel wall to wall flowing was given the high performance than other flowing condition with observing in the case of phase change materials. Furthermore, the heat removal factor F_R was influenced to the melting of PCM more than the mass flow rate, during phase change the PCM absorbed thermal energy which was decreased the factor F_R, increased during the sensible heat stage. Koyuncu et al. (Koyuncu and Lüle, 2015) studied the performance of a domestic chromium solar water collector with PCM which arranged tube for water circulated and filled PCM. The results showed the collector efficiency was equal to 59% at the mass flow rate of 0.02 kg/s·m². Papadimitratos et al. (Papadimitratos et al., 2016) studied the performance of solar water heater with evacuated tube filled the dual phase change materials. The efficiency could improve of 26% for the normal operation and 66% for stagnation mode.

In this research aims to investigate the novel solar collector integrated with phase change materials (PCM) filled inside copper tube. The PCM riser would be inserted through the absorber plate tube with using water as a working fluid for directly heat exchanger between the absorber plate and PCM. The experimental data was studied parameters for thermal efficient analysis following to the ASHRAE Standard test (Polvongsri, 2013).

2 EXPERIMENTAL SETUP
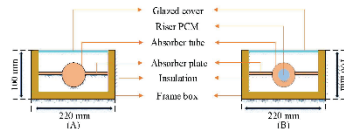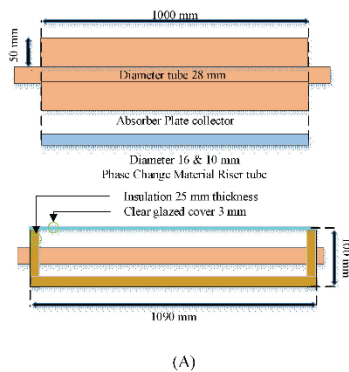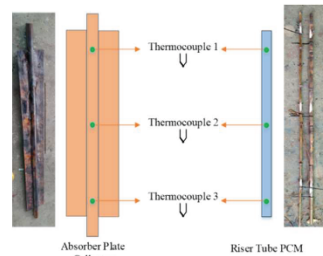
2.1 Solar collector configuration

Figure 1: Schematic of (A) The solar collector without PCM and (B) The novel solar collector integrated PCM.

(A)

(B)

Figure 2: The novel solar collector (A) The absorber plate tube 28 mm of diameter and (B) The riser tube 10 mm and 16 mm of diameter.

The novel solar collector was built from a single copper tube as absorber plate tube of 28.7 mm outside diameter, 1 mm thickness and 1,000 mm length. The riser copper tube of 10 mm diameter and 16 mm diameter were inserted through the single copper tube and filled with RT42 phase change material (PCM) fully. The melting point of PCM between 38-42 °C (ICNQT, 2018). The absorber plate was painted as a normal black color for solar radiation absorption. A single clear glass of 3 mm thick was installed above the solar collector for make the inside temperature of collector higher than environment. The 25 mm of thickness rubber insulation was installed around the side and back of aluminum frame (Aroflex rubber with density of 40-70 kg/m³) for heat loss reducing in the side and back. The final dimensions of novel solar collector are length 1090 mm the width 220 mm and height 100 mm as showed in the Figure 1 and Figure 2.

2.2 Experiment procedure

The novel solar water heater collectors integrated with phase change materials riser were given an abbreviation following the Table 1.

Table 1: The characteristic of solar collector integrated with PCM 1, PCM 2 and without PCM.

Category	Diameter	Unit	Inside
PCM 1	Ø 16	mm	RT 42
PCM 2	Ø 10	mm	RT 42
Without PCM	-	-	-

The experiment tested at the School of Renewable Energy, Maejo University, Chiang Mai, Thailand where located at 18.92 °N latitude and 99° E longitude. In Figure 3 showed the novel and conventional solar collectors were installed at 18° tile angle facing to the south. Water was pumped from storage tank through the collectors by electric pump. The resistant heater in storage tank was used to regulate the water temperature during testing. The performance testing following to the ASHRAE Standard test 93-2003 (Polvongsri, 2013) which the most often used to evaluate of any solar collector design. The standard suggested the testing requires measurement under steady state condition which the solar radiation is more than 790 W/m², and the mass flow rate of water per collector area is equal to 0.02 kg/s·m². The rang of water temperature through solar collector was set up following 35, 40, 45, 50, 55, 60, 65 °C, respectively. The mass flow rate of water was measured by the manual

The 1st International Conference on Smart Community Development in the Asia Pacific (iSCAP2020)

flow meter (Platon), gauge valve adjustment flow and has a bypass for overload preventing in the case of overpressure occurring. The solar radiation was collected by the pyranometer (Apogee SP-110-L-10). The thermocouple type K was used to measure the temperature that related many parameters and recorded in the data logger (TD-1947 SD and Adam 5000 PBC) every 5 minutes.
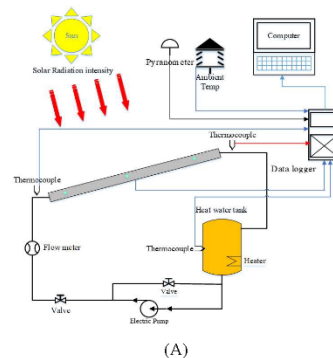

(A)

(B)

Figure 3: The experimental set-up (A) Diagram of testing (B) View of experimental collector.

2 THEORY

The performance of the solar collector is described by energy balance that indicates the incident solar energy and useful energy gain. In the steady state the useful energy output with the absorber plate area (A_C) and heat removal factor (F_R) which is mention by Bliss-William (Duffie and Beckman, 2013) as following eq. (1);

$$Q_u = A_c F_R \left[S - U_L \left(T_i - T_a \right) \right] \qquad (1)$$

or the useful energy of the solar collector experiment of the energy output is calculated following eq. (2);

$$Q_u = \dot{m} C_P \left(T_o - T_i \right) \qquad (2)$$

The thermal efficiency of solar collector is defined as the ratio between the heat gain from working fluid and the total incident solar radiation on the absorber plate area of solar collector (Duffie and Beckman, 2013, Polvongsri, 2013) as following eq.(3);

$$\eta = \frac{Q_u}{A_C I_T} = \frac{\dot{m} C_p \left(T_o - T_i \right)}{A_C I_T} \qquad (3)$$

$$\eta = F_R \left(\tau \alpha \right)_e - F_R U_L \frac{\left(T_i - T_a \right)}{I_T} \qquad (4)$$

The thermal efficiency test is presented at near normal incidence conditions therefore, that F_R is constant of maximum efficient, F_R and U_L are constant within the range of temperature. The linear will result when the efficiency is obtained from averaged data plated against $(T_i-T_a)/I_T$ according to Eq. (4). The intersection of the vertical line of efficiency axis is equal to $F_R(\tau\alpha)_e$. At this axis the temperature of working fluid that entered the collector near ambient temperature means that the collector efficient is nearly maximum. So, the slope of the linear line is equal to $F_R U_L$ shows that the way energy has removed from the solar collector. At the intersection of the line with the horizontal axis collector efficiency is zero and this point normally calls the stagnation, usually occurs when no fluid flows in the collector.

*The 1st International Conference on Smart Community Development
in the Asia Pacific (iSCAP2020)*

3 RESULTE AND DISCUSSION

For solar collector performance analysis shows in the Figure 4 and Figure 5. Figure 4 presents the useful heat gain due to the inlet water temperature variation. Both of heat gain from the novel solar collectors integrated with PCM (PCM 1, PCM 2) showed that were higher than the collector without PCM at the mass flow rate of 0.02 kg/s·m^2. The PCM 2 with riser of 10 mm diameter was given higher heat gain than the PCM 1 with riser of 16 mm diameters which may effect of the energy storage in the phase change material that filled in the riser. Due to the heat gain of collector was influence with the temperature therefore the heat gains at the low inlet water temperature had slightly heat loss to environment while the high inlet temperature would give much losing thermal energy.
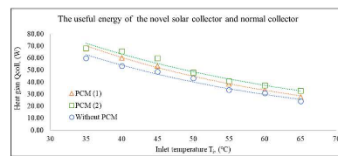
Figure 4: Useful energy gain of novel and conventional solar collectors.
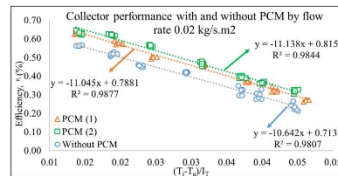
Figure 5: The thermal efficiency of novel and conventional solar collectors.

In the Figure 5 shows the thermal efficiency of the novel and conventional solar collectors were analyzed following the ASHRAE standard 93-2003. The linear equations of both collectors PCM 2 and PCM 1 could identify of the better system performance than the conventional solar collector without PCM. The range of inlet temperature, ambient temperature and solar radiation were given the relation of $(T_i-T_a)/I_T$ at X-axis, its value changed cause of the variation of inlet temperature during testing with steady state condition while the intersection on Y-axis presented the thermal efficiency $F_R(\tau\alpha)_e$. According to eq.(4), if the relation $(T_i-T_a)/I_T$ was slightly different, the collected thermal energy was closely to the maximum energy input as solar radiation. On the opposite, when the relation of $(T_i-T_a)/I_T$ had grown up, the energy loss would increase cause of the ambient temperature variation that showed as the slope of the linear equation or F_RU_L. The results showed that $(T_i-T_a)/I_T$ was varied from 0.01-0.05 °C·m^2/W. Both the novel solar collectors integrated with PCM were performed that PCM 1 and PCM 2 provided the $F_R(\tau\alpha)_e$ of 0.788, 0.815 and F_RU_L was 11.05, 11.14 W/m^2·°C, respectively while the solar collector without PCM got 0.713, and 10.64 W/m^2·°C as shown as in Table 2 with all case studies had the correlation on coefficient over than 0.98.

Table 2: The values of $F_R(\tau\alpha)_e$ and F_RU_L for the novel solar collectors comparing the conventional solar collector.

The standard test mass flow rate 0.02 kg/s·m^2

Category	$F_R(\tau\alpha)_e$	F_RU_L	R^2
PCM 1	0.788	11.05	0.987
PCM 2	0.815	11.14	0.984
Without PCM	0.713	10.64	0.981

In order to analyze the system analysis, the novel solar collectors and conventional collector were tested in daytime since 8:40 AM to 15:55 PM. The experimental results present by Figure 6 to Figure 9 that described the collector performance and showed the several of inlet temperature, outlet temperature and the storage tank temperature. In the Figure 6 shows the changing of the solar radiation intensity and ambient temperature during daytime. The maximum solar radiation was around 800 W/m^2 and the ambient temperature was about 31 °C.
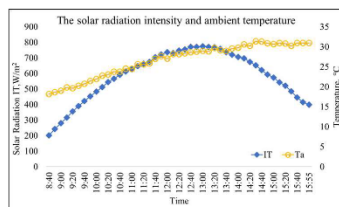
Figure 6: The variation of solar radiation and ambient temperature.

The experiment was investigated at the initial temperature in 10-liter storage tank of 25 °C and set the water mass flow rate of 0.02 kg/s·m². In the Figure 7 and Figure 8 were presented the variation of temperature change of the novel solar collector (PCM 1 and PCM 2). The maximum temperature different between inlet and outlet temperature was around 5.1 and 5.5 °C, respectively during peak solar radiation and the ambient temperature average of 27.2 °C. For the maximum temperature of both water storage tanks were 50.2 and 51.5 °C, respectively while the conventional solar collector in Figure 9 shows the temperature different was around 4.8 °C and temperature close to the 50 °C.

Figure 7: The temperature variation of the novel solar collector (PCM 1) during daytime.

Figure 8: The temperature variation of novel solar collector (PCM 2) during daytime.

Figure 9: The temperature variation of conventional solar collector (without PCM) during daytime.

In Figure 10 shows the heat gain in the storage tank of each case studies. The heat gain (Q_s) would be varied by the solar radiation variation. At the solar radiation lower than 600 W/m², the heat gains both the novel collectors (PCM1 and PCM 2) and conventional collector (without PCM) were similar. When the solar radiation more than 600 W/m², the heat gain of both novel collectors were higher than the conventional solar collector. The calculated heat gains of using PCM 1, PCM 2 and without PCM were 1,126.3, 1,219.7 and 1,059.01 MJ, respectively. When considered in the term of thermal efficiency, both PCM collectors given the greater thermal efficiency about 8-10%.

Figure 10: The heat gain in water storage tank of novel solar collectors and conventional solar collector.

4 CONCLUSIONS

The novel solar collector integrated with RT42 phase change material riser in difference diameter of 16 and 10 mm were tested under the ASHRAE standard testing with the mass flow rate per collector area of 0.02 kg/s·m² and the adjusted the inlet water temperature from 35, 40, 45, 50, 55, 60 and 60 °C. The results showed that solar collector that integrates with PCM in 10 mm diameter riser tube (PCM2) was demonstrated the

highest $F_R(\tau\alpha)_e$ and $F_R U_L$ of 0.815 and 11.140 $W/m^2 \cdot K$. The collected data have been trust with the correlation coefficient over than 0.98. Moreover, both of novel solar collectors were given the higher thermal performance than conventional collector.

ACKNOWLEDGEMENTS

REFERENCES

BELLAN, S., ALAM, T. E., GONZÁLEZ-AGUILAR, J., ROMERO, M., RAHMAN, M. M., GOSWAMI, D. Y. & STEFANAKOS, E. K. 2015. Numerical and experimental studies on heat transfer characteristics of thermal energy storage system packed with molten salt PCM capsules. *Applied Thermal Engineering,* 90, 970-979.

DUFFIE, J. A. & BECKMAN, W. A. 2013. Solar engineering of thermal processes. 4th ed. Hoboken, New Jersey: Wiley,.

EIAMSA-ARD, S. & SEEMAWUTE, P. 2012. Decaying swirl flow in round tubes with short-length twisted tapes. *International Communications in Heat and Mass Transfer,* 39, 649-656.

GAUTAM, A., CHAMOLI, S., KUMAR, A. & SINGH, S. 2017. A review on technical improvements, economic feasibility and world scenario of solar water heating system. *Renewable and Sustainable Energy Reviews,* 68, 541-562.

GUPTA, A., GAUR, M. K., CROOK, R. & DIXON-HARDY, D. W. 2017. Experimental investigation of heat removal factor in solar flat plate collector for various flow configurations AU - Malvi, C. S. *International Journal of Green Energy,* 14, 442-448.

ICNQT 2018. Nano PCM.

JAISANKAR, S., RADHAKRISHNAN, T. K. & SHEEBA, K. N. 2009. Experimental studies on heat transfer and friction factor characteristics of thermosyphon solar water heater system fitted with spacer at the trailing edge of twisted tapes. *Applied Thermal Engineering,* 29, 1224-1231.

KALOGIROU, S. A. 2014. Flat-plate collector construction and system configuration to optimize the thermosiphonic effect. *Renewable Energy,* 67, 202-206.

KHALIFA, A. J. N. & ABDUL JABBAR, R. A. 2010. Conventional versus storage domestic solar hot water systems: A comparative performance study. *Energy Conversion and Management,* 51, 265-270.

KIATSIRIROAT, T. 2014. Performance Analysis of Flat-Plate Solar Collector Having Silver Nanofluid as a Working Fluid AU - Polvongsri, Sarawut. *Heat Transfer Engineering,* 35, 1183-1191.

KOYUNCU, T. & LÜLE, F. 2015. Thermal Performance of a Domestic Chromium Solar Water Collector with Phase Change Material. *Procedia - Social and Behavioral Sciences,* 195, 2430-2442.

LOEM, S., DEETHAYAT, T., ASANAKHAM, A. & KIATSIRIROAT, T. 2019. Thermal characteristics on melting/solidification of low temperature PCM balls packed bed with air charging/discharging. *Case Studies in Thermal Engineering,* 14, 100431.

MIRZAEI, M. 2017. Experimental investigation of the assessment of Al2O3–H2O and CuO–H2O nanofluids in a solar water heating system. *Journal of Energy Storage,* 14, 71-81.

MUHAMMAD, M. J., MUHAMMAD, I. A., SIDIK, N. A. C., YAZID, M. N. A. W. M., MAMAT, R. & NAJAFI, G. 2016. The use of nanofluids for enhancing the thermal performance of stationary solar collectors: A review. *Renewable and Sustainable Energy Reviews,* 63, 226-236.

MURUGAN, M., VIJAYAN, R., SARAVANAN, A. & JAISANKAR, S. 2019. Performance enhancement of centrally finned twist inserted solar collector using corrugated booster reflectors. *Energy,* 168, 858-869.

PAPADIMITRATOS, A., SOBHANSARBANDI, S., POZDIN, V., ZAKHIDOV, A. & HASSANIPOUR, F. 2016. Evacuated tube solar collectors

The 1st International Conference on Smart Community Development in the Asia Pacific (iSCAP2020)

integrated with phase change materials. *Solar Energy,* 129, 10-19.

POLVONGSRI, S. 2013. ASHRAE STANDARD 93-2003 METHODS OF TESTING TO DETERMINE THE THERMAL PERFORMANCE OF FLAT-PLATE SOLAR COLLECTORS. CHING MAI: THERMAL SYSTEM RESEARCH UNIT.

SARAVANAN, A., SENTHILKUMAAR, J. S. & JAISANKAR, S. 2016. Experimental studies on heat transfer and friction factor characteristics of twist inserted V-trough thermosyphon solar water heating system. *Energy,* 112, 642-654.

SHARAFELDIN, M. A. & GRÓF, G. 2018. Experimental investigation of flat plate solar collector using CeO2-water nanofluid. *Energy Conversion and Management,* 155, 32-41.

SHARAFELDIN, M. A., GRÓF, G. & MAHIAN, O. 2017. Experimental study on the performance of a flat-plate collector using WO3/Water nanofluids. *Energy,* 141, 2436-2444.

SYAM SUNDAR, L., KIRUBEIL, A., PUNNAIAH, V., SINGH, M. K. & SOUSA, A. C. M. 2018. Effectiveness analysis of solar flat plate collector with Al2O3 water nanofluids and with longitudinal strip inserts. *International Journal of Heat and Mass Transfer,* 127, 422-435.

APPENDIX

Nomenclature

$\dot{m}$	Mass flow rate of water	kg/s
C_p	Specific heat capacity	$J/kg.^oC$
I_T	Incident radiation intensity	W/m^2
A_c	Surface area of solar collector	m^2
F_R	Heat removal factor	-
T_o	Outlet water temperature	^oC
T_a	Ambient temperature	^oC
T_i	Inlet water temperature	^oC
T_{Tank}	Water tank temperature	^oC

Q_s	Energy gain of storage tank	MJ
$\dot{Q}_u$	Rate of useful heat gain	W
U_L	Overall loss coefficient of collector	$W/m^2\,^oC$
R^2	Correlation coefficient	
$(\tau\alpha)_e$	Absorptance-Transmittance produce	
η	Solar collector efficiency	

Table 3: value of parameters

Category	Value	Unit
I_T	801.21	W/m^2
$\dot{m}$	0.02	kg/s.m^2
T_i	35.6	°C
T_o	44.9	°C
C_p	4187	J/kg. °C
A_c	0.128	m^2

The useful energy calculation according to the Eq. (2): from the Table 3:

$$Q_u = 0.02 \times (0.127) \times 4187 \times (44.9 - 35.6)$$
$$= 65.028\,W$$

The thermal efficiency of the solar collector could be calculated according to the Eq.(3): from Table 3:

$$\eta = \frac{65.028}{801.21 \times 0.128}$$
$$= 0.62$$

Effect of mass flow rate on thermal performance of flat-plate solar collector integrated with phase change material riser

5th RSU National and International Research Conference on Science and Technology, Social Science and Humanities 2020, Rangsit University, on 1 May 2020

RSUSSH
2020

Proceedings of
The 5th RSU International Research Conference
on Science and Technology, Social Science,
and Humanities 2020

1 May 2020

"THE CHALLENGES IN THE UPSHOT OF CANNABIS FOR MEDICINE"

BIOMEDICAL ENGINEERING/ DENTAL SCIENCE

MEDICAL/ PHARMACEUTICAL AND BIOMEDICAL SCIENCE

APPLIED SCIENCE / ENGINEERING/ FOOD AND AGRICULTURAL

ARCHITECTURE AND DESIGN/ PERFORMANCE ART

EDUCATION

FINANCIAL/ BANKING/ BUSINESS/ MANAGEMENT/ COMMUNICATION ARTS AND TOURISM

LIBERAL ART

HUMANITY AND SOCIAL SCIENCE

CHINESE STUDY

RSUSSH
2020

"THE CHALLENGES IN THE UPSHOT OF CANNABIS FOR MEDICINE"

RANGSIT UNIVERSITY

MCL
Malayan Colleges Laguna

Fontys

BIOMEDICAL ENGINEERING/ DENTAL SCIENCE

MEDICAL/ PHARMACEUTICAL AND BIOMEDICAL SCIENCE

APPLIED SCIENCE / ENGINEERING/ FOOD AND AGRICULTURAL

ARCHITECTURE AND DESIGN/ PERFORMANCE ART

EDUCATION

FINANCIAL/ BANKING/ BUSINESS/ MANAGEMENT/ COMMUNICATION ARTS AND TOURISM

LIBERAL ART

HUMANITY AND SOCIAL SCIENCE

CHINESE STUDY

Effect of mass flow rate on thermal performance of flat-plate solar collector integrated with phase change material riser

Bundarith Nhel and Sarawut Polvongsri*

School of Renewable Energy, Maejo University, Chiang Mai, Thailand
*Corresponding author, E-mail: saravooth@hotmail.com

Abstract

The solar energy is clean, environmentally renewable energy and can be used in both electricity and heat function. In part of heat production, it commonly used a solar collector that can integrate with many techniques for offering the highest thermal performance which one method is to use the phase change material (PCM). The goal of this research is to study the thermal performance of solar collector with and without phase change material (PCM) riser. The various water mass flow rate per collector area were observed at 0.01, 0.02 and 0.03 kg/s·m², respectively. The two novel solar collectors were built in a single copper tube as absorber plate tube with 28.7 mm of outside diameter, 1 mm of thickness and 1,000 mm of length inserted with copper tube riser with diameter of 10 mm and 16 mm which were filled with RT42 phase change material (a melting point between 38 ℃ to 42 ℃). The novel solar collectors were installed for thermal performance testing following ASHRAE standard 93-2003 comparing with the solar collector without PCM riser.

The experiment results show that both of the novel solar collectors were given the thermal performance greater than the solar collector without PCM riser. The novel solar collector that integrated with phase change material riser of 16 mm diameter (PCM1) at 0.03 kg/s·m² demonstrated the best of $F_R(\tau\alpha)_e$ and $F_R U_L$ of 0.811 and 9.753 (W/m²·K)following by the mass flow rate of 0.02 kg/s·m² and 0.01 kg/s·m², respectively. For the novel solar collector integrated with phase change materials riser of 10 mm diameter (PCM2) gave the $F_R(\tau\alpha)_e$ and $F_R U_L$ of 0.815 and 11.140 (W/m²·K) at 0.02 kg/s·m² following by the results of mass flow rate 0.03 kg/s·m² and 0.01 kg/s·m², respectively.

Keywords: Thermal performance, Solar flat plate collector, Phase change material, PCM RT42.

1. Introduction

The Presently, the energy demand is increased rapidly around the world (UN(unitednation), 2018) along the global economic growth, while energy resource has limited and has decreased amount of fossil fuel such as coal, natural gas and crude oil. Burning of fossil fuel increases the amount of greenhouse gas in the atmosphere that causes of the global warming (WHO, 2018). Solar energy is a potential renewable energy. It's free and environmentally save more than fossil fuel energy. The useful of solar energy can be used in both functional electricity and heat. Heating system by using solar flat plate collector is used in the low range temperature which less than 100 ℃ especially using for water heating production (Gautam, Chamoli, Kumar, & Singh, 2017; Kalogirou, 2014). Although, the solar collector is widely used but many researchers try to enhance its thermal performance by many methods (Cabeza, Castell, Barreneche, de Gracia, & Fernández, 2011). Using phase change materials (PCM) integrated with solar collector is an alternative method. PCM is a chemical composite that can store a large amount of thermal energy during melting or freezing in the storage tank. The thermal accumulation of PCM has been given a large quantity when integrates in the collector, and it can reduce heat loss. The suitable outlet temperature could provide in cloudy day when operated comparing without PCM (Bellan et al., 2015; Cabeza et al., 2011; Gupta, Gaur, Crook, & Dixon-Hardy, 2017; Khalifa, Suffer, & Mahmoud, 2013; Koca, Oztop, Koyun, & Varol, 2008; Koyuncu & Lüle, 2015; Lin, Al-Kayiem, & Aris, 2012; Loem, Deethayat, Asanakham, & Kiatsiriroat, 2019; Wu et al., 2018). The research study between PCM and flat plate solar collector had been published by various techniques, for example: (Koyuncu & Lüle, 2015) studied the domestic chromium solar water collector with PCM filling which the system arranged an absorber pipe for water circulating at 0.02 kg/s·m², (Lin et al., 2012) studied the flat-plate solar collector integrated with phase change materials below the absorber plate as thermal energy storage. The absorber plate was modified by the surface

[555]

extending into the PCM reservoir for heat transfer increasing. The results showed that the comparison of solar flat plate collector in different inclination angles from 10°-20° in the case of with and without phase change materials can operate the promising 38 ℃ of hot water temperature for daytime demand and give 52 % of system efficiency, and (Mettawee & Assassa, 2006) studied the compact solar collector that contained the PCM and a copper pipe embedded inside for carrying the heat transfer of system. The result showed that the PCM would be melted by solar radiation with temperature increases gradually by its low-temperature gradient due to the low thermal conductivity and the natural convection grew strongly to solid-liquid interface by re-circulated flow.

In this experiment, it investigates the novel Flat-Plate solar collector which water exchanges accumulation heat directly with absorber plate, the PCM is filled in the copper tube riser that inserts in the copper absorber tube of collector. During operation testing, the solar collector will absorb heat from solar radiation and transfer to the working fluid and PCMs. The thermal performance of this novel system is tested as following to ASHRAE standard 93-2003.

2. Objectives

1. To study the solar Flat-Plate collector integrated with phase change material riser tube.
2. To find thermal efficiency of novel solar collector (PCM 1 and PCM 2) to conventional solar collector using the Ashrae standard 93-2003.
3. To find the effect of mass flow rate on thermal performance Flat-Plate collector integrated performance.

3. Materials and Methods

3.1 The novel solar collector

The novel solar collectors in this experiment had two prototype flat-plate solar collectors. Each set consisted of a single copper tube as absorber plate tube with an outside diameter of 28.7 mm, thickness of 1 mm and length of 1000 mm, inside a copper tube was inserted a copper riser. The first prototype was filled with RT42 Phase Change Material (PCM) in riser tube with a diameter of 16 mm and the second one was filled with the same PCM in a diameter of 10 mm. PCM melting point is between 38-42 ℃ (ICNQT, 2018) were inserted into the absorber plate of flat-plate collector. The copper tube plate was welded with a copper absorber plate for increasing aperture surface and painted a black color on the absorber plate. On the above, a single clear glass of 3 mm thickness was installed as a cover greenhouse effect. Around the aluminum frame of novel solar collector was enfolded by the Aroflex foam rubber (density of 40-70 kg/m³) with thickness 25 mm for heat loss reduction. The perspective dimension of the novel solar collectors was 1090 mm of length, 220 mm of width, and 100 mm of height that shows in Figure 1 and Figure 2.
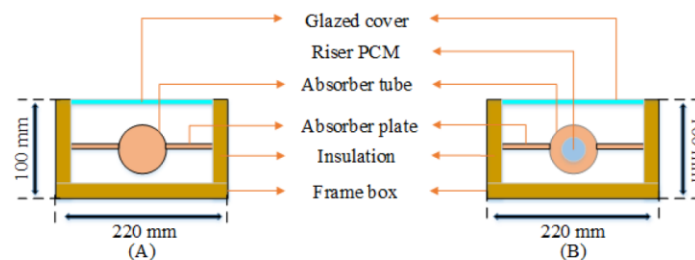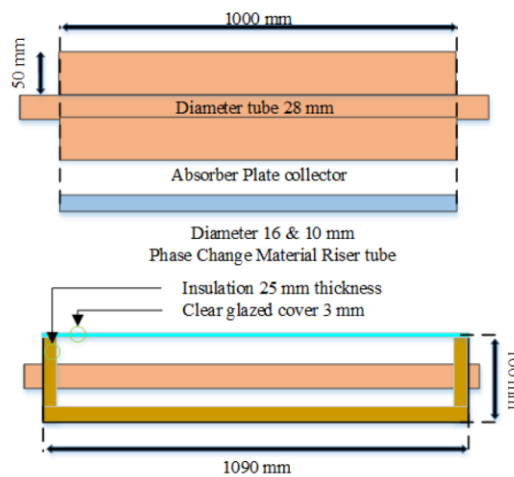

Figure 1 Schematic of (A) The normal collector and (B) The novel solar collector integrated PCM

Figure 2 Absorber plate and PCM riser with measure points both novel and conventional solar collector

3.2 Experimental procedure

The experiment divided in three case studies for example, testing with 16 mm of riser diameter (called PCM 1), 10 mm of diameter (called PCM 2) and without PCM riser and was undertaken at the School of Renewable Energy, Maejo University, Chiang Mai, Thailand. All of collectors were installed at 18° of tilt angle facing to the south as shown in

Figure **3**. The water flow rate was circulated through the system by the electrical pump. Each solar collector had own 11 kg of water storage tank with a resistance heater and stored water circulating that collected heat gain from the collector. The mass flow rate was measured by the manual flow meter (Platon), installed the gauge valve to regulate the mass flow rate of water in solar collector system and the bypass valve was used to reduce overload from overpressure in system.

The experiment method was conducted following ASHRAE standard 93-2003 (Polvongsri, 2013) to find out the thermal performance of solar collector. All of parameters, for example, the solar radiation, the ambient temperature, the inlet water temperature, and the outlet water temperature, were set following ASHRAE standard and the mass flow rate of working fluid is adjusted under steady state condition. The resistance heater used to modify the range inlet temperature from 35 °C to 65 °C during testing. Before doing experiment, the set temperature was pumped with a small pump into the storage tank runs in 5 minutes to make sure the water was stable. While testing, the hot water from solar collector is going through to the storage tank which was collected thermal energy. It made hot water remained on the top of the tank while the bottom still remains the set-inlet temperature even though the temperature water in the storage tank changed as a small value which could be accepted as following to the standard (± Max of (0.1 °C, 2%)). The type K thermocouple was used to measure the temperature parameters and recorded in the multi channels data logger (Model Lutron, TD-1947 SD). The total solar radiation at a tilt angle of the solar collector was measured by pyranometer (Model Apogee, SP-110) and recorded in data logger (Model Adam 5000 PBC). The error of each instruments was calibrated independently after the experimental data collection.
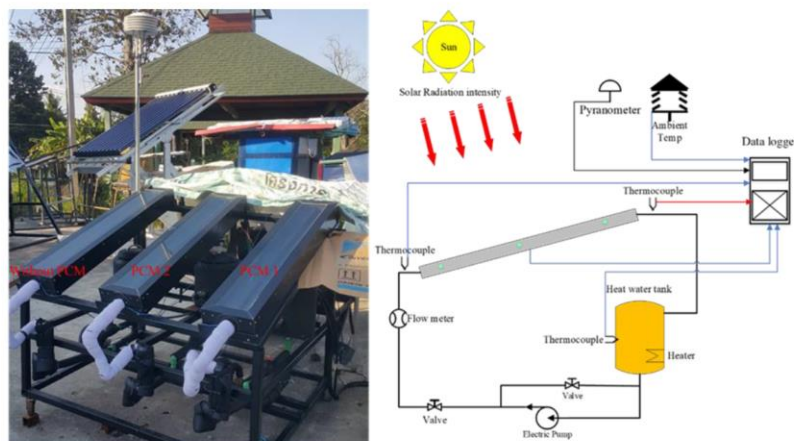
Figure 3 The novel solar collectors integrated with PCM and Conventional collector installation

3.3 Analysis

The data measurement of ambient temperature, inlet water temperature, outlet water temperature, water temperature of storage tank, solar radiation, and mass flow rate would be used to calculate thermal efficiency of solar collector as following Eq.(1) to Eq.(3). The collected heat gained for the solar is calculated by Eq.(1) (Duffie & Beckman, 2013).

$$\dot{Q} = \dot{m}C_p \left(T_o - T_i\right) \tag{1}$$

The Eq.(1) is definition of the collected ability of all kind solar collector which gave the energy output of the collected heat gain $\dot{Q}$, with the mass flow rate through   the collector $\dot{m}$, following the temperature of the water before flow through the inside and after leave the collector to the storage tank T_i and T_o. The specific heat of the water as working fluid C_p.

The thermal efficiency of solar collector can be determined as following Eq.(2) and Eq.(3) (Duffie & Beckman, 2013; Polvongsri, 2013).

$$\eta = \frac{\dot{m}c_p \left(T_o - T_i\right)}{I_T A_C} \tag{2}$$

$$\eta = F_R \left(\tau\alpha\right)_e - F_R U_L \frac{\left(T_i - T_a\right)}{I_T} \tag{3}$$

The thermal efficient of the solar collector in Eq.(2) could calculate the collector energy gain as energy output or collected energy of collector and the solar radiation I_T with the collector area A_c as the energy input. In Eq.(3), the thermal efficiency is presented at linear equation relation. The linear equation will result when the efficiencies are obtained from averaged data plated against $(T_i-T_a)/I_T$ according to Eq.(3). The intersection of the Y-axis is equal to $F_R(\tau\alpha)_e$, and on this axis, the temperature of working fluid entering the collector is nearly the means ambient temperature that the collector efficiency is nearly a

[558]

maximum value. Therefore, the slope of the linear equation is equal to $F_R U_L$. This slope indicates that heat loss has been removed from the solar collector that nominated as removed energy parameter. At the intersection of X-axis, the collector efficiency is equal to zero and this point normally called stagnation which usually occurs when there is no fluid flows in the collector.

4. Results and Discussion
4.1 Thermal efficiency of collector

The experimental conditions were set as followed ASHRAE standard 93-2003 (Polvongsri, 2013) which are, the solar radiation intensity is equal or more than 790 W/m^2 and the air velocity set from 2.2-4.4 m/s. The two novel collectors with PCM riser and conventional collector without PCM were tested with various mass flow rate 0.01, 0.02 and 0.03 kg/s·m^2 and the inlet water temperatures were varied at 35, 40, 45, 50, 55, 60, 65 ℃, respectively.
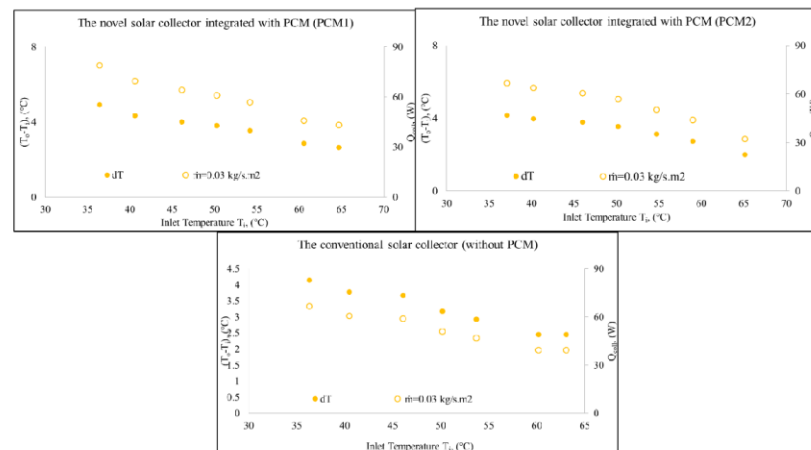

Figure 4 The temperature difference of (T_o-T_i) and collected heat gain from novel solar collector with PCM 1, PCM 2, and the conventional collector without PCM

The temperature difference of (T_o-T_i) and collected heat gain Q_{coll} of novel collector PCM1, PCM2 and without PCM is shown in Figure 4. The results found that in the case of PCM1, PCM2 and without PCM showed the temperature difference between the outlet water temperature and inlet water temperature would give the maximum value to the minimum value at the mass flow rate of 0.01, 0.02 and 0.03 kg/s·m^2, respectively, because the high mass flow rate could gather heat gain of collector more than low mass flow rate. Therefore, the temperature difference (T_o-T_i) was different less than the operation at the higher mass flow rate. Moreover, the temperature difference (T_o-T_i) was changed following to the temperature setting from 35-65 ℃ with the low inlet water temperature through to the solar collector that could collected high thermal energy with less thermal loss. When the inlet water temperature (T_i) increased, the efficiency of the solar collector was decreased because of the large amount of heat that was loosening to the low ambient temperature. At the mass flow rate at 0.01 kg/s·m^2, the temperature differences of (T_o-T_i) PCM 1, PCM 2, and without PCM were 10.1-4.2 ℃, 9.2-4.1℃ and 8.5-3.2 ℃, respectively. At the mass flow rate of 0.02 kg/s·m^2 was 6.1-2.5 ℃, 6.2-2.8 ℃ and 5.5-2 ℃ and the mass flow rate of 0.03 kg/s.m^2 obtained 4.9-4.6 ℃, 4.2-2.1℃ and 4.2-2.4℃, respectively.

[559]

The amount of collected heat gain (Q_{coll}) was decreased following the arrangement of inlet water temperature while the high mass flow rate was given a high amount of thermal energy. Otherwise, the collected heat gain (Q_{coll}) was showed that the PCM 1 and without PCM case study were given the highest thermal energy at the mass flow rate of 0.03 kg/s·m² while the PCM 2 demonstrated that the mass flow rate of 0.02 kg/s□m² gave the highest thermal energy. The various flow rates (0.01, 0.02 and 0.03 kg/s·m²) given by the Q_{coll} were 78.6-42.5 W, 67.5-26.8 W and 70.6-29.5 W of the PCM 1. In the case of PCM 2 gave 65.7-32.1 W, 69.3-32.4 W and 64.3-28.6 W and finally in the case of without PCM gave 67.4-38.5 W, 60-21.8 W, and 58-22.4 W, respectively.
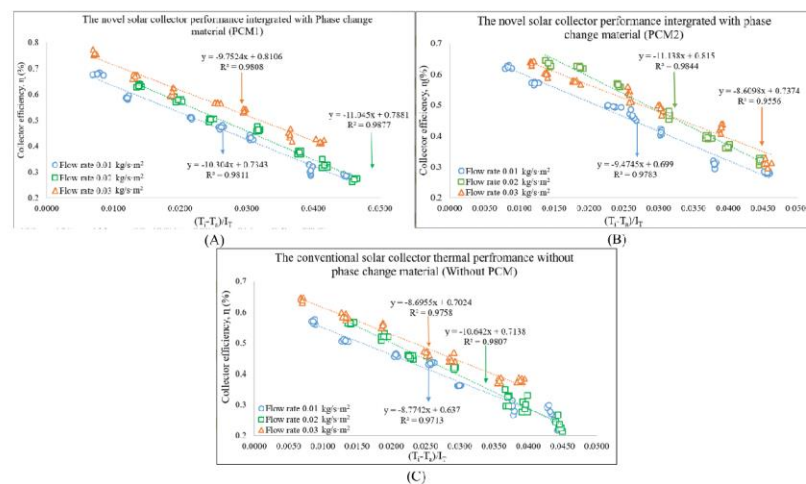
Figure 5 The thermal efficiency of novel solar collector with (A), PCM 1,(B) PCM 2, and (C) conventional collector without PCM

Table 1 The thermal performance analysis data of each collectors

PCM 1 (The novel solar collector integrated with riser phase change materials 16 mm of diameter)			
Category	$F_R(\tau\alpha)_e$	$F_R U_L$	R^2
Flow rate 0.01 kg/s·m²	0.734	10.30	0.981
Flow rate 0.02 kg/s·m²	0.788	11.05	0.987
Flow rate 0.03 kg/s·m²	0.811	9.752	0.981
PCM 2 (The novel solar collector integrated with riser phase change materials 10 mm of diameter)			
Category	$F_R(\tau\alpha)_e$	$F_R U_L$	R^2
Flow rate 0.01 kg/s□m²	0.699	9.474	0.978
Flow rate 0.02 kg/s□m²	0.815	11.14	0.984
Flow rate 0.03 kg/s□m²	0.737	8.609	0.956
Without PCM (The conventional flat-plated solar collector)			
Category	$F_R(\tau\alpha)_e$	$F_R U_L$	
Flow rate 0.01 kg/s□m²	0.637	8.774	0.97
Flow rate 0.02 kg/s□m²	0.714	10.642	0.98
Flow rate 0.03 kg/s□m²	0.702	8.695	0.97

Figure 5 showed that the thermal efficiency of various mass flow rate 0.01, 0.02, 0.03 kg/s□m² of novel solar collector integrated with phase change material and conventional collector. The results are represented by the linear regression function between $(T_i-T_a)/I_T$ and thermal efficiency (η). The mass flow rate of the $F_R(\tau\alpha)_e$ in each case were performed on the intersection of Y-axis representing the maximum efficiency and the slope of the equation as the heat loss to environment by following the Eq.(3). The novel solar collector integrated with PCM of riser tube 16 mm outside diameter (PCM1) was given the value $F_R(\tau\alpha)_e$ of 0.734, 0.788 and 0.811, and heat loss F_RU_L of 10.30, 11.05 and 9.75 W/m²·K by testing various flow rates was showed in Table 1 (PCM1). The novel collector PCM1 tested with mass flow rate at 0.03 kg/s□m² is given a highest thermal performance with $F_R(\tau\alpha)_e$ of 0.811 and F_RU_L of 9.75 W/m²·K.

The novel solar collector integrated with PCM of riser tube 10 mm outside diameter (PCM2) was given the value $F_R(\tau\alpha)_e$ of 0.699, 0.815 and 0.737 and heat loss F_RU_L of 9.474, 11.14 and 8.609 W/m²·K, respectively, by testing various flow rates was showed in Table 1 (PCM2). The novel collector PCM1 tested with mass flow rate at 0.02 kg/s□m² is given a highest thermal performance with $F_R(\tau\alpha)_e$ of 0.815 and F_RU_L of 11.14 W/m²·K, respectively.

The conventional solar collector without PCM (without PCM) was given the value $F_R(\tau\alpha)_e$ of 0.637, 0.714 and 0.702 and heat loss F_RU_L of 8.774, 10.642 and 8.695 W/m²·K, respectively, by testing various flow rates was showed in Table 1 (without PCM). The conventional collector tested with mass flow rate at 0.02 kg/s□m² is given a highest thermal performance with $F_R(\tau\alpha)_e$ of 0.714 and F_RU_L of 10.642 W/m²·K, respectively.

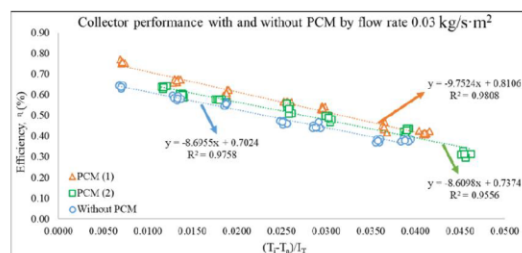**Figure 6** The thermal efficiency of all case studies at the mass flow rate of 0.03 kg/s□m²

Figure 6 shows the collector efficiency at 0.03 kg/s□m² of novel and conventional solar collectors. The result of the experiment confirmed that the both prototype novel solar collectors were given the greater thermal efficiency than the conventional collector. The best mass flow arte was selected at 0.03 kg/s□m² which the novel collector PCM 1 was given the highest thermal efficiency than other cases in the Table 1.

4.2 Daily system operation
The novel solar collectors and the conventional collector were experimented for analysis system operation since 8:30 a.m. to 03:00 p.m. under clear sky day condition. The system operated at the best mass flow rate of 0.03 kg/s□m² and circulated the water from the 10-liter storage tank to the collector. The results in Figure 7 and Figure 8 showed that the storage tank with initial temperature (T_s) was about 25 °C and when the solar radiation (I_T) increased, the storage tank temperature was raised continuously following the variation of solar radiation. The maximum solar radiation was around 830 W/m² at 12:30 PM, the temperature T_s of storage tank were increased to 45, 46, and 44 °C, respectively. The PCM 1 was collected more thermal energy than other collectors until the end of the operating at 3:00 p.m. which the storage tank temperature was 55 °C while PCM 2 and without PCM was 53 °C and 51°C, respectively.
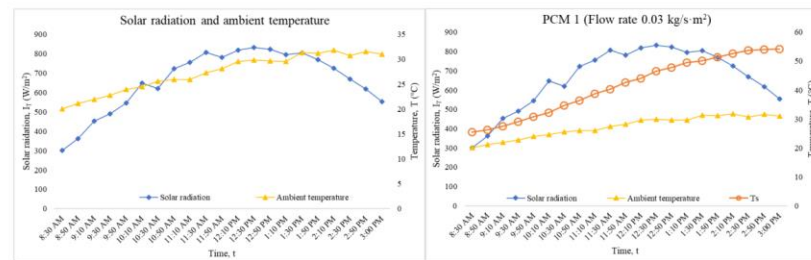
Figure 7 Solar radiation, ambient temperature and the result of daily system operation of novel solar collectors (PCM 1) of the mass flow rate of 0.03 kg/s·m²
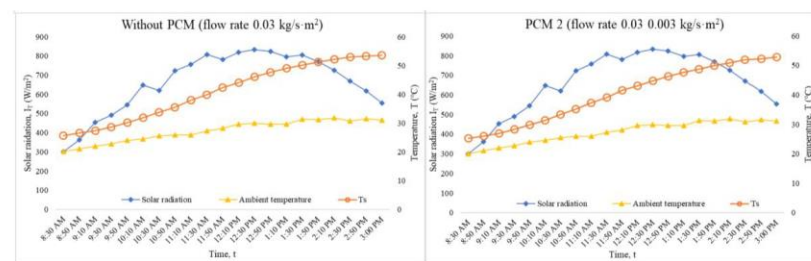
Figure 8 The result of daily system operation of novel solar collectors (PCM 2) of the mass flow rate of 0.03 kg/s·m²

5. Conclusion

The novel solar collectors that integrated with the phase change materials riser of 16 mm diameter (PCM 1) and 10 mm diameter (PCM2) were experimented comparing the conventional solar collector without PCM riser. The thermal performance testing was conducted following by ASHRAE standard 93-2003. The discovered results showed that both of the novel solar collectors were given the thermal performance greater than the collector without PCM riser. The novel solar collector with 16 mm diameter of riser (PCM 1) represented the suitable $F_R(\tau\alpha)_e$ and $F_R U_L$ which were 0.811 and 9.753 (W/m²·K) at 0.03 kg/s·m², and then was followed as 0.01 kg/s·m² and 0.02 kg/s·m², respectively. The novel solar collector integrated with phase change material RT42 (melting point between 38 to 43 °C) is $14.76 per kilogram (Australia Dollar) which was used in the experimental study.

6. Acknowledgements

7. References

Bellan, S., Alam, T. E., González-Aguilar, J., Romero, M., Rahman, M. M., Goswami, D. Y., & Stefanakos, E. K. (2015). Numerical and experimental studies on heat transfer characteristics of thermal energy storage system packed with molten salt PCM capsules. *Applied Thermal Engineering, 90*, 970-979. doi:https://doi.org/10.1016/j.applthermaleng.2015.07.056

Cabeza, L. F., Castell, A., Barreneche, C., de Gracia, A., & Fernández, A. I. (2011). Materials used as PCM in thermal energy storage in buildings: A review. *Renewable and Sustainable Energy Reviews, 15*(3), 1675-1695. doi:https://doi.org/10.1016/j.rser.2010.11.018

Duffie, J. A., & Beckman, W. A. (2013). *Solar engineering of thermal processes.* US: Wiley&Sons.

Gautam, A., Chamoli, S., Kumar, A., & Singh, S. (2017). A review on technical improvements, economic feasibility and world scenario of solar water heating system. *Renewable and Sustainable Energy Reviews, 68*, 541-562. doi:https://doi.org/10.1016/j.rser.2016.09.104

Gupta, A., Gaur, M. K., Crook, R., & Dixon-Hardy, D. W. (2017). Experimental investigation of heat removal factor in solar flat plate collector for various flow configurations AU - Malvi, C. S. *International Journal of Green Energy, 14*(4), 442-448. doi:10.1080/15435075.2016.1268619

ICNQT. (2018). Nano PCM. doi:http://icnqt.com/nano-products/nano-pcm/

Kalogirou, S. A. (2014). Flat-plate collector construction and system configuration to optimize the thermosiphonic effect. *Renewable Energy, 67*, 202-206. doi:https://doi.org/10.1016/j.renene.2013.11.021

Khalifa, A. J. N., Suffer, K. H., & Mahmoud, M. S. (2013). A storage domestic solar hot water system with a back layer of phase change material. *Experimental Thermal and Fluid Science, 44*, 174-181. doi:https://doi.org/10.1016/j.expthermflusci.2012.05.017

Koca, A., Oztop, H. F., Koyun, T., & Varol, Y. (2008). Energy and exergy analysis of a latent heat storage system with phase change material for a solar collector. *Renewable Energy, 33*(4), 567-574. doi:https://doi.org/10.1016/j.renene.2007.03.012

Koyuncu, T., & Lüle, F. (2015). Thermal Performance of a Domestic Chromium Solar Water Collector with Phase Change Material. *Procedia - Social and Behavioral Sciences, 195*, 2430-2442. doi:https://doi.org/10.1016/j.sbspro.2015.06.267

Lin, S. C., Al-Kayiem, H. H., & Aris, M. (2012). Experimental investigation on the performance enhancement of integrated PCM-flat plate solar collector. *Journal of Applied Sciences, 12*(24), 2390-2396.

Loem, S., Deethayat, T., Asanakham, A., & Kiatsiriroat, T. (2019). Thermal characteristics on melting/solidification of low temperature PCM balls packed bed with air charging/discharging. *Case Studies in Thermal Engineering, 14*, 100431. doi:https://doi.org/10.1016/j.csite.2019.100431

Mettawee, E.-B. S., & Assassa, G. M. R. (2006). Experimental study of a compact PCM solar collector. *Energy, 31*(14), 2958-2968. doi:https://doi.org/10.1016/j.energy.2005.11.019

Polvongsri, S. (2013). ASHRAE STANDARD 93-2003: Methods of Testing to Determine the Thermal Performance of Flat-Plate Solar Collectors: Chieng Mai: Thermal System Research Unit.

UN(unitednation). (2018). The world population. https://www.un.org/development/desa/publications/.

WHO. (2018). Pollution. https://www.who.int/airpollution/en/.

Wu, W., Dai, S., Liu, Z., Dou, Y., Hua, J., Li, M., . . . Wang, X. (2018). Experimental study on the performance of a novel solar water heating system with and without PCM. *Solar Energy, 171*, 604-612. doi:https://doi.org/10.1016/j.solener.2018.07.005

CURRICULUM VITAE

NAME	Bundarith Nhel
DATE OF BIRTH	25 November 1994

EDUCATION

2000-2006	Primary School of Kampong Beung, Kampong Leng, Kampong Chhang Province
2006-2010	Hun Sen Kampong Leng High School, Kampong Leng, Kampong Chhnang Province
2011-2012	High School Diploma, Preah Bat Soramarith High School, Kampong Chhnang Province, Cambodia
2012-2014	Foundation year (General Study) at the Institute of Technology of Cambodia
2014-2017	Bachelor Degree of Industrial and Mechanical Engineering of Institute of Technology of Cambodia
2018-Present	Master Degree student of School of Renewable Energy, Maejo University, Chiang Mai, Thailand.

WORK EXPERIENCE

2017-2018	Former of (MVAC) CAD design engineer at Team-Cambodia Co., Ltd
2017	Trainee student at Lotus Green Team Co., Ltd